

Toxicological Evaluation of Poly(ethylene imine) -based non-viral vector systems for pulmonary siRNA application

Dissertation

zur Erlangung des Doktorgrades

der Naturwissenschaften

(Dr. rer. nat.)

dem Fachbereich Pharmazie der Philipps Universität Marburg vorgelegt von

Christiane **Andrea** Barbara **Beyerle**

aus Neuss

Marburg/Lahn 2010

Vom Fachbereich Pharmazie der Philipps-Universität Marburg als Dissertation am
13.04.2010 angenommen.

Erstgutachter: Prof. Dr. Thomas Kissel

Zweitgutachter: Prof. Dr. Carsten Culmsee

Tag der mündlichen Prüfung am 14.04.2010

Die vorliegende Arbeit entstand auf Anregung und unter Anleitung von
Herrn Prof. Dr. Thomas Kissel

am Institut für Pharmazeutische Technologie und Biopharmazie
der Philipps-Universität Marburg

und in enger Zusammenarbeit mit der Arbeitsgruppe von
Herrn Dr. Tobias Stöger

am Institut für Lungenbiologie
Comprehensive Pneumology Center

im Helmholtz Zentrum München

„Es geht darum, all das, was man zum Ausdruck bringen will, lange und intensiv genug zu betrachten, um etwas daran zu entdecken, das noch von niemandem gesehen und ausgesprochen worden ist. In allem gibt es etwas Unbekanntes, denn wir sind daran gewöhnt, uns beim Schauen stets an das zu erinnern, was man vor uns über das Betrachtete gedacht hat.“

Guy de Maupassant, Reisen nach Nordafrika

Meinen Eltern und Großeltern

in Liebe und Dankbarkeit

Table of content

1	Introduction.....	1
	<i>The lung.....</i>	<i>2</i>
	<i>1.1 Anatomical and physiological aspects.....</i>	<i>2</i>
	<i>1.2 Basic considerations for lung delivery.....</i>	<i>7</i>
	<i>1.3 Cellular Transport mechanisms.....</i>	<i>13</i>
	<i>1.4 Barriers for pulmonary administration.....</i>	<i>17</i>
	<i>1.5 Non viral vector systems for pulmonary siRNA application.....</i>	<i>19</i>
	<i>1.6 Aspects of Nanotoxicology in Nanomedicine.....</i>	<i>25</i>
	<i>1.7 Aim of this thesis.....</i>	<i>30</i>
	<i>1.8 References.....</i>	<i>32</i>
2	In vitro cytotoxic and immuno-modulatory profiling of low molecular weight polyethylen-imines for pulmonary application	38
	<i>2.1 Abstract.....</i>	<i>39</i>
	<i>2.2 Introduction.....</i>	<i>40</i>
	<i>2.3 Materials and Methods.....</i>	<i>43</i>
	<i>2.4 Results.....</i>	<i>48</i>
	<i>2.5 Discussion.....</i>	<i>57</i>
	<i>2.6 Supplementary material.....</i>	<i>62</i>
	<i>2.7 References.....</i>	<i>67</i>
3	PEGylation affects cytotoxicity and cell-compatibility of Poly(ethylene imine) for lung application: structure-function-relationships.....	69
	<i>3.1 Abstract.....</i>	<i>70</i>
	<i>3.2 Introduction.....</i>	<i>71</i>
	<i>3.3 Materials and Methods.....</i>	<i>74</i>
	<i>3.4 Results.....</i>	<i>80</i>
	<i>3.5 Discussion.....</i>	<i>90</i>
	<i>3.6 Supplementary material.....</i>	<i>95</i>
	<i>3.7 References.....</i>	<i>96</i>
4	Toxicity pathway focused gene expression profiling of PEI-based polymers for pulmonary applications.....	100
	<i>4.1 Abstract.....</i>	<i>101</i>
	<i>4.2 Introduction.....</i>	<i>102</i>
	<i>4.3 Experimental Section.....</i>	<i>105</i>
	<i>4.4 Results.....</i>	<i>110</i>
	<i>4.5 Discussion.....</i>	<i>118</i>
	<i>4.6 Supporting Information.....</i>	<i>124</i>
	<i>4.7 References.....</i>	<i>130</i>
5	Investigations on mutant frequency induced by PEI in FE1-Muta™ Mouse lung epithelial cells.....	134
	<i>5.1 Abstract.....</i>	<i>135</i>
	<i>5.2 Introduction.....</i>	<i>136</i>
	<i>5.3 Materials and Methods.....</i>	<i>138</i>
	<i>5.4 Results and Discussion.....</i>	<i>141</i>
	<i>5.5 Conclusion.....</i>	<i>147</i>
	<i>5.6 References.....</i>	<i>148</i>

6	Side-effects of PEI-based siRNA nanocarriers for pulmonary application in mice	150
	6.1 <i>Abstract</i>	151
	6.2 <i>Introduction</i>	152
	6.3 <i>Materials and Methods</i>	154
	6.4 <i>Results</i>	157
	6.5 <i>Discussion</i>	168
	6.6 <i>Supplementary Material</i>	174
	6.7 <i>References</i>	183
7	Fatty acid modification of low molecular weight polyethylenimine-mediated siRNA delivery to lung leucocytes after intratracheal instillation in mice	185
	7.1 <i>Abstract</i>	186
	7.2 <i>Background</i>	187
	7.3 <i>Methods</i>	189
	7.4 <i>Results</i>	194
	7.5 <i>Discussion</i>	205
	7.6 <i>Supplementary data</i>	208
	7.7 <i>References</i>	211
8	Summary and Perspectives	214
	8.1 <i>Summary</i>	215
	8.2 <i>Perspectives</i>	217
	8.3 <i>Zusammenfassung</i>	220
	8.4 <i>Ausblick</i>	223
9	Appendices	226
	9.1 <i>Abbreviations</i>	227
	9.2 <i>List of publications</i>	229
	9.3 <i>Poster presentations</i>	230
	9.4 <i>Lectures</i>	231
	9.5 <i>Curriculum vitae</i>	232
	9.6 <i>Danksagung</i>	234

1 Introduction

The lung

1.1 Anatomical and physiological aspects

Anatomy of the lung

The lung represents one very sensitive organ which gives animals and humans the breath of life. The primary functions of the lungs are to enable gas exchange between the blood and the external environment, and to maintain homeostatic systemic pH. To perform this very important task the lung consists of two distinct zones: i) conducting and ii) respiratory, within which the airway and vascular compartments are situated (Fig. 1).

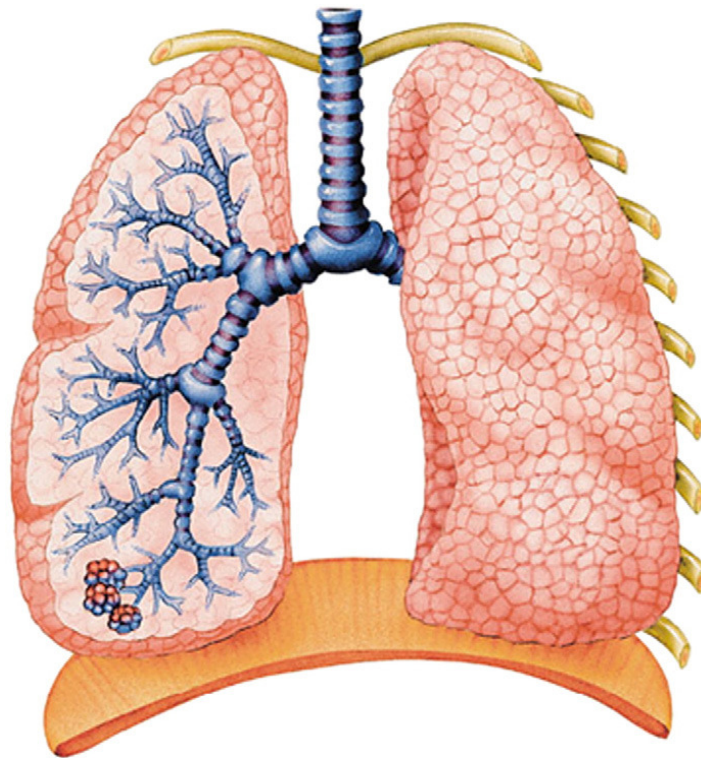


Figure 1: Schematic presentation of the lung showing conducting airways (blue) and alveolar gas exchange region (pink), adapted from [1].

The function of the conducting zone is to move air by bulk flow into and out of the lung during each breath. This zone consists of the first sixteen generations of airways and the air follows the way of the bronchi and bronchioles with low resistance. Generation zero represents the trachea, which bifurcates into the two main bronchi, which further subdivided into bronchi that enter respectively the left and right lung lobes. The intrapulmonary bronchi

continue to subdivide into progressively smaller diameter bronchi and bronchioles. The conducting zone ends with terminal bronchioles, which are devoid of alveoli (Fig.2).

		Generation	Diameter (cm)	Length (cm)	Number	Total cross-sectional area, cm ²
Conducting zone	Trachea	0	1.80	12.0	1	2.54
	Bronchi	1	1.22	4.8	2	2.33
		2	0.83	1.9	4	2.13
	Bronchioles	3	0.56	0.8	8	2.00
		4	0.45	1.3	16	2.48
	Terminal bronchioles	5	0.35	1.07	32	3.11
Respiratory zones		16	0.06	0.17	6×10^4	180.0
	Respiratory bronchioles	17	↓	↓	↓	↓
		18	↓	↓	↓	↓
		19	0.05	0.10	5×10^5	10^3
	Alveolar ducts	T ₃ 20	↓	↓	↓	↓
		T ₂ 21	↓	↓	↓	↓
	Alveolar sacs	T ₁ 22	↓	↓	↓	↓
		T 23	0.04	0.05	8×10^6	10^4

Figure 2: Scheme of airway branching in the human lung with the representative generation including in the upper and lower airways, containing their representative lung structures with their respective diameter (cm), length (cm), number, and total cross-sectional area (cm²), adapted from [2, 3].

Since the first 16 generations of airways contain no alveoli they are anatomically incapable of gas exchange with the venous blood and constitute the so-called anatomic dead space. The respiratory zone consists of all structures that participate in gas exchange and begins with respiratory bronchioles containing alveoli. These bronchioles subdivide into additional respiratory bronchioles eventually giving rise to alveolar ducts and finally to alveolar sacs. The acinus is defined as the unit comprised of a primary respiratory bronchiole, alveolar ducts, and alveolar sacs. The total cross-sectional area from trachea to terminal bronchioles (from 2.5 to 180 cm²) [4] provides optimal conditions for bulk flow of air through the large airways down to the terminal bronchioles. In the terminal airways that comprise the respiratory zone and acini, airways continue dichotomous branching, but diameters of

respiratory bronchioles and alveolar ducts change very little with each generation (from 0.06 to 0.024 cm). Thus, the total airway cross-sectional area nearly doubles with each generation beyond generation 16 (from 180 to 10 000 cm²). As a result of the enormous increase in surface area, bulk flow of air decreases rapidly within the respiratory zone until movement of air within alveoli occurs entirely by diffusion. The large area needed for molecular diffusion is provided by the respiratory zone, since 96 % of increase of the total cross-sectional area of airways occurs over the final 2.6 mm of the airway system and entirely within the respiratory zone.

The structure of the airways varies considerably depending on their location in the tracheobronchial tree. The trachea is a fibromuscular tube supported ventrolaterally by c-shaped cartilage and completed dorsally by smooth muscle. It provides the path of least resistance to airflow due to its large diameter. As the airways penetrate the lung parenchyma and continues dichotomous branching, cartilage continues to decrease in size and amount. Bronchioles are distinguished from bronchi by the lack of cartilage altogether, making them far less rigid and more distensible and collapsible than bronchi.

Pulmonary cell types

The conducting airways condition the inspired air and clear it from many environmental pollutants before reaching the respiratory zone. While this partly depends upon the branching pattern, the cells lining the airways play an important role.

In human four major cell types represent the surface epithelium and two main immunocompetent cell types are responsible for uptake and clearance of foreign materials like bacteria, pollutants or particles as well as communication to the cell environment:

i) Ciliated cells

Nearly half of the epithelial cells in the normal human airway are ciliated at all airway generations except for the respiratory units distal to the terminal bronchioles.

The surface of the ciliated cell is covered by cilia, about 200 per cell, each normally beating about 1000 times per minute with its effective stroke generally in the cranial direction and coordinated with those on adjacent cells. The cilia move the overlying mucus layer only with their tips up to the airways, away from the alveoli and toward the pharynx. Mucus that reaches the pharynx is usually swallowed or expectorated.

ii) Goblet cells

In the human trachea there are between six and seven thousand mucus secreting goblet cells/mm². In adults 30 to 40 % of the total cells in the larger airways are mucus cells. The basal cells are thought to be major stem cells from which ciliated mucus cells derived. Numbers and activity of goblet cells are induced by a variety of acute and chronic inflammatory stimuli.

iii) Clara cells

Clara cells are nonciliated bronchiolar cells and are restricted to the terminal bronchioles, where they represent around 20 % of the cell population. They produce a bronchiolar surfactant and have oxidative activity as well as being involved in the fluid absorption.

iv) Type I and type II epithelial cells

The alveolar surface is mostly covered by alveolar epithelium, made up of type I cells or pneumocytes. Type I pneumocytes cover 5000 mm² of the alveolar surface by each cell, and measure only 0.2 mm in length, and with a low volume density of subcellular organelles, and they are connected to each other. There are approximately 300 million alveoli in the lungs, with a combined surface area that is greater than 100 m², and with an alveolar epithelium as thin as 0.1 μm. Due to their thinness they prevent fluid loss, while facilitating rapid gas exchange, but make them extremely sensitive to injury. Type I pneumocytes are not capable of regeneration or reproduction in contrast to type II pneumocytes. Type II pneumocytes are smaller, more compact, and cuboidal with a high density of subcellular organelles and are twice as numerous as the type I cells, but cover only about 7 % of the surface area. Lamellar

bodies and surfactant-storing organelles characterized type II pneumocytes. They often occupy the corners of alveoli and their surface has abundant microvilli, and they are connected to each other by tight junction. Type II cells are metabolic active and responsible for both epithelial cell renewal and synthesis of surfactant, and acting as an ion and fluid pump to move fluid out of the air spaces. Its cuboidal shape facilitates rapid communication within the cells. In addition, there must be an extracellular signal following injury of type I cells that induces bordering type II cells to divide, hypertrophy, change their organelle composition, flatten out, and become new type I cells.

v) *Alveolar macrophages*

Alveolar macrophages are located at the interphase between air and lung tissue. They provided the first line of phagocytic defense against microbial invasion in the non-inflamed lower respiratory tract. Besides their phagocytic and mircobicidal functions, alveolar macrophages secrete numerous chemical mediators, mainly cytokines and chemokines, upon stimulation and playing an important role in inflammatory regulation in the lung.

vi) *Dendritic cells*

The lung is equipped with an elaborate network of dendritic cells (DCs) that can be found throughout the conducting airways, lung interstitium, lung vasculature, pleura, and bronchial lymph nodes. DCs perform a unique sentinel function in the pulmonary immune response in that they recognize inhaled antigens through expression of ancient pattern-recognition receptors such as Toll-like receptors, nucleotide-binding oligomerization domain (NOD)-like receptors, and C-type lectin receptors that will recognize motifs on virtually any inhaled pathogen, allergen, or substance. In addition, lung DCs express numerous receptors for inflammatory mediators that are released upon damage to tissue by pathogens, trauma, vascular damage, or necrosis. In summary, DCs bridge the innate and the adaptive immune system in humans.

1.2 Basic considerations for lung delivery

Pulmonary ventilation, lung function parameter

Alveolar ventilation is the exchange of gas between the alveoli and the external environment. In this process oxygen is brought into the lungs from the atmosphere and carbon dioxide carried into the lungs in the mixed venous blood is expelled from the body. Thus, alveolar ventilation is normally defined as the volume of gas per unit time that reaches the alveoli.

The volume of air inspired or expired during a normal breath (tidal volume; V_t) of a 70 kg adult is about 500 ml per breath. The vital capacity (VC) is the volume of air that can be expired from the lungs after maximal inspiration (about 4.5 l in a healthy 70 kg adult). The residual volume (RV) is the volume of gas left in the lungs after maximal forced expiration. It is determined by the force generated by the muscles of expiration and the inward elastic recoil of the lungs as they oppose the outward elastic recoil of the chest wall. The total volume of air that a person breathes each minute is measured by the expired volume of air for each breath (represents V_t) and the number of breaths over a fixed period of time. To determine alveolar ventilation, the amount of air present in the conducting zone of the airways (where gas exchange does not occur) has to be subtracted out of this calculation. This volume is known as anatomic dead space (V_d) and is approximately 150 ml in the adult male. Thus, alveolar ventilation is defined as: ***Alveolar ventilation = $(V_t - V_d) * \text{respiratory rate}$*** , where V_t represents the tidal volume and V_d the dead volume.

However, both tidal volume and respiratory rate vary enormously according to age and clinical status and should be kept in mind for drug delivery scenario. In addition, there are regional differences in ventilation due to topographical reasons, alteration in lung distensibility or airway resistance. Figure 3 shows the different lung capacities and volumes described above:

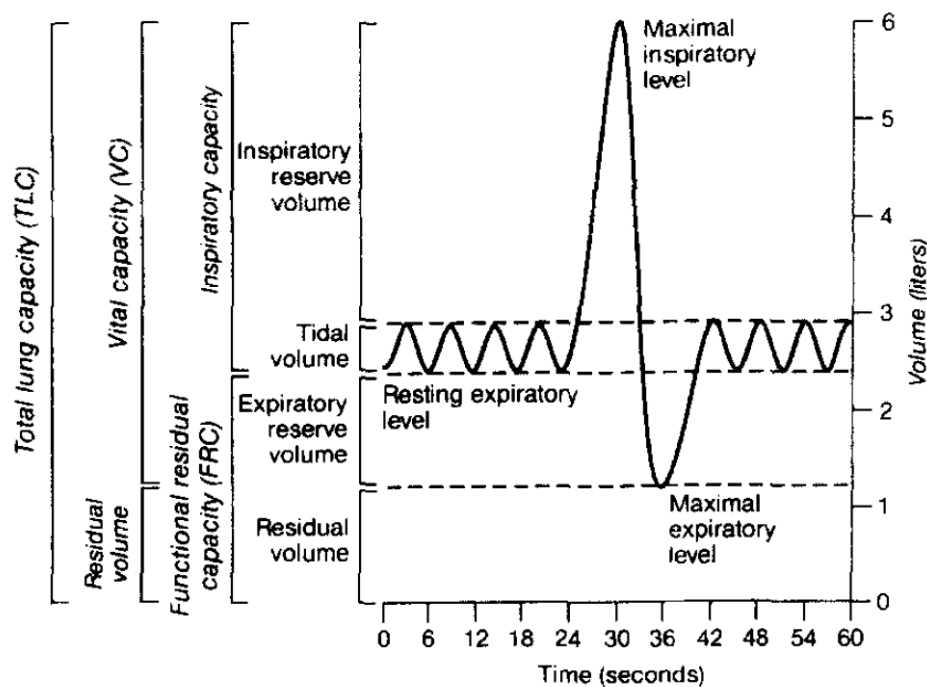


Figure 3: Capacities and volumes of the human lung, representing one breath showing the maximal inspiratory level and the maximal respiratory level with the resting expiratory level. Total lung capacity (TLC), vital capacity (VC), respiratory capacity, functional residual capacity (FRC), residual volume, expiratory reserve volume, are additionally presented, adapted from [2, 5].

Pulmonary administration, deposition modelling

When using the inhalation route for local and systemic drug delivery an efficient and reproducible lung deposition of inhaled aerosol particles is essential. Once deposited, particles encounter a variety of physiochemical and biological barriers. These include mucus barriers and catabolic enzymes in the tracheobronchial region, and macrophages in the alveolar region.

With the approval of inhaled insulin in 2006 an important milestone was achieved and more biotherapeutics will be tested for pulmonary administration. However, most pulmonary drug delivery technologies work with an efficiency of less than 20 % and lung dose might change from patient to patient by more than 100 %. Thus, the technology used for pulmonary drug delivery is quite important and must be suitable for patients to perform an efficient and reproducible delivery to the lungs.

The most important biophysical parameters determining regional drug deposition in human lungs are:

- i) aerodynamic particle behaviour
- ii) breathing pattern of particles
- iii) time of aerosol injection into the breathing cycle
- iv) airway anatomy and morphology of the patient

The aerodynamic particle diameter (d_{ae}) is defined as the diameter of a sphere with a density of 1 g/cm³ that has the same aerodynamic behaviour as the particle which will be characterized:

$$d_{ae} = \sqrt{(\rho/\rho_a * d_g)}$$

where ρ is the mass density of the particle, ρ_a the unit density (1 g/cm³) and d_g is the geometric diameter. The d_{ae} is mainly depending on the diffusion of the particle and the equation follows the Stoke-Einstein relationship: $D = k * T / 6 \pi \eta r$, where D is diffusion coefficient, k is the Boltzmann constant, T is temperature, η is viscosity, and r is aerodynamic radius. Thus, particles with different density and shape could be distinguished using their aerodynamic properties.

The most relevant mechanisms for therapeutic aerosols in the airways are:

- i) **Diffusion by Brownian motion** ($d_{ae} < 0.5 \mu\text{m}$)

Particle deposition by diffusion is based on Brownian motion. An aerosol particle, which is suspended in gas is moved by collisions with gas molecules. This leads to an irregular and unoriented movement of particles that causes contact with an airway wall. The probability that a particle is deposited on an airway wall by Brownian motion is dependent on the size of the particle and the residence time of the particle in the respiratory tract. Thus, the deposition by diffusion is defined as: $DE_{diff} \sim t/d_{ae}$, where DE_{diff} is deposition by diffusion, t represents the residence time in the respiratory tract and d_{ae} is the aerodynamic diameter of the particle. Deposition by diffusion is only relevant for aerosol particles with an aerodynamic diameter below 0.5 μm . Conventional drugs usually obtain diameters between 1-10 μm . Therefore, this

mechanism has no significant influence on drug deposition within the lung. But for nanoparticles less than 500 nm diffusion by Brownian motion could be important for deposition of such nanoparticles into the lungs (Fig. 4).

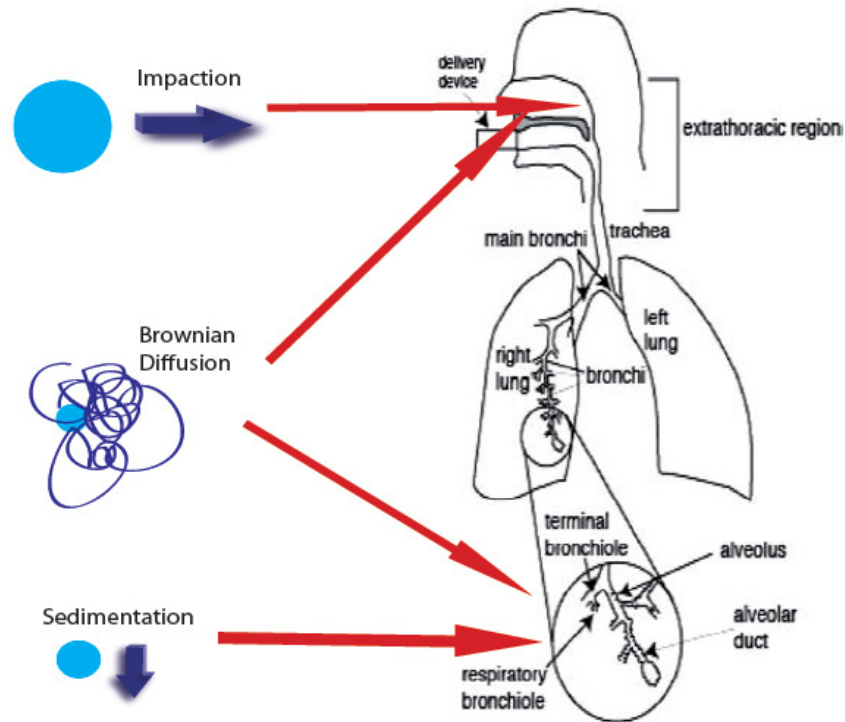


Figure 4: Deposition mechanism of inhaled particles in the lungs are presented, adapted and modified from [6, 7]. The deposition of particles mainly depends on the aerodynamic diameter of the particles. To reach the upper airways particles with diameters of 3-5 μm are appropriated (impaction), whereas smaller particles with diameter between 0.5-3 μm are deposited in the lower airways by sedimentation. Diffusion occurs when particle size is smaller than 0.5 μm and particles are either exhaled or deposit in the lower airways depending on the rate of inspiration and expiration.

ii) **Sedimentation by gravitational force** ($d_{ae} > 0.5 \mu\text{m}$)

Deposition by sedimentation is caused by the gravity of the earth. By this gravitational force an aerosol particle will be accelerated so long until the counterpoise caused by the resistance of the air equals the gravitational force. At this point the particle will deposit with a constant settling velocity. Deposition by sedimentation is described as: $DE_{sed} \sim d_{ae}^2 * t$, where DE_{sed} represents deposition by sedimentation, d_{ae} is the aerodynamic diameter, and t is the residence time in the respiratory tract. Particles with diameters $< 1 \mu\text{m}$ have only negligible

sedimentation velocity. With increasing particle size, the settling velocity is so large that within the time of a breath the particle will reach an airway wall.

iii) **Impaction** ($d_{ae} > 3 \mu\text{m}$)

Impaction is caused by the inertia of aerosol particles. Larger particles with a diameter above $3 \mu\text{m}$ are too inert and tend to fly straight ahead. This mechanism leads to particle deposition in the extrathoracic airways, but also on bifurcations at the intrathoracic airways. Deposition by impaction is defined as: $DE_{im} \sim d_{ae}^2 * V$, where DE_{im} is deposition by impaction, d_{ae} represents the aerodynamic diameter and V is the settling velocity of the particle. Particle deposition by impaction is the main cause that prevents aerosol particles from entering into the lungs.

The upper human airways have anatomical structures acting as efficient filters for inhaled natural pollutants. Fast inhalation leads to enhanced deposition by impaction at the larynx and in the nose and prevents particle penetration into the lungs. This extrathoracic deposition efficiency has a high inter-subject variability because of biological and anatomical differences of mouth and throat. This variability can be reduced, when inhaling very slowly and/ or using smaller particles ($1-3 \mu\text{m}$), which leads to a small impaction parameter and results in minimal extrathoracic deposition. It has to be noted that particle size should be not too small because these particles are exhaled and tend to aggregated very fast. Particles with aerodynamic diameter of 1 to $3 \mu\text{m}$ have shown to deposit optimally in the alveolar region of the lungs [8, 9] (Fig. 5).

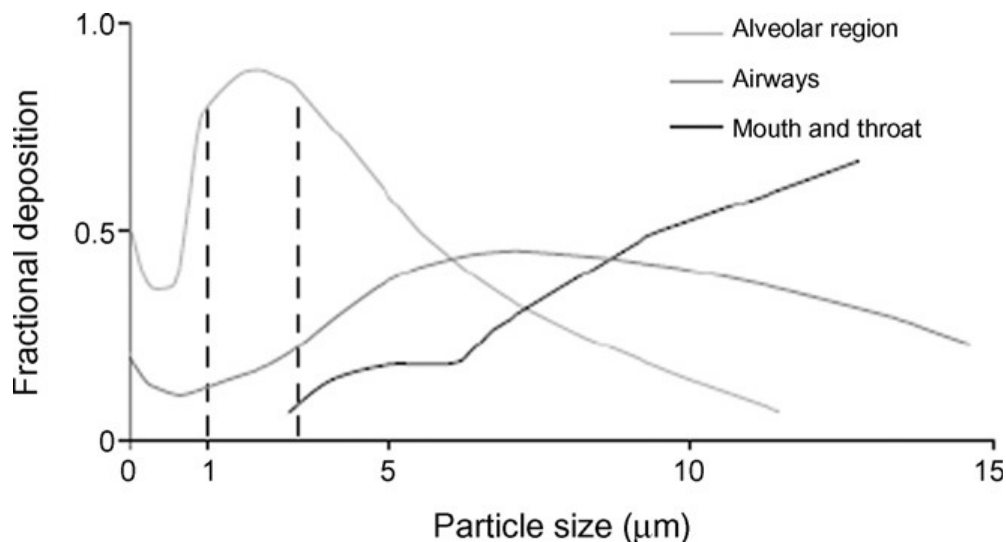


Figure 5: Effect of particle size on the deposition of aerosol particles in the human respiratory tract following a slow inhalation and a five seconds breath hold, adapted from [10]. Light grey line shows the deposition of particles in the alveolar region, dark grey line represents the deposition in the airways, and the black line presents the deposition in mouth and trachea, depending on the particle diameter (μm).

For particles $> 1 \mu\text{m}$ deposition occurs by sedimentation or impaction and these mechanisms are responsible for the site of deposition within the respiratory system and is normally called regional deposition. Some mathematical models described the determination of the deposition in different regions in the respiratory system and allow the estimation of regional deposition of inhaled aerosol particles.

Under normal breathing conditions the lungs usually contain only about half the volume of air they can hold. The airways contain only four percent of the lung air, the alveoli the rest. Depending on the breathing pattern regional deposition is changed dramatically in addition to the influence of the particle size. Thus, for pulmonary application not only an efficient therapeutic substance but also an efficient delivery system to transport the drug to its intended target in the lung is needed. Aerodynamic particle behaviour, breathing pattern and lung morphology have to be considered.

1.3 Cellular Transport mechanisms

Intracellular membrane traffic guided cellular processes, which are trafficked lipids, proteins, receptor ligands and soluble molecules to distinct compartments within the cell. Compartmentalization is maintained through the organization of the cytoplasm into multiple intracellular structures that have their own distinct identity and function. Individual compartments are continually in flux and proteins and lipids are continually moving between compartments and the balance of traffic between them defines the steady-state localization. Macromolecular therapeutics and nanosized delivery systems are all candidates for cellular uptake by the mechanism of endocytosis [11]. Modern drug delivery design is characterized by the delivery of drugs to a specific cellular target. The target site of action may be exclusively within the inside of a range of organelles or the agent may require escape from endosomes or lysosomes prior to reaching its target. In most cases, it is also important that the drug is not exported from the cell following its entry into recycling or secretion pathways. The plasma membrane and downstream organelles therefore pose major barriers to effective drug delivery. Endocytosis describes multiple methods of internalisation that can be classified into two broad categories: i) phagocytosis (“cell eating - the uptake of large particles”) and ii) pinocytosis (“cell drinking – the uptake of fluid and solutes”) [12]. Phagocytosis is normally restricted to specialized cells, including macrophages, monocytes, and neutrophils. This mechanism is mainly responsible for clearance of pathogens such as bacteria and yeast, and large debris of cells. In contrast to that, pinocytosis occurs in all cell types and is currently subdivided into i) clathrin-mediated endocytosis, ii) macropinocytosis, iii) internalisation via caveoli, and iv) clathrin-and caveoli-independent endocytosis [12, 13] (Fig 6). Many agents that are delivered to cells will also be delivered to compartments outside of the classical endocytotic pathway.

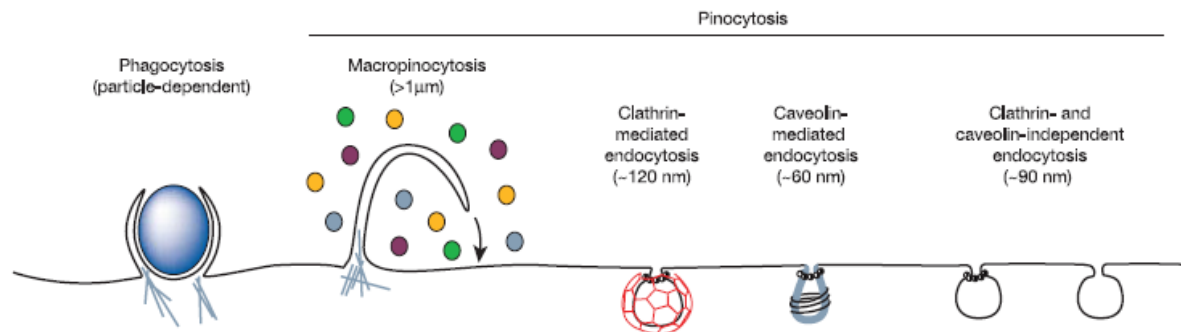


Figure 6: *Endocytotic pathways into the mammalian cell adapted from [12]. Phagocytosis is characterized by particle uptake by specialized cells like macrophages, monocytes, or neutrophils and represents the first way of defense against foreign material. Pinocytosis occurs in all cell types and is divided in four main subdivisions (i) macropinocytosis, (ii) clathrin-dependent, (iii) caveolin-dependent, and (iv) clathrin-/caveolin-independent endocytotic pathway. Macropinocytosis (i) is represented by uptake of soluble particles with diameter above 300nm. Clathrin-mediated endocytosis (ii) allows the internalisation of proteins and other molecules into the cell by using specific receptors expressed on the cell surface, and represents the preferred pathway for microspheres up to 200 nm in size. Caveolin-mediated endocytosis (iii) is characterized by uptake via caveolae, small (50-80nm) invagination of the plasma membrane. The clathrin- and caveolin-independent pinocytosis (iv) used other cholesterol-rich microdomains on the plasma membrane than caveolae and clathrin, which are smaller in diameter and mainly located in the brain in neurons and neuroendocrine cells.*

Macropinocytosis is a nonselective endocytotic pathway for internalization of suspended macromolecules and the internalized vesicles or macropinosomes can have sizes up to 5 μm [14]. During macropinocytosis, membrane protrusions, often called ruffles, are formed which can subsequently fuse with each other or with the plasma membrane to enclose large volumes. Clathrin-mediated endocytosis allows the internalisation of proteins and other molecules into the cell through the use of specific receptors expressed on the cell surface, e.g. ligand-activated receptors such as the epidermal growth factor (EGF) receptor, transferrin receptor, or low-density lipoprotein receptor. Clathrin-dependent endocytosis is said to be the preferred pathway for microspheres up to 200 nm in size [15], macropinocytosis is essential in the internalization of particles larger than 300 nm in diameter, and represent the first line of

defense against foreign material and removal of damaged host cells. Noncoated vesicle (non-clathrin/caveoli coated) formation (i.e. clathrin independent endocytosis) also contributes to internalization from the cell membrane. Although the details of this pathway have not been completely elucidated, it is currently subclassified based on the role of dynamin and several small GTPases [16]. These include uptake from lipid rafts in caveolae or via a flotillin-dependent pathway, from which the caveolae-mediated endocytosis is probably the best characterized pathway. Caveolae are small (50 - 80 nm), smooth, flask-shaped invaginations of the plasma membrane that are characterized by the presence of caveolin-1. Certain pathogens like SV40 virus and cholera toxin subunit B specifically use this pathway to enter cells. However, a significant fraction of cholera toxin subunit B is also taken up on clathrin-coated vesicles.

A number of endocytotic pathways have been demonstrated to be involved in the uptake of DNA complexes [17], and this is highly dependent on cell type, the nature of the gene carrier, and the particle size [18]. This variability stresses the necessity of studying the internalization of each of the different types of non-viral gene carriers in an appropriate cell line model. A quantification of the contribution for each endocytotic pathway to the overall cellular uptake is essential for elucidating the corresponding intracellular pharmacokinetic models.

For uptake of cationic complexes (cationic polymers with plasmid DNA) syndecans are proposed to be the main receptors involved in adherent cells, illustrated in Fig.7, adapted from [19]. Syndecans are ubiquitous transmembrane adhesion molecules. Their polyanionic heparin sulphate moieties are bound at the distal end of their ectodomain, thus facilitating extracellular matrix binding, but also interaction with large cationic particles. PEI takes advantage of the extracellular matrix catabolism by adherent cells. After initial binding of PEI-nucleic acid complexes to their receptor, gradual electrostatic zippering of the plasma membrane around the particle is sustained by lateral diffusion of many syndecan molecules that cluster into cholesterol-rich rafts. Clustering, in turn, triggers protein kinase C (PKC)

activation and linker protein-mediated actin binding to the cytoplasmic tail of syndecan. Resulting tension fibers and a growing network of cortical actin can then pull the particle into the cell [20].

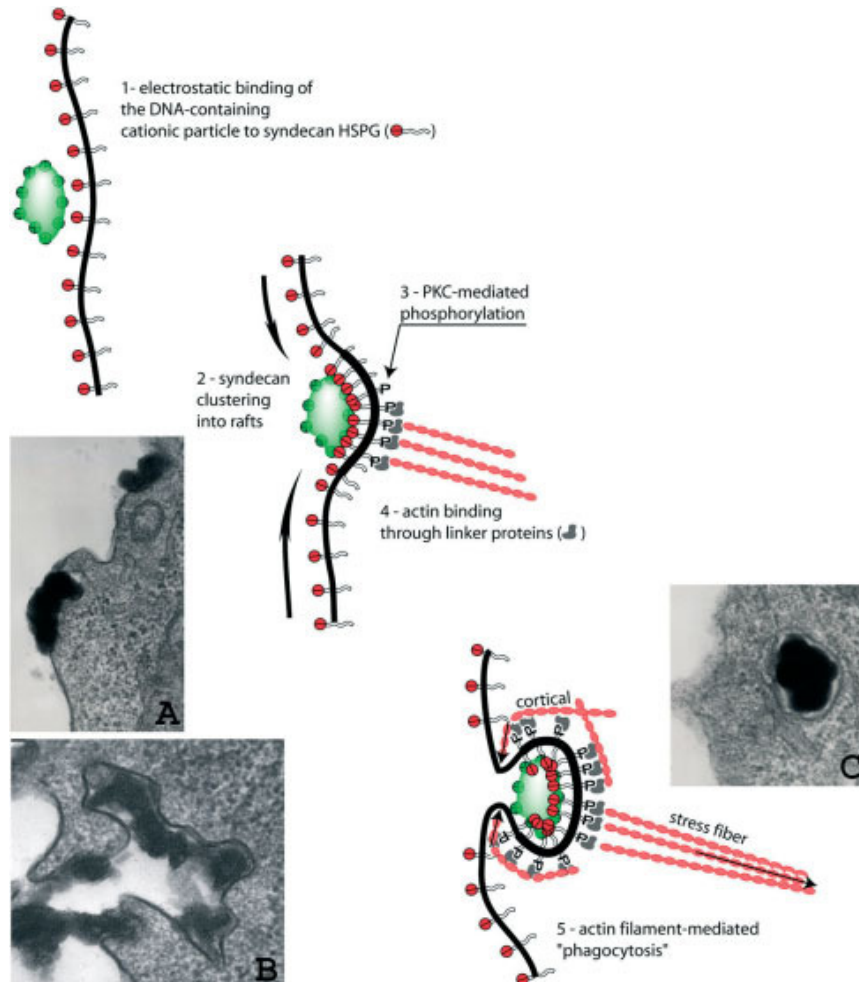


Figure 7: A model for the uptake of cationic complexes by adherent cells, suggested from Kopatz et al. [19]. The hypothesized mechanism for the entry of cationic complexes into adherent cells in culture was divided in five steps: 1) Electrostatic binding of the cationic particle to syndecans (transmembrane heparan sulphate proteoglycans (HSPGs)), 2) Particle-induced syndecan clustering into cholesterol-rich rafts, 3) protein kinase C (PKC) mediated phosphorylation, 4) actin binding through linker proteins, 5) actin-mediated engulfment of the particle.

1.4 Barriers for pulmonary administration

In the lungs the major barriers for efficient local non-viral based gene delivery are the mucus layer secreted by goblet cells, the apical membrane glycol-conjugates, and the airway epithelium with tight junctions inhibiting the intracellular transport. Surfactant produced by type II pneumocytes may facilitate nucleic acid delivery due to increased complex stability and condensation [21-24]. In many airway diseases mucus viscosity and airway microenvironment are extremely altered and may enhance the barrier to airway gene transfer to the lungs [23, 25-27]. Normal airway mucus lines the epithelial surface and provides an important innate immune function by detoxifying noxious molecules and by trapping and removing pathogens and particulates from the airway via mucociliary clearance. The major macromolecular constituents of normal mucus, the mucin glycoproteins, are large, heavily glycosylated proteins with a defining feature of tandemly repeating sequences of amino acids rich in serine and threonine, the linkage sites for large carbohydrate structures. For normal function, mucus must be cleared by ciliary motion and this process requires a balance between the volume and composition of the mucus, adequate periciliary liquid volume, and normal ciliary beat frequency. Normal mucus has been found to inhibit gene delivery [28], but also sputum and broncho-alveolar fluid recovered from cystic fibrosis (CF) patients were shown to inhibit PEI-mediated gene transfer efficiency [29]. In addition, the role of bacteria infection in gene transfer specially the massive colonization of CF airways by *Pseudomonas aeruginosa* and other bacteria modified the microenvironment in the airways and has to be taken into account when non-viral vector systems are investigated. For example, it was described that mice infected with *P.aeruginosa* showed a 5-fold increase in gene transfer whereas infection with *E.coli* did not show any implementation on gene transfer [30].

Surfactant produced by type II cells reduces surface tension in the lung and prevent the alveoli from collapsing. The amount of surfactant required by the lung is a function of tidal volume/functional residual capacity ratio (V_t / FRC), the radius of curvature of the alveoli, and

the compliance of the chest wall. The lower the ratio V_t to FRC, the less surfactant needed. According to LaPlace's law the greater the radius of the curvature of the lung, the less surfactant is required to prevent collapse. Interaction with surfactant proteins did not affect PEI-mediated gene transfer [21, 24, 31].

1.5 Non viral vector systems for pulmonary siRNA application

RNA interference (RNAi) based therapeutics represent a fundamentally new way to treat human disease by addressing targets that are otherwise “undruggable” with existing medicines [32, 33]. The nobel-prize winning discovery of RNAi in the worm *Caenorhabditis elegans* in 1998 [34], and the subsequent demonstration that RNAi operates in mammalian cells revolutionized the current understanding of endogenous mechanisms of gene regulation and provided powerful new tools for biological research and drug discovery. RNAi pathways are guided by small RNAs that include small interfering RNAs (siRNAs) and mirco RNAs (miRNAs) with the latter deriving from imperfectly paired non-coding hairpin RNA structures that are naturally transcribed by the genome. Gene silencing can be induced by siRNA through sequence-specific cleavage of perfectly complementary messenger RNA (mRNA), whereas miRNAs mediate translational repression and transcript degradation for imperfectly complementary targets (Fig.8).

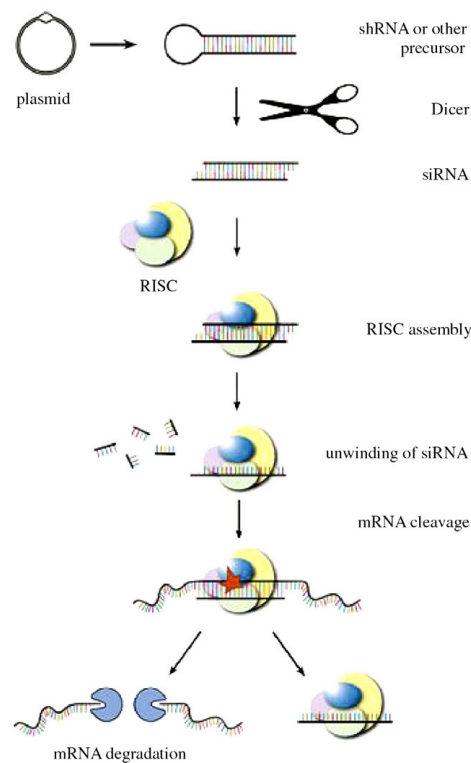


Figure 8: RNAi machinery adapted from [35]. Short hairpin RNAs (shRNAs) expressed from plasmid or delivered intracellularly are processed into 21-23 base pair siRNA fragments by enzyme Dicer. A multiprotein complex called RISC (RNA Induced Silencing Complex) assembles with the

siRNA, retaining the guide strand and discarding the passenger strand. The siRNA then guides RISC to complementary mRNA molecules in the cytosol and through Watson-Crick base pairing selectively binds and cleaves the mRNA in the region of homology. The mRNA is then degraded by the endonuclease region of the RISC complex, thus translation into protein cannot occur.

The goal of RNAi-based therapy represents the activation of selective mRNA cleavage for efficient gene silencing. There are two possibilities to harness the endogenous pathway: either i) by using viral vector to express short hairpin RNA (shRNA) that resembles miRNA precursors, or (ii) by introducing siRNAs that mimic Dicer cleavage product into the cytoplasm. Synthetic siRNAs utilize the naturally occurring RNAi pathway in a manner that is consistent and predictable, thus making them particularly attractive as therapeutics. Since they enter RNAi pathway later, siRNAs are less likely to interfere with gene regulation by endogenous miRNAs [36, 37]. The most important characteristics for effective design and selection of siRNAs are potency, specificity, and nuclease stability. Two types of off-target effects need to be avoided or minimized: i) silencing of genes sharing partial homology to the siRNA and ii) immune stimulation induced by recognition of certain siRNAs by the innate immune system. The activation of the innate immune systems by siRNA could be induced by recognition of dsRNAs by the serine/threonine protein kinase receptor (PKR) [38]. This pathway is normally triggered by dsRNAs that are more than 30 nucleotides long, but at higher concentrations also siRNAs may be able to activate this pathway resulting in global translational blockade and cell death. The potential to activate toll-like receptors (TLRs) in the endosomal pathway is more likely to occur after siRNA delivery due to recognition of specific nucleotide sequence motifs (e.g. GU) by TLRs. TLR activation could trigger the production of type I interferons and pro-inflammatory cytokines, and induce nuclear factor kappa B (NF- κ B) activation [39, 40]. For example, the presence of 2'-O-methyl modifications within the siRNA duplex could abrogate the binding to TLR7 in endosomes and abolish immunostimulatory response. In addition, these modifications also reduce sequence-dependent off-target silencing and may be particularly beneficial in enhancing siRNA target

specificity [41-43]. Due to increasing mortality and morbidity caused by several lung diseases, RNAi strategies have attracted particular attention and the lung as target organ provides an attractive tool because of the accessibility via non-invasive routes, e.g. nasal or pulmonary applications. The clinical success of siRNA-mediated interventions critically depends upon the safety and efficacy of the delivery methods and agents. Naked siRNAs are degraded in human plasma with a half-life of minutes [44, 45]. Thus, the search for optimized nanocarriers to deliver siRNA is still under intensive investigation. The negative charge and chemical degradability of siRNA under physiologically relevant conditions make its delivery a major challenge [35]. Depending on their origin, two types of positively charged carriers could be distinguished: i) lipid-based and ii) polymeric-based carrier systems. Both systems provided several advantages to deliver siRNA. Liposome formation agents like Lipofectamine 2000 [46, 47] and cardiolipin analogues [48, 49] have been successfully used for the delivery of siRNA. Negatively charged nucleic acids and positively charged lipids spontaneously form nanoparticles, known as lipoplexes, of 50-200 nm in diameter [50]. Interaction with serum components represents one of the major hurdles that influence the performance when used systemically [27]. Recently, lipid-mediated delivery of siRNA against apolipoprotein B (ApoB) has been used to target ApoB mRNA to the liver [51, 52]. The *in vivo* use of cationic lipids especially by *i.v.* administration presents significant problems as these reagents can be quite toxic. Despite problems with *i.v.* use, cationic lipids are employed for *i.p.* injection [53-55], for CNS injection [56, 57] or in topical epithelial surface application [58, 59] and intratracheal [60]. Toxicity varies with the precise chemical composition of the lipids employed, dose, and the delivering route. Variations in chemical composition can have a large impact on the functional properties of cationic lipid mixtures [61], and lipoplex/liposomal preparations have been devised with decreased toxicity that are more compatible with *i.v.* administration. Liposomes can be modified with ligands such as folate or small peptides, which assist with delivery and help target specific cell types or tissues [62, 63]. Through the

use of neutral polyethylene glycol-substituted surfaces and other approaches, liposomes can be stabilized and made more “stealthy” showing reduced clearance and improved pharmacokinetics [64, 65]. These kinds of lipid nanoparticles have been successfully used to deliver antisense oligonucleotides and siRNAs in vivo [48, 49, 66].

Similar to the lipid-based non viral vector systems, the positive charges of polycations allow an efficient interaction with siRNAs to form so-called polyplexes, which can bind onto cell plasma membrane and be endocytosed. In contrast to the lipid-based systems that rely on the fusogenic property of the liposomes to mediate endosomal escape, polymeric carriers such as poly(ethylene imine) (PEI) use the so-called “proton-sponge” effect to enhance endosomal release of endocytosed polyplexes [20, 67-70] (Fig.9).

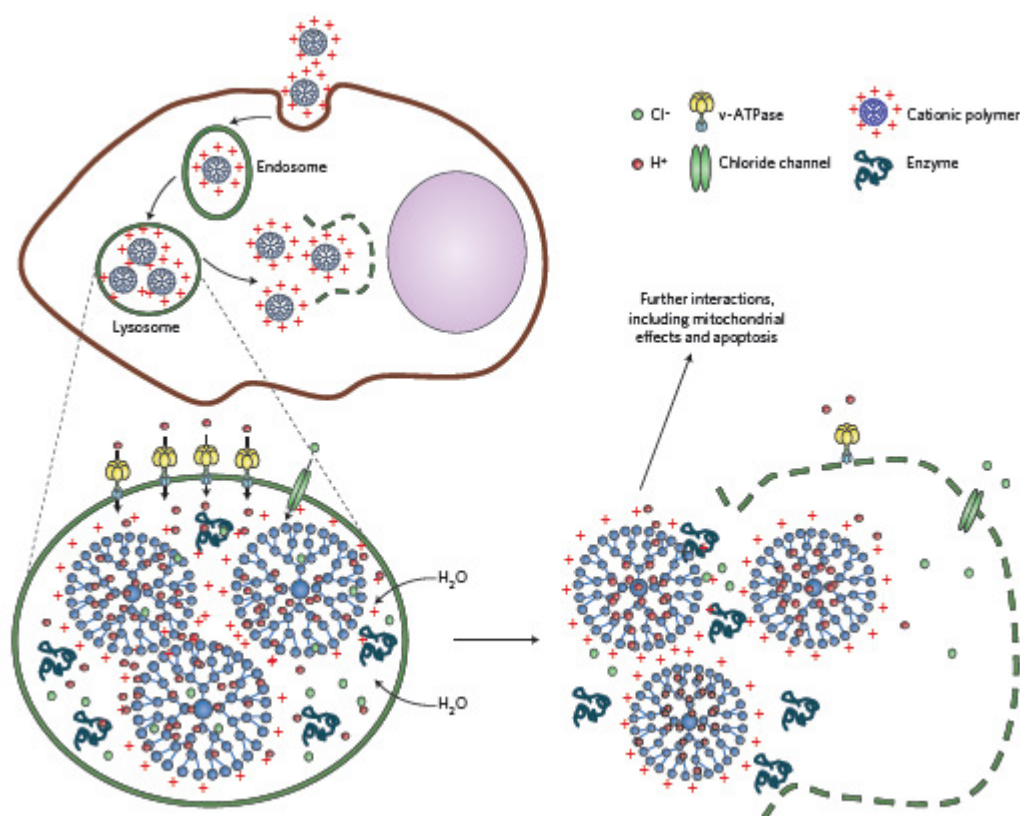


Figure 9: Proton sponge mechanism adapted from [69]. Cationic polymers bind to negatively charged nucleic acids and forms so-called polyplexes with positive surface charge. Polyplexes binds with high affinity to negatively charged lipid groups on the plasma membrane and are endocytosed in the tight fitting vesicles (endosome). Once entered into an acidifying lysosomal compartment, the unsaturated amino groups are capable of sequestering protons that are supplied by the ATP-ase (proton pump). This process keeps the pump functioning and leads to the retention of one chloride ion

(Cl⁻) and one water molecule (H₂O) per proton. Subsequent lysosomal swelling and rupture leads to deposition of nucleic acid and polymer in the cytoplasm and the spillage of the lysosomal content. Due to the high buffering capacity in the lysosome positively charged polymers the mechanism is called proton sponge.

According to this mechanism, the deprotonated amines with different pK_a values confer a buffer effect over a wide range of pH. This buffering may protect the siRNA from degradation in the endosomal compartment during maturation of the early endosomes to late endosomes and their subsequent fusion with the lysosomes. The buffering property also allows the polyplex to escape from the endosome. At lower pH the buffering capacity causes an influx of chloride ions and water into the endosomes, which burst due to osmotic pressure and facilitating intracellular release of PEI - siRNA polyplexes. PEI has been used for many years to facilitate nucleic acid delivery [20, 68]. However, due to toxicity and variable performance it has not found generalized acceptance as a delivery tool for either antisense oligonucleotides or siRNAs. Nevertheless, PEI can be used as a prototype for formulation of more complex particles with improved properties [71]. For example, a PEGylated PEI particle with a vasculature-targeting RDG peptide has been shown to deliver siRNAs successfully in a mouse xenograft tumor model [72]. Deacylation of PEI reduces toxicity and improves pulmonary delivery of siRNAs in mice [73] and folate-modified PEGylated PEI is being tested for siRNA delivery in tumor cells [74]. Although a large number of studies have reported successful in vivo delivery of nucleic acids using liposome or polyplex reagents, issues of toxicity persist and must be addressed. Much of the toxicity of cationic lipids relates to electrostatic effects, and precise complexation ratios of the positively charged reagent with the negatively charged cargo nucleic acid are important. Interaction with negatively charged serum proteins can inactivate the complex [75], and particle aggregation with clumping in capillary beds can be problematic; interaction with complement proteins can

lead to inflammation. When loaded with a nucleic acid cargo, cationic reagent can trigger the release of a variety of cytokines (see discussion of TLR activation above).

Synthetic polymers and nanomaterials display selective phenotypic effects in cells and in the body that affect signal transduction mechanisms involved in inflammation, differentiation, proliferation, and apoptosis. When physically mixed or covalently conjugated with cytotoxic agents, bacterial DNA or antigens, polymers can drastically alter specific genetically controlled responses to these agents [76]. These effects, in part, result from cooperative interactions of polymers and nanomaterials with plasma cell membranes and trafficking of polymers and nanomaterials to intracellular organelles. Cells and whole organism responses to these materials can be phenotype or genotype dependent. In selected cases, polymer agents can bypass limitations to biological responses imposed by the genotype, for example, phenotypic correction of immune response by polyelectrolytes. Overall, these effects are relatively benign as they do not result in cytotoxicity or major toxicities in the body. Collectively, however, these studies support the need for thoroughly assessing pharmacogenomic effects of polymer materials to maximize clinical outcomes and understand the pharmacological and toxicological effects of polymer formulations of biological agents, i.e. polymer genomics. In addition, it is well described in the literature that cationic nanoparticles disrupt lipid bilayers [77, 78], induce oxidative stress inside the cell as a result of cell-type interplay and cause in some cases acute lung inflammation when administered intratracheally [79, 80]. Intensive efforts have to be focus on the issue of cytotoxicity to obtain more insight in the exact mechanisms behind, which are multidimensional and largely depend on the application route as well as the formulation that is delivered. Therefore, toxicity profiles are still needed and represent a great implement in improving non-viral delivery systems.

1.6 Aspects of Nanotoxicology in Nanomedicine

Nanotechnology has the potential to revolutionize medicine, and has already presented new regulatory challenges. This technology represents a manipulation of matter near atomic-size scale (1 - 100 nm) to engineer new structures, materials, and devices. Considering the rapid growth of nanotechnology and the variety of nanomaterials potentially used in the future, identifying, quantifying and managing potential health risks is essential, especially in the respiratory tract that may serve as the portal of entry for inhaled nanoparticles and nanofibers. [81]. Nanoparticle behaviour and toxicity in the lungs and translocation from the lungs has been investigated over decades in the environmental health field with a focus on (ambient) ultrafine particles (UFP). UFP are defined as particles with an aerodynamic diameter below 100 nm [82]. Their small size distinguishes them from larger coarse (aerodynamic diameter < 10 μm , PM₁₀) and fine (aerodynamic diameter < 2.5 μm , PM_{2.5}) air pollution particles. Epidemiological studies have shown that a sudden surge in the level of particulate matter (PM) can be linked to increased cardio-respiratory morbidity and mortality including asthma, chronic obstructive pulmonary disease (COPD) and arteriosclerosis [83, 84]. The small size and the huge surface area of UFPs might be the main factors contributing to their toxicity and adverse side-effects in humans. UFPs are taken up by lung cells and are able to cross the epithelial barrier to enter the blood and lymph stream by transcytosis and getting distributed to the body. The large surface area per mass of nanoparticles causes them to be more biologically active, thus initiated inflammatory and oxidative stress responses. Physicochemical particle properties such as size, surface charge and hydrophilicity define the fate of particles in vivo. Because synthetic nanomaterials often occur in size ranges similar to ultrafine airborne particles that are considered to be a major factor contributing to adverse health effects of air pollution, information on the biological reactivity of these particulates is also necessary to allow their safety evaluation. One important note is that these environmental toxicological studies focus on insoluble materials, such as carbon or titanium dioxide,

whereas therapeutic nanoparticulate systems are composed of materials that will eventually degrade into biocompatible components. Thus, depending on the speed of degradation, biodegradable nanoparticles may be anticipated to elicit toxicological responses quite different from non-biodegradable materials. Therefore, further investigations of the health ramifications of medical nanoparticles as a function of their physicochemical characteristics are still needed [81]. As exposure to PM from vehicle exhaust, combustion, road dust and windblown soil has been associated with increases in respiratory and cardiovascular morbidity and mortality biomarkers of inflammation and oxidative stress should be provided to predict and assess the risk of particulate therapeutic systems. Nel and colleagues have introduced a hierarchical oxidative stress model as a predictive toxicological tool for assessment of nanomaterial hazards [85]. They defined the predictive toxicological approach as establishing and using mechanisms and pathways of injury at a cellular and molecular level to prioritize screening for adverse biological effects and health outcomes *in vivo* [86]. Experimental evidence exists about the hazard that nanomaterials cause and a lot of studies dealt with the possible toxicological mechanisms and pathways behind each nanomaterial [83, 86-95]. Currently, there is considerable debate about the right nanomaterial toxicity testing with regard to correct toxicological screening endpoints for the correct balance of *in vitro* and *in vivo* testing, the cost of the effort and who should be responsible for screening and safety assessment of nanomaterials [96, 97]. The hierarchical oxidative stress paradigm postulates that oxidative stress leads to incremental cellular responses that can be classified as antioxidant defense (tier1), pro-inflammatory effects (tier2) and cytotoxicity (tier3) (Fig 10).

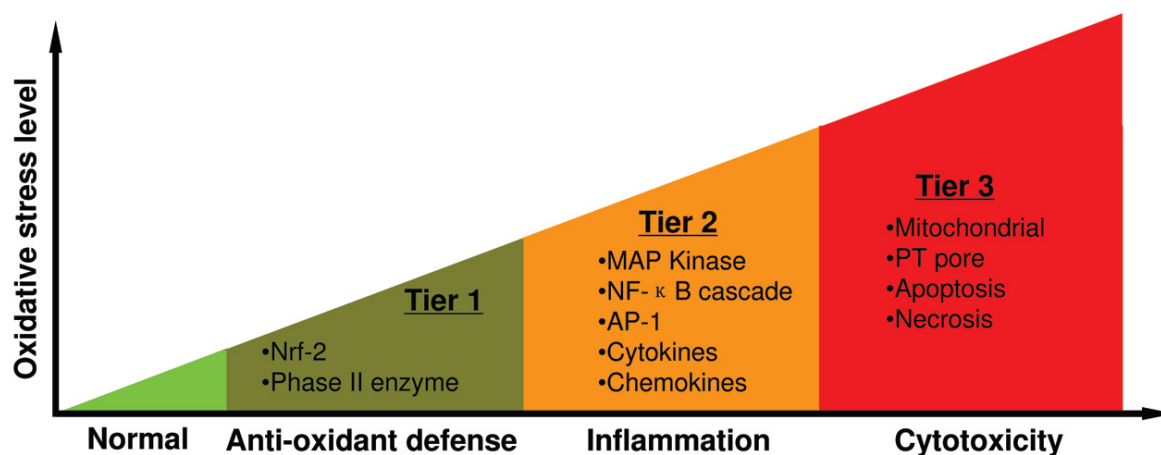


Figure 10: Hierarchical oxidative stress model adapted from [86] – an example of a predictive paradigm. At a lower amount of oxidative stress (tier 1), phase II antioxidative enzymes are induced via transcriptional activation of the antioxidant response element by Nrf-2 to restore cellular redox homeostasis. At an intermediate amount of oxidative stress (tier2), activation of MAPK and Nf-kB cascades induces pro-inflammatory responses. At a high amount of oxidative stress (tier 3), perturbation of the mitochondrial PT pore and disruption of electron transfer results in apoptosis or necrosis.

Each of these response tiers are initiated by specific biological sensors and activation mechanisms. In Tier 1, the transcription factor Nrf-2 is activated to enhance the expression of phase II enzymes, which attempt to restore redox equilibrium. If the level of oxidant injury increases (Tier 2), cells express pro-inflammatory cytokines by activating signalling pathways such as the mitogen-activated protein kinase (MAPK) and nuclear factor-kappa B (Nf-kB) cascades. At the highest level of oxidative stress (Tier 3), interference in mitochondrial inner membrane electron transfer or changing open/closed status of permeability transition pore could lead to effects on ATP synthesis and release of pro-apoptotic factors.

Application of nanotechnology to medical problems – nanomedicine – offers a wide range of therapeutical and diagnostical approaches. Material at the nanometer scale exploits several novel physiochemical and biological properties. Mainly increased surface area and nano-sized effects provided higher reactivity, strength and electrical characteristics of nanomaterial. Nanotechnology provides many advantages also for drug delivery to improve targeted side of

action as well as more controlled release to better manage drug pharmacokinetics, pharmacodynamics, non-specific toxicity, immunogenicity and biorecognition of systems in the quest for improved efficacy [98]. Two main factors are important to investigate: i) drug formulation and ii) route of application. Demonstration of optimal drug loading and release properties, long shelf-life and low toxicity are the main issues to be overcome for development of successful drug carrier systems. The route of administration is as important as the drug itself for a therapeutic success. Nanocarriers for drug delivery are intended to cross physical barriers and avoid toxic effects [69].

Implementation of RNAi technology and integration to nanomedicine may be of great clinical relevance to improve treatment strategies in a wide range of disorders. Table 1 summarized ongoing clinical trials using siRNAs for different targets.

Table 1: Summary of ongoing clinical trials for siRNA delivery

Company	siRNA	target	Disease/disorder	Status
Acuity Pharmaceuticals	Bevasiranib (Cand5)	VEGF	AMD, DME	Phase II _{completed} , Phase III _{planned}
	ACU-HTR-OOX	TGF- β	fibrosis	Phase II
Alnylam	ALN-RSV-01 ALN-RSV-02	RSV Pediatric RSV	RSV Pediatric RSV	Phase IIb preclinical
	ALN-VSP	KSP and VEGF	Liver cancer	Phase I
Silence Therapeutics	Atu21		Advanced solid cancer	Phase I
	Atu134		Acute lung injury	Preclinical
Sirna Therapeutics (Quark Pharmaceuticals & Pfizer)	RTP801		DME	Phase I
Sirna Therapeutics (Quark Pharmaceuticals)		p53	Acute kidney injury	Phase I
Sirna Therapeutics (Calando Pharmaceuticals)	CALAA-01	RRM2	Solid tumor cancer	Phase I
Sirna Therapeutics (TransDerm Inc.)	TD101	PC keratin K6a	Pachyonychia congenita	Phase Ib
Sirna Therapeutics	AGN211745 (Sirna-027)		AMD, CNV & AMD	Phase II
	I5NP		Delayed graft function, Kidney transplantation	Phase I Phase II
		PAI-1 in monocytes	Atherosclerosis	preclinical

Table 1: Summary of ongoing clinical trials for siRNA delivery, source: http://clinicaltrials.ifpma.org/no_cache/en/search-trials-ongoing/all/index.htm, abbreviations used: VEGF: vascular endothelial growth factor, TGF- β : transforming growth factor beta, KSP: kinesin spindle protein; RSV: respiratory syncytial virus; RRM2: ribonucleotide reductase M2 polypeptide; PC: Pachyonychia congenita; PAI-1: plasminogen activator inhibitor; AMD: age related macular degeneration; DME: diabetic macular edema,; CNV: choroidale Neovascularization

In conclusion, recently discovered posttranscriptional gene silencing, material science and nanotechnology represent the basis of innovative delivery techniques that offer great potential benefits to patients and new markets to pharmaceutical and drug delivery companies.

1.7 Aim of this thesis

Pulmonary application of nucleic acids such as pDNA and siRNA gained increasing attention for treatment of various lung disorders, e.g. viral infections (influenza, RSV), lung cancer or acute lung injury. Because of the high lability of nucleic acids, various non-viral vector systems for the improved nucleic acids delivery were developed and intensively investigated. Many studies focused on physicochemical characterization and transfection studies, but failed to elucidate in more detail the cytotoxicity of the nanocarriers and the nanocomplexes. Several clinical trials using gene therapy or siRNA to treat different kind of hereditary or acquired diseases are ongoing, but mostly failed to enter the clinics due to safety and efficacy reasons. The aim of this thesis was to gain more detailed insight in the toxicity pathways of non-viral vector system, especially poly(ethylene imine) (PEI)-based nanocarriers, for pulmonary siRNA delivery. PEI serves as gold standard for in vitro transfection of pDNA [20, 68, 70, 99] and has been shown to successfully deliver pDNA via the inhalative route [22, 100, 101] to the lungs. In our group, some promising PEI-modifications for siRNA delivery were developed and investigated for their efficacy, and (within this thesis) for their toxicity, especially in lung cells. The overall aim of this thesis presents the development of tools to predict toxicity and immunomodulation of non-viral vector systems for pulmonary siRNA delivery and to evaluate in more detail the mechanisms behind the toxicity of PEI-based non-viral vector systems.

Basic informations of the lung anatomy and physiology as well as considerations for pulmonary application, and nanotoxicology when using polymeric non-viral vector systems were provided in *Chapter 1* of this thesis. The first part of this thesis (*Chapter 2-5*) deals with in vitro evaluation of different PEI-based nanocarriers regarding their cytotoxicity and immunomodulatory effects in different lung cells. The second part (*Chapter 6-7*) represents in vivo studies for toxicity and efficacy of pre-selected PEI-based nanocomplexes with siRNA

in mice. *Chapter 8* summarizes the *in vitro* and *in vivo* results and gives an outlook of further investigations on optimized polymeric nanocarriers.

The search for predictive toxicity tools is still needed and the mechanisms behind the toxicity of PEI-based nanocarriers should be further investigated with regard to optimization of the cationic polymers on the one hand and on the other with regard to establishment of optimized and predictive toxicity models.

1.8 References

- 1 Griesenbach, U. and E.W. Alton, *Gene transfer to the lung: lessons learned from more than 2 decades of CF gene therapy*. *Adv Drug Deliv Rev*, 2009. 61(2): p. 128-39.
- 2 Patton, J.S., *Mechanisms of macromolecule absorption by the lungs*. *Advanced Drug Delivery Reviews*, 1996. 19: p. 3-36.
- 3 Weibel, *Morphometry of the Human Lung*. 1963, New York: Academic Press.
- 4 Kohlhäufl, M., *Understanding Clinical Aerosol Therapy: Physiological Aspects of the Respiratory System and Current Inhalation Therapy in Chronic Obstructive Pulmonary Disease and Asthma*. *Pulmonary Drug Delivery*, ed. K. Bechthold-Peters and H. Luessen. Vol. 2. 2007, Aulendorf, Germany: Editor Cantor Verlag.
- 5 Phalen, *Inhalation studies: Foundations and Techniques*. 1984, FL: CRC Press, Inc. Boca Raton.
- 6 Finlay, W., *Mechanics of Inhaled Pharmaceutical Aerosols*. 2001, New York: Academic Press. 94.
- 7 Gill, S., R. Löbenberg, T. Ku, S. Azarmi, W. Roa, and E.J. Prenner, *Nanoparticles: Characteristics, Mechanisms of Action, and Toxicity in Pulmonary Drug Delivery—A Review*. *J. Biomed. Nanotechnol.*, 2007. 3: p. 107-119.
- 8 Asghariana, B., O.T. Pricea, and W. Hofmann, *Prediction of particle deposition in the human lung using realistic models of lung ventilation*. *J Aerosol Sci*, 2006. 37(10): p. 1209-1221.
- 9 Heyder, J., J. Gebharta, G. Rudolfa, C. Schillera, and W. Stahlhofen, *Deposition of particles in the human respiratory tract in the size range 0.005–15 μm* . *J Aerosol Sci*, 1986. 17(5): p. 811-25.
- 10 Yang, W., J.I. Peters, and R.O. Williams, 3rd, *Inhaled nanoparticles--a current review*. *Int J Pharm*, 2008. 356(1-2): p. 239-47.
- 11 Wattiaux, R., N. Laurent, S. Wattiaux-De Coninck, and M. Jadot, *Endosomes, lysosomes: their implication in gene transfer*. *Adv Drug Deliv Rev*, 2000. 41(2): p. 201-8.
- 12 Conner, S.D. and S.L. Schmid, *Regulated portals of entry into the cell*. *Nature*, 2003. 422(6927): p. 37-44.
- 13 Watson, P., A.T. Jones, and D.J. Stephens, *Intracellular trafficking pathways and drug delivery: fluorescence imaging of living and fixed cells*. *Adv Drug Deliv Rev*, 2005. 57(1): p. 43-61.
- 14 Grimmer, S., B. van Deurs, and K. Sandvig, *Membrane ruffling and macropinocytosis in A431 cells require cholesterol*. *J Cell Sci*, 2002. 115(Pt 14): p. 2953-62.
- 15 Rejman, J., V. Oberle, I.S. Zuhorn, and D. Hoekstra, *Size-dependent internalization of particles via the pathways of clathrin- and caveolae-mediated endocytosis*. *Biochem J*, 2004. 377(Pt 1): p. 159-69.
- 16 Mayor, S. and R.E. Pagano, *Pathways of clathrin-independent endocytosis*. *Nat Rev Mol Cell Biol*, 2007. 8(8): p. 603-12.
- 17 Medina-Kauwe, L.K., J. Xie, and S. Hamm-Alvarez, *Intracellular trafficking of nonviral vectors*. *Gene Ther*, 2005. 12(24): p. 1734-51.
- 18 von Gersdorff, K., N.N. Sanders, R. Vandenbroucke, S.C. De Smedt, E. Wagner, and M. Ogris, *The internalization route resulting in successful gene expression depends on both cell line and polyethylenimine polyplex type*. *Mol Ther*, 2006. 14(5): p. 745-53.
- 19 Kopatz, I., J.S. Remy, and J.P. Behr, *A model for non-viral gene delivery: through syndecan adhesion molecules and powered by actin*. *J Gene Med*, 2004. 6(7): p. 769-76.
- 20 Demeneix, B. and J.P. Behr, *Polyethylenimine (PEI)*. *Adv Genet*, 2005. 53: p. 217-30.

- 21 Kleemann, E., M. Neu, N. Jekel, L. Fink, T. Schmehl, T. Gessler, W. Seeger, and T. Kissel, *Nano-carriers for DNA delivery to the lung based upon a TAT-derived peptide covalently coupled to PEG-PEI*. *J Control Release*, 2005. 109(1-3): p. 299-316.
- 22 Bragonzi, A., G. Dina, A. Villa, G. Calori, A. Biffi, C. Bordignon, B.M. Assael, and M. Conese, *Biodistribution and transgene expression with nonviral cationic vector/DNA complexes in the lungs*. *Gene Ther*, 2000. 7(20): p. 1753-60.
- 23 Rudolph, C., J. Lausier, S. Naundorf, R.H. Muller, and J. Rosenecker, *In vivo gene delivery to the lung using polyethylenimine and fractured polyamidoamine dendrimers*. *J Gene Med*, 2000. 2(4): p. 269-78.
- 24 Nguyen, J., R. Reul, T. Betz, E. Dayyoub, T. Schmehl, T. Gessler, U. Bakowsky, W. Seeger, and T. Kissel, *Nanocomposites of lung surfactant and biodegradable cationic nanoparticles improve transfection efficiency to lung cells*. *J Control Release*, 2009. 140(1): p. 47-54.
- 25 Griesenbach, U., D.M. Geddes, and E.W. Alton, *Gene therapy progress and prospects: cystic fibrosis*. *Gene Ther*, 2006. 13(14): p. 1061-7.
- 26 Griesenbach, U., C. Meng, R. Farley, S.H. Cheng, R.K. Scheule, M.H. Davies, P.C. Wolstenholme-Hogg, W. ten Hove, P. van der Hoeven, P.L. Sinn, P.B. McCray, Jr., M. Inoue, D.M. Geddes, M. Hasegawa, G. Frankel, S. Wiles, and E.W. Alton, *In vivo imaging of gene transfer to the respiratory tract*. *Biomaterials*, 2008. 29(10): p. 1533-40.
- 27 Zuhorn, I.S., J.B. Engberts, and D. Hoekstra, *Gene delivery by cationic lipid vectors: overcoming cellular barriers*. *Eur Biophys J*, 2007. 36(4-5): p. 349-62.
- 28 Ferrari, S., C. Kitson, R. Farley, R. Steel, C. Marriott, D.A. Parkins, M. Scarpa, B. Wainwright, M.J. Evans, W.H. Colledge, D.M. Geddes, and E.W. Alton, *Mucus altering agents as adjuncts for nonviral gene transfer to airway epithelium*. *Gene Ther*, 2001. 8(18): p. 1380-6.
- 29 Rosenecker, J., S. Naundorf, S.W. Gersting, R.W. Hauck, A. Gessner, P. Nicklaus, R.H. Muller, and C. Rudolph, *Interaction of bronchoalveolar lavage fluid with polyplexes and lipoplexes: analysing the role of proteins and glycoproteins*. *J Gene Med*, 2003. 5(1): p. 49-60.
- 30 Rejman, J., S. Di Gioia, A. Bragonzi, and M. Conese, *Pseudomonas aeruginosa infection destroys the barrier function of lung epithelium and enhances polyplex-mediated transfection*. *Hum Gene Ther*, 2007. 18(7): p. 642-52.
- 31 Ernst, N., S. Ulrichskotter, W.A. Schmalix, J. Radler, R. Galneder, E. Mayer, S. Gersting, C. Plank, D. Reinhardt, and J. Rosenecker, *Interaction of liposomal and polycationic transfection complexes with pulmonary surfactant*. *J Gene Med*, 1999. 1(5): p. 331-40.
- 32 de Fougerolles, A., H.P. Vornlocher, J. Maraganore, and J. Lieberman, *Interfering with disease: a progress report on siRNA-based therapeutics*. *Nat Rev Drug Discov*, 2007. 6(6): p. 443-53.
- 33 Novina, C.D. and P.A. Sharp, *The RNAi revolution*. *Nature*, 2004. 430(6996): p. 161-4.
- 34 Fire, A., S. Xu, M.K. Montgomery, S.A. Kostas, S.E. Driver, and C.C. Mello, *Potent and specific genetic interference by double-stranded RNA in *Caenorhabditis elegans**. *Nature*, 1998. 391(6669): p. 806-11.
- 35 Gary, D.J., N. Puri, and Y.Y. Won, *Polymer-based siRNA delivery: perspectives on the fundamental and phenomenological distinctions from polymer-based DNA delivery*. *J Control Release*, 2007. 121(1-2): p. 64-73.
- 36 Grimm, D., K.L. Streetz, C.L. Jopling, T.A. Storm, K. Pandey, C.R. Davis, P. Marion, F. Salazar, and M.A. Kay, *Fatality in mice due to oversaturation of cellular microRNA/short hairpin RNA pathways*. *Nature*, 2006. 441(7092): p. 537-41.

- 37 Jackson, A.L., S.R. Bartz, J. Schelter, S.V. Kobayashi, J. Burchard, M. Mao, B. Li, G. Cavet, and P.S. Linsley, *Expression profiling reveals off-target gene regulation by RNAi*. *Nat Biotechnol*, 2003. 21(6): p. 635-7.
- 38 Schlee, M., V. Hornung, and G. Hartmann, *siRNA and isRNA: two edges of one sword*. *Mol Ther*, 2006. 14(4): p. 463-70.
- 39 Hornung, V., M. Guenther-Biller, C. Bourquin, A. Ablasser, M. Schlee, S. Uematsu, A. Noronha, M. Manoharan, S. Akira, A. de Fougères, S. Endres, and G. Hartmann, *Sequence-specific potent induction of IFN- α by short interfering RNA in plasmacytoid dendritic cells through TLR7*. *Nat Med*, 2005. 11(3): p. 263-70.
- 40 Judge, A.D., V. Sood, J.R. Shaw, D. Fang, K. McClintock, and I. MacLachlan, *Sequence-dependent stimulation of the mammalian innate immune response by synthetic siRNA*. *Nat Biotechnol*, 2005. 23(4): p. 457-62.
- 41 Judge, A.D., G. Bola, A.C. Lee, and I. MacLachlan, *Design of noninflammatory synthetic siRNA mediating potent gene silencing in vivo*. *Mol Ther*, 2006. 13(3): p. 494-505.
- 42 Robbins, M., A. Judge, E. Ambegia, C. Choi, E. Yaworski, L. Palmer, K. McClintock, and I. MacLachlan, *Misinterpreting the therapeutic effects of small interfering RNA caused by immune stimulation*. *Hum Gene Ther*, 2008. 19(10): p. 991-9.
- 43 Robbins, M., A. Judge, and I. MacLachlan, *siRNA and innate immunity*. *Oligonucleotides*, 2009. 19(2): p. 89-102.
- 44 Chong, S., Y.J. Kim, S. Kim, H.O. Park, and Y.C. Choi, *Chemical modification of siRNAs to improve serum stability without loss of efficacy*. *Biochem Biophys Res Commun*, 2006. 342(3): p. 919-27.
- 45 Layzer, J.M., A.P. McCaffrey, A.K. Tanner, Z. Huang, M.A. Kay, and B.A. Sullenger, *In vivo activity of nuclease-resistant siRNAs*. *Rna*, 2004. 10(5): p. 766-71.
- 46 Dalby, B., S. Cates, A. Harris, E.C. Ohki, M.L. Tilkins, P.J. Price, and V.C. Ciccarone, *Advanced transfection with Lipofectamine 2000 reagent: primary neurons, siRNA, and high-throughput applications*. *Methods*, 2004. 33(2): p. 95-103.
- 47 Santel, A., M. Aleku, O. Keil, J. Endruschat, V. Esche, G. Fisch, S. Dames, K. Löffler, M. Fechtner, W. Arnold, K. Giese, A. Klippel, and J. Kaufmann, *A novel siRNA-lipoplex technology for RNA interference in the mouse vascular endothelium*. *Gene Ther*, 2006. 13(16): p. 1222-34.
- 48 Chien, P.Y., J. Wang, D. Carbonaro, S. Lei, B. Miller, S. Sheikh, S.M. Ali, M.U. Ahmad, and I. Ahmad, *Novel cationic cardiolipin analogue-based liposome for efficient DNA and small interfering RNA delivery in vitro and in vivo*. *Cancer Gene Ther*, 2005. 12(3): p. 321-8.
- 49 Pal, A., A. Ahmad, S. Khan, I. Sakabe, C. Zhang, U.N. Kasid, and I. Ahmad, *Systemic delivery of RafsiRNA using cationic cardiolipin liposomes silences Raf-1 expression and inhibits tumor growth in xenograft model of human prostate cancer*. *Int J Oncol*, 2005. 26(4): p. 1087-91.
- 50 Sitterberg, J., A. Ozcetin, C. Ehrhardt, and U. Bakowsky, *Utilising atomic force microscopy for the characterisation of nanoscale drug delivery systems*. *Eur J Pharm Biopharm*. 74(1): p. 2-13.
- 51 Soutschek, J., A. Akinc, B. Bramlage, K. Charisse, R. Constien, M. Donoghue, S. Elbashir, A. Geick, P. Hadwiger, J. Harborth, M. John, V. Kesavan, G. Lavine, R.K. Pandey, T. Racie, K.G. Rajeev, I. Rohl, I. Toudjarska, G. Wang, S. Wuschko, D. Bumcrot, V. Kotliansky, S. Limmer, M. Manoharan, and H.P. Vornlocher, *Therapeutic silencing of an endogenous gene by systemic administration of modified siRNAs*. *Nature*, 2004. 432(7014): p. 173-8.
- 52 Zimmermann, T.S., A.C. Lee, A. Akinc, B. Bramlage, D. Bumcrot, M.N. Fedoruk, J. Harborth, J.A. Heyes, L.B. Jeffs, M. John, A.D. Judge, K. Lam, K. McClintock, L.V.

- Nechev, L.R. Palmer, T. Racie, I. Rohl, S. Seiffert, S. Shanmugam, V. Sood, J. Soutschek, I. Toudjarska, A.J. Wheat, E. Yaworski, W. Zedalis, V. Koteliansky, M. Manoharan, H.P. Vornlocher, and I. MacLachlan, *RNAi-mediated gene silencing in non-human primates*. *Nature*, 2006. 441(7089): p. 111-4.
- 53 Flynn, M.A., D.G. Casey, S.M. Todryk, and B.P. Mahon, *Efficient delivery of small interfering RNA for inhibition of IL-12p40 expression in vivo*. *J Inflamm (Lond)*, 2004. 1(1): p. 4.
- 54 Verma, U.N., R.M. Surabhi, A. Schmaltieg, C. Becerra, and R.B. Gaynor, *Small interfering RNAs directed against beta-catenin inhibit the in vitro and in vivo growth of colon cancer cells*. *Clin Cancer Res*, 2003. 9(4): p. 1291-300.
- 55 Miyawaki-Shimizu, K., D. Predescu, J. Shimizu, M. Broman, S. Predescu, and A.B. Malik, *siRNA-induced caveolin-1 knockdown in mice increases lung vascular permeability via the junctional pathway*. *Am J Physiol Lung Cell Mol Physiol*, 2006. 290(2): p. L405-13.
- 56 Hassani, Z., G.F. Lemkine, P. Erbacher, K. Palmier, G. Alfama, C. Giovannangeli, J.P. Behr, and B.A. Demeneix, *Lipid-mediated siRNA delivery down-regulates exogenous gene expression in the mouse brain at picomolar levels*. *J Gene Med*, 2005. 7(2): p. 198-207.
- 57 Luo, M.C., D.Q. Zhang, S.W. Ma, Y.Y. Huang, S.J. Shuster, F. Porreca, and J. Lai, *An efficient intrathecal delivery of small interfering RNA to the spinal cord and peripheral neurons*. *Mol Pain*, 2005. 1: p. 29.
- 58 Maeda, Y., K. Fukushima, K. Nishizaki, and R.J. Smith, *In vitro and in vivo suppression of GJB2 expression by RNA interference*. *Hum Mol Genet*, 2005. 14(12): p. 1641-50.
- 59 Palliser, D., D. Chowdhury, Q.Y. Wang, S.J. Lee, R.T. Bronson, D.M. Knipe, and J. Lieberman, *An siRNA-based microbicide protects mice from lethal herpes simplex virus 2 infection*. *Nature*, 2006. 439(7072): p. 89-94.
- 60 Griesenbach, U., C. Kitson, S. Escudero Garcia, R. Farley, C. Singh, L. Somerton, H. Painter, R.L. Smith, D.R. Gill, S.C. Hyde, Y.H. Chow, J. Hu, M. Gray, M. Edbrooke, V. Ogilvie, G. MacGregor, R.K. Scheule, S.H. Cheng, N.J. Caplen, and E.W. Alton, *Inefficient cationic lipid-mediated siRNA and antisense oligonucleotide transfer to airway epithelial cells in vivo*. *Respir Res*, 2006. 7: p. 26.
- 61 Spagnou, S., A.D. Miller, and M. Keller, *Lipidic carriers of siRNA: differences in the formulation, cellular uptake, and delivery with plasmid DNA*. *Biochemistry*, 2004. 43(42): p. 13348-56.
- 62 Dubey, P.K., V. Mishra, S. Jain, S. Mahor, and S.P. Vyas, *Liposomes modified with cyclic RGD peptide for tumor targeting*. *J Drug Target*, 2004. 12(5): p. 257-64.
- 63 Meyerhoff, A., *U.S. Food and Drug Administration approval of AmBisome (liposomal amphotericin B) for treatment of visceral leishmaniasis*. *Clin Infect Dis*, 1999. 28(1): p. 42-8; discussion 49-51.
- 64 Moghimi, S.M. and J. Szebeni, *Stealth liposomes and long circulating nanoparticles: critical issues in pharmacokinetics, opsonization and protein-binding properties*. *Prog Lipid Res*, 2003. 42(6): p. 463-78.
- 65 Oupicky, D., M. Ogris, K.A. Howard, P.R. Dash, K. Ulbrich, and L.W. Seymour, *Importance of lateral and steric stabilization of polyelectrolyte gene delivery vectors for extended systemic circulation*. *Mol Ther*, 2002. 5(4): p. 463-72.
- 66 Braasch, D.A., S. Jensen, Y. Liu, K. Kaur, K. Arar, M.A. White, and D.R. Corey, *RNA interference in mammalian cells by chemically-modified RNA*. *Biochemistry*, 2003. 42(26): p. 7967-75.

- 67 Akinc, A., M. Thomas, A.M. Klibanov, and R. Langer, *Exploring polyethylenimine-mediated DNA transfection and the proton sponge hypothesis*. J Gene Med, 2005. 7(5): p. 657-63.
- 68 Boussif, O., F. Lezoualc'h, M.A. Zanta, M.D. Mergny, D. Scherman, B. Demeneix, and J.P. Behr, *A versatile vector for gene and oligonucleotide transfer into cells in culture and in vivo: polyethylenimine*. Proc Natl Acad Sci U S A, 1995. 92(16): p. 7297-301.
- 69 Nel, A.E., L. Madler, D. Velegol, T. Xia, E.M. Hoek, P. Somasundaran, F. Klaessig, V. Castranova, and M. Thompson, *Understanding biophysicochemical interactions at the nano-bio interface*. Nat Mater, 2009. 8(7): p. 543-57.
- 70 Behr, J., *The proton sponge: A trick to enter cells the viruses did not exploit*. chimia, 1997. 51: p. 34-36.
- 71 Kim, W.J. and S.W. Kim, *Efficient siRNA delivery with non-viral polymeric vehicles*. Pharm Res, 2009. 26(3): p. 657-66.
- 72 Schiffelers, R.M., A. Ansari, J. Xu, Q. Zhou, Q. Tang, G. Storm, G. Molema, P.Y. Lu, P.V. Scaria, and M.C. Woodle, *Cancer siRNA therapy by tumor selective delivery with ligand-targeted sterically stabilized nanoparticle*. Nucleic Acids Res, 2004. 32(19): p. e149.
- 73 Thomas, M., J.J. Lu, Q. Ge, C. Zhang, J. Chen, and A.M. Klibanov, *Full deacylation of polyethylenimine dramatically boosts its gene delivery efficiency and specificity to mouse lung*. Proc Natl Acad Sci U S A, 2005. 102(16): p. 5679-84.
- 74 Hwa Kim, S., J. Hoon Jeong, K. Chul Cho, S. Wan Kim, and T. Gwan Park, *Target-specific gene silencing by siRNA plasmid DNA complexed with folate-modified poly(ethylenimine)*. J Control Release, 2005. 104(1): p. 223-32.
- 75 Yang, J.P. and L. Huang, *Overcoming the inhibitory effect of serum on lipofection by increasing the charge ratio of cationic liposome to DNA*. Gene Ther, 1997. 4(9): p. 950-60.
- 76 Kabanov, A.V., *Polymer genomics: an insight into pharmacology and toxicology of nanomedicines*. Adv Drug Deliv Rev, 2006. 58(15): p. 1597-621.
- 77 Hong, S., P.R. Leroueil, E.K. Janus, J.L. Peters, M.M. Kober, M.T. Islam, B.G. Orr, J.R. Baker, Jr., and M.M. Banaszak Holl, *Interaction of polycationic polymers with supported lipid bilayers and cells: nanoscale hole formation and enhanced membrane permeability*. Bioconj Chem, 2006. 17(3): p. 728-34.
- 78 Leroueil, P.R., S. Hong, A. Mecke, J.R. Baker, Jr., B.G. Orr, and M.M. Banaszak Holl, *Nanoparticle interaction with biological membranes: does nanotechnology present a Janus face?* Acc Chem Res, 2007. 40(5): p. 335-42.
- 79 Beyerle, A., O.M. Merkel, T. Stoeger, and T. Kissel, *PEGylation affects cytotoxicity and cell-compatibility of poly(ethylene imine) for lung application: structure-function-relationships* Toxicol Appl Pharmacol, 2009. in press.
- 80 Beyerle, A., A. Braun, A. Banerjee, N. Ercal, O. Eickelberg, T. Kissel, and T. Stoeger, *Side-effects of PEI-based siRNA nanocarriers for pulmonary application in mice*. Eur Res J, under review.
- 81 Mossman, B.T., P.J. Borm, V. Castranova, D.L. Costa, K. Donaldson, and S.R. Kleeberger, *Mechanisms of action of inhaled fibers, particles and nanoparticles in lung and cardiovascular diseases*. Part Fibre Toxicol, 2007. 4: p. 4.
- 82 Oberdorster, G., E. Oberdorster, and J. Oberdorster, *Nanotoxicology: an emerging discipline evolving from studies of ultrafine particles*. Environ Health Perspect, 2005. 113(7): p. 823-39.
- 83 Nemmar, A.H.M.F., Hoet Peter H.M., Vermeylen Josef, Nemery Benoit, *Size effect of intratracheally instilled particles on pulmonary inflammation and vascular thrombosis*. Toxicol Appl Pharmacol, 2003. 186: p. 38-45.

- 84 Pope, C.A., 3rd, M. Ezzati, and D.W. Dockery, *Fine-particulate air pollution and life expectancy in the United States*. *N Engl J Med*, 2009. 360(4): p. 376-86.
- 85 Nel, A., T. Xia, L. Madler, and N. Li, *Toxic potential of materials at the nanolevel*. *Science*, 2006. 311(5761): p. 622-7.
- 86 Meng, H., T. Xia, S. George, and A.E. Nel, *A Predictive Toxicological Paradigm for the Safety Assessment of Nanomaterials*. *ACS Nano*, 2009. 3(7): p. 1620–1627.
- 87 Brown, D.M., K. Donaldson, P.J. Borm, R.P. Schins, M. Dehnhardt, P. Gilmour, L.A. Jimenez, and V. Stone, *Calcium and ROS-mediated activation of transcription factors and TNF-alpha cytokine gene expression in macrophages exposed to ultrafine particles*. *Am J Physiol Lung Cell Mol Physiol*, 2004. 286(2): p. L344-53.
- 88 Donaldson, K., and Stone, V. , *Current hypotheses on the mechanisms of toxicity of ultrafine particles*. *Ann Ist Super Sanità*, 2003. 39(3): p. 405-410.
- 89 Schins, R.P., *Mechanisms of genotoxicity of particles and fibers*. *Inhal Toxicol*, 2002. 14(1): p. 57-78.
- 90 Schins, R.P., J.H. Lightbody, P.J. Borm, T. Shi, K. Donaldson, and V. Stone, *Inflammatory effects of coarse and fine particulate matter in relation to chemical and biological constituents*. *Toxicol Appl Pharmacol*, 2004. 195(1): p. 1-11.
- 91 Xia, T., M. Kovochich, J. Brant, M. Hotze, J. Sempf, T. Oberley, C. Sioutas, J.I. Yeh, M.R. Wiesner, and A.E. Nel, *Comparison of the abilities of ambient and manufactured nanoparticles to induce cellular toxicity according to an oxidative stress paradigm*. *Nano Lett*, 2006. 6(8): p. 1794-807.
- 92 Knaapen, A.M., P.J. Borm, C. Albrecht, and R.P. Schins, *Inhaled particles and lung cancer. Part A: Mechanisms*. *Int J Cancer*, 2004. 109(6): p. 799-809.
- 93 Knaapen, A.M., R.P. Schins, D. Polat, A. Becker, and P.J. Borm, *Mechanisms of neutrophil-induced DNA damage in respiratory tract epithelial cells*. *Mol Cell Biochem*, 2002. 234-235(1-2): p. 143-51.
- 94 Sayes, C.M., K.L. Reed, and D.B. Warheit, *Assessing toxicity of fine and nanoparticles: comparing in vitro measurements to in vivo pulmonary toxicity profiles*. *Toxicol Sci*, 2007. 97(1): p. 163-80.
- 95 Warheit, D.B., T.R. Webb, and K.L. Reed, *Pulmonary toxicity screening studies in male rats with M5 respirable fibers and particulates*. *Inhal Toxicol*, 2007. 19(11): p. 951-63.
- 96 Borm, P.J. and D. Berube, *A tale of opportunities, uncertainties, and risks*. *Nano Today*, 2008. 3(1-2): p. 56-59.
- 97 Donaldson, K., P.J. Borm, V. Castranova, and M. Gulumian, *The limits of testing particle-mediated oxidative stress in vitro in predicting diverse pathologies; relevance for testing of nanoparticles*. *Part Fibre Toxicol*, 2009. 6: p. 13.
- 98 Pison, U., T. Welte, M. Giersig, and D.A. Groneberg, *Nanomedicine for respiratory diseases*. *Eur J Pharmacol*, 2006. 533(1-3): p. 341-50.
- 99 Fischer, D., Y. Li, B. Ahlemeyer, J. Krieglstein, and T. Kissel, *In vitro cytotoxicity testing of polycations: influence of polymer structure on cell viability and hemolysis*. *Biomaterials*, 2003. 24(7): p. 1121-31.
- 100 Rudolph, C., R.H. Muller, and J. Rosenecker, *Jet nebulization of PEI/DNA polyplexes: physical stability and in vitro gene delivery efficiency*. *J Gene Med*, 2002. 4(1): p. 66-74.
- 101 Densmore, C.L., F.M. Orson, B. Xu, B.M. Kinsey, J.C. Waldrep, P. Hua, B. Bhogal, and V. Knight, *Aerosol delivery of robust polyethyleneimine-DNA complexes for gene therapy and genetic immunization*. *Mol Ther*, 2000. 1(2): p. 180-8.

2 In vitro cytotoxic and immuno-modulatory profiling of low molecular weight poly(ethylene imines) for pulmonary application

Andrea Beyerle, Sabrina Höbel, Frank Czubayko, Holger Schulz, Thomas Kissel, Achim Aigner, and Tobias Stoeger.

Published in *Toxicology in vitro* 23 (2009) 500–508

Authors's Contributions:

A.B. prepared the manuscript draft and wrote the manuscript, carried out the experimental work, analyzed and interpreted the data; S.H. did the preparation of the PEI F 25-LMW, F.C. provided the PEI F25-LMW, H.S. provided the financial support of the cell culture studies, T.K. reviewed and edited the manuscript, A.A. provided the PEI F25-LMW and reviewed and edited the manuscript, T.S. was involved in the data interpretation, reviewed and edited the manuscript. All authors read and approved the final version of the manuscript.

2.1 Abstract

Polyethylenimines (PEI) are potent non-viral nucleic acid delivery vehicles used for gene delivery and RNA interference (RNAi). For non-invasive pulmonary RNAi therapy the respiratory tissue is an attractive application route, but offers particularly unwanted side effects like cytotoxicity as well as inflammatory and immune responses.

In the current study, we determined the most crucial issues of pulmonary applications for two low molecular weight PEIs in comparison to the well known lung toxic crystalline silica. Cytotoxic effects and inflammatory responses were evaluated in three murine pulmonary target cell lines, the alveolar epithelial (LA4), the alveolar macrophage (MH-S) and the macrophage-monocyte-like (RAW 264.7) cell line.

For both PEIs, cytotoxicity was detected most prominently in the alveolar epithelial cells and only at high doses. Cytokine responses, in contrast were observed already at low PEI concentrations and could be divided into three groups, induced (i) by free PEI (IL-6, TNF- α , G-CSF), (ii) by PEI/siRNA complexes (CCL2, CCL5, CXCL1, CXCL10), or (iii) unaffected by either treatment (IL-2, -4, -7, -9, and CCL3).

We conclude that even for the respiratory tissue both PEIs represent powerful siRNA delivery tools with reduced cytotoxicity and minor proinflammatory potency. However, in relation to response levels observed upon crystalline silica exposures, some PEI induced proapoptotic and proinflammatory responses might not be considered completely harmless, therefore further *in vivo* investigations are advisable.

Keywords: Polyethylenimine, Pulmonary inflammation, Nanocarrier, Cytotoxicity

2.2 Introduction

RNA interference (RNAi) represents a powerful method for specific gene silencing and RNAi therapeutics achieve a fundamentally new way to treat human diseases by activating selective mRNA cleavage for efficient ablation of the expression of any target gene [1, 2]. Due to their instability and poor tissue and cell penetration, the delivery of RNAs to their sites of action is one of the most challenging aspects, particularly *in vivo*. The use of nanoparticles for encapsulating therapeutic agents represents an advanced class of drug delivery systems for both conventional drugs as well as for nucleic acids, i.e. plasmid DNA, coding for therapeutically relevant genes, antisense oligonucleotides and small interfering RNA (siRNA). For the induction of siRNA-mediated gene-targeting *in vivo* the efficient protection of siRNAs against enzymatic or non-enzymatic degradation is most important due to their short biological half-life. One promising strategy is the complexation of siRNAs with poly(ethylene imine) (PEI). Initially, PEI was introduced as an efficient non-viral transfection reagent for the delivery of plasmid DNA, demonstrating high transfection efficiency *in vitro* and *in vivo* [3]. In more recent studies, the PEI-mediated delivery of nucleic acids was extended towards small RNA molecules, i.e. siRNAs [4]. Due to its high cationic charge density and a large number of protonable nitrogen atoms, PEI is able to form stable, water-soluble non-covalent complexes with nucleic acids. These complexes are efficiently taken up by cells through endocytosis and subsequently, based on the so-called ‘proton-sponge effect’ [5], intracellularly released without the support of endosome disruptive agents for lysosomal escape. Since a high efficacy of nucleic acid delivery generally requires an excess of PEI thus leading to a net positive surface charge, non-specific interactions of the complexes with negatively charged cellular structures may result in decreased efficiency and increased toxicity. To reduce PEI cytotoxicity, several studies have introduced modified PEIs such as block or graft copolymers containing cationic and hydrophilic non-ionic components [6]. Furthermore, increased biocompatibility without modifications of the polymer structure was

achieved by employing low molecular weight PEIs, which displayed significantly reduced cytotoxicity [7, 8]. Additionally, it was shown that certain low molecular weight PEIs provide increased transfection efficacies for DNA as well as for siRNA. This is particularly true for the commercially available linear 22 kDa jet-PEI (Polyplus, France) as well as for the branched 4-10 kDa PEI F25-LMW, which was obtained through size fractionation of commercially available 25 kDa branched PEI by gel permeation chromatography [9].

With regard to the therapeutic application in humans, high efficacy as well as safety and biocompatibility are among the most critical issues for any gene delivery system including PEI. Therefore, in this study we focused on the two low molecular weight PEIs of different structure described above, which have already been employed *in vitro* and *in vivo*, and thus have been established as relevant delivery reagents for systemic application [4, 9-11]. Targeted delivery of polyplexes to the lung is an emerging area of gene therapy research. The main attraction of using sub-micron sized particles, particularly below 300 nm in size for pulmonary delivery, is the observation that these particles tend to escape the detection by the macrophage clearance system and remain in the lung sufficiently long enough to release their 'payload' in a controlled manner [12]. However, instilled non-biodegradable polystyrene nanospheres with small diameters and thus large surface areas have been shown to induce pulmonary inflammation [13]. In comparison to micron-sized particles, a given mass of the sub-micron fraction is considered to be in particular hazardous and might be more reactive due to their increased surface area-to-mass ratio, since they not only escape clearance mechanisms resulting in increased retention time [12]. In addition, upon pulmonary delivery of positively charged amine-polystyrene particles even systemic effects like enhanced thrombosis via platelet activation have been observed [14]. Thus, *in vitro* toxicity studies are considered as an important adjunct to *in vivo* studies [15] and, due to possible toxic or inflammatory effects of the particles employed, need to precede any *in vivo* study also with regard to identifying optimal and maximum dosages.

To study cytotoxic and proinflammatory effects of nanoplexes in the lung, three cell lines were selected: the alveolar epithelial cells (LA4), the alveolar macrophages (MH-S) and the macrophage-monocyte like cell line RAW 264.7. This selection of relevant cell lines is based on the fact that (i) for inhaled particles, the fragile, alveolar epithelium represents the first barrier, and (ii) macrophages are vital to the regulation of immune response and the development of inflammation.

In our study, cell-based assays for cytotoxic and proinflammatory endpoints were performed with two already established PEIs, namely branched PEI F25-LMW and linear jet-PEI, and their corresponding PEI/siRNA complexes, since the complexes may dissociate making the toxicity of free PEI a relevant issue [16]. To benchmark putative adverse effects related to PEI exposure, we included respirable crystalline silica particles (α -quartz) as lung toxic positive control, which are considered as a well recognized health hazard known to cause pulmonary inflammation and severe lung diseases [12, 17].

Hence, the goal of this study was to evaluate the (dose-dependent) inflammatory and toxic effects of PEI and PEI/siRNA complexes, in order to assess the safety of these nanoplexes formulated as therapeutic aerosols. The correlation of these data with physicochemical particle properties may also help to design novel, optimized, non-viral vector systems for pulmonary application and to establish, which molecules are relevant to estimate.

2.3 Materials and Methods

Polymers and particles

PEI F25-LMW was purified from 25 kDa branched PEI (Al 25-kDa, free base, water free, Sigma-Aldrich, Taufkirchen, Germany) by gel permeation chromatography as described previously [9]. The obtained low molecular weight fraction of 25 kDa PEI was characterized by a size of 4-10 kDa and accordingly termed PEI F25-LMW. PEI F25-LMW featured highest transfection efficiency for different stable tumor cell lines (SKOV-3, SW-13, and ME-180) which was comparable to the commercially available jetPEI. For details see [9, 11]. JetPEI was purchased from Polyplus (Ilkirch, France), and represents a linear polyethylenimine (PEI) with a molecular weight of ~22 kDa according to the informations provided by the manufacturer. Min-U-Sil 5 (crystalline silica, α -quartz) was obtained from U.S. Silica Company, Berkeley Springs, WV, USA. According to the datasheet this frequently used reference material is characterized by a median diameter of 1.7 μm and a purity of 98 % SiO_2 .

Cell culture

Cell culture experiments were carried out using murine alveolar epithelial – like type II cells (LA4; ATCC No. CCL-196TM) and murine alveolar macrophages (MH-S; ATCC No. CRL-2019) as well as the mouse leukaemic monocyte macrophage cell line RAW 264.7 (ATCC No. TIB-71). LA4 cells were grown in HAM's F12 medium with stable L-glutamine (Biochrom AG, Seromed, Germany) containing 15 % fetal bovine serum (FBS, Gibco, Germany) and 1 % non essential amino acids (Biochrom AG, Seromed, Germany) and 100 U/ml penicillin and 100 mg/ml streptomycin (Biochrom AG Seromed, Germany), MH-S cells were cultured in RPMI 1640 (Biochrom AG, Seromd, Germany) with stable L-glutamine supplemented with 10 % fetal bovine serum (FBS, Gibco, Germany), 50 μM 2-mercaptoethanol (Gibco, Germany), 10 mM HEPES (Gibco, Germany), 1 mM Na-pyruvate (Gibco, Germany), 50 U/ml penicillin and 50 mg/ml streptomycin (Biochrom AG Seromed,

Germany), RAW 264.7 cells were grown in Dulbecco's modified Eagle's medium with stable L-glutamine (DMEM, Biochrom AG, Seromed, Germany) supplemented with 10 % fetal bovine serum (FBS, Gibco, Germany) and 100 U/ml penicillin and 100 mg/ml streptomycin (Biochrom AG Seromed, Germany). All cells were grown in a humidified incubator at 37 ° C and 5 % CO₂ and passaged every 2-3 days.

Exposure experiments

Cells were exposed to pure polymer (PEI F25-LMW, jetPEI), the corresponding polyplexes with siGL3, or Min-U-Sil 5 particles as reference particle. Polyplexes were prepared with the siRNA siGL3 (Sense: 5' – CUU-ACG-CUG-AGU-ACU-UCG-ATT-3'; Antisense: 5' – UCG-AAG-UAC-UCA-GCG-UAA-GTT-3' MWG, Ebersberg, Germany) as described previously [4, 9, 11]. Briefly, appropriate amounts of siGL3 (10 µg) and PEI solution were each separately diluted in 50 µl HEPES (10 mM) buffered sodium chloride solution (150 mM), pH 7.4. After 10 min the siRNA solution was mixed with the PEI solution, resulting in a final volume of 100 µl, followed by an incubation of 30 min at room temperature. PEI/siGL3 ratios were calculated on the basis of PEI nitrogen per siRNA phosphate and expressed as PEI/siRNA equivalent (N/P ratio). In the current study we used N/P ratios in the range of 0.05 – 5 to obtain the desired concentration of PEI from 0.5-50 µg/ml, which corresponds to a dose range of 0.25-25 µg/cm²/0.5*10⁶ cells. The suspension of Min-U-Sil 5 was prepared in double-distilled, sterile water. The stock solution was sonicated for 15 min, and rigorously vortexed and then diluted in double-distilled, sterile water.

0.25*10⁶ cells/ well were seeded in 24-well-plates (FALCON, Germany) with a final volume of 500 µl cell culture medium supplemented with 10 % serum (DMEM and RPMI 1640, respectively), or 15 % serum (HAM's F12) and containing antibiotics 24 h prior to particle treatment. After 24 h cell culture medium was replaced and 400 µl of fresh, prewarmed cell culture medium without antibiotics and reduced serum (2 %) was added to each well. 100 µl of the appropriate concentration of polymer, polyplex as well as Min-U-Sil suspension was

added to obtain a final volume of 500 μ l per well. Previous experiments confirmed, that regarding cell viability and cytotoxicity untreated cells and solvent treated cells, i.e. cells treated with 100 μ l of HEPES(10 mM) buffered sodium chloride solution (150 mM) or 100 μ l double-distilled, sterile water in 400 μ l cell culture medium (supplemented with 2 % FBS and without antibiotics) for 24 h revealed no detectable responses (data not shown). Therefore, we tested the particle treated cells in comparison to untreated cells as control. After 24 h treatment aliquots of the supernatants were taken for cytokine and LDH release studies and cells were subsequently incubated with the WST-1 reagent for cell viability determination. Each single experiment was carried out in triplicates and was repeated three times.

Cell viability

Cell viability was determined using the Cell Proliferation Reagent WST-1 (Roche Diagnostics, Germany) to quantify mitochondrial activity according to the method of Mosmann [18]. After 24 h exposure the relative viability [%] related to control samples (untreated cells) was calculated by the following equation:

$$\text{Cell viability} = (\text{OD}_{\text{sample}} / \text{OD}_{\text{control}}) * 100.$$

Cytotoxicity (LDH-assay)

For detection of the cytosolic enzyme lactate dehydrogenase (LDH) characteristic for membrane damaging effects we used the Cytotoxicity Detection Kit (Roche Diagnostics, Germany) according to the manufacturer's instructions. After 24 h exposure, the LDH concentration in the cell culture supernatant was spectrophotometrically determined with an ELISA reader (Labsystems iEMS Reader MF, Helsinki, Finland) at a wavelength of 492 nm. Cells treated with 2 % (w/v) Triton X-100 served as high control and were set as maximum of LDH release (100 %) according to the manufacturer's instructions. The relative LDH release is defined by the ratio of LDH released over total LDH in the intact cells (high control). Less than 10 % LDH release was regarded as non-toxic effect level in our experiments [19].

Cytokine detection

Multiplexed Immunoassays (Multi-Analyte Profiling)

In all cell lines, 22 cytokines/chemokines were detected simultaneously in cell culture supernatant by using a microsphere based multiplexing system (Linco Research, St. Charles, MO). In this study, the secretion of the following cytokines/chemokines was investigated: IL-1 α , IL-1 β , IL-4, IL-5, IL-6, IL-7, IL-9, IL-10, IL-12p70, IL-13, IL-15, IL-17, TNF-alpha, INF- γ , G-CSF, GM-CSF, CXCL1 CXCL10, CCL2, CCL3, and CCL5. The assay was performed as described previously [20]. The mean fluorescence intensity (MFI) was detected by the Multiplex plate reader (Luminex System, Bio-Rad Laboratories, Germany) for each sample (50 μ l) with a minimum of 50 beads per region being analyzed. Raw data (MFI) was captured using the Multiplex plate reader software (Bioplex Manager, Version 2.0). For data analysis, a 4-parameter logistic curve fit was applied to each standard curve and sample.

ELISA studies

Additionally, supernatants of LA4 and RAW 264.7 cells were used to quantify the secretion of four proinflammatory, acute phase cytokines by enzyme-linked immunosorbent assays (ELISA) using the following kits according to the manufacturer's protocols: BD OptEIA™ Mouse TNF ELISA Kit II, BD OptEIA™ Set Mouse IL-1 β , BD OptEIA™ Mouse IL-6 ELISA Kit and Quantikine® Mouse KC (R&D Systems) according to the manufacturer's protocols. Briefly, samples and standards diluted in the assay diluent provided with the kit were incubated at room temperature either in wells already supplied or in 96-well plates (NUNC, Wiesbaden, Germany) freshly precoated with specific capturing antibodies in the case of IL-1 β . After washing steps, the detection antibody-conjugate was added and incubated at room temperature prior to washing steps. The subsequent addition of substrate solution then resulted in color development and after the addition of stop solution the color intensity was measured with an ELISA reader (Labsystems iEMS Reader MF, Helsinki, Finland) at the corresponding wavelength with wavelength correction as detailed in the kits.

Detection limits for each cytokine in the multiplex-ELISA and the ELISA studies were listed in Table S1.

Statistics

All values are presented as mean \pm standard error (SEM) of three independent experiments for the polymer and five for the quartz exposures with all experiments run in triplicates. Significant differences between two groups were evaluated by Student's *t*-test or between more than two groups by one-way ANOVA followed by Tukey's multiple comparison test. Statistical analysis was performed using the program STATGRAPHICS PLUS Version 5.0 (Statpoint, Inc., Virginia, USA).

2.4 Results

PEI polymers induce cell-type-dependent decrease in metabolic activity

Treatment of the selected cell lines with various amounts of polymers or polyplexes, respectively, revealed marked differences in their cellular sensitivity with the alveolar epithelial cells (LA4) being more susceptible than the two macrophage-like cell lines (Figures 1 A-F).

Figure 1: Cell viability

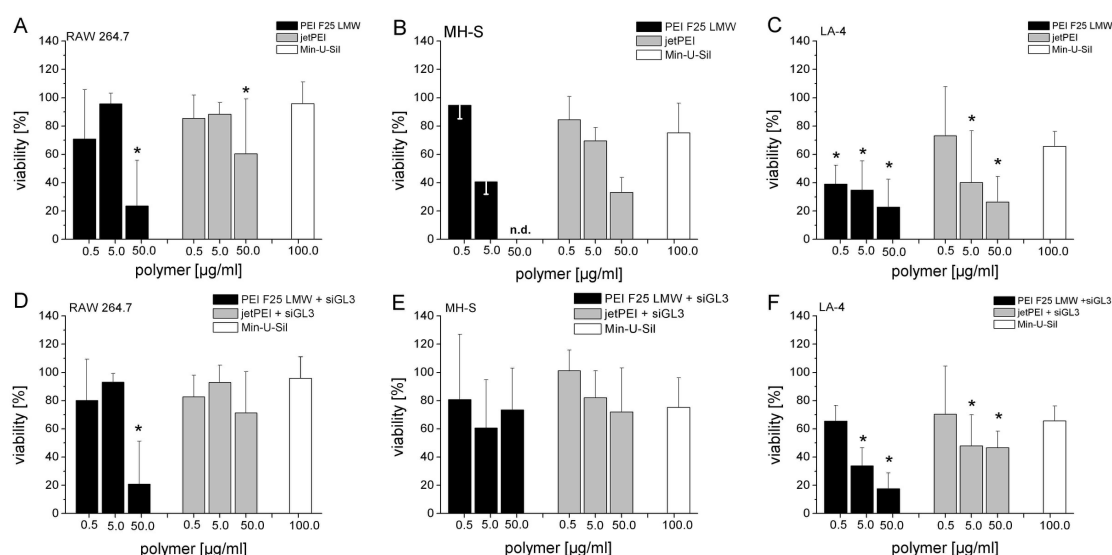


Figure 1 A-F: Cell viability as determined by WST-1 Cell Proliferation Assay. Values are expressed as mean±SEM (n=3 for PEI and PEI/siRNA treatment and n=5 for Min-U-Sil exposure). Cells were exposed with three different concentrations (0.5, 5, 50 µg/ml) of PEI F25-LMW (black bars), jetPEI (grey bars) or Min-U-Sil 5 (100 µg/ml), which served as benchmark. Figures A-C showed the cell viability after treatment with free PEI, figures D-F represented the cell viability after treatment of the corresponding PEI/siRNA complexes. Differences to control (untreated cells) with (p)<0.05 were considered statistically significant and marked with an asterisk, n.d.= not detectable.

More specifically, in LA4 cells the lowest dose of the branched PEI F25-LMW (0.5 µg/ml) caused already more than 50 % decrease in cell viability, thus exceeding even the effects of crystalline silica which served as a benchmark for particle induced pulmonary toxicity. In contrast, viability of macrophages remained unaffected at this concentration with decreased

metabolic activity only being observed at higher doses of 5 $\mu\text{g/ml}$ (MH-S) or 50 $\mu\text{g/ml}$ (RAW 264.7). The linear jetPEI caused a dose-dependent decrease in metabolic activity, but appeared generally less toxic (Figures 1 A-C). Furthermore, in all three cell lines, polyplexes were less toxic compared to the free polymers (Figures 1 D-F), and complexes based on PEI F25-LMW generated stronger decreases in cell viability than jetPEI, but differences failed to be statistically significant.

PEI polymers cause only marginal membrane damage

In agreement with the WST-1 data, the release of LDH after 24h particle exposure indicating membrane damage proved to depend on the cell line, on the polymer/complex and on the concentration (Figures 2 A-F).

Figure 2: Cytotoxicity

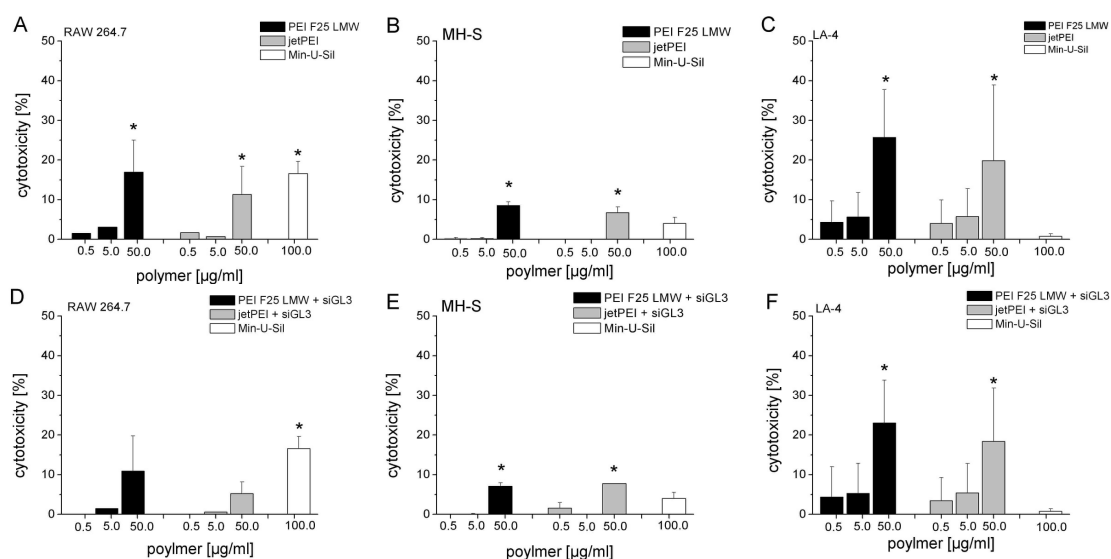


Figure 2 A-F: Influence of cell membrane integrity was observed by measuring LDH in the cell culture supernatant after 24h exposure of three different concentrations of PEI (0.5, 5, 50 $\mu\text{g/ml}$) with PEI F25-LMW (black bars), jetPEI (grey bars) and Min-U-Sil 5 (white bars). Values are expressed as mean \pm SEM ($n=3$ for PEI and PEI/siRNA treatment and $n=5$ for Min-U-Sil exposure). Min-U-Sil 5 (100 $\mu\text{g/ml}$) served as benchmark. Figures A-C represented the cytotoxicity upon free PEI exposure and figures D-F upon PEI/siRNA complex exposure. Probability (p) < 0.05 was considered as significant compared to control (untreated cells) and indicated with an asterisk.

More specifically, for the macrophage cell lines, the LDH release in response to the polyplex or free polymer was negligible with values around the non-toxic threshold of 10 % LDH release [19] only being observed at the highest PEI concentration (50 $\mu\text{g/ml}$). Again, in comparison to the macrophages, the alveolar epithelial cells were more susceptible to both polymers and polyplexes. In contrast, crystalline silica particles caused a high LDH release only in the macrophage cell line RAW 264.7. On the other hand, the membrane integrity of the epithelial cells was not affected by crystalline silica, regardless of the reduced viability determined by the WST assay (compare Figures 1C and 2C). Both PEIs, the branched PEI F25-LMW, as well as the linear jetPEI, revealed significant membrane toxicity only at the highest dose of 50 $\mu\text{g/ml}$ and the alveolar epithelial cells yielded the most prominent dose-dependent LDH release. No differences in LDH release were detected comparing free polymers to PEI/siRNA complexes.

Multiplex cytokine profiling of PEI/siRNA exposed cells

Cytokine secretion in response to the particles was determined 24 h after exposure in all three cell lines. Remarkably, for five cytokines (IL-1 α , CCL2, CCL5, CXCL1, and CXCL10) increased concentrations were observed after 24 h PEI/siRNA treatment in the alveolar cell lines MH-S and LA4 (see table S2B and S2C), but not in RAW 264.7 macrophages. Highest induction rates in cytokine release were detected for the CXC chemokines CXCL1, the murine functional homologue of human IL-8, and CXCL10, also called interferon- γ (IFN- γ) inducible protein 10. For both chemokines PEI/siRNA exposure caused 10-fold increased levels, which for CXCL1 was confined to LA4 cells (PEI F25 LMW/siRNA 50 $\mu\text{g/ml}$: 1530 \pm 188 pg/ml vs. ctrl. 104 \pm 45 pg/ml). PEI F25-LMW/siRNA polyplexes yielded a statistically significantly ($p < 0.05$) 3-fold higher release of CXCL1 compared to jetPEI/siRNA polyplexes (jetPEI/siRNA 50 $\mu\text{g/ml}$: 500 \pm 144 pg/ml vs. ctrl. 104 \pm 45 pg/ml). In contrast, the CXCL10 concentration was 10 times elevated only after jetPEI/siRNA treatment

(jetPEI/siRNA 5 μ g/ml: 1903 \pm 1844 pg/ml vs. PEI F25 LMW/siRNA 5 μ g/ml: 195 \pm 57 pg/ml and vs. 196 \pm 47 pg/ml for ctrl) (Tables S2B and S2C and Figure 3).

Interestingly, the often in the field of inhalation toxicology used macrophage-monocyte cell line RAW 264.7, did not match these response pattern described above, as CCL2 and CXCL1 failed to respond, and CCL5 and CXCL10 at the lowest dose showed even reduced cytokine levels upon PEI/siRNA complexes treatment relative to controls (for CXCL10: PEI F25 LMW/siRNA 50 μ g/ml: 1152 \pm 391 pg/ml and jetPEI/siRNA 50 μ g/ml 1556 \pm 1004 pg/ml vs. 1644 \pm 980 pg/ml for ctrl. and for CCL5: PEI F25 LMW/siRNA 50 μ g/ml: 3 \pm 2 pg/ml and jetPEI/siRNA 50 mg/ml: 6 \pm 4 pg/ml vs. 12 \pm 3 pg/ml for ctrl.) (Table S2A). Statistically significant ($p < 0.05$) changes in cytokine release were only detected in the epithelial cell line (LA4) after PEI/siRNA treatment for CCL2 and CXCL1 in a dose-dependent manner (Figure 3). For the high dose response of these two chemokines the exposures with jetPEI/siRNA complexes resulted in significant weaker effects.

In contrast, a different set of cytokines was affected by exposure to crystalline silica used as lung toxicity benchmark particles. In fact, of the cytokines released upon polyplex treatment (IL-1a, CCL2, -5, CXCL1, and -10), crystalline silica affected only the release of CXCL10 in LA4 cells (Tables S2A-C) was detected. In agreement to the PEI data, the most prominent effects following exposure to silica particles were detected in LA4 cells.

Figure 3: Cytokine release of PEI LMW/siRNA polyplexes

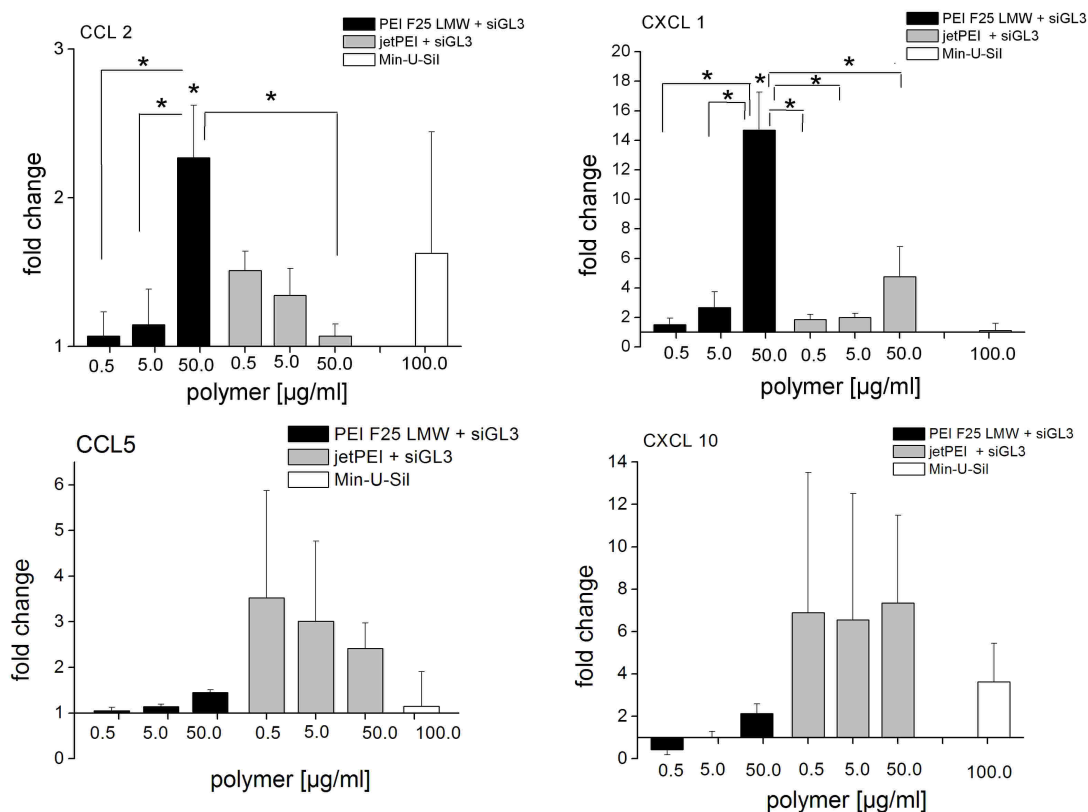


Figure 3: Quantification of cytokine concentrations after 24h exposure to PEI F25-LMW/siGL3 polyplexes (black bars), and jetPEI/siGL3 polyplexes (grey bars) at three different PEI concentrations 0.5, 5, 50µg/ml, and Min-U-Sil 5 (100µg/ml) (white bars) in LA4 alveolar epithelial cells using a multi analyte detection immunoassay. Values represent relative changes (mean±SEM) of three independent experiments compared to levels of untreated cells. Asterisk indicates statistically significant changes (p-value<0.05).

Multiplex cytokine profiling of PEI exposed cells

In order to distinguish between polymer and polyplex effects possibly related to the different physicochemical properties of the free PEI and the nucleic acid/PEI complexes, the cytokine responses were analyzed with a comprehensive panel. In view of our data from the cytokine profiling of PEI/siRNA exposed cells, we focused here on the most relevant cytokines showing at least 1.5 induction either by polyplexes or by the silica benchmark (IL-6, TNF- α , CXCL1, CXCL10, CCL2, G-CSF). In addition to that IL-1 β was included in the panel because of its immunological potency. The highest response levels were observed in the

RAW 264.7 cells for the acute phase cytokines TNF- α , IL-6, and the granulocyte-colony-stimulating factor (G-CSF) and to lesser extent for the IFN- γ inducible Th1 cytokine CXCL10 (Figure 4 and Table S2A). Here the most prominent changes were detected for G-CSF already at the moderate dose of 5 μ g/ml PEI with increased levels up to 20- or 80-fold for PEI F25-LMW (414 \pm 310 pg/ml vs. 15 \pm 1 pg/ml for ctrl.) and jetPEI (1131 \pm 935 pg/ml vs. 15 \pm 1 pg/ml for ctrl.) respectively. Crystalline silica particles actually caused nearly identical response pattern with a two-fold increase in G-CSF in all three cell lines (LA4: 47 \pm 15 pg/ml vs. 23 \pm 2 pg/ml for ctrl., MH-S: 87 \pm 25 pg/ml vs. 47 \pm 5 pg/ml for ctrl., RAW264.7: 593 \pm 434 pg/ml vs. 260 \pm 159 pg/ml for ctrl.).

In RAW 264.7 cells IL-6 levels were more than 10-fold elevated following jetPEI exposure (139 \pm 56 pg/ml vs. 11 \pm 4 pg/ml for ctrl.) and more than 5-fold due to PEI F25-LMW treatment (80 \pm 53 pg/ml vs. 11 \pm 4 pg/ml for ctrl.), but changes were characterized by high variability. However, no changes in IL-6 release were detected for the two alveolar cell lines (LA4 and MH-S). TNF- α levels were up to 4-fold increased after both polymer exposure, and again confined to RAW 264.7 cells (PEI F25 LMW 5 μ g/ml: 154 \pm 39 pg/ml and jetPEI 5 μ g/ml: 150 \pm 23 pg/ml vs. 37 \pm 16 pg/ml for ctrl.). Notably, the cytokines induced by free PEI polymer (IL-6, G-CSF, CXCL10, and TNF α) were also increased upon silica exposures in all three cell lines, with epithelial LA4 cells demonstrating the highest responsiveness.

Figure 4: Cytokine release of LMW PEIs

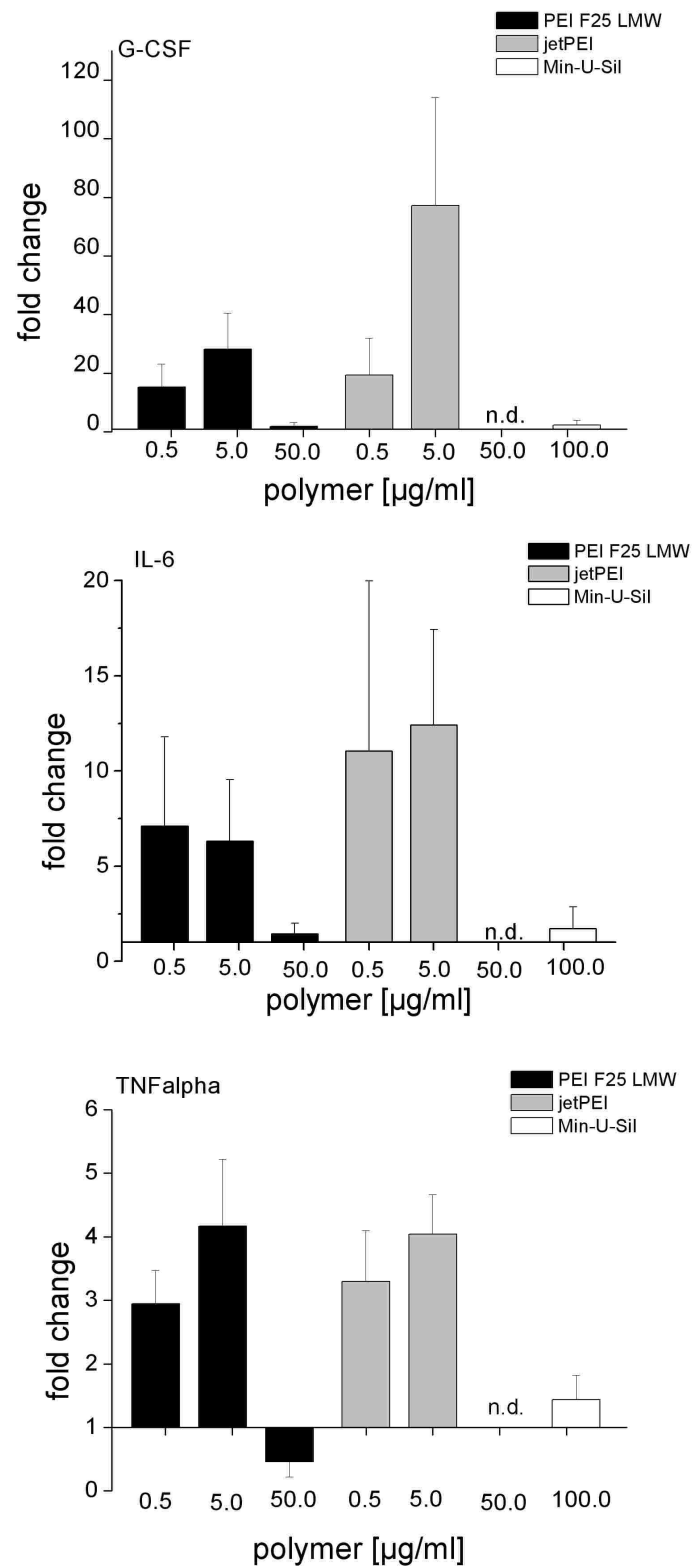


Figure 4: Quantification of cytokine concentrations in RAW 264.7 cultures after 24h exposure to 0.5, 5, 50 µg/ml PEI F25-LMW (black bars), and jetPEI (grey bars), and Min-U-Sil 5 (100 µg/ml) (white bars) cells using a multi analyte detection immunoassay. Values represent relative changes (mean±SEM) of three independent experiments compared to levels of untreated cells. Statistically significance was represented as asterisk with a p-value of 0.05.

ELISA based reexamination of acute phase cytokines

To compare our multiplex cytokine profiling data with the most commonly used ELISA-based results, the levels of the four major pro-inflammatory cytokines (IL-1 β , IL-6, CXCL-1 and TNF- α) were additionally quantified by ELISA (Table S3). Measurements were restricted to LA4 and RAW 264.7 cells, since these two cell lines revealed to be the most sensitive to the PEI exposures described above. After treatment with the lowest dose of jetPEI (0.5 μ g/ml), TNF- α levels increased 3-fold in RAW 264.7 cells (3459.4 \pm 470.9 pg/ml vs. 986.5 \pm 74.7 pg/ml for ctrl.), which confirmed our multiplex data. IL-6 secretion in the ELISA experiments corresponded well with the multiplex data and seems to be more prominent in the macrophages than in the epithelial cells, but again the values were close to the lower detection limit of the assay. As with the multiplex profiling, exposure related changes in IL-1 β release were not detectable with the traditional ELISA technique.

Noteworthy, the statistically significant changes ($p < 0.05$) in cytokine levels matched well in both test systems: CXCL1 concentrations were increased up to 15-fold detected by multiplex technique after treatment of LA4 cells with 50 μ g/ml PEI F25-LMW/siRNA (1530 \pm 188 pg/ml vs. ctrl. 104 \pm 45 pg/ml) compared to a 7-fold increase observed by ELISA (605.7 \pm 13.9 pg/ml vs. 81.9 \pm 30.5 pg/ml). In the RAW 264.7 macrophages, both systems revealed a 3-fold increase for TNF- α after treatment with 0.5 μ g/ml jetPEI (ELISA: 3459.4 \pm 470.9 pg/ml vs. 986.5 \pm 74.7 pg/ml for ctrl. and multiplex: 122 \pm 30 pg/ml vs. 37 \pm 16 pg/ml for ctrl.).

In summary, we categorized the proinflammatory response pattern in two groups: (i) an acute phase like cytokine group consisting of IL-6, G-CSF and TNF α , which showed to be induced by free PEI polymer, and mainly in proinflammatory macrophages, and (ii) a chemokine group, in particular represented by CCL2, CCL5, CXCL1, and CXCL10 being induced primarily in by PEI/siRNA complexes exposed to the resident alveolar cell types (LA4 and MH-S), see table 1.

Table 1: Cytokine release induced by

	I. free PEI	II. PEI/siRNA complexes	III. unaffected by either treatment in all cell lines
LA4			
PEI F25 LMW jetPEI	G-CSF	CXCL1>CCL2 CXCL10>CXCL1>CCL5	
Min-U-Sil 5	IL-6>TNF-a>CXCL10>G-CSF		
MH-S			
PEI F25 LMW JetPEI	G-CSF	CCL5>IL-1a CXCL10>CCL5	IL-2, -4,-7, -9, and CCL3
Min-U-Sil 5	TNF-a>G-CSF		
RAW264.7			
PEI F25 LMW jetPEI	G-CSF>TNF-a>IL-6 G-CSF>IL-6>TNFa>CXCL10		
Min-U-Sil 5	G-CSF		
Category	“acute-phase-cytokines”	“viral defense”	“non responder”

Table 1: Cytokine release induced by (I.) free PEI (first column), (II.) PEI/siRNA polyplexes (second column), and (III.) unaffected by either treatment (third column). The mainly observed cytokines were listed in descendent manner of released levels in the three different cell lines (LA4, MH-S, RAW264.7). Min-U-Sil 5 100 µg/ml represented the reference for highly, acute phase cytokine release in the lung.

2.5 Discussion

Our study aimed at an *in vitro* assessment of the cytotoxic and in particular of the immunomodulatory effects of two low molecular weight PEI polymers, namely the branched PEI F25-LMW and the commercially available linear jetPEI, as well as their corresponding siRNA polyplexes, to allow a prediction for safe *in vivo* dosing. For better correlation to further *in vivo* studies in mice, the murine system was chosen at the *in vitro* level. To analyze cell interactions in response to particle, we investigated different cell types which represent professional phagocytes (macrophages) but also cell types contributing to the innate immune response in the lung (alveolar macrophages and epithelial type II cells). Classical submerge culture conditions of these adherent cells were chosen to screen for unwanted side-effects of the non-viral gene carriers in regard to a prospective aerosol therapy by using those non-viral gene carriers. In addition, crystalline silica was used as a reference particle at a concentration of 100 $\mu\text{g/ml}$ corresponding to a surface dose of 25 $\mu\text{g/cm}^2$. This dose was deduced from our previous cytotoxic and inflammation dose-response data covering a range from 5 to 250 $\mu\text{g/cm}^2$. In that study 25 $\mu\text{g/cm}^2$ (100 $\mu\text{g/ml}$) crystalline silica yielded moderate but significant effects on cytotoxicity as well as on the inflammatory response in lung target cells (data not shown). A crucial issue represents the specific selection of an optimal reference particle, in our study crystalline silica served as benchmark particle although it causes toxic and proinflammatory effects to the lung via different pathways as compared to our PEI based carriers. Nevertheless, we selected crystalline silica, because it is one of the best described lung toxic substances, that causes cytotoxicity and inflammatory responses *in vitro* and *in vivo* [17].

PEI particles were exposed to the cells in a dose range from 0.5 to 50 $\mu\text{g/ml}$ representing a broad range of concentrations generally used for transfection studies *in vitro* and *in vivo* (0.5-5 $\mu\text{g/ml}$), up to an extremely high PEI dose of 50 $\mu\text{g/ml}$ to demonstrate a worst case scenario regarding cytotoxic effects. We did not investigate the effects of free siRNA treatment to the

cells, because it is well described in the literature that without any vehicle, siRNA is rapidly degraded by nucleases and thus would not effectively reach its intracellular site of action without any vehicle or techniques like electroporation [16].

Cytotoxic response

In the present study, we demonstrated a cell-type dependent reduction of the cell viability in response to two different low molecular weight PEIs and their corresponding PEI/siRNA complexes, which clearly showed the epithelial cell line to be the most sensitive. Since the decrease in cell viability was not accompanied by membrane damage (Fig. 1 and 2), necrosis could be excluded as underlying cell death pathway, respectively at low doses. Therefore, we suggest rather an apoptotic-like way, according to Moghimi and colleagues who recently demonstrated that PEI can react as a proapoptotic agent [21]. Only the highest dose of PEI reduced the metabolic activity of the two macrophage cell lines to levels below 50 %. This cell type dependence suggests that PEI polymer and polyplex uptake by phagocytosis has no major contribution to carrier toxicity, on the contrary endocytotic uptake processes involving epithelial cell surface proteins, like sulfate group rich, negatively charged proteoglycans might rather be of importance [22].

Our data also indicate that the exposure to the corresponding polyplexes caused generally less cytotoxicity regarding mitochondrial dehydrogenases activity and membrane integrity. A similar relation has been demonstrated for PEGylated PEIs by Malek and colleagues [23]. Both could argue for the importance of charge based cell particle interactions.

With regard to safety, based on our *in vitro* cytotoxicity data, and in view of a reduced toxicity of the PEI/siRNA polyplexes, the dose range of 0.5 – 5 µg/ml might be considered as adequate for future *in vivo* studies. However, the proapoptotic potency for susceptible cells, like the alveolar epithelium might bring along some perturbation that would have to be examined *in vitro* in more detail before starting *in vivo* studies. Caution is also advised, since both PEIs

affected cell viability even at moderate doses much more than our lung toxicity benchmark, the crystalline silica particles.

Cell membrane toxicity followed a different cell-type-dependence for Min-U-Sil (LA4 < MH-S << RAW246.7) as compared to PEI particles (MH-S < RAW264.7 << LA4). Accordingly for the silica exposure phago- rather than endocytosis seems to be responsible for the macrophage susceptibility, and necrosis is in this case indicated by a significant release of cellular LDH (Fig. 2A and D).

Immunomodulatory effects

The PEI particles investigated here are characterized by a size below 100nm for the polymers and around 50-200 nm for the polyplexes with siRNA [4, 9, 10] and could thus be classified to the category of nanoparticles. Because of the fraction of molecules represented at the surface of the particle, it is generally accepted, that at a given mass, smaller sized particles (nanoparticles) are more reactive or even toxic than larger sized particles [15]. However, for PEI or PEI/siRNA the surface toxicity and in particular the inflammatory potential to lung tissue, which will be one critical factor for their pulmonary administration, is largely unknown. So far, only few studies dealt with the immunomodulatory effects of PEI [24] and [25], but the rapidly increasing application of siRNA requires a high attention to the innate immune response not merely caused by the siRNA itself [26], but also by the non-viral vector systems [24].

In our study we screened the release of cytokines using the broadest available panel of pro- and anti-inflammatory mouse cytokines in three different immune competent lung target cells. Upon exposures to free PEI the acute phase response cytokines IL-6, G-CSF and TNF- α were much more pronounced in the macrophage-monocyte like (RAW 264.7) cells as compared to the alveolar resident like MH-S cells. Alveolar MH-S cells otherwise mediated, similar to the epithelial LA4 cells, a significant release of CCL and CXCL chemokines upon siRNA complexed PEI, see table 1. In the case of the alveolar epithelial cells statistically significant

increases in CCL2 and CXCL1 levels were detected with the highest dose of 50 $\mu\text{g/ml}$ PEI F25-LMW/siRNA polyplexes. In addition, CCL5 and CXCL10 concentrations were 5- to 10-fold elevated after jetPEI/siRNA exposure at the lower dose regime, but changes were statistically not significant. The chemokines CCL5 and CXCL10 but also CXCL1 could functionally be called 'viral defense' like cytokines, characterized by the IFN-stimulated response promoter element and their ability to be immediately expressed and released due to cellular detection of viral infections [27]. This observation allows us to categorize the proinflammatory response pattern in two groups: (i) the acute phase cytokines, like IL-6, G-CSF and TNF α , which are induced by free PEI polymer, and mainly in proinflammatory macrophages, and (ii) the 'viral defense' like cytokines, in particular represented by CCL2, CCL5, CXCL1, and CXCL10 which are induced primarily in by PEI/siRNA complexes exposed resident alveolar cell types (LA4 and MH-S). Upon endocytosis of PEI polyplexes and subsequent endosomal RNA release into the cytoplasm it might be speculated, that specific intracellular receptors of the innate immune system, like TLR3, could activate an antiviral like cytokine response [28]. According to this hypothesis, the highly inflammatory crystalline silica particles induced only IL-6, G-CSF and TNF- α (and to a minor extend CXCL10) but not CCL2, CCL5 or CXCL1. Therefore CCL2 and CCL5 might represent the primary 'RNA' specific indicators under these conditions.

Interestingly, the release levels of IL-1 β were not affected by the particle exposures. This finding could either be related to the fact that the here assessed exposure setting did not induce IL-1 β expression or, that pathways upstream the subsequent secretion of mature IL-1 β have not been triggered in a cell-autonomous way.

Our study confirms that cell types differ in their responsiveness and susceptibility to the respective particles analyzed, hence the validity of studies limited to only one cell line might be not sufficient. Moreover our cytokine screen demonstrated that the best known and thus most often analyzed cytokines, like TNF or IL-1 might not necessarily be the most sensitive

representatives for proinflammatory changes, therefore we suggest to analyze a comprehensive panel of cytokines/chemokines.

In summary in our *in vitro* experiments both PEIs either as polyplex or free polymers provoked within a therapeutically relevant concentration range corresponding to 0.5 – 5 µg/ml PEI, no cytotoxicity and only minor immunomodulatory responses since the dose effective to cause statistically significant cytokine releases exceeded any realistic exposure deduced from the dose range used for *in vitro* or *in vivo* transfection studies. Nevertheless, the high dose effects even exceeded the effect levels of crystalline silica which was used as lung toxic benchmark control, and thus should be considered for further *in vivo* application studies.

Conflict of Interest Statement

None of the authors has any competing or financial interest in relation to the submission. No involvement of study sponsors in the study design to declare.

Acknowledgments

This study was supported by a grant of the German Research Council (DFG-Forschergruppe 627). We would like to thank Michael Krumpel for his excellent technical assistance and Dr. Maria Diedrich-Möhring for her kind introduction in the multiplex technique.

2.6 Supplementary material

Table S1: Detection limits

Cytokine	lower detection limit			upper detection limit		
	22-er panel pg/ml	8-er panel pg/ml	ELISA pg/ml	22-er panel pg/ml	8-er panel pg/ml	ELISA pg/ml
MIP1a	16.6			10010.0		
GMCSF	61.6			9215.0		
MCP1	68.0	93.6		9934.1	2020.1	
KC	68.0	14.9	16.0	2741.0	2003.0	1000.0
RANTES	2.3			805.1		
IFN γ	58.0			3269.1		
IL-1 β	23.0		31.3	8504.0		1700.0
IL-2	2.8			3669.1		
IL-1a	24.8	84.9		6502.0	2004.5	
IL_7	2.4			9868.0		
IL-15	13.3			4753.0		
IL-4	3.1			1738.1		
IL_5	57.6			2943.0		
IL-6	19.3	10.0	16.0	5429.0	2006.0	1000.0
IL-10	20.8			4882.1		
IL-12p70	58.1	7.8		8184.0	2003.0	
TNF α	3.2	6.2	124.0	1716.0	327.1	1700.0
IL-9	15.6			10000.0		
IL-13	16.9			8612.0		
IL-17	8.8			1879.1		
IP-10	43.0			10570.1	2024.0	
G-CSF	15.3			5797.1	2012.0	

Table S1: Detection limits of the investigated cytokines obtained for each panel in the appropriate experiment from the standard curves.

Table S2A: Cytokine response in RAW 264.7

RAW 264.7	IL-1a	IL-2	IL-4	IL-6	IL-7	IL-9	G-CSF	CXCL10	TNFalpha	CCL3	CCL2	CCL5	CXCL1
PEI F25 LMW													
0.5µg/ml + siRNA	b.d.l.	b.d.l.	b.d.l.	b.d.l.	b.d.l.	0.7±0.2	b.d.l.	0.3±0.1	0.4±0.0	0.9±0.4	0.4±0.2	0.2±0.1	b.d.l.
5µg/ml + siRNA	b.d.l.	b.d.l.	b.d.l.	b.d.l.	b.d.l.	1.0±0.3	b.d.l.	0.9±0.5	0.5±0.1	1.3±0.0	0.8±0.2	0.4±0.1	b.d.l.
50µg/ml + siRNA	b.d.l.	b.d.l.	b.d.l.	b.d.l.	b.d.l.	1.2±0.5	b.d.l.	0.7±0.3	0.5±0.2	0.8±0.4	0.6±0.4	0.3±0.1	b.d.l.
jetPEI													
0.5 µg/ml+siRNA	b.d.l.	b.d.l.	b.d.l.	b.d.l.	b.d.l.	1.0±0.3	b.d.l.	0.5±0.1	0.4±0.7	1.2±0.0	0.6±0.1	0.3±0.2	b.d.l.
5 µg/ml+siRNA	b.d.l.	b.d.l.	b.d.l.	b.d.l.	b.d.l.	0.7±0.1	b.d.l.	0.6±0.1	0.4±0.1	1.3±0.0	0.9±0.2	0.3±0.1	b.d.l.
50 µg/ml+siRNA	b.d.l.	b.d.l.	b.d.l.	b.d.l.	b.d.l.	0.7±0.1	b.d.l.	0.9±0.4	1.1±0.7	1.3±0.1	1.2±0.4	0.6±0.2	b.d.l.
PEI F25 LMW													
0.5µg/ml	b.d.l.	n.d.	n.d.	7.1±4.7	n.d.	n.d.	15.3±7.8	1.9±0.4	2.9±0.5	n.d.	1.3±0.0	n.d.	b.d.l.
5µg/ml	b.d.l.	n.d.	n.d.	6.3±3.2	n.d.	n.d.	28.2±12.2	1.9±0.5	4.2±1.1	n.d.	1.2±0.0	n.d.	b.d.l.
50µg/ml	b.d.l.	n.d.	n.d.	1.4±0.8	n.d.	n.d.	1.8±2.0	0.6±0.3	0.5±0.2	n.d.	0.8±0.3	n.d.	b.d.l.
jetPEI													
0.5 µg/ml	b.d.l.	n.d.	n.d.	11.1±8.9	n.d.	n.d.	19.4±12.7	2.0±0.4	3.3±0.8	n.d.	1.3±0.0	n.d.	b.d.l.
5.0µg/ml	b.d.l.	n.d.	n.d.	12.4±5.1	n.d.	n.d.	77.2±36.9	1.7±0.4	4.0±0.6	n.d.	1.1±0.2	n.d.	b.d.l.
50µg/ml	b.d.l.	n.d.	n.d.	n.d.	n.d.	n.d.	n.d.	n.d.	n.d.	n.d.	n.d.	n.d.	n.d.
Min-U-Sil													
100µg/ml	b.d.l.	b.d.l.	b.d.l.	1.7±1.1	b.d.l.	0.7±0.1	2.3±1.7	0.6±0.2	1.4±0.4	1.1±0.1	b.d.l.	0.9±0.2	b.d.l.

Table S2A:

Relative cytokine secretion (fold change) in RAW 264.7 cells after exposure to free PEI or PEI/siRNA complexes for 24h, as detected by a multiple analyte detection immunoassay. Means were normalized to control cells (untreated cells). Values represent mean ± SEM, n=2-3; b.d.l. = below detection limit; statistically significant ($p < 0.05$) changes compared to control levels (untreated cells) are marked with an asterisk; n.d. = not done.

Table S 2B: Cytokine response in MH-S

MH-S	IL-1a	IL-2	IL-4	IL-6	IL-7	IL-9	G-CSF	CXCL1	TNFalpha	CCL3	CCL2	CCL5	CXCL1
PEI F25 LMW													
0.5µg/ml+siRNA	1.0±0.1	1.1±0.5	1.0±0.1	0.1±0.1	0.8±0.3	b.d.l.	b.d.l.	0.8±0.2	1.0±0.0	1.1±0.0	0.8±0.2	1.2±0.5	b.d.l.
5 µg/ml+siRNA	1.0±0.2	0.3±0.1	1.0±0.1	0.5±0.1	0.8±0.4	b.d.l.	b.d.l.	1.0±0.2	1.0±0.2	1.1±0.0	1.1±0.5	1.1±0.3	b.d.l.
50 µg/ml+siRNA	2.6±1.7	1.7±0.5	1.0±0.1	0.6±0.0	0.9±0.3	b.d.l.	b.d.l.	1.6±0.8	0.9±0.2	0.8±0.3	1.8±1.5	5.2±4.4	b.d.l.
jetPEI													
0.5µg/ml+siRNA	0.3±0.6	0.8±0.5	1.0±0.0	0.5±0.9	0.8±0.2	b.d.l.	b.d.l.	7.0±3.0	0.5±0.5	1.1±0.0	1.4±0.0	3.2±1.2	b.d.l.
5 µg/ml+siRNA	1.1±0.0	0.3±0.1	0.9±0.0	0.9±0.5	1.0±0.5	b.d.l.	b.d.l.	10.7±7.6	0.9±0.6	1.0±0.1	1.1±0.3	2.1±1.4	b.d.l.
50 µg/ml+siRNA	0.4±0.2	1.2±0.0	1.0±0.0	0.5±0.1	0.7±0.3	b.d.l.	b.d.l.	2.2±0.9	1.7±1.6	0.2±0.2	0.5±0.1	1.6±0.6	b.d.l.
PEI F25 LMW													
0.5µg/ml	b.d.l.	n.d.	n.d.	0.4±0.4	n.d.	n.d.	1.7±1.7	1.0±0.0	0.6±0.3	n.d.	1.0±0.0	n.d.	1.2±0.4
5 µg/ml	b.d.l.	n.d.	n.d.	0.3±0.3	n.d.	n.d.	1.6±1.6	1.0±0.0	0.3±0.2	n.d.	0.9±0.0	n.d.	0.6±0.3
50 µg/ml	b.d.l.	n.d.	n.d.	0.2±0.2	n.d.	n.d.	0.4±0.3	1.0±0.0	0.3±0.2	n.d.	0.3±0.1	n.d.	1.4±0.6
jetPEI													
0.5µg/ml	b.d.l.	n.d.	n.d.	0.4±0.4	n.d.	n.d.	2.4±1.9	1.0±0.0	0.3±0.2	n.d.	1.0±0.0	n.d.	0.8±0.0
5 µg/ml	b.d.l.	n.d.	n.d.	0.3±0.3	n.d.	n.d.	2.0±1.7	1.0±0.0	0.3±0.2	n.d.	1.0±0.0	n.d.	0.5±0.0
50µg/ml	b.d.l.	n.d.	n.d.	n.d.	n.d.	n.d.	n.d.	n.d.	n.d.	n.d.	n.d.	n.d.	n.d.
Min-U-Sil													
100µg/ml	1.4±0.3	1.1±0.6	1.0±0.0	1.5±0.3	1.4±0.1	1.4±0.7	2.4±0.7	1.6±0.6	2.6±1.0	0.8±0.1	0.9±0.2	0.8±0.0	1.3±0.2

Table S2B:

Relative cytokine secretion (fold change) in MH-S cells after exposure to free PEI or PEI/siRNA complexes for 24h, as detected by a multiple analyte detection immunoassay. Means were normalized to control cells (untreated cells). Values represent mean ± SEM, n=2-3; b.d.l. = below detection limit; statistically significant ($p<0.05$) changes compared to control levels (untreated cells) are marked with an asterisk; n.d.= not done.

Table S2C: Cytokine response in LA4

LA4	IL-1a	IL-2	IL-4	IL-6	IL-7	IL-9	G-CSF	CXCL10	TNFalpha	CCL3	CCL2	CCL5	CXCL1
PEI F25 LMW													
0.5µg/ml+siRNA	0.3±0.0	0.2±0.0	1.1±0.0	1.0±0.0	0.7±0.3	b.d.l.	b.d.l.	0.4±0.2	1.4±0.3	0.9±0.1	1.1±0.2	1.1±0.1	1.5±0.4
5µg/ml+siRNA	0.4±0.0	0.2±0.1	0.9±0.1	0.8±0.2	1.2±0.2	b.d.l.	b.d.l.	1.0±0.3	1.1±0.0	0.8±0.1	1.1±0.2	1.1±0.1	2.7±1.1
50 µg/ml+siRNA	1.0±0.2	0.7±0.1	1.0±0.1	1.6±0.8	0.9±0.1	b.d.l.	b.d.l.	2.1±0.5	1.2±0.1	0.8±0.1*	2.3±0.4	1.4±0.1*	14.7±2.6
jetPEI													
0.5 µg/ml+siRNA	0.2±0.2	0.3±0.0	1.1±0.0	1.5±0.4	1.1±0.1	b.d.l.	b.d.l.	10.1±6.6	0.7±0.3	0.9±0.0	1.6±0.1	4.7±2.4	2.0±0.3
5µg/ml+siRNA	0.3±0.1	0.2±0.1	1.1±0.0	1.1±0.1	1.1±0.1	b.d.l.	b.d.l.	9.7±8.8	0.9±0.1	0.3±0.2	1.3±0.2	3.0±1.8	2.0±0.3
50µg/ml+siRNA	1.8±0.6	0.7±0.2	1.0±0.0	1.7±0.7	0.8±0.2	b.d.l.	b.d.l.	7.3±4.1	1.1±0.2	0.9±0.0	1.1±0.1	2.4±0.6	4.8±2.1
PEI F25 LMW													
0.5 µg/ml	b.d.l.	n.d.	n.d.	0.4±0.1	n.d.	n.d.	6.3±5.5	1.2±0.6	b.d.l.	n.d.	1.1±0.5	n.d.	1.2±0.4
5µg/ml	b.d.l.	n.d.	n.d.	0.0±0.0	n.d.	n.d.	1.4±0.9	0.7±0.7	b.d.l.	n.d.	1.0±0.5	n.d.	1.3±0.3
50µg/ml	b.d.l.	n.d.	n.d.	0.4±0.2	n.d.	n.d.	7.6±6.8	0.9±0.6	b.d.l.	n.d.	1.1±0.5	n.d.	1.2±0.5
jetPEI													
0.5µg/ml	b.d.l.	n.d.	n.d.	0.1±0.1	n.d.	n.d.	0.7±0.3	0.9±0.6	b.d.l.	n.d.	1.0±0.5	n.d.	1.2±0.5
5µg/ml	b.d.l.	n.d.	n.d.	0.1±0.1	n.d.	n.d.	0.5±0.3	0.7±0.6	b.d.l.	n.d.	0.2±0.1	n.d.	0.6±0.5
50µg/ml	b.d.l.	n.d.	n.d.	n.d.	n.d.	n.d.	n.d.	n.d.	n.d.	n.d.	n.d.	n.d.	n.d.
Min-U-Sil													
100µg/ml	1.2±0.0	0.6±0.1	0.8±0.0	4.6±2.3	0.8±0.3	b.d.l.	2.0±0.6	2.9±2.9	3.4±2.5	0.7±0.3	1.6±0.8	1.2±0.8	1.1±0.5

Table S2:

Relative cytokine secretion (fold change) in LA4 cells after exposure to free PEI or PEI/siRNA complexes for 24h, as detected by a multiple analyte detection immunoassay. Means were normalized to control cells (untreated cells). Values represent mean ± SEM, n=2-3; b.d.l. = below detection limit; statistically significant ($p<0.05$) changes compared to control levels (untreated cells) are marked with an asterisk; n.d.= not done.

Table S3: Cytokine secretion of LA4 and RAW264.7 detected by ELISA technique

	CXCL1		TNF α	
	LA-4	RAW 264.7	LA-4	RAW 264.7
control	81.9 \pm 30.5	b.d.l.	b.d.l.	986.5 \pm 74.7
0.5μg/ml polymer				
PEI F25-LMW/siGL3	100.0 \pm 4.3	b.d.l.	b.d.l.	1380.7 \pm 120.5
jetPEI/siGL3	74.6 \pm 19.4	b.d.l.	b.d.l.	1921.7 \pm 389.3
PEI F25-LMW	81.6 \pm 5.1	b.d.l.	b.d.l.	1179.3 \pm 319.6
jetPEI	133.0 \pm 11.6	b.d.l.	b.d.l.	*3459.4\pm470.9
5μg/ml polymer				
PEI F25-LMW/siGL3	98.7 \pm 13.7	b.d.l.	b.d.l.	1237.5 \pm 151.7
jetPEI/siGL3	91.6 \pm 15.6	b.d.l.	b.d.l.	1279.3 \pm 172.3
PEI F25-LMW	69.4 \pm 11.7	b.d.l.	b.d.l.	1494.3 \pm 214.3
jetPEI	112.3 \pm 20.0	b.d.l.	b.d.l.	1487.1 \pm 210.3
50μg/ml polymer				
PEI F25-LMW/siGL3	*605.7\pm13.9	b.d.l.	b.d.l.	1197.8 \pm 73.3
jetPEI/siGL3	157.4 \pm 25.1	b.d.l.	b.d.l.	1612.0 \pm 432.9
PEI F25-LMW	342.3 \pm 13.2	b.d.l.	b.d.l.	1620.4 \pm 291.3
jetPEI	129.9 \pm 17.6	b.d.l.	b.d.l.	1187.4 \pm 140.6

Table S3: Cytokine secretion [pg/ml] in LA4(left) and RAW 264.7 cells (right)

after exposure to free PEI or PEI/siRNA complexes for 24h, as detected by

enzyme-linked immunosorbent assay. Values represented mean \pm SEM, n=5,

statistically significance was marked as an asterisk with a p-value of 0.05 and

b.d.l. means below detection limit.

2.7 References

- 1 Aigner, A., *Delivery Systems for the Direct Application of siRNAs to Induce RNA Interference (RNAi) In Vivo*. J Biomed Biotechnol, 2006. 2006(4): p. 71659.
- 2 Fougerolles de, A., H.P. Vornlocher, J. Maraganore, and J. Lieberman, *Interfering with disease: a progress report on siRNA-based therapeutics*. Nat Rev Drug Discov, 2007. 6(6): p. 443-53.
- 3 Boussif, O., F. Lezoualc'h, M.A. Zanta, M.D. Mergny, D. Scherman, B. Demeneix, and J.P. Behr, *A versatile vector for gene and oligonucleotide transfer into cells in culture and in vivo: polyethylenimine*. Proc Natl Acad Sci U S A, 1995. 92(16): p. 7297-301.
- 4 Urban-Klein, B., S. Werth, S. Abuharbeid, F. Czubayko, and A. Aigner, *RNAi-mediated gene-targeting through systemic application of polyethylenimine (PEI)-complexed siRNA in vivo*. Gene Ther, 2005. 12(5): p. 461-6.
- 5 Behr, J., *The proton sponge: A trick to enter cells the viruses did not exploit*. chimia, 1997. 51: p. 34-36.
- 6 Park, T.G., J.H. Jeong, and S.W. Kim, *Current status of polymeric gene delivery systems*. Adv Drug Deliv Rev, 2006. 58(4): p. 467-86.
- 7 Fischer, D., T. Bieber, Y. Li, H.P. Elsassser, and T. Kissel, *A novel non-viral vector for DNA delivery based on low molecular weight, branched polyethylenimine: effect of molecular weight on transfection efficiency and cytotoxicity*. Pharm Res, 1999. 16(8): p. 1273-9.
- 8 Kunath, K., A. von Harpe, D. Fischer, H. Petersen, U. Bickel, K. Voigt, and T. Kissel, *Low-molecular-weight polyethylenimine as a non-viral vector for DNA delivery: comparison of physicochemical properties, transfection efficiency and in vivo distribution with high-molecular-weight polyethylenimine*. J Control Release, 2003. 89(1): p. 113-25.
- 9 Werth, S., Urban-Klein, B., Dai L., Höbel S., Grzelinski M., Bakowsky U., Czubayko F., Aigner A., *A low molecular weight fraction of polyethylenimine (PEI) displays increased transfection efficiency of DNA and siRNA in fresh or lyophilized complexes*. J Control Rel, 2006. 112: p. 257-270.
- 10 Grzelinski, M., B. Urban-Klein, T. Martens, K. Lamszus, U. Bakowsky, S. Hobel, F. Czubayko, and A. Aigner, *RNA interference-mediated gene silencing of pleiotrophin through polyethylenimine-complexed small interfering RNAs in vivo exerts antitumoral effects in glioblastoma xenografts*. Hum Gene Ther, 2006. 17(7): p. 751-66.
- 11 Beyerle, A., S. Hobel, F. Czubayko, H. Schulz, T. Kissel, A. Aigner, and T. Stoeger, *In vitro cytotoxic and immunomodulatory profiling of low molecular weight polyethylenimines for pulmonary application*. Toxicol In Vitro, 2009. 23(3): p. 500-8.
- 12 Oberdorster, G., E. Oberdorster, and J. Oberdorster, *Nanotoxicology: an emerging discipline evolving from studies of ultrafine particles*. Environ Health Perspect, 2005. 113(7): p. 823-39.
- 13 Brown, D.M., Wilson M.R., MacNee W., Stone V., Donaldson K., *Size-dependent proinflammatory effects of ultrafine polystyrene particles: a role for surface area and oxidative stress in the enhanced activity of ultrafines*. Toxicol Appl Pharmacol, 2001. 175: p. 191-199.
- 14 Nemmar, A.H.M.F., Hoet Peter H.M., Vermeylen Josef, Nemery Benoit, *Size effect of intratracheally instilled particles on pulmonary inflammation and vascular thrombosis*. Toxicol Appl Pharmacol, 2003. 186: p. 38-45.
- 15 Oberdorster, G., A. Maynard, K. Donaldson, V. Castranova, J. Fitzpatrick, K. Ausman, J. Carter, B. Karn, W. Kreyling, D. Lai, S. Olin, N. Monteiro-Riviere, D.

- Warheit, and H. Yang, *Principles for characterizing the potential human health effects from exposure to nanomaterials: elements of a screening strategy*. Part Fibre Toxicol, 2005. 2: p. 8.
- 16 Akhtar, S. and I. Benter, *Toxicogenomics of non-viral drug delivery systems for RNAi: potential impact on siRNA-mediated gene silencing activity and specificity*. Adv Drug Deliv Rev, 2007. 59(2-3): p. 164-82.
- 17 Sayes, C.M., K.L. Reed, and D.B. Warheit, *Assessing toxicity of fine and nanoparticles: comparing in vitro measurements to in vivo pulmonary toxicity profiles*. Toxicol Sci, 2007. 97(1): p. 163-80.
- 18 Mosmann, T., *Rapid colorimetric assay for cellular growth and survival: application to proliferation and cytotoxicity assays*. J Immunol Methods, 1983. 65(1-2): p. 55-63.
- 19 Choksakulnimitr Suthummar, M.S., Tokuda Hideaki, Takakura Yoshinobu, Hashida Mitsuru, *In vitro cytotoxicity of macromolecules in different cell culture systems*. J Control Release, 1995. 34: p. 233-214.
- 20 Prabhakar, U., E. Eirikis, M. Reddy, E. Silvestro, S. Spitz, C. Pendley, 2nd, H.M. Davis, and B.E. Miller, *Validation and comparative analysis of a multiplexed assay for the simultaneous quantitative measurement of Th1/Th2 cytokines in human serum and human peripheral blood mononuclear cell culture supernatants*. J Immunol Methods, 2004. 291(1-2): p. 27-38.
- 21 Moghimi, S.M., P. Symonds, J.C. Murray, A.C. Hunter, G. Debska, and A. Szewczyk, *A two-stage poly(ethylenimine)-mediated cytotoxicity: implications for gene transfer/therapy*. Mol Ther, 2005. 11(6): p. 990-5.
- 22 Paris, S., A. Burlacu, and Y. Durocher, *Opposing roles of syndecan-1 and syndecan-2 in polyethyleneimine-mediated gene delivery*. J Biol Chem, 2008. 283(12): p. 7697-704.
- 23 Malek, A., F. Czubayko, and A. Aigner, *PEG grafting of polyethylenimine (PEI) exerts different effects on DNA transfection and siRNA-induced gene targeting efficacy*. J Drug Target, 2008. 16(2): p. 124-39.
- 24 Gautam, A., C.L. Densmore, E. Golunski, B. Xu, and J.C. Waldrep, *Transgene expression in mouse airway epithelium by aerosol gene therapy with PEI-DNA complexes*. Mol Ther, 2001. 3(4): p. 551-6.
- 25 Kawakami, S., Y. Ito, P. Charoensit, F. Yamashita, and M. Hashida, *Evaluation of proinflammatory cytokine production induced by linear and branched polyethylenimine/plasmid DNA complexes in mice*. J Pharmacol Exp Ther, 2006. 317(3): p. 1382-90.
- 26 Robbins, M., A. Judge, E. Ambegia, C. Choi, E. Yaworski, L. Palmer, K. McClintock, and I. MacLachlan, *Misinterpreting the therapeutic effects of small interfering RNA caused by immune stimulation*. Hum Gene Ther, 2008. 19(10): p. 991-9.
- 27 Melchjorsen, J., L.N. Sorensen, and S.R. Paludan, *Expression and function of chemokines during viral infections: from molecular mechanisms to in vivo function*. J Leukoc Biol, 2003. 74(3): p. 331-43.
- 28 Matsukura, S., F. Kokubu, M. Kurokawa, M. Kawaguchi, K. Ieki, H. Kuga, M. Odaka, S. Suzuki, S. Watanabe, H. Takeuchi, T. Kasama, and M. Adachi, *Synthetic double-stranded RNA induces multiple genes related to inflammation through Toll-like receptor 3 depending on NF-kappaB and/or IRF-3 in airway epithelial cells*. Clin Exp Allergy, 2006. 36(8): p. 1049-62.

3 PEGylation affects cytotoxicity and cell-compatibility of Poly(ethylene imine) for lung application: structure-function-relationships

Andrea Beyerle, Olivia Merkel, Tobias Stoeger, Thomas Kissel

Published in *Toxicology Applied Pharmacology* (2010); 242(2):146-54.

Author's contributions::

A.B. prepared the manuscript draft and wrote the manuscript, carried out the experimental work, analyzed and interpreted the data; O.M. measured the buffer capacity and provided the PEI-PEG polymers, T.S. reviewed and edited the manuscript, T.K. provided the PEI-PEG polymers, reviewed and edited the manuscript. All authors read and approved the final version of the manuscript.

3.1 Abstract

Poly(ethylene imine) (PEI) has widely been used as non-viral gene carrier due to its capability to form stable complexes by electrostatic interactions with nucleic acids. To reduce cytotoxicity of PEI, several studies have addressed modified PEIs such as block or graft copolymers containing cationic and hydrophilic non-ionic components. Copolymers of PEI and hydrophilic poly(ethylene glycol) (PEG) with various molecular weights and graft densities were shown to exhibit decreased cytotoxicity and potential for DNA and siRNA delivery.

In this study, we evaluated the cytotoxicity and cell-compatibility of different PEGylated PEI polymers in two murine lung cell lines. We found that the degree of PEGylation correlated with both cytotoxicity and oxidative stress, but not with proinflammatory effects. AB type copolymers with long PEG blocks caused high membrane damage and significantly decreased the metabolic activity of lung cells. In addition, they significantly increased the release of two lipid mediators such as 8-isoprostanes (8-IP) and prostaglandin E₂ (PGE₂) in a dose-dependent manner. In contrast, the cytokine profiles which indicated high levels of acute-phase cytokines such as TNF- α , IL-6, and G-CSF did not follow any clear structure-function relationship.

In conclusion, we found that modification of PEI 25 kDa with high degree of PEGylation and low PEG chain length reduced cytotoxic and oxidative stress response in lung cells, while the proinflammatory potential remained unaffected. A degree of substitution in the range of 10 to 30 and PEG-chain lengths up to 2000 Da seem to be beneficial and merit further investigations.

Key Words: poly(ethylene imine), lung, cytotoxicity, inflammation, membrane interaction

3.2 Introduction

The modification of cytotoxic properties of polycations remains a considerable challenge as biocompatible polymers are needed for repeated biomedical applications. A fundamental understanding of cytotoxic effects is of particular importance for the design of pulmonary delivery systems containing siRNA and plasmid DNA (pDNA). Targeted loco-regional delivery of polyplexes to the lung represents an emerging area of gene therapy research [1-3]. Poly(ethylene imine) (PEI) is one of the most extensively investigated polymers for gene delivery. One drawback of PEI is its relatively high cytotoxicity due to the aggregation of huge clusters of PEI on cell membranes, which can induce necrosis [4], and its interaction with blood components [5, 6]. The functionality of PEI as a gene carrier was significantly improved by grafting with hydrophilic poly(ethylene glycol) (PEG) to yield PEG-PEI copolymers [7, 8]. Complexation of PEG-PEI copolymers with nucleic acids generated nano-scale polyelectrolyte complexes (polyplexes) with a core-shell structure. In general, PEGylation improved solubility and colloidal stability [9], reduced surface charges [8], prolonged circulation time [6], and reduced complement activation [10], hence reducing interactions with plasma proteins and cells. The precise effect of PEGylation depends on many factors including molecular weight of PEG and PEI, density of PEG grafting, type of nucleic acid, and environment. PEG-PEIs were extensively studied for delivery of plasmids [11, 12] as well as recently for oligonucleotides [13] and siRNA [14]. Often the molecular weight of PEG was suggested as the main factor determining polyplex size and colloidal stability [15]. However, the chain length and grafting density of PEG strongly affects pDNA and siRNA condensation and stability in different ways [8, 14]. Therefore, siRNA delivery and gene transfer should be considered separately regarding transfection efficiency [16]. Studies of PEG-PEI as a carrier for nucleic acids focused mainly on polyplex properties, but failed to report the toxicity profiles of copolymers alone [15]. PEI based polyplexes usually contain an excess of uncomplexed PEI which cannot be degraded in the body [5, 17].

Therefore, we focused in this study on the free PEI based polymers. As cationic nanoparticles disrupt lipid bilayers [18, 19], we studied the structure-function relationship of four different PEGylated PEI25kDa copolymers concerning cytotoxicity and cell-compatibility. With regard to the therapeutic application in humans, high efficiency as well as safety and biocompatibility are the most critical issues for any gene delivery system. The interaction of cationic polymers with the negatively charged cell surface has been described in the literature to cause high cytotoxicity [20] but only a few studies systematically investigated the interaction of soluble polymers with the cell surface [21, 22]. To our knowledge, no mechanistic study of the cytotoxicity and cell-compatibility of polymeric non-viral vector systems alone have been reported so far.

Promising results of pulmonary application of PEI-based non-viral nucleic acid vector systems were recently communicated under *in vivo* conditions after inhalation [23, 24]. One potential advantage of nanocarriers could be that these particles tend to escape the detection by the macrophage clearance system and remain in the lung sufficiently long to release their 'payload' in a controlled manner [25]. However, instilled non-biodegradable polystyrene nanospheres have been shown to induce pulmonary inflammation [26] and pulmonary delivery of positively charged amine-polystyrene particles caused systemic effects like enhanced thrombosis via platelet activation [27]. Thus, *in vitro* toxicity studies are considered as an important adjunct to *in vivo* studies [25] and need to precede any *in vivo* study.

In this study we evaluated structure-function relationships of polymeric non-viral vector systems regarding cytotoxicity and cell-compatibility. The cytotoxic and proinflammatory effects as well as the oxidative potential of four different PEI-PEG copolymers was evaluated in comparison to PEI 25kDa (standard). Two murine alveolar cell lines were selected based on the fact that (i) for inhaled particles, the fragile, alveolar epithelium represents the first barrier, and that (ii) macrophages are vital to the regulation of immune response and the development of inflammation. Our aim was an increased understanding of the toxicity of PEI-

based polymeric non-viral vector systems on a cellular level to delineate optimal structure-function properties for optimized synthesis of such vector systems for *in vivo* applications.

3.3 Materials and Methods

Materials

Branched poly(ethylene imine) (PEI) with a molecular weight of 25 kDa (Polymin, water-free, 99 %) was a gift of BASF, Ludwigshafen. The copolymers poly(ethylene imine)-graft-poly(ethylene glycol) (PEI-PEG) with a PEG content of approximately 50 % (w/w) were synthesized as previously described [8, 11] by grafting linear PEG of 0.55, 2, 5, and 20 kDa onto branched PEI 25 kDa. These graft copolymers were designated using following nomenclature: PEI(25k)-g-PEG(x)_n. The number in brackets (25k or x, where x= 0.55 k, 2 k, 5 k, and 20 k) represents the molecular weight of the PEI or PEG block in Da, and the index n is the average number of PEG blocks per PEI molecule. This number was calculated on the basis of ¹H-NMR spectra as described previously [11]. Polymer dilutions were prepared in sterile, sodium chloride solution (0.9 %).

Polymer buffer capacity

The buffer capacity of all polymers was measured in potentiometric titration assays using a Mettler Toledo DL50 Titrator (Mettler-Toledo GmbH, Giessen, Germany). Polymers were dissolved in distilled water and briefly sonicated. All polymer solutions were prepared to contain the same number of PEI amine groups (20 mg PEI 25 kDa in 20 ml, equivalent to 23 mM amines), which allows for a direct comparison of the buffering capacity of each polymer per mole of amine. The pH of the polymer was measured during slow addition of 0.1 N HCl under vigorous stirring. All experiments were run in duplicate and evaluated by the LabX Software (Mettler-Toledo GmbH, Giessen, Germany) concerning equivalence points and pKa values.

Cell culture

Experiments were carried out using murine alveolar epithelial – like type II cells (LA4; ATCC No. CCL-196TM) and murine alveolar macrophages (MH-S; ATCC No. CRL-2019). LA4 cells were grown in HAM's F12 medium with stable L-glutamine containing 15 % fetal

bovine serum (FBS, Gibco, Germany) and 1 % non essential amino acids and 100U/ml penicillin and 100mg/ml streptomycin. MH-S cells were cultured in DMEM medium with stable L-glutamine supplemented with 10 % fetal bovine serum (FBS, Gibco, Germany) and 100 U/ml penicillin and 100 mg/ml streptomycin at 37 ° C and 5 % CO₂. All cells were passaged every 2-3 days. All cell culture reagents were obtained from Biochrom AG, Seromed, Germany, unless otherwise stated.

Cell Proliferation assay

The metabolic cell activity was determined using the Cell Proliferation Reagent WST-1 (Roche Diagnostics, Germany) according to [28]. Briefly, LA4 and MH-S cells were seeded at a density of 8×10^3 cells/well in 96-well-plate in cell culture medium containing FBS and grown overnight in an incubator at 37 ° C and 5 % CO₂. Medium was replaced before cells were treated. The polymer dilutions were prepared as described above and added to the appropriate wells. After 72 h of incubation, the relative viability [%] related to control samples (untreated cells) was calculated by following equation: Cell viability = $(OD_{\text{sample}}/OD_{\text{control}}) * 100$. All data represent three independent experiments. IC₅₀ values were calculated as polymer concentration which inhibits growth of 50 % of cells relative to untreated control cells according to [29]. The results of optical density measurements were fitted logistically by the Levenberg-Marquardt method of least-squares minimization for nonlinear equations under default conditions using Origin 7.0 (Origin LabSoftware, Northampton, USA) by the following equation: $Y = Y_0 + (Y_m - Y_0) / (1 + (C/C_0))$, where C₀ is the IC₅₀ dose, Y is the optical density in a well containing a particular polymer/extract of concentration C. Y₀ and Y_m are the optical densities corresponding to 0 % viability and 100 % viability, respectively.

Cytotoxicity (LDH-assay)

For detection of the cytosolic enzyme lactate dehydrogenase (LDH) the Cytotoxicity Detection Kit (Roche Diagnostics, Germany) was used according to the manufacturer's

protocol. Briefly, cells were cultured in 24-well-plates at a density of 0.25×10^6 cells/well and incubated in an incubator overnight for adherence. To avoid interference with the assay reagents, the cell culture medium was replaced with serum-reduced (2% FBS) cell culture medium without antibiotics before addition of polymers. The polymer dilutions were added to the appropriate wells and LDH kinetic was observed after 0.5 h, 1 h, 2 h, 4 h, 6 h, and 24 h exposure time. The LDH concentration in the cell culture supernatant was determined spectrophotometrically at a wavelength of 492 nm using an ELISA reader (Labsystems iEMS Reader MF). Cells treated with 2 % (w/v) Triton X-100 served as a control according to the manufacturer's protocol and revealed maximum LDH release (100 %) corresponding to $OD_{\text{high control}}$. The relative LDH release is defined by the ratio of LDH released over total LDH (high control) and was calculated as follows: Cytotoxicity [%] = $(OD_{\text{sample}} - OD_{\text{low control}}) / (OD_{\text{high control}} - OD_{\text{low control}}) * 100$, where $OD_{\text{low control}}$ was the absorption from the supernatant of the untreated cells. Less than 10 % LDH release was regarded as non-toxic effect level in our experiments according to [21]. All data represents three independent experiments.

Lipid mediators

Extracellular appearance of 8-Isoprostanes (8-IP) and prostaglandin E_2 (PGE_2) was investigated in the cell culture supernatants according to [30]. Briefly, the supernatants of the cell culture experiments were deproteinized by adding an 8-fold volume of 90 % methanol containing 0.5 mM EDTA and 1mM 4-hydroxy-2,2,6,6,-tetramethylpiperidine-1oxyl, pH 7.4. To completely remove proteins, the suspensions were stored at -80°C for 24h followed by a centrifugation step at 10.000 g for 20 min at 4°C . Aliquots of the supernatants were dried in a vacuum centrifuge, dissolved in assay buffer, and used for quantification of 8-IP and PGE_2 using their specific enzyme immunoassays (Cayman Chemical Company, Ann Arbor, MI, USA) according to the manufacturer's instructions.

Cytokine release

In a multiplexing Luminex assay (Linco Research, St. Charles, MO), 8 cytokines/chemokines were simultaneously detected in the cell culture supernatant. In this study, the secretion of the following cytokines/chemokines was investigated: IL-1 α , IL-6, TNF- α , G-CSF, CXCL1, CXCL10, CCL2, and CCL3. The assay was performed as described previously [31] and mean fluorescence intensity (MFI) was detected by the Multiplex plate reader (Luminex System, Bio-Rad Laboratories, Germany) for each sample (50 μ l) with a minimum of 100 beads per region being analyzed. The raw data (MFI) were captured using the Multiplex plate reader software (Bioplex Manager, Version 2.0). For data analysis, a 5-parameter logistic curve fit was applied to each standard curve and sample.

Quantitative reverse –transcriptase polymerase chain reaction (qRT-PCR)

Cells were seeded at a density of 0.5×10^6 cells/well (2ml) in 6-well-plates (FALCON, Germany) and were allowed to adhere overnight in an incubator at 37 ° C and 5 % CO₂. After 24 h, cell culture medium was replaced and the appropriate amount of polymer dilution was added to the well in a final volume of 2ml/well. Cells were treated with the polymers for 2 h or 6 h, respectively. At these two different time points, RNA was isolated from the cells using the RNeasy Mini Kit (Qiagen, Hilden, Germany). DNase digestion was carried out using DNase I (Qiagen, Hilden, Germany). The quality of RNA was checked in an agarose-gel (1%) containing SYBR Safe (Invitrogen, Karlsruhe, Germany) and the RNA amount was quantified using an ND-1000 Spectrophotometer (NanoDrop Technologies, Inc., Wilmington, DE, US) at the absorbance ratio of 260 and 280 nm. 1 μ g of total DNase I treated RNA was used for the first-strand cDNA reaction using nonamer primers (Metabion, München, Germany) and Superscript II reverse transcriptase (Invitrogen, Karlsruhe, Germany). Quantitative transcript levels were analyzed using Absolute QPCR SYBR Green Mix plus ROX kit (ABgene, Hamburg, Germany) with the ABI Prism 7000 Sequence detection System (Applied Biosystems, Foster City, CA, USA). The comparative threshold cycle (CT) method was carried out to calculate the relative abundance of transcript [32]. Following genes were

investigated and normalized to the house keeping gene hydroxanthine guanine phosphoribosyltransferase 1 (*Hprt1*): glutathione-S-transferase, alpha 1 (*Gst1a*), glutathionreductase 1 (*Gsr*), heme oxygenase (*Hmox-1*), metallothionein 2 (*Mt2*) and cyclooxygenase 2 (*Ptgs2*). The primer pairs, which were used for the gene expression profiling are listed in table 1.

Statistical analyses

All values are presented as mean±standard error (SEM) of at least three independent experiments, unless otherwise stated. Significant differences between two groups were evaluated by Student's t-test and between more than two groups by one-way analysis of variance followed by Tukey's multiple comparison test. In case of highly different variances, we evaluated significant differences by using the two-tailed t-test with Welch's correction. Statistical analysis were performed using the program STATGRAPHICS PLUS Version 5.0 (Statpoint, Inc., Virginia, USA) and GraphPad Prism 5.0 (GraphPad Software, Inc., La Jolla, CA 92037 USA).

Table 1: *List of primer sequences*

<u>Ref.sequence¹</u>	<u>Gene abbr.¹</u>	<u>Gene name</u>	<u>forward primer sequence²</u>	<u>reverse primer sequence²</u>
NM_008181	Gst1a	glutathione-S-transferase, alpha 1	AGG AGA GAG CCC TGA TTG	CTG TTG CCC ACA AGG TAG
NM_010344	Gsr	glutathione reductase 1	AGG GCC ACA TCC TAG TAG AC	GTC GCT GAA GAC CAC AGT AG
NM_010442	Hmox-1	heme oxygenase (decycling) 1	TTCTGGTATGGGCCTCACTGG	ACCTCGTGGAGACGCTTTACA
NM_008630	Mt2	metallothionein 2	TAG ATG GAT CCT GCT CCT GC	CAC TTG TCG GAA GCC CTC TT
NM_011198	Ptgs2	prostaglandin-endoperoxide synthase 2	CAA CAC CTG AGC GGT TAC	GTT CCA GGA GGA TGG AGT
NM_013556	Hprt1	hypoxanthine guanine phosphor- ribosyltransferase 1	GTT GGA TAC AGG CCA GAC TTT GT	CAC AGG CTA GAA CAC CTG C

¹All genes are abbreviated by their official MGI symbol (Mouse Genome Informatics, <http://www.informatics.jax.org>).

²Transcript sequences are identified by the NCBI Reference Sequences ID. Primer were derived by Primer3 open source software, (<http://primer3.sourceforge.net/>) using the primer picking conditions: GC: 55-60%; annealing: 55°C.

3.4 Results

In this study, we investigated the structure-function relationship of PEGylated PEI copolymers concerning their cytotoxicity and cell-compatibility in comparison to the backbone polymer, PEI 25kDa. PEI 25kDa was grafted with PEG chains of different molecular weights (0.55 kDa, 2 kDa, 5 kDa, and 20 kDa), but the PEG weight ratio of approximately 50 % was kept constant. We hypothesized that the degree of PEGylation and the PEG chain length might affect not only cytotoxicity but might also modify their biocompatibility, especially their proinflammatory effects.

Buffer capacity

Polymer solutions of equivalent nitrogen concentrations were examined by potentiometric titration to evaluate the influence of PEGylation on the buffer capacity. Potentiometric titration curves are shown in supplementary material, S1. PEGylation reduced the buffer capacity of the polymers. Higher degrees of PEGylation caused lower pKa values due to PEG grafting of amino groups. The reduced buffer capacity could be explained by the reduced amount of secondary amines which were less abundant in the stronger PEGylated PEI copolymers, namely PEI(25)-PEG(0.55)30 and PEI(25)-PEI(2)10. The buffer capacities of stronger PEGylated PEI-PEG copolymers were approximately at the physiological pH of 7.4, whereas the AB diblock-copolymer PEI(25)-PEG(20)1 yielded a similar pKa value to unmodified PEI 25 kDa of 8.36. It has to be noted that in the range of pH 4-6, usually attributed to the lyso-/ endosomal compartment, buffer capacity was not significantly different for all polymers. In general, regarding the pKa values, PEI 25kDa and PEI(25)- PEG(20)1 had more basic properties compare to the higher modified PEG-PEI copolymers. It can therefore be hypothesized that these polymers have a more pronounced ability to balance the acidic endosomal environment and chloride influx during the endosomal ripening and strongly promote the osmotic swelling of endosomes.

Cell proliferation study

For each polymer, the influence on metabolic activity was analyzed in two cell types by estimating the IC₅₀ values (Table 2). The IC₅₀ values clearly depended on the grafting degree of PEG on PEI 25 kDa and were similar in both cell lines. The higher the degree of PEGylation, the higher was the IC₅₀ value, pointing out that PEI(25)-PEG(0.55)30 and PEI(25)-PEG(2)10 were the most favourable copolymers for further *in vivo* investigation with regard to their reduced impact on cell viability.

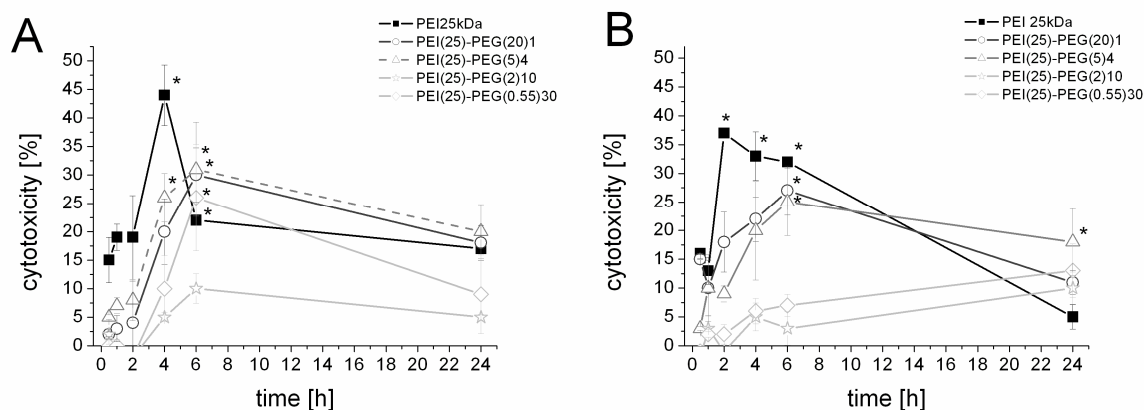
Table 2: IC₅₀ values

Polymer	LA4 ¹	r ²	MH-S ¹	r ²
PEI25kDa	0.002±1.94*10E-4	0.996	0.005±6,46*10E-4	0.983
PEI(25)-PEG(20)1	0.014±0.0035	0.967	0.011±0.0031	0.98
PEI(25)-PEG(5)4	0.014±0.003	0.985	0.007±3.71*10E-4	0.998
PEI(25)-PEG(2)10	0.022±0.0088	0.988	0.027±0.003	0.99
PEI(25)-PEG(0.55)30	0.033±0.004	0.968	0.021±0.006	0.995

¹IC₅₀ values were given in mg/ml as mean±SD of three independent experiments. Cell proliferation in LA4 and MH-S was analyzed using WST-1 assay after 72h particle exposure and IC₅₀ values were calculated using sigmoidal fitting as described in material and methods.

Cytotoxicity

In addition to the influence of metabolic activity, the kinetics of membrane damage effects caused by PEI-PEG derivatives and PEI 25 kDa were analyzed. In both cell lines, the maximal leakage of LDH was determined after 6h for all PEI-PEG molecules and PEI 25 kDa (Fig. 1).

Figure 1: Cytotoxicity**Figure 1: Cytotoxicity**

LDH leakage correlated to degree of PEGylation [11] at the highest dose of 50 $\mu\text{g/ml}$ PEI. LDH release was determined using Cytotoxicity detection kit (Roche) after 0.5, 1, 2, 4, 6, and 24 h polymer treatment in LA4 cells (A) and MH-s cells (B). For each time point three independent experiments were carried out and the values were expressed as mean \pm SD. Less than 10% LDH release were regarded as non-toxic effect level in our experiments [21]. Significant difference to control was presented as asterisk with $*p < 0.05$.

According to the IC_{50} values, the degree of PEGylation on PEI 25 kDa correlated well with the cytotoxic effect at high PEI concentrations and the membrane damage in a time-dependent manner. Again, the higher the PEGylation degree and the lower the molecular weight of PEG, the lower was the cytotoxic effect.

Lipid mediators

Because polycations are in general known for their strong interaction with the plasma-membrane, it was assumed that the generation of lipid mediators could be one toxicological mechanism explaining the cytotoxic behaviour of PEI-PEG and PEI. Therefore, the extracellular release of two major lipid mediators, namely 8-isoprostanes (8-IP) and prostaglandin E_2 (PGE_2) was investigated. After treatment for 24 h, the release of the lipid mediators were similar in both cell lines. PEI 25 kDa, PEI(25)-PEG(20)1, and PEI(25)-PEG(5)4 caused the strongest release of the two lipid mediators, which was detected to be more than 25-fold increased compared to control. The higher the degree of PEGylation on

PEI 25 kDa, the lower were the levels of 8-IP and PGE₂, showing the same trend as observed for the metabolic activity and LDH leakage (Fig. 2).

Figure 2: Release of lipid mediators

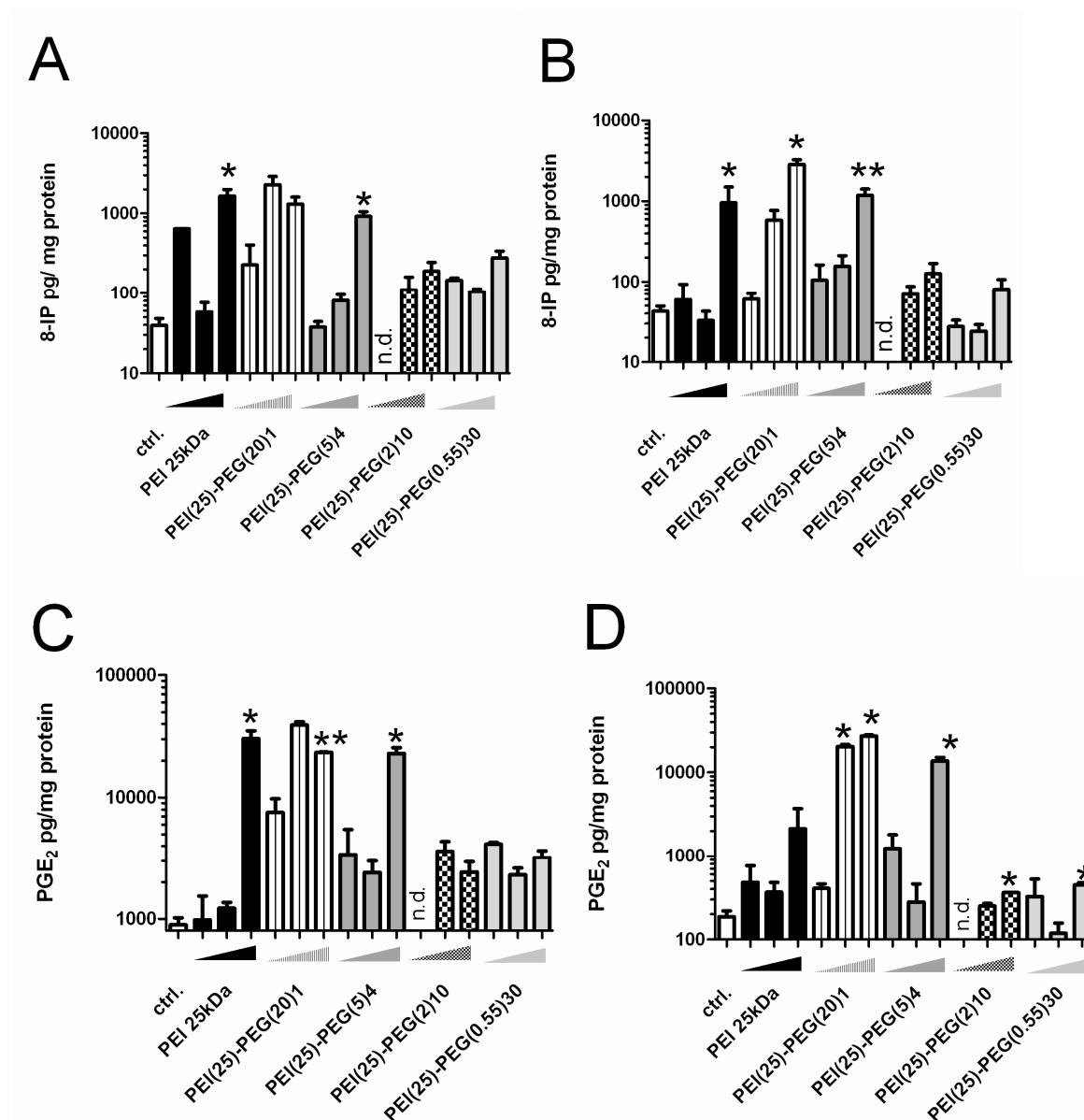


Figure 2: Release of lipid mediators

Determination of 8-Isprostanes (upper panel) and Prostaglandin E₂ (lower panel) in the supernatant, after 24 h polymer treatment of LA4 cells (A and C) and MH-S cells (B and D). Control is given in white bars, PEI 25 kDa in black bars, PEI(25)-PEG(20)1 in bars with vertical lines, PEI(25)-PEG(5)4 in dark grey bars, PEI(25)-PEG(2)10 in chequered bars and PEI(25)-PEG(0.55)30 in light grey bars. Polymer concentrations were indicated as increasing triangle with concentration of 0.5 μg/ml, 5 μg/ml and 50 μg/ml PEI. Each value was normalized to the protein amount of the supernatant and was

presented as mean \pm SEM, $n=3$; *n.d.*= not determined. Asterisks expressed significant changes vs. control (supernatant from untreated cells), * $p<0.05$ and ** $p<0.01$.

Proinflammatory effects

As any inflammatory reaction related to the therapeutic application of PEI-based vectors could be of general concern, the release of eight proinflammatory cytokines after treatment for 24 h with different PEI-PEG copolymers was investigated. The cytokine release was highly different for all polymers and caused mainly high levels of acute-phase cytokines such as IL-1 α , IL-6, TNF- α , and G-CSF. None of the investigated polymers elevated the chemokines levels of CXCL1, CXCL10, CCL2, and CCL3 after polymer treatment compared to control (data not shown). A clear dose-response or difference in the pattern of cytokine response regarding the degree of PEGylation of the polymers could not be found, (Fig. 3).

Figure 3 A-B: Cytokine response

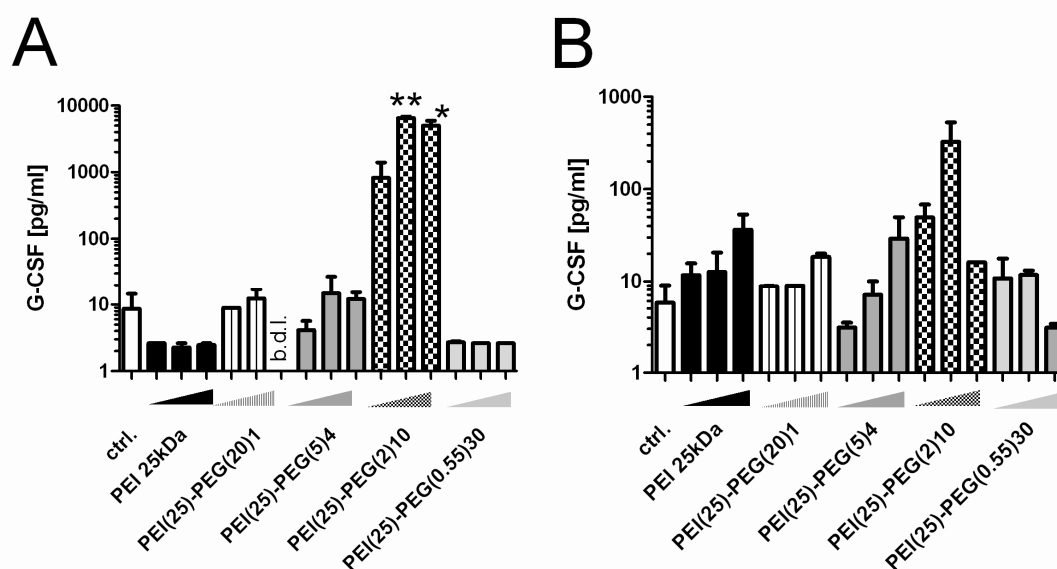


Figure 3 A-B: Cytokine response

G-CSF release was measured after 24h polymer treatment in LA4 cells (A) and MH-S cells (B). Three polymer concentrations (0.5, 5, 50 μ g/ml) were exposed to the cells; control is given in white bars, PEI 25 kDa in black bars, PEI(25)-PEG(20)1 in bars with vertical lines, PEI(25)-PEG(5)4 in dark grey bars, PEI(25)-PEG(2)10 in chequered bars and PEI(25)-PEG(0.55)30 in light grey bars. Values were presented as mean \pm SEM and asterisks expressed significant changes vs. control (supernatant

from untreated cells), * $p < 0.05$ and ** $p < 0.01$, values under the detection limit of each cytokine were indicated with *b.d.l.*: below detection limit.

The highly grafted polymer PEI(25)-PEG(0.55)30 caused the lowest proinflammatory response in the alveolar epithelial cells, but high levels of IL-6 were found in an inverted dose-response (0.5 $\mu\text{g/ml}$: 37.91 ± 7.35 pg/ml, 5 $\mu\text{g/ml}$: 22.35 ± 8.1 pg/ml, 50 $\mu\text{g/ml}$: 15.1 ± 2.23 pg/ml vs. ctrl. 2.48 pg/ml). In the alveolar macrophages, 5 $\mu\text{g/ml}$ PEI(25)-PEG(0.55)30 caused elevated levels of TNF- α and G-CSF (TNF- α : 23.92 ± 2.97 pg/ml vs. ctrl. 6.07 pg/ml, G-CSF: 11.78 ± 1.34 pg/ml vs. ctrl. 2.49 pg/ml). In comparison, PEI 25 kDa elicited IL-6 levels in the epithelial cells in a similar inverted dose-response manner like PEI(25)-PEG(0.55)30 (IL-6 values for PEI 25 kDa: 0.5 $\mu\text{g/ml}$: 15.18 ± 6.96 pg/ml, 5 $\mu\text{g/ml}$: 12.31 ± 3.58 pg/ml, 50 $\mu\text{g/ml}$: 2.96 ± 0.32 pg/ml vs. ctrl. 2.48 pg/ml) and yielded high levels of G-CSF in the macrophages in a dose-dependent manner (0.5 $\mu\text{g/ml}$: 11.73 ± 4 pg/ml, 5 $\mu\text{g/ml}$: 4.77 ± 0.57 pg/ml, 50 $\mu\text{g/ml}$: 52.81 ± 5.61 pg/ml vs. ctrl. 2.49 pg/ml). Interestingly, PEI(25)-PEG(2)10 caused the highest proinflammatory response and released high levels of IL-6, G-CSF and TNF- α in both cell lines. Despite no clear structure-function relationship of the cytokine profile, cytokine response was cell type dependent. In the alveolar epithelial cells, IL-6 release seemed to be more prominent and in most cases non linear to the dose, whereas in the alveolar macrophages the growth factor G-CSF and TNF- α were in most cases significantly elevated after treatment with high doses of polymer.

Gene expression analysis

To get an insight in the underlying pathways related to the observed polymer-cell interactions, first the expression profile of prostaglandin endoperoxide synthase (*Ptgs2*, the rate-limiting enzyme in the conversion of membrane derived inflammatory intermediates like prostaglandin E_2) and second four genes mainly related to oxidative stress response (*Hmox-1*, *Gst1a*, *Gsr*, and *Mt2*) were analyzed upon PEI treatment over 2 h and 6 h.

In both cell lines, the levels of *Ptgs2* expression were strongly induced by PEI polymer treatment (Fig. 4).

Figure 4 A-B: Gene expression of prostaglandin endoperoxide synthase 2 (*Ptgs2*)

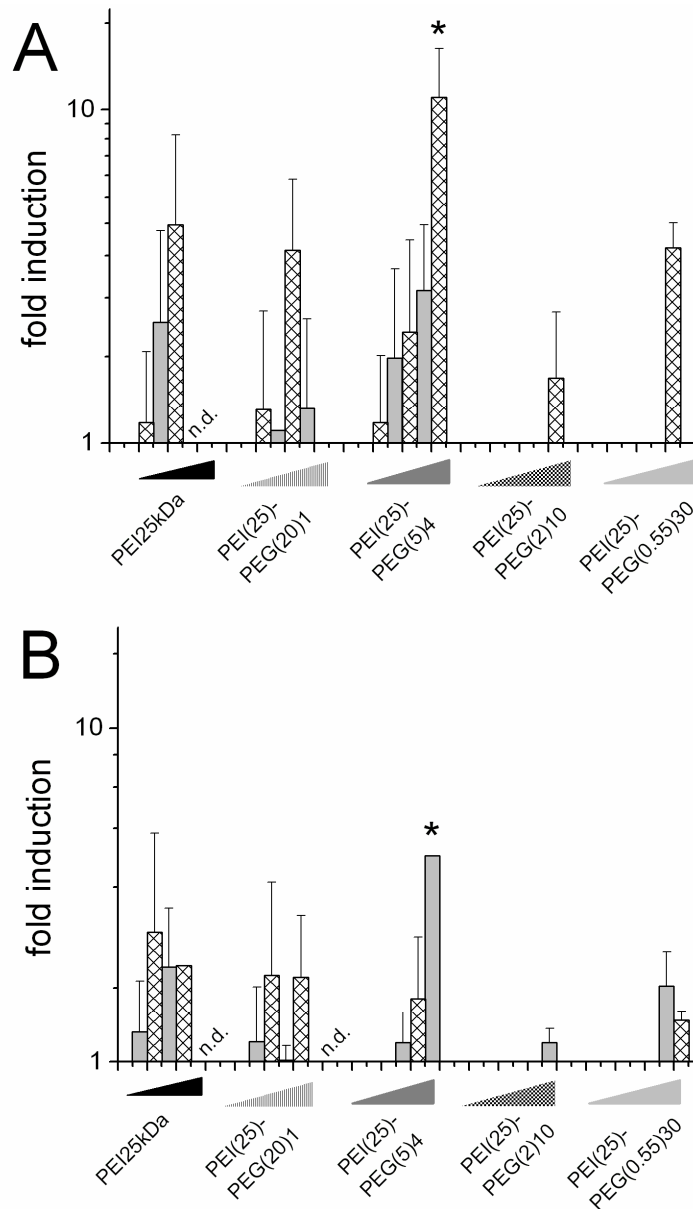


Figure 4 A-B: Gene expression of prostaglandin endoperoxide synthase 2 (*Ptgs2*)

Gene expression of *Ptgs2* after 2 h (gray bars) and 6 h (sparsed bars) treatment of polymer in LA4 (A) and MH-S (B) cells; PEI 25 kDa and PEI-PEG copolymers were fold induction was calculated using comparative cycle threshold (CT) method normalized to the house keeping gene *Hprt 1*. Values were presented as mean \pm SD and asterisks expressed significant changes vs. control (untreated cells), * $p < 0.05$.

Strongest expressions were detected upon treatment with 50 µg/ml PEI(25)-PEG(5)4 yielding 11-fold induction after 6 h in LA-4 and 4-fold induction after 2 h in MH-S cells. Other polymers like PEI(25)-PEG(0.55)30, PEI(25)-PEG(2)10 and PEI25 kDa caused moderate *Ptgs2* expression of 4-fold induction in LA-4 and 2-fold induction in MH-S cells. Overall, *Ptgs2* expression matches well with the release pattern of the arachidonic acid derivatives 8-IP and PGE₂. To address the oxidative stress potential of the polymers, four additional genes related to antioxidative stress response were investigated. The mean induction of all four genes was calculated and is shown in Table 3 for both cell lines. PEI 25 kDa yielded the highest induction (4.5-fold) of the four oxidative stress genes in MH-S cells after 2 h. PEI(25)-PEG(20)1 and PEI(25)-PEG(5)4 showed induction levels of more than 1.5-fold, and stronger PEGylated PEI copolymers induced oxidative stress response less than 1.5-fold induction after incubation for 2 h and 6 h. Oxidative stress responses differed between epithelial and macrophage cells, but respective transcript levels were overall higher after 2 h exposure compared to 6h. Regarding their potency to induce intracellular oxidative stress, the polymers can be arranged in the following ascending order: LA4: PEI(25)-(20)1 = PEI(25)-(2)10 < PEI(25)-(0.55)30 < PEI25 kDa < PEI(25)-(5)4 and MH-S: PEI(25)-(2)10 = PEI(25)-(0.55)30 < PEI(25)-(20)1 = PEI(25)-(5)4 < PEI25 kDa. In both cell lines, PEI25 kDa revealed to be one of the highly active polymer inducing an antioxidative response.

Table 3: *Oxidative stress response*¹

	<i>GstYa</i>		<i>Gsr</i>		<i>Hmox-1</i>		<i>Mt-2</i>	
	<i>LA4</i>	<i>MH-S</i>	<i>LA4</i>	<i>MH-S</i>	<i>LA4</i>	<i>MH-S</i>	<i>LA4</i>	<i>MH-S</i>
2h								
PEI 25kDa								
0.5µg/ml	0.87	0.90	0.66	1.13	0.97	1.31	1.81	2.86
5µg/ml	0.99	0.75	0.75	1.05	1.32	1.25	*7.64	3.69
50µg/ml	n.d.	1.00	n.d.	1.54	n.d.	1.65	n.d.	0.79
PEI(25)-PEG(20)1								
0.5µg/ml	1.00	0.91	1.00	1.05	0.91	1.00	2.14	2.20
5µg/ml	1.03	1.06	0.79	0.93	0.88	1.08	0.48	3.41
50µg/ml	1.23	n.d.	0.74	n.d.	0.99	n.d.	0.63	n.d.
PEI(25)-PEG(5)4								
0.5µg/ml	1.41	0.97	1.07	0.95	0.65	0.69	5.60	1.84
5µg/ml	1.17	1.14	1.15	1.16	0.96	0.72	5.84	1.97
50µg/ml	1.09	n.d.	1.12	n.d.	1.61	n.d.	1.35	n.d.
PEI(25)-PEG(2)10								
0.5µg/ml	0.88	0.99	0.94	0.98	0.81	0.98	1.00	1.64
5µg/ml	0.79	0.83	0.96	0.94	0.84	0.97	0.93	1.54
50µg/ml	0.80	0.83	1.04	1.04	0.88	0.99	0.88	1.15
PEI(25)-PEG(0.55)30								
0.5µg/ml	1.37	1.21	1.00	1.00	0.78	0.92	2.49	1.50
5µg/ml	1.28	1.14	0.95	1.01	0.73	0.87	4.13	1.73
50µg/ml	1.14	0.97	0.95	0.95	0.73	1.10	3.87	1.74
6h								
PEI 25kDa								
0.5µg/ml	0.95	0.71	1.01	1.25	1.26	1.32	1.37	3.74
5µg/ml	0.95	1.20	1.00	1.02	1.77	1.06	2.69	3.49
50µg/ml	n.d.	n.d.	n.d.	n.d.	n.d.	n.d.	n.d.	n.d.
PEI(25)-PEG(20)1								
0.5µg/ml	1.06	0.71	0.95	0.94	1.17	1.07	1.43	3.81
5µg/ml	0.87	1.20	1.13	1.18	1.32	1.14	1.45	1.64
50µg/ml	n.d.	n.d.	n.d.	n.d.	n.d.	n.d.	n.d.	n.d.
PEI(25)-PEG(5)4								
0.5µg/ml	1.06	0.91	0.93	1.62	1.36	0.93	1.53	2.75
5µg/ml	1.07	1.17	0.81	1.19	1.55	1.38	2.29	3.86
50µg/ml	3.16	n.d.	1.46	n.d.	*11.50	n.d.	*9.60	n.d.
PEI(25)-PEG(2)10								
0.5µg/ml	1.23	0.79	1.23	0.86	1.18	0.82	1.37	1.65
5µg/ml	1.10	0.75	0.90	0.89	1.04	0.76	1.33	1.77
50µg/ml	0.77	0.73	0.87	0.91	1.15	0.78	1.00	1.24
PEI(25)-PEG(0.55)30								
0.5µg/ml	0.82	0.71	0.88	0.90	1.26	0.81	1.20	1.65
5µg/ml	0.83	1.04	0.83	1.06	1.19	1.04	1.34	2.04
50µg/ml	0.70	1.16	0.78	0.91	1.38	1.10	1.13	1.87

¹Oxidative stress response expressed as fold induction of glutathione-S-transferase, alpha 1 (*Gst1a*), glutathione reductase (*Gsr*), heme oxygenase 1 (*Hmox-1*), and metallothionein 2 (*Mt2*) after 2h and 6h in LA4 (left) and MH-S cells (right) after treatment with PEI 25kDa and PEI-PEG copolymers (0.5µg/ml, 5.0µg/ml and 50µg/ml). Gene induction more than 2-fold increase were bold highlighted, asterisks expressed significant changes vs. control (untreated cells), *p<0.05.

3.5 Discussion

Cytotoxicity

PEI is one of the most efficient non-viral vector system for transfection of plasmid DNA (pDNA) and siRNA in cell culture as well as *in vivo* [33, 34]. However, pronounced cellular toxicity of PEI and severe systemic side effects limit the use of PEI polyplexes *in vivo* [5, 20]. Since there was evidence that toxicity is attributed to free PEI present in polyplexes, we intensively analyzed the structure-function relationship with regard to cytotoxicity and biocompatibility for pulmonary application of four differently PEGylated PEI 25 kDa copolymers in comparison to PEI 25 kDa. We evaluated a broad range of PEI concentrations (0.5-50 $\mu\text{g/ml}$) that were in a therapeutically relevant concentration range. The highest concentration of 50 $\mu\text{g/ml}$ represented an overload dose of PEI to mimic the worst case scenario. In regard to patients or animal experiments, 50 $\mu\text{g/ml}$ corresponds to 25 $\mu\text{g/cm}^2$ dose and 6 mg/lung in small animals like mice [35]. Such high concentrations possibly also occur after repeated administrations and retention of PEI in the lung due to the lack of biodegradability of PEI. However, 0.5 $\mu\text{g/ml}$ (or 0.25 $\mu\text{g/cm}^2$) and 5 $\mu\text{g/ml}$ (or 2.5 $\mu\text{g/cm}^2$) were in the range of therapeutically applied PEI doses with N/P ratios up to 20 when siRNA is administered in a range of 2-5 nmol. According to the cytotoxicity studies, there was clear evidence that the higher the degree of PEGylation and the lower the PEG chain length, the less was the cytotoxic effects observed by regarding metabolic activity and LDH release (Table 2 and Fig. 1). Interestingly, the LDH kinetic in this report corresponded well with the proposed proton sponge effect for PEI. Polyplexes were taken up by cells via endocytosis and the high buffering capacity of PEI and the passive chloride ion influx into the endosome is reported to cause osmotic swelling and subsequent endosome disruption and release of pDNA or siRNA into the cytoplasm during 4-6 h after application [36-39]. For all PEI-PEG polymers and PEI 25 kDa, maximal leakage of LDH could be detected in the first 4-6 h after treatment, except for PEI(25)-PEG(2)10 and PEI(25)-PEG(0.55)30 in MH-S cells.

Inflammatory potential

A lot of studies described apoptotic cell death as one event in PEI mediated toxicity [40, 41], but Fischer et al. (2003) postulated necrosis as alternative pathway of cell death for PEI treated cells [20]. In our study, the cytokine profile did not match the structure-function relationship of cytotoxicity and lipid peroxidation. Mainly four acute-phase cytokines such TNF- α , IL-6, IL-1 α and G-CSF were released after polymer treatment. PEI(25)-PEG(2)10 caused the highest proinflammatory response in both cell lines, e.g. up to 80-fold elevated levels of G-CSF (Fig. 3), whereas this polymer was one of the very promising polymers for *in vivo* application because of its low cytotoxic and oxidative stress potential. For all other polymers, the four acute-phase cytokine levels (TNF- α , IL-6, IL-1 α and G-CSF) were up to 5-fold elevated in both cell lines without any structure-function relationship. The apoptotic cell death seemed to be more prominent because of the highly dose-dependent reduction of metabolic activity in the mitochondria and the alteration of the mitochondrial membrane potential and most probably the mitochondrial membrane itself. Due to very high cytotoxicity of PEI 25 kDa and the lower PEGylated PEI-PEG copolymers it could be suggested that the cells were leaking of energy and therefore could not release any cytokine for their defence at 24h treatment. Nevertheless, these data highlighted the membrane interaction with PEI as one of the most prominent effect to understand the toxicity of this polymer. PEI (25)-PEG(2)10 and PEI(25)-PEG(0.55)30 seemed to be promising non-viral vector systems for pulmonary application of siRNA or pDNA *in vivo* regarding their cytotoxic profiles.

Oxidative stress responses

Oxidative stress response caused by PEI polymers in the cell was investigated. It is well known and described in the literature that oxidative stress caused by nanomaterials exposed to the lung is a critical issue [42-44]. Nel and colleagues introduced a *hierarchical oxidative stress model* [43, 45] that divided the oxidative stress caused by nanoparticles deposited in the lung into a tripartite tier hierarchy. Tier 1 is the lowest oxidative stress level, characterized by

antioxidative responses like activation of transcription factors Nrf2. Tier 2 described subsequent ongoing inflammatory processes based on the ability of reactive oxygen species (ROS) to induce redox-sensitive signalling pathways such as MAP kinases and NFκB cascades, and tier 3 is the highest oxidative stress level, where cytotoxic events occur like alteration of the mitochondrial activity, apoptotic or necrotic cell death pathways. To investigate the underlying mechanisms of polymer-mediated toxicity, the release of two major lipid mediators, 8-IP and PGE₂, both known to be indicative for cellular ROS production and lipid peroxidation [30], was determined. Remarkably, in both cell lines PEI-PEG copolymers caused similar release pattern of the two lipid mediators in comparison to the cytotoxic data (Fig.2).

To confirm the underlying pathway of the lipid peroxidation, gene induction of cyclooxygenase 2 (*Ptgs2*) and four characteristically oxidative stress genes like heme oxygenase 1 (*Hmox-1*), glutathione-S-transferase, alpha 1 (*Gst1a*), glutathione reductase (*Gsr*), and metallothionein 2 (*Mt2*) was investigated in response to the polymer treatment for 2h and 6h. At this point, it should be mentioned that mRNA could not be isolated after exposures with high doses (50 µg/ml) of PEI25 kDa in both cell lines and PEI(25)-PEG(20)1 in MH-S cells. The failure to prepare RNA could be explained by the high toxic properties of these polymers and their strong binding to RNA due to their high positive surface charge. Thus, no gene expressions analysis could be performed in these cases. The gene expression profile of *Ptgs2* yielded similar pattern as the PGE₂ release after 24 h in both cell lines. Again, a high shielding effect of PEG on PEI 25 kDa reduced lipid peroxidation. PEI 25 kDa and two of the PEG modified PEI polymers, namely PEI (25)-PEG(5)4 and PEI(25)-PEG(20)1 caused statistically significantly elevated levels of 8-IP as well as PGE₂ in the same manner at high doses of 50 µg/ml. The increased levels of the two lipid mediators have to be kept in mind because PGE₂ acts as an immune modulator to promote humoral and Th2-type immune responses and represents a key regulator of inflammation [46]. Additionally, 8-IP is driven by

non-enzymatic events like reactive oxygen species or free radicals which are responsible for modulation of inflammation and are generally considered as oxidative stress markers, especially in the lung. From these data, we concluded that PEG shielded not only the cytotoxic effect of the highly positively charged polymer PEI but also protected cells from lipid peroxidation via the non enzymatic pathway (8-IP) and cyclooxygenase mediated pathway (PGE₂). To confirm our hypothesis that PEI-based copolymers caused oxidative stress inside the cell and that generation of reactive oxygen species occurred, the induction of *Hmox-1*, *Gst1a*, *Gsr*, and *Mt2* as oxidative stress markers was analyzed. The results clearly showed high levels of oxidative stress response, especially for PEI 25 kDa and the AB diblock-copolymer, PEI(25)-PEG(20)1. The stress response was much more prominent in the macrophages than in the epithelial cells. The cell type difference could be explained by the differences in gene induction of the genes analyzed. Therefore, it was concluded that the non-enzymatic pathway caused by free radical-initiated peroxidation of arachidonic acid, should be taken in consideration. High levels of 8-IP play a dominant role in pulmonary disorders like cystic fibrosis, chronic obstructive pulmonary disease and asthma [47, 48] and might interfere with possible therapeutic approaches.

Concluding Remarks for pulmonary application

The structure-function-relationships of the investigated PEI-PEG copolymers resulted in clear evidence that PEI 25 kDa highly grafted with short PEG chain length strongly reduced cytotoxicity from PEI 25 kDa and in addition yielded less release of lipid mediators, but still showed high proinflammatory cytokine levels. Tier 2 represented ongoing inflammatory processes induced by redox-sensitive signalling in the cells and could be evaluated as a strong unwanted side-effect, especially for loco-regional administration into the lung. A lot of studies described negative outcomes like cardiovascular events [27, 49, 50] and carcinogenesis [51] resulted from initial acute inflammatory processes in the lung, but cytotoxicity is one event which should be reduced when regarding repetitive application of

such non-viral vector systems. Concerning the respective treatment of lung disorders like cystic fibrosis, allergic asthma or chronic obstructive pulmonary disease we hypothesized that cytotoxicity has to be avoided much stronger than proinflammatory events, but especially for pulmonary application proinflammatory events should be kept in mind and need intensively mechanistic evaluation *in vivo*.

Conflict of interest statement

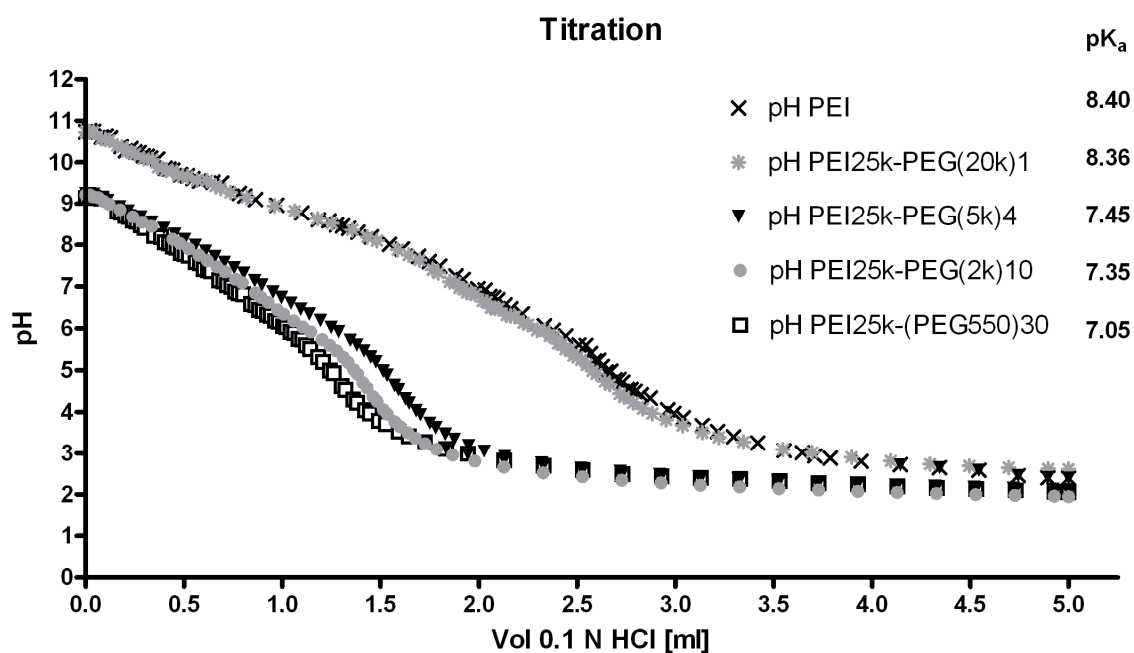
None of the authors have any competing of financial interest in relation to submission. No involvement of study sponsors in the study design has to be declared.

Acknowledgment

Financial support of the Deutsche Forschungsgemeinschaft (DFG, Forschergruppe 627) is gratefully acknowledged. We would like to thank Barbara Oswald for her excellent technical assistance and Dr. Maria Diedrich-Möhring for her kind introduction in the multiplex technique and Klaus Keim for his excellent technical support.

3.6 Supplementary material

S1: Buffer capacity



S1: Buffer capacity

Buffer capacity of four different PEI-PEG copolymers in comparison to PEI 25kDa; pK_a values were calculated with LabX (Mettler Toledo GmbH, Giessen, Germany). Equivalent nitrogen amount of each polymer were titrated in duplicate

3.7 References

- 1 Densmore, C.L., F.M. Orson, B. Xu, B.M. Kinsey, J.C. Waldrep, P. Hua, B. Bhogal, and V. Knight, *Aerosol delivery of robust polyethyleneimine-DNA complexes for gene therapy and genetic immunization*. *Mol Ther*, 2000. 1(2): p. 180-8.
- 2 Gautam, A., C.L. Densmore, B. Xu, and J.C. Waldrep, *Enhanced gene expression in mouse lung after PEI-DNA aerosol delivery*. *Mol Ther*, 2000. 2(1): p. 63-70.
- 3 Rudolph, C., R.H. Muller, and J. Rosenecker, *Jet nebulization of PEI/DNA polyplexes: physical stability and in vitro gene delivery efficiency*. *J Gene Med*, 2002. 4(1): p. 66-74.
- 4 Fischer, D., T. Bieber, Y. Li, H.P. Elsasser, and T. Kissel, *A novel non-viral vector for DNA delivery based on low molecular weight, branched polyethylenimine: effect of molecular weight on transfection efficiency and cytotoxicity*. *Pharm Res*, 1999. 16(8): p. 1273-9.
- 5 Boeckle, S., K. von Gersdorff, S. van der Piepen, C. Culmsee, E. Wagner, and M. Ogris, *Purification of polyethylenimine polyplexes highlights the role of free polycations in gene transfer*. *J Gene Med*, 2004. 6(10): p. 1102-11.
- 6 Ogris, M., S. Brunner, S. Schuller, R. Kircheis, and E. Wagner, *PEGylated DNA/transferrin-PEI complexes: reduced interaction with blood components, extended circulation in blood and potential for systemic gene delivery*. *Gene Ther*, 1999. 6(4): p. 595-605.
- 7 Park, T.G., J.H. Jeong, and S.W. Kim, *Current status of polymeric gene delivery systems*. *Adv Drug Deliv Rev*, 2006. 58(4): p. 467-86.
- 8 Petersen, H., P.M. Fechner, A.L. Martin, K. Kunath, S. Stolnik, C.J. Roberts, D. Fischer, M.C. Davies, and T. Kissel, *Polyethylenimine-graft-poly(ethylene glycol) copolymers: influence of copolymer block structure on DNA complexation and biological activities as gene delivery system*. *Bioconjug Chem*, 2002. 13(4): p. 845-54.
- 9 Kichler, A., M. Chillon, C. Leborgne, O. Danos, and B. Frisch, *Intranasal gene delivery with a polyethylenimine-PEG conjugate*. *J Control Release*, 2002. 81(3): p. 379-88.
- 10 Finsinger, D., J.S. Remy, P. Erbacher, C. Koch, and C. Plank, *Protective copolymers for nonviral gene vectors: synthesis, vector characterization and application in gene delivery*. *Gene Ther*, 2000. 7(14): p. 1183-92.
- 11 Petersen, H., P.M. Fechner, D. Fischer, and T. Kissel, *Synthesis, Characterization, and Biocompatibility of Polyethylenimine-graft-poly(ethylene glycol) Block Copolymers*. *Macromolecules*, 2002. 35(18): p. 6867-6874.
- 12 Kunath, K., A. von Harpe, D. Fischer, and T. Kissel, *Galactose-PEI-DNA complexes for targeted gene delivery: degree of substitution affects complex size and transfection efficiency*. *J Control Release*, 2003. 88(1): p. 159-72.
- 13 Brus, C., H. Petersen, A. Aigner, F. Czubayko, and T. Kissel, *Physicochemical and biological characterization of polyethylenimine-graft-poly(ethylene glycol) block copolymers as a delivery system for oligonucleotides and ribozymes*. *Bioconjug Chem*, 2004. 15(4): p. 677-84.
- 14 Mao, S., X. Shuai, F. Unger, M. Wittmar, X. Xie, and T. Kissel, *Synthesis, characterization and cytotoxicity of poly(ethylene glycol)-graft-trimethyl chitosan block copolymers*. *Biomaterials*, 2005. 26(32): p. 6343-56.
- 15 Glodde, M., S.R. Sirsi, and G.J. Lutz, *Physicochemical properties of low and high molecular weight poly(ethylene glycol)-grafted poly(ethylene imine) copolymers and their complexes with oligonucleotides*. *Biomacromolecules*, 2006. 7(1): p. 347-56.

- 16 Malek, A., F. Czubayko, and A. Aigner, *PEG grafting of polyethylenimine (PEI) exerts different effects on DNA transfection and siRNA-induced gene targeting efficacy*. *J Drug Target*, 2008. 16(2): p. 124-39.
- 17 Fahrmeir, J., M. Gunther, N. Tietze, E. Wagner, and M. Ogris, *Electrophoretic purification of tumor-targeted polyethylenimine-based polyplexes reduces toxic side effects in vivo*. *J Control Release*, 2007. 122(3): p. 236-45.
- 18 Hong, S., P.R. Leroueil, E.K. Janus, J.L. Peters, M.M. Kober, M.T. Islam, B.G. Orr, J.R. Baker, Jr., and M.M. Banaszak Holl, *Interaction of polycationic polymers with supported lipid bilayers and cells: nanoscale hole formation and enhanced membrane permeability*. *Bioconjug Chem*, 2006. 17(3): p. 728-34.
- 19 Leroueil, P.R., S. Hong, A. Mecke, J.R. Baker, Jr., B.G. Orr, and M.M. Banaszak Holl, *Nanoparticle interaction with biological membranes: does nanotechnology present a Janus face?* *Acc Chem Res*, 2007. 40(5): p. 335-42.
- 20 Fischer, D., Y. Li, B. Ahlemeyer, J. Krieglstein, and T. Kissel, *In vitro cytotoxicity testing of polycations: influence of polymer structure on cell viability and hemolysis*. *Biomaterials*, 2003. 24(7): p. 1121-31.
- 21 Choksakulnimitr, S., S. Masuda, T. Hideaki, Y. T., and H. Mitsuru, *In vitro cytotoxicity of macromolecules in different cell culture systems*. *J Control Release*, 1995. 34: p. 233-214.
- 22 Teramura, Y., Y. Kaneda, T. Totani, and H. Iwata, *Behavior of synthetic polymers immobilized on a cell membrane*. *Biomaterials*, 2008. 29(10): p. 1345-55.
- 23 Dif, F., C. Djediat, O. Alegria, B. Demeneix, and G. Levi, *Transfection of multiple pulmonary cell types following intravenous injection of PEI-DNA in normal and CFTR mutant mice*. *J Gene Med*, 2006. 8(1): p. 82-9.
- 24 Oberdorster, G., E. Oberdorster, and J. Oberdorster, *Nanotoxicology: an emerging discipline evolving from studies of ultrafine particles*. *Environ Health Perspect*, 2005. 113(7): p. 823-39.
- 25 Brown, D.M., W. M.R, M. W., S. V., and D. K., *Size-dependent proinflammatory effects of ultrafine polystyrene particles: a role for surface area and oxidative stress in the enhanced activity of ultrafines*. *Toxicol Appl Pharmacol*, 2001. 175: p. 191-199.
- 26 Nemmar, A., H.M. F., H.P. H.M., V. Josef, and N. Benoit, *Size effect of intratracheally instilled particles on pulmonary inflammation and vascular thrombosis*. *Toxicol Appl Pharmacol*, 2003. 186: p. 38-45.
- 27 Oberdorster, G., A. Maynard, K. Donaldson, V. Castranova, J. Fitzpatrick, K. Ausman, J. Carter, B. Karn, W. Kreyling, D. Lai, S. Olin, N. Monteiro-Riviere, D. Warheit, and H. Yang, *Principles for characterizing the potential human health effects from exposure to nanomaterials: elements of a screening strategy*. *Part Fibre Toxicol*, 2005. 2: p. 8.
- 28 Mosmann, T., *Rapid colorimetric assay for cellular growth and survival: application to proliferation and cytotoxicity assays*. *J Immunol Methods*, 1983. 65(1-2): p. 55-63.
- 29 Minko, T., P. Kopeckova, V. Pozharov, and J. Kopecek, *HPMA copolymer bound adriamycin overcomes MDR1 gene encoded resistance in a human ovarian carcinoma cell line*. *J Control Release*, 1998. 54(2): p. 223-33.
- 30 Beck-Speier, I., N. Dayal, E. Karg, K.L. Maier, G. Schumann, H. Schulz, M. Semmler, S. Takenaka, K. Stettmaier, W. Bors, A. Ghio, J.M. Samet, and J. Heyder, *Oxidative stress and lipid mediators induced in alveolar macrophages by ultrafine particles*. *Free Radic Biol Med*, 2005. 38(8): p. 1080-92.
- 31 Prabhakar, U., E. Eirikis, M. Reddy, E. Silvestro, S. Spitz, C. Pendley, 2nd, H.M. Davis, and B.E. Miller, *Validation and comparative analysis of a multiplexed assay for the simultaneous quantitative measurement of Th1/Th2 cytokines in human serum*

- and human peripheral blood mononuclear cell culture supernatants. *J Immunol Methods*, 2004. 291(1-2): p. 27-38.
- 32 Livak, K.J. and T.D. Schmittgen, *Analysis of relative gene expression data using real-time quantitative PCR and the 2(-Delta Delta C(T)) Method*. *Methods*, 2001. 25(4): p. 402-8.
- 33 Grayson, A.C., A.M. Doody, and D. Putnam, *Biophysical and structural characterization of polyethylenimine-mediated siRNA delivery in vitro*. *Pharm Res*, 2006. 23(8): p. 1868-76.
- 34 Jere, D., C.X. Xu, R. Arote, C.H. Yun, M.H. Cho, and C.S. Cho, *Poly(beta-amino ester) as a carrier for si/shRNA delivery in lung cancer cells*. *Biomaterials*, 2008. 29(16): p. 2535-47.
- 35 Stone, K.C., M. R.R., G. P., S. B., and C. J., *Allometric relationships of cell numbers and size in the mammalian lung*. *Am J Resp Cell Mol Biol*, 1992. 6: p. 235-243.
- 36 Godbey, W.T., K.K. Wu, G.J. Hirasaki, and A.G. Mikos, *Improved packing of poly(ethylenimine)/DNA complexes increases transfection efficiency*. *Gene Ther*, 1999. 6(8): p. 1380-8.
- 37 Godbey, W.T., K.K. Wu, and A.G. Mikos, *Tracking the intracellular path of poly(ethylenimine)/DNA complexes for gene delivery*. *Proc Natl Acad Sci U S A*, 1999. 96(9): p. 5177-81.
- 38 Godbey, W.T., K.K. Wu, and A.G. Mikos, *Poly(ethylenimine)-mediated gene delivery affects endothelial cell function and viability*. *Biomaterials*, 2001. 22(5): p. 471-80.
- 39 Zaric, V., D. Weltin, P. Erbacher, J.S. Remy, J.P. Behr, and D. Stephan, *Effective polyethylenimine-mediated gene transfer into human endothelial cells*. *J Gene Med*, 2004. 6(2): p. 176-84.
- 40 Hunter, A.C., *Molecular hurdles in polyfectin design and mechanistic background to polycation induced cytotoxicity*. *Adv Drug Deliv Rev*, 2006. 58(14): p. 1523-31.
- 41 Regnstrom, K., E.G. Ragnarsson, M. Fryknas, M. Koping-Hoggard, and P. Artursson, *Gene expression profiles in mouse lung tissue after administration of two cationic polymers used for nonviral gene delivery*. *Pharm Res*, 2006. 23(3): p. 475-82.
- 42 Donaldson, K., and Stone, V. , *Current hypotheses on the mechanisms of toxicity of ultrafine particles*. *Ann Ist Super Sanità*, 2003. 39(3): p. 405-410.
- 43 Nel, A., T. Xia, L. Madler, and N. Li, *Toxic potential of materials at the nanolevel*. *Science*, 2006. 311(5761): p. 622-7.
- 44 Xia, T., M. Kovichich, M. Liang, J.I. Zink, and A.E. Nel, *Cationic polystyrene nanosphere toxicity depends on cell-specific endocytic and mitochondrial injury pathways*. *ACS Nano*, 2008. 2(1): p. 85-96.
- 45 Li, N., T. Xia, and A.E. Nel, *The role of oxidative stress in ambient particulate matter-induced lung diseases and its implications in the toxicity of engineered nanoparticles*. *Free Radic Biol Med*, 2008. 44(9): p. 1689-99.
- 46 Harris, S.G., J. Padilla, L. Koumas, D. Ray, and R.P. Phipps, *Prostaglandins as modulators of immunity*. *Trends Immunol*, 2002. 23(3): p. 144-50.
- 47 Janssen, L.J., *Isoprostanes: an overview and putative roles in pulmonary pathophysiology*. *Am J Physiol Lung Cell Mol Physiol*, 2001. 280(6): p. L1067-82.
- 48 Morrow, J.D. and L.J. Roberts, *The isoprostanes: their role as an index of oxidant stress status in human pulmonary disease*. *Am J Respir Crit Care Med*, 2002. 166(12 Pt 2): p. S25-30.
- 49 Mills, N.L., K. Donaldson, P.W. Hadoke, N.A. Boon, W. MacNee, F.R. Cassee, T. Sandstrom, A. Blomberg, and D.E. Newby, *Adverse cardiovascular effects of air pollution*. *Nat Clin Pract Cardiovasc Med*, 2009. 6(1): p. 36-44.

- 50** Muhlfield, C., B. Rothen-Rutishauser, F. Blank, D. Vanhecke, M. Ochs, and P. Gehr, *Interactions of nanoparticles with pulmonary structures and cellular responses*. *Am J Physiol Lung Cell Mol Physiol*, 2008. 294(5): p. L817-29.
- 51** Roller, M., *Carcinogenicity of inhaled nanoparticles*. *Inhal Toxicol*, 2009. 21(S1): p. 144-157.

4 Toxicity pathway focused gene expression profiling of PEI-based polymers for pulmonary applications

Andrea Beyerle, Martin Irmeler, Johannes Beckers, Thomas Kissel, Tobias Stoeger

Submitted to *Molecular Pharmaceutics* (Manuscript ID: mp-2009-00278x, under revision)

Author's contributions:

A.B. prepared the manuscript draft and wrote the manuscript, designed and performed the experimental work, analyzed and interpreted all data, M.I. did the analysis of the biological network interactions using Ingenuity Systems pathway software, and analyzed the qRT-PCR data, J.B. provided the Ingenuity Systems pathway software, T.K. provided the PEI-PEG polymers, reviewed and edited the manuscript, T.S interpreted the qRT-PCR data, reviewed and edited the manuscript. All authors read and approved the final version of the manuscript.

4.1 Abstract

Polyethylene imine (PEI) based polycations, successfully used for gene therapy or RNA interference *in vitro* as well as *in vivo* have been shown to cause well known adverse side effects, especially high cytotoxicity. Therefore, various modifications have been developed to improve safety and efficiency of these non-viral vector systems, but profound knowledge about the underlying mechanisms responsible for the high cytotoxicity of PEI is still missing. In this *in vitro* study, we focused on stress and toxicity pathways triggered by PEI-based vector systems to be used for pulmonary application in comparison to two well known lung toxic particles: fine crystalline silica (CS) and nano-sized ZnO (NZO). The cytotoxicity profiles of all stressors were investigated in alveolar epithelial like type II cells (LA4) to define concentrations with matching toxicity levels (cell viability >60 % and LDH release <10%) for subsequent qRT-PCR based gene array analysis.

Within the first 6 h pathway analysis revealed for CS an extrinsic apoptotic signaling (TNF pathway) in contrast to the intrinsic apoptotic pathway (mitochondrial signaling) which was induced by PEI25kDa after 24 h treatment. The following causative chain of events seems conceivable: reactive oxygen species derived from particle surface toxicity triggers TNF signaling in the case of CS, whereby endosomal swelling and rupture upon endocytotic PEI 25 kDa uptake causes intracellular stress and mitochondrial alterations, finally leading to apoptotic cell death at higher doses.

PEG modification most notably reduced the cytotoxicity of PEI 25 kDa but increased proinflammatory signaling on mRNA and even protein level. Hence in view of the lung as a sensitive target organ this inflammatory stimulation might cause unwanted side-effects related to respiratory and cardiovascular disorders. Thus further optimization of the PEI-based vector systems is still needed for pulmonary application.

Keywords: toxicity, gene expression profiling, poly(ethylene imine), inflammation, pulmonary application

4.2 Introduction

Viral and non-viral vectors have widely been used in gene therapy as delivery systems for nucleic acids. The transfer of viral vector technology to clinical gene therapy trials has raised safety issues such as unexplained cytotoxicity and immunogenicity in target cells and tissues despite their high transfection efficiency [1, 2]. Therefore, non-viral vector systems were promoted as promising and safer alternatives for gene and siRNA delivery [3, 4]. So far, the main focus of gene therapy and RNA interference was on increasing efficiency and bioavailability while decreasing toxicity on a systemic and cellular level [5-8].

In this context the identification of mechanisms and pathways underlying cellular perturbation and toxicity caused by exposure of target cells and tissues to polymeric non-viral delivery systems would help to improve their safety profile dramatically. In particular toxicogenomics have proved to be a powerful tool for the direct monitoring of patterns of cellular perturbation by various exogenous agents at the molecular level [9]. To study alteration of gene expression caused by the interaction between the structure and activity of a defined stressor and a selected cellular system can be an effective method to gain a first insight into this complex biological response. One major issue of PEI-based non-viral vector systems is their strong cytotoxicity [10, 11] In fact PEI-based vector systems have been shown to cause considerable changes of gene expression *in vitro*, effects that might also have the potential to enhance off-target effects also *in vivo* like it has been observed for siRNA targeting [12, 13]. Indeed in the literature cationic polymers, dendrimers, and lipid-based transfection reagents were shown to alter cellular gene expression, but the consequences of these expression changes on biological systems remain largely unknown at present.

The lung represents a promising target organ for non invasive local therapy of pulmonary diseases including asthma, chronic obstructive pulmonary disorder, cystic fibrosis, ischemic reperfusion injury and infection with respiratory viruses. Hence this study focuses on the use of poly(ethylene imine) (PEI) based carrier systems for pulmonary delivery of nucleic acids

like siRNA. Respective PEI polymers were selected from previous studies [14] because of their promising cytotoxic profile, and CS and NZO particles were chosen due to their well-known lung toxicity. CS it is a long established lung carcinogen which induces severe pulmonary inflammation often resulting in fibrosis [15, 16]. For NZO several studies described the high proinflammatory potential, possibly caused by the fraction of soluble Zn ions released in acidic cell compartments like endosomes [10]. Moreover, exposure to zinc fume can cause metal fume fever, an illness usually related to inhalation of fumes from welding, cutting, or brazing, on galvanized metal [17, 18]. The detected gene expression pattern were classified on the basis of the *hierarchical oxidative stress model* [7, 19] developed for ambient particulate matter and nanoparticles. Nel and colleagues introduced a three tier hierarchy that subdivided oxidative stress caused by (nano)particles deposited in the lung in three categories. Tier 1 represents the lowest oxidative stress level characterized by expression of genes important for the cellular antioxidant response and which are regulated via the antioxidant response element binding transcription factor Nrf2. Tier 2 describes subsequent ongoing inflammatory processes based on the ability of unbalanced reactive oxygen species (ROS) to induce redox-sensitive signalling pathways such as MAP kinases and NFκB cascades. Finally the highest oxidative stress level is named tier 3, where cytotoxic events occur like alterations of the mitochondrial activity, cell cycle progression and apoptotic or necrotic cell death pathways optimal doses for each of the five stressors, which causes a moderate, comparable level of cytotoxicity, therefore to allow for the subsequent comparative mechanistic investigations based on mRNA and protein expression levels. Secondly, we evaluated alterations in gene expression pattern after treatment of alveolar epithelial like type II cells with the two lung benchmark particles and the three different PEI-based polymers applying a qRT-PCR based pathway focused gene array covering 84 genes related to oxidative stress, inflammation, cell growth and proliferation, or cell death (necrosis and apoptosis). Since upon treatment with PEG modified PEI copolymers significant inductions of

proinflammatory gene expression were detected, we followed the inflammatory response on protein level by cytokine quantification.

4.3 Experimental Section

Particles

Branched poly(ethylene imine) (PEI) with a molecular weight of 25 kDa (Polymin™, water-free, 99 %) was a gift of BASF, Ludwigshafen. The polyethylene imine-graft-poly(ethylene glycol)s (PEI-PEG) with a PEG content of approximately 50 % (w/w) were synthesized as previously described [6, 20] by grafting linear PEG of 0.55 kDa and 2 kDa, respectively, onto branched PEI 25 kDa. These graft copolymers were designated using following nomenclature: PEI(25k)-g-PEG(x)n. The number in brackets (25k or x, where x=0.55 k, 2 k) represents the molecular weight of PEI or PEG block in Daltons, and the index n is the average number of PEG blocks per PEI molecule. The number was calculated on the basis of ¹H-NMR spectra as described previously [20]. Min-U-Sil 5 (crystalline silica) was obtained from U.S. Silica Company, Berkeley Springs, WV, USA, with a median diameter of 1.7 μm as specified by the manufacturer. Zinc oxide (CAS-No: 1314-13-2) was obtained from Alfa Aesar (A Johnson Matthey Company, Karlsruhe, Germany) with a nominal average diameter of 70nm, it is designated as nano-sized ZnO (NZO).

Polymers were diluted in sterile sodium chloride (150 mM) solution and vigorously vortexed directly before use. Crystalline silica and nano-sized ZnO suspensions were prepared in sterile, double-distilled water. Stock solutions (10 mg/ml) were sonicated for 15 min prior to serial dilution and each suspension was sonicated for 10 min directly before use.

Cell culture

Cell culture experiments were performed using the murine alveolar epithelial – like type II cells (LA4; ATCC No. CCL-196™). Cells were grown in HAM's F12 medium with stable Glutamax containing 15 % fetal bovine serum (FBS, Gibco, Germany) and 1% non essential amino acids and 100 U/ml penicillin and 100 mg/ml streptomycin at 37 ° C and 5 % CO₂. All cells were passaged every 2-3 days. All reagents were obtained from Biochrom AG, Seromed, Germany or otherwise signed. LA4 cells were seeded at a density of $0.5 \cdot 10^6$ cells/well (2 ml)

in 6-well-plates (FALCON, Germany) and were allowed to adhere overnight in an incubator at 37 ° C and 5 % CO₂. After 24 h cell culture medium was replaced and the appropriate amount of the particle dilution was added to the well in a final volume of 2 ml/well. Cells were treated with the polymers and particles for 6 h and 24 h.

Cell viability

Cell viability was determined using the Cell Proliferation Reagent WST-1 (Roche Diagnostics, Germany) according to the method of Mosmann[21]. Briefly, LA4 cells were seeded at a density of 0.25×10^6 cells/well/2cm² in 24-well-plates in cell culture medium containing 15 % FBS and grown overnight in an incubator at 37 ° C and 5 % CO₂. For the treatment, the cell culture medium was replaced by freshly, pre-warmed, serum-reduced (2 % FBS) cell culture medium without antibiotics. Particles were exposed to the cells for 24h and the relative viability [%] related to control samples (untreated cells) was calculated by following equation: Cell viability = $(OD_{\text{sample}} / OD_{\text{control}}) \times 100$. All data represent at least three independent experiments. In addition IC₅₀ values were determined following a 72 h incubation of LA4 cells (8000 cells/well) in 96-well-plate with particle and polymer concentrations in the range from 0.001-1 mg/ml. After 72 h treatment metabolic activity was detected as described above and IC₅₀ values were calculated as concentration which inhibits cell viability by 50 % relative to untreated control cells according to Minko [22] . The results of optical density measurements were fitted logistically by the Levenberg-Marquardt method of least-squares minimization for nonlinear equations under default conditions using Origin 7.0 (Origin LabSoftware, Northampton, USA) by the following equation: $Y = Y_0 + (Y_m - Y_0) / (1 + (C/C_0))$, where C₀ is the IC₅₀ dose, Y is the optical density in a well containing a particular polymer/extract of concentration C. Y₀ and Y_m are the optical densities corresponding to 0 % viability and 100 % viability, respectively.

Cytotoxicity

For detection of the cytosolic enzyme lactate dehydrogenase (LDH) in the culture supernatant, a characteristic of membrane damage we used the Cytotoxicity Detection Kit (Roche Diagnostics, Germany) according to the manufacturer's protocol. The experiments were carried out according to the conditions of WST-1 assay. After 24 h the LDH concentration in the cell culture supernatant was spectrophotometrically determined in an ELISA reader (Labsystems iEMS Reader MF) at a wavelength of 492 nm. According to the manufacturer's protocol cells treated with 2 % (w/v) Triton X-100 served as control and set as maximum of LDH release (100 %). The relative LDH release is defined by the ratio of LDH released over total LDH in the intact cells (high control). Less than 10 % LDH release were regarded as non-toxic effect level in our experiment [23]. All data represent at least three independent experiments.

RNA isolation

After 6 h and 24 h incubation RNA was isolated from the cells by using RNeasy Mini Kit (Qiagen, Hilden, Germany). Briefly, cell culture medium was removed and cells were washed two times with pre-warmed, sterile PBS without Mg^{2+} and Ca^{2+} , pH 7.4. Cells were lysed with 350 μ l RLT buffer containing 1 % (v/v) 2-mercaptoethanol. The cell lysate was collected in an Eppendorf tube and the tube was vigorously vortexed. 350 μ l cold (4 ° C) ethanol (70 %) was added to each cell lysate to precipitate the RNA. 700 μ l lysate was placed onto a Qiagen column and were centrifuged at 15.000 g for 1 min. The flow through was discarded and DNase digestion was carried out using DNase I (Qiagen, Hilden, Germany). 350 μ l RW1 buffer was added to the column and the column was centrifuged at 15.000 g x 1 min. The flow through was discarded and the column was placed in a new collection tube. In the same way 500 μ l RPE buffer containing ethanol was added twice and centrifuged at first 15.000 g for 1 min, and at the second time 15.000 g for 2 min. The column was placed in a new tube and the RNA was eluted from the column with 30 μ l RNase-free water by centrifugation at

15.000 g for 1 min. RNA was directly frozen at -80 ° C and stored for further investigations. The quality of RNA was checked in an agarose-gel (1 %) containing SYBRGold (Invitrogen, Germany, Karlsruhe) and the RNA amount was quantified using ND-1000 Spectrophotometer (NanoDrop Technologies, Inc., Wilmington, DE, US) at the absorbance ratio of 260 and 280 nm.

Gene expression profiling

cDNA synthesis was performed using RT² First Strand Kit (Superarray, Catalog-No.: C-03) following the instructions of the manufacturer. Briefly, genomic DNA was eliminated using Genomic DNA Elimination Mixture provided in the Kit. RT Cocktail was prepared and First Strand cDNA synthesis reaction was carried out according to the manufacturer's instructions. For detailed information regarding the genes applied on this array RT² Profiler™ PCR Array Mouse Stress & Toxicity Pathway Finder (Superarray, Cat-no.: APMM-003A) see supplementary material S1.

Array was performed according to the instructions of the manufacturer and the qRT-PCR was carried out with ABI Prism 7000 Sequence detection System (Applied Biosystems, Foster City, CA, USA). Briefly, cDNA was diluted in appropriate amount of master mix (RT² Real-Time SYBR Green/ ROX PCR Master Mix) and RNase-free water and loaded onto the array plate. The qRT-PCR was performed using a two-step cycling program with an initial heating for 2 min. at 50 ° C followed by two stages with one cycle of 10 min at 95 ° C and 40 cycles of 15 sec at 95 ° C and 1min at 60 ° C. Immediately after the cycling program a melting curve program was running to generate a first derivative dissociation curve.

Genes were clustered according to the seven clusters of the RT² Profiler™ PCR Array Mouse Stress & Toxicity Pathway Finder provided from the manufacturer and the gene expression pattern was illustrated in a heat map (Supporting information S2) using free software called CARMAweb from Graz University of Technology, Institute of Genomics and Bioinformatics,[24] <https://carmaweb.genome.tugraz.at/carma/>. Log₂ ratios were used as

input, with red colours indicating up-regulation (treated vs control) and green colours indicating down-regulation of the respective genes. Biological network interactions of genes regulated more than 2-fold were analyzed using the Ingenuity Systems pathway software (<http://www.ingenuity.com>), which is based on an expert curated interaction database. For clarity, some interactions were not shown. A small number of relations were added manually based on literature research, Fig.2A and B.

Cytokine release

Eight cytokines/chemokines were detected simultaneously in the cell culture supernatant using Luminex technology (Linco Research, St. Charles, MO). In this study, the secretion of following cytokines/chemokines was investigated: IL-1 α , IL-6, TNF-alpha, G-CSF, CXCL1, CXCL10, CCL2, and CCL3. The assay was performed as described previously [25]. The mean fluorescence intensity (MFI) was detected by the Multiplex plate reader (Luminex System, Bio-Rad Laboratories, Germany) for each sample (50 μ l) with a minimum of 100 beads per region being analyzed. The raw data (MFI) were captured using the Multiplex plate reader software (Bioplex Manager, Version 2.0). For data analysis, a 5-parameter logistic curve fit was applied to each standard curve and sample.

Statistics

All values are presented as mean \pm standard error (SEM) of at least three independent experiments. Significant differences between two groups were evaluated by Student's t-test or between more than two groups by one-way ANOVA followed by Tukey's multiple comparison test. Statistical analysis was performed using the program STATGRAPHICS PLUS Version 5.0 (Statpoint, Inc., Virginia, US).

4.4 Results

Cytotoxicity evaluation

For all particles and polymers a clear dose-dependent cytotoxicity was found after 24 h treatment (Fig. 1A-F).

Figure 1: Cytotoxicity evaluation

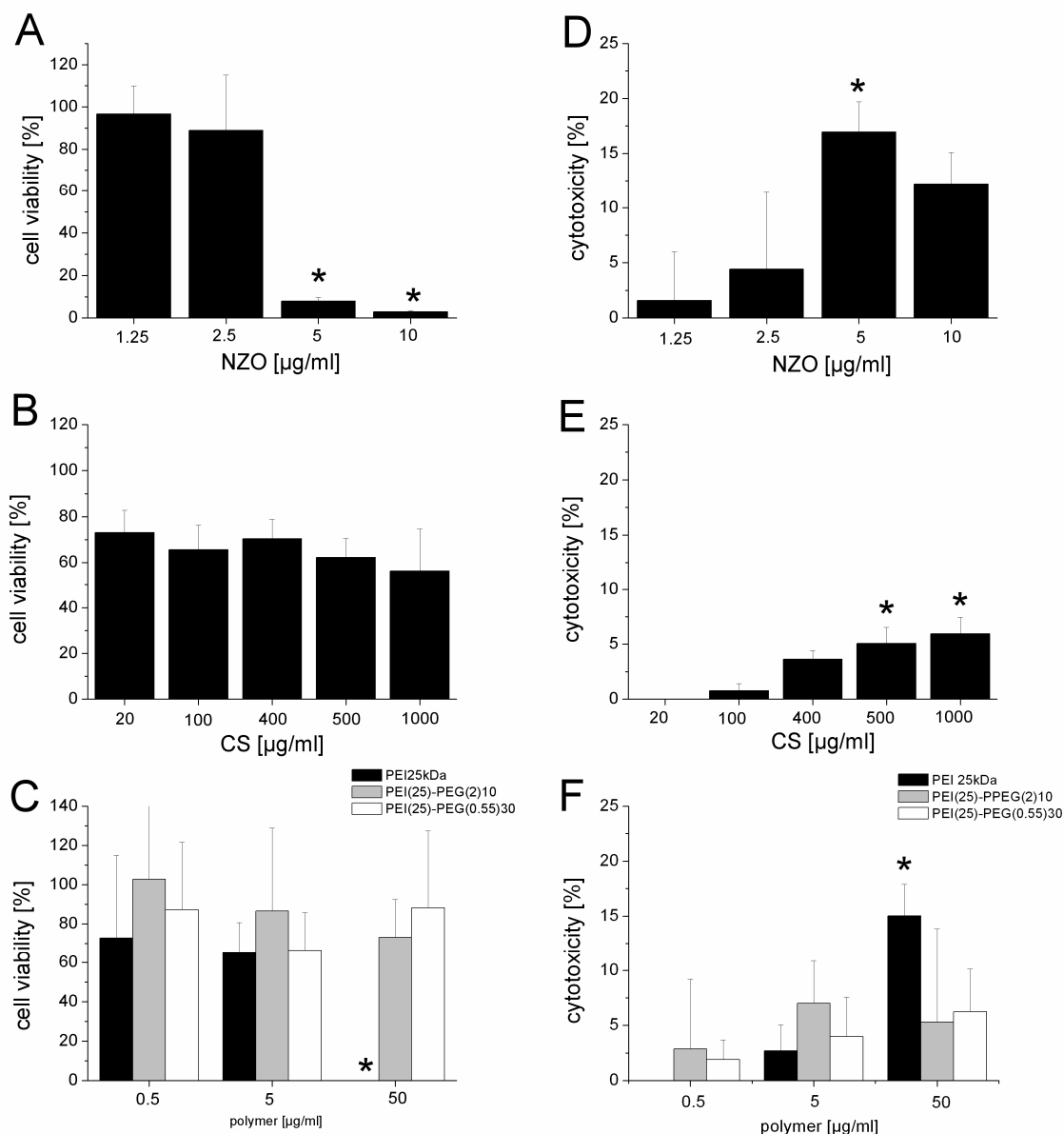


Figure 1: Cytotoxicity evaluation

Left panel (A-C) shows cell viability and right panel (D-F) cytotoxicity (LDH release) in LA4 cells after 24h treatment with nano-sized ZnO (NZO), crystalline silica (CS), PEI 25kDa (black), PEI(25)-PEG(2)10 (grey), and PEI(25)-PEG(0.55)30 (white). Values are given in mean \pm SEM, experiments were repeated three times in case of the PEI based polymers and five times in case of NZO and CS.

Statistically significant changes were represented by an asterisk with p -value < 0.05 vs. control (untreated cells).

Considering a mass based dose metric NZO was the most cytotoxic agent, resulting in cell viability reduction of over 90% and cell membrane damage (LDH release) of 15 % already at a dose of 5 $\mu\text{g/ml}$. Particles and polymers show decreasing cytotoxicity as estimated by their IC_{50} values in the following order: PEI25 kDa $>$ NZO $>$ PEI(25)-PEG(2)10 $>$ PEI(25)-PEG(0.55)30 $>$ CS (Table 1).

Table 1: IC_{50} value

Particle/polymer	IC_{50} [mg/ml]
CS	> 1
NZO	0.014 ± 0.003
PEI25kDa	0.003 ± 0.000
PEI(25)-PEG(2)10	0.022 ± 0.009
PEI(25)-PEG(0.55)30	0.033 ± 0.004

Table 1: IC_{50} values were presented as mean \pm SD of three independent experiments. Cell proliferation in LA4 cells was analyzed using WST-1 assay after 72 h particle exposure and IC_{50} values were calculated using sigmoidal fitting using Boltzmann equation.

In comparison to PEI 25 kDa, PEGylated PEI co-polymers showed significantly reduced cytotoxicity ($p < 0.05$) (Fig. 1C and F and Table 1). For PEI 25 kDa the highest concentration of 50 $\mu\text{g/ml}$ caused severe toxicity yielding cell viability levels below detection and significantly elevated levels of LDH (15.03 ± 2.86 , $p < 0.05$). To ensure sufficient RNA integrity for the subsequent qRT-PCR based toxicity pathways focused gene array we used conditions resulting in low to moderate cytotoxicity levels as characterized by the WST-related toxicity below 40 %, and the membrane toxicity (LDH) below 10 %. The following doses were selected in the gene array study: 400 $\mu\text{g/ml}$ for CS, 2.5 $\mu\text{g/ml}$ for NZO, and 5 $\mu\text{g/ml}$ for each of the three PEI-based polymers.

Toxicological focused gene expression profiling

We selected a pathway focused design with a representative set of genes indicative for a broad range of toxicological responses covering seven different stress and toxicity pathway clusters: Metabolic and Oxidative Stress (1), Heat Shock (2), Proliferation and Carcinogenesis (3), Growth Arrest and Senescence (4), Inflammation (5), Necrosis or Apoptosis: DNA Damage and Repair (6) and Necrosis or Apoptosis: Apoptosis Signalling (7) (Supporting information S1).

Two time points were investigated to detect acute and prolonged effects, namely 6 h and 24 h after treatment. From the 84 genes analyzed the expression of 35 genes (42 %) was altered for all particles and polymers investigated at both time points (Supporting information S2). For a more comprehensive arrangement of the observed expression changes we categorized them according to the three tier levels of the hierarchical oxidative stress model from Nel and colleagues [19] (Table 2).

Table 2: *Gene expression profiling*

Particle/polymer	pathway	gene name	GenBank	fold change	
				Early response 6h	Late response 24h
CS	Cytotoxicity	E2f1	NM_007891	3.7	0.6
	Cytotoxicity	Tnfsf10	NM_009425	3.4	n.d.
	Cytotoxicity	Gadd45a	NM_007836	3.0	0.7
	Cytotoxicity	Cdkn1a	NM_007669	2.4	0.8
	Cytotoxicity	Ddit3	NM_007837	2.3	0.7
	Cytotoxicity	Bax	NM_007527	2.2	0.4
	Cytotoxicity	Tnfrsf1a	NM_011609	2.0	0.3
	Cytotoxicity	Ceng1	NM_009831	2.0	0.2
	Inflammation	Cxcl10	NM_021274	11.6	6.6
	Inflammation	Casp1	NM_009807	8.0	0.1
	Inflammation	Nos2	NM_010927	7.8	0.8
	Inflammation	Nfkbia	NM_010907	4.4	1.1
	Inflammation	IL18	NM_008360	3.9	0.0
	Inflammation	Lta	NM_010735	3.0	0.6
	Inflammation	Serpine1	NM_008871	-3.3	3.9
	Inflammation	Csf2	NM_009969	1.0	2.9
	Ox.stress	Ugt1a2	NM_013701	14.9	0.3
	Ox.stress	Cryab	NM_009964	6.1	0.1
	Ox.stress	Hspa1b	NM_010478	2.2	0.5
	Ox.stress	Mt2	NM_008630	1.8	2.3
Ox.stress	Hmox1	NM_010442	1.7	2.1	
NZO	Inflammation	Nfkbia	NM_010907	3.9	0.4
	Inflammation	Cxcl10	NM_021274	2.2	0.5
	Ox.stress	Hspb1	NM_013560	9.8	0.4

Table 2: Gene expression profiling (continued)

Particle/polymer	pathway	gene name	GenBank	fold change	fold change	
NZO	Ox.stress	Ugt1a2	NM_013701	6.8	0.6	
	Ox.stress	Hmox1	NM_010442	3.0	0.4	
	Ox.stress	Mt2	NM_008630	2.2	0.3	
PEI 25kDa	Cytotoxicity	E2f1	NM_007891	2.1	1.5	
	Cytotoxicity	Bcl2l1	NM_009743	-1.5	3.2	
	Cytotoxicity	Bax	NM_007527	1.0	2.4	
	Cytotoxicity	Atm	NM_007499	-1.3	2.2	
	Cytotoxicity	Ercc4	NM_015769	-1.3	2.0	
	Cytotoxicity	Anxa5	NM_009673	1.3	2.0	
	Inflammation	Nfkbia	NM_010907	3.3	1.5	
	Inflammation	Csf2	NM_009969	2.4	0.8	
	Ox.stress	Ugt1a2	NM_013701	10.0	0.7	
	Ox.stress	Mt2	NM_008630	2.1	0.8	
	Ox.stress	Hspa1b	NM_010478	-1.4	4.7	
	Ox.stress	Cyp1b1	NM_009994	-2.8	2.6	
	Ox.stress	Hmox2	NM_010443	-2.5	2.4	
	PEI(25)-PEG(2)10	Cytotoxicity	E2f1	NM_007891	2	0.7
		Inflammation	Cxcl10	NM_021274	4.1	0.1
Inflammation		Nfkbia	NM_010907	3.5	1.7	
Inflammation		Casp1	NM_009807	2.1	1.0	
Inflammation		Nos2	NM_010927	2.0	0.9	
Ox.stress		Ugt1a2	NM_013701	7.1	0.4	
PEI(25)-PEG(0.55)30	Ox.stress	Cryab	NM_009964	3.0	0.9	
	Ox.stress	Hspa1b	NM_010478	1.6	3.1	
	Cytotoxicity	E2f1	NM_007891	3.0	0.9	
	Inflammation	Nfkbia	NM_010907	7.4	2.7	
	Inflammation	Nos2	NM_010927	4.5	2.8	
	Inflammation	Casp1	NM_009807	4.1	1.1	
	Inflammation	Cxcl10	NM_021274	2.5	0.3	
	Inflammation	Mif	NM_010798	2.1	0.8	
	Inflammation	Serpine1	NM_008871	2.0	1.4	
	Inflammation	IL1b	NM_008361	1.3	5.9	
PEI(25)-PEG(2)10	Ox.stress	Ugt1a2	NM_013701	10.0	0.8	
	Ox.stress	Cryab	NM_009964	2.5	1.2	
	Ox.stress	Hspa1b	NM_010478	1.7	4.8	

Table 2: Genes were clustered in three tier levels (Tier 3: cytotoxicity, tier 2: inflammation, tier 1: oxidative stress) according to the hierarchical oxidative stress model from Nel and colleagues [19]. Shown are genes with change of expression of more than 2-fold after 6h and 24h treatment with CS (Min-U-Sil 5 400 µg/ml), NZO (2.5 µg/ml), PEI25 kDa (5 µg/ml), PEI(25)-PEG(2)10 (5 µg/ml), and PEI(25)-PEG(0.55)30 (5 µg/ml). Fold changes (linear) were calculated using comparative cycle threshold (CT) method and normalized to the house keeping gene Hprt 1.

Lung toxic benchmarks

The highest number of changes in gene expression was observed upon treatment with CS after 6 h and 24 h (Table 2). The following genes were more than 2-fold up-regulated after 6 h

treatment and the corresponding tier levels are indicated: Cytotoxicity: *NfkBia*, *E2f1*, *Tnfsf10*, *Gadd45*, *Cdkn1a*, *Ddit*, *Bax*, *Tnfrsf1a*, and *Ccng* Inflammation: *Cxcl10*, *Casp1*, *Nos2*, *NfkBia*, *Il-18*, and *Lta*, Oxidative stress: *Ugt1a2*, *Cryab*, and *Hspa1b*. Most genes regulated after 6 h of treatment were related to inflammation and/or to cell survival/apoptosis pathways. After 24 h treatment, only five genes showed elevated mRNA levels which were either related to a sustained proinflammatory state (*Cxcl10* and *Serpine 1*) or to an oxidative stress response (*Mt2* and *Hmox1*).

In contrast NZO treatment induced expression for oxidative and heat shock stress genes after 6 h (*Hspa1b* and *Hspb1*, *Ugt1a2*, *Hmox1*, *Mt2*) but returned to baseline levels (or even below) after the 24 h treatment. Exceptions were *NfkBia* and *Cxcl10*, which are indicative of inflammation.

PEI-based non-viral carrier systems

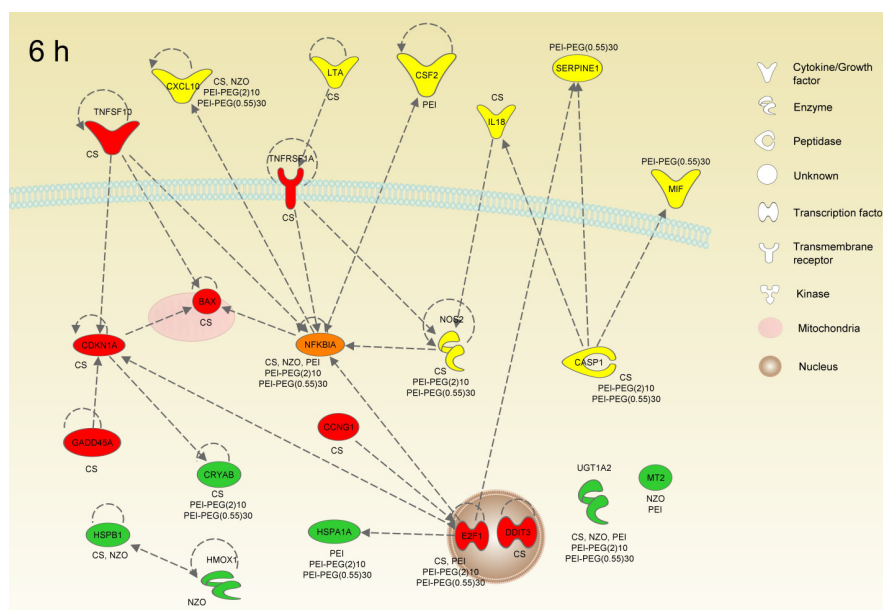
Within the first 6 h PEI 25 kDa induced only for a few gene expression changes above a factor of 2 with the most notable markers indicating oxidative stress (*Ugt1a2* and *Mt2*), and to a lesser extent also anti-apoptotic, survival and proinflammatory (*Cxcl10*, *Csf2*, *Nfkbia*) responses. The response pattern changed considerably for the second phase of analysis with an increasing contribution of apoptosis-related markers. Compared to the PEG-modified PEI copolymers after 24 h PEI 25 kDa treatment was the only polymer causing obvious apoptotic gene expression (*Bcl2l1*, *Bax*, *Anxa5*, *Ercc4* and *Atm*) a pattern not at all observed for the two lung toxic benchmark particles NZO and CS after 24 h treatment, but after 6 h for CS.

During the early response after 6 h highly elevated expression levels of *E2f1*, a cell cycle regulating transcription factor, and *NfkBia*, an important component of the NF κ B machinery, involved in many proinflammatory and apoptosis/survival signalling pathways, were detected for all three PEI polymers, as well as oxidative stress indicating phase II metabolizing enzyme *Ugt1a2*.

Overall, during the first 6 h treatment PEGylated copolymers but not PEI 25 kDa caused mainly an up-regulation of proinflammatory genes including *Cxcl10*, *Caps1*, *Nos2*, and *Nfkb1a*. The cellular stress response markers *Cryab* and *Hsp1b* showed a similar expression pattern with high levels for *Hspa1b* only after 24 h for both PEGylated PEIs. Only PEI(25)-PEG(0.55)30 induced particular high levels of *Mif* and *Serpine 1* after 6 h and *Il1b*, *Nos2* and *Nfkb1a* after 24 h, all well described proinflammatory marker genes (Fig.2A and B).

Figure 2: Pathway modeling

A



B

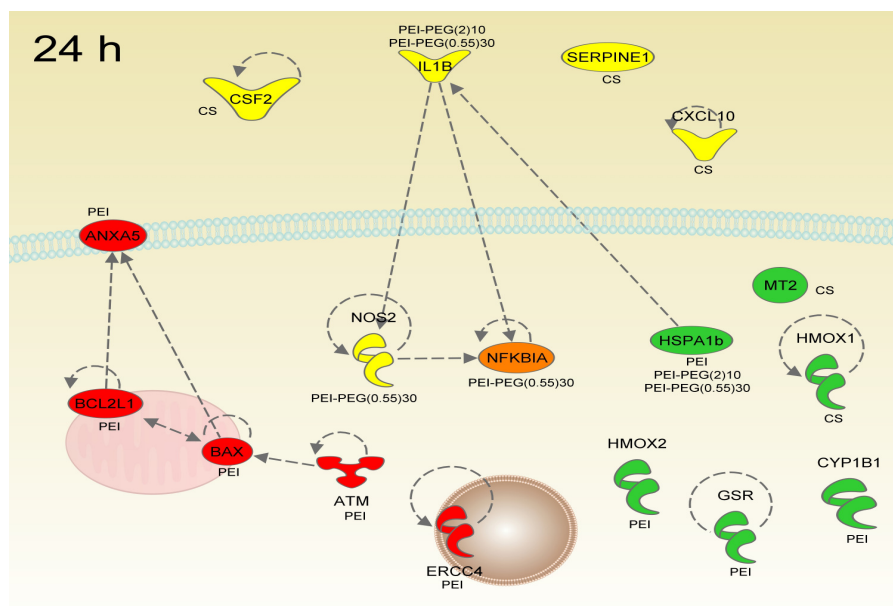
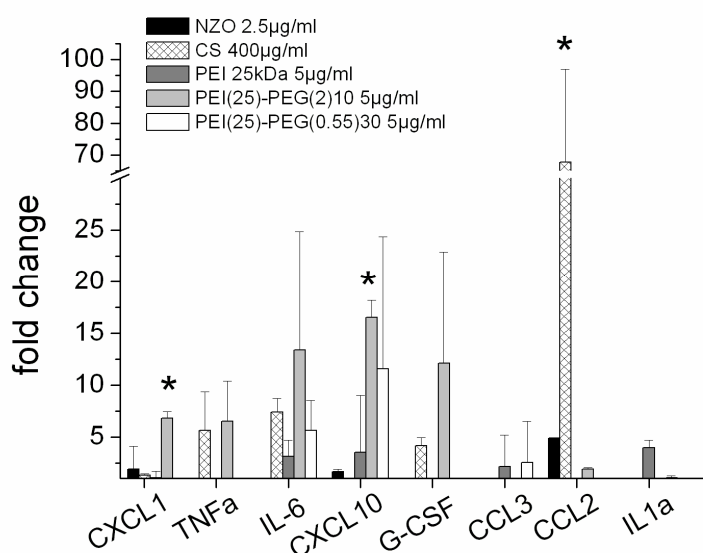


Figure 2A-B: Pathway modeling

Network of all more than 2 fold induced genes at 6 h (A) or 24 h (B). Interactions are based on the Ingenuity pathway software and the different treatments are indicated. Genes are highlighted according to Nel and colleagues [19] (green/oxidative stress, yellow/inflammation, red/cytotoxicity), orange (inflammation/cytotoxicity-overlap).

Cytokine Profiling

For lung particle interactions the proinflammatory effect is a sensitive and critical response to foreign material, which is induced already at doses below significant cytotoxicity. To confirm the gene array results the induction of a proinflammatory state was also investigated at the protein level. A panel of eight representative cytokines (IL-1 α , IL-6, TNF-alpha, G-CSF, CXCL1 CXCL10, CCL2, and CCL3) was assessed for their release from LA4 cells upon 24h treatment with the above selected doses. Corresponding to the gene expression data, CS and PEI(25)-PEG(2)10 showed the most prominent proinflammatory response (Fig.3).

Figure 3: Cytokine release**Figure 3: Cytokine release**

Cytokine release was determined in LA4 cells after 24 h treatment. Values are represented as fold changes compared to the control (untreated cells; mean \pm SEM). Statistically significant changes with a p -value < 0.05 compared to controls are indicated by an asterisk.

Experiments were repeated three times in case of the PEI based polymers and five times in case of NZO and CS.

Increased levels were mainly detected for the acute-phase cytokines like CXCL1, CXCL10, TNF, IL-6, and G-CSF (CSF2) upon CS and PEGylated PEI treatment, with a more than 10 fold elevated protein release for IL-6, CXCL10 and G-CSF caused by PEI(25)-PEG(2)10. In addition, monocyte chemoattractant protein 1 (MCP-1, also known as CCL2) showed up to 70-fold elevated levels after 24 h treatment with CS. At the concentration used in the qRT-PCR array as well as at higher doses of up to 1000 $\mu\text{g/ml}$ for CS and NZO and 50 $\mu\text{g/ml}$ for PEI 25 kDa (data not shown), both treatments caused only negligible release levels of the investigated proinflammatory cytokines.

4.5 Discussion

Cytotoxicity

To overcome the high cytotoxicity of PEI-based non viral vector systems is a major challenge towards an improved safety and efficiency of gene therapy and RNAi. Some modifications of standard PEI 25 kDa already yielded promising carriers. For example, as previously described[26] PEGylation of PEI 25kDa with a PEG chain length of up to 2 kDa and a grafting degree higher than 10 strongly reduced cytotoxicity of PEI 25 kDa. In comparison to the lung toxic benchmark particles we showed here similar cytotoxicity levels for PEI 25 kDa and NZO, but much less for CS.

For the qRT-PCR pathway-focused gene array particle concentrations with moderate cytotoxic effects were used as clearly shown by the data on membrane damage and metabolic activity. By avoiding a state of full-blown cell death we were able to study underlying toxicity mechanisms under well-defined cell culture setting.

Stress and Toxicity Pathway Finder

Lung toxic benchmarks

Inhalation of CS has long been associated with lung disease such as silicosis and lung cancer [27, 28]. The typical involved processes were generation of oxidative species, release of inflammatory cytokines and chemokines as well as proliferative factors. In our *in vitro* study we were able to reproduce and distinguish these processes by gene expression profiling and by that validate our system. In accordance to previous results we observed a strong up-regulation of genes related to oxidative stress response and detoxification (*Ugt1a2*, *Cryab*, *Mt2*, *Hmox1*), inflammation (*Nfkb1a*, *Cxcl10*, *Casp1*, *Nos2*, *Il18*, *Lta*, *Hspa1b*, *Serpine1*, *Csf2*), and cytotoxicity pathways (*Tnfsf10*, *E2f*, *Gadd45*, *Cdkn1a*, *Ddit3*, *Bax*, *Tnfrsf1a*, *Ccng1*).

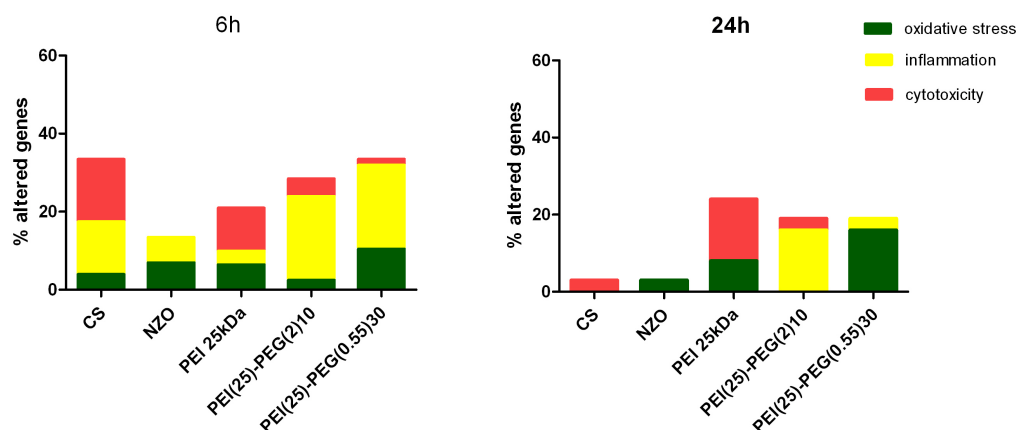
ZnO particles and Zn²⁺ ions have been described to stimulate oxygen radical formation and cause metal fume fever [17, 18, 29]. In particular Zn is a potent and well known inducer of heat shock protein transcription [30], a phenomenon that might be seen as a protective mechanism of these chaperons for recovery from stress situations.

In our study we observed a pronounced stress response characterized by heat shock and oxidative stress marker expression like *Hspb1*, *Hmox1*, *Mt2*, *Ugt1a2* as well as minor indications for proinflammatory reactions (*NfkBia* and *Cxcl10*) after 6 h. After 24 h no up-regulated genes but rather repressed expression levels were detected (Supporting material, S2). Even though the transcriptional pathways leading to gene repression are less understood compared to those of induction, the repression of the major oxidative stress marker heme oxygenase 1 (*Hmox1*), has been discussed as potential defense strategy upon hypoxic conditions. Besides that, Zn exposed cells, have been found to react with an overall inhibition of protein synthesis[31].

PEI-based non-viral vector systems

PEI-based non-viral vector systems caused all together less alteration of gene expression levels as compared to our lung toxic benchmark particles, but we could still detect a prominent cytotoxic (PEI 25 kDa) as well as proinflammatory response to PEG modified PEI copolymers.

In detail after 6 h treatment several genes related to inflammatory signalling were especially altered upon treatment with PEG modified PEI-based non-viral vectors. After 24 h notably more genes, mainly related to apoptosis, were induced by PEI 25KDa (Fig.2 and 4).

Figure 4: *Expression Synopsis*Figure 4: *Expression Synopsis*

Genes were clustered in three tier levels (tier 1 (green): oxidative stress, tier 2: inflammation (yellow), tier 3: cytotoxicity (red)) according to the hierarchical oxidative stress model from Nel and colleagues[19]. The percentage of altered genes (> 2-fold) after 6 h (left) and 24 h (right) treatment with CS (400 $\mu\text{g/ml}$), NZO (2.5 $\mu\text{g/ml}$), PEI25kDa (5 $\mu\text{g/ml}$), PEI(25)-PEG(2)10 (5 $\mu\text{g/ml}$), and PEI(25)-PEG(0.55)30 (5 $\mu\text{g/ml}$) was calculated based on the number of genes more than 2 fold induced, related to the number of genes representing the tier level on the array.

Nfkb and *E2f* seem to be key players induced by the inflammatory response after 6 h. *Nfkb* triggers inflammation mediated by chemokines and cytokines as well as apoptotic signalling pathways a process that is well described in the literature [32]. The transcription factor *E2f* is a potent activator for genes involved in cell cycle regulation, DNA synthesis and replication [33], but is also known to promote apoptotic signaling [34, 35].

High levels of *Cxcl10* and *Nos2* were observed after treatment with PEG-modified PEI polymers. These genes are well known for their immunomodulatory potential and are known to be highly induced during inflammation [36]. Both, PEI(25)-PEG(2)10 and PEI(25)-PEG(0.55)30 treatment induced stress response proteins, in particular antioxidant defence pathways represented by *Ugt1a2*, *Mt2*, and *Hmox1*, which are possibly upstream of the inflammatory cascade (*Il18*, *Cxcl10*, *Nfkb*, *Casp1*, *Nos2*). PEI 25 kDa caused high up-regulation of genes like *Bax*, *Bcl2l1*, *Atm*, *Anxa5*, and *Ercc4* related to apoptotic cell death,

whereas PEG-PEI copolymers induced high levels of genes related to inflammation like *Casp1*, *Il1b*, *Hspa1b*, *Nos2*, and *NfkBia*. Since the observed long lasting inflammatory potential of CS [37-40], was found to be associated with its hazard to cause chronic lung disease [28, 41], our observation might raise serious concerns about the safety of non-degradable, PEGylated polymers like PEI(25)-PEG(0.55)30,

Inflammatory response

Sensitive organs such as the lung are well known for their high sensitivity to particle treatment, especially for so called nano-sized particles in a size range below 100nm [41-43]. Exposure of the respiratory system to particles triggers proinflammatory effects and can directly cause tissue damage and alteration of lung function and adverse cardiovascular effects [29, 44]. Therefore any inflammatory stimulation caused by inhalation of a therapeutic agent has to be monitored carefully. In our study prominent up-regulation of genes related to inflammation (*Cxcl10*, *Nos2*, *IL-1b*, *Casp1*, *NfkBia*, *Csf2*, *Mif*, *Serpine1*, *Lta*, *Il-18*) was observed after treatment with PEI(25)-PEG(2)10, PEI(25)-PEG(0.55)30 and CS. This result is in good accordance to other studies [28, 45, 46], where CS was used as positive control for lung inflammation. At protein level PEGylated copolymers and CS caused abundant cytokine release with patterns similar to our qRT-PCR data. The proinflammatory potential of the PEI-based non-viral vector systems seems to be promoted by the PEG-modification of PEI 25 kDa with a PEG chain length of 2 kDa and grafting densities higher than 10.

Two different underlying mechanisms could be highlighted when comparing the cytotoxicity (apoptosis) pathways triggered by CS after 6h with those by PEI25 kDa after 24 h as illustrated in Fig. 2A and B: For CS it seems to be likely that during the onset of the cascade, the TNF-receptor has been activated by reactive oxygen species generated by particle surface reactivity. This rapid activation will subsequently be transduced, depending on the cellular stress levels, via the cellular NFκB - switchpoint into signaling causing either inflammatory

(*Cxcl10*, *Lta*, *Casp1*, *Il18* and *Nos2*) or apoptotic responses (*Tnfr10*, *Cdkn1a*, *Ccng1*, *Gadd45a*). In contrast to this extrinsic apoptotic pathway, PEI 25 kDa caused high induction of genes related to the intrinsic apoptotic pathway like *Bcl2l1*, *Bax* and DNA damage response like *Atm* and *Ercc4*. This intrinsic response could be induced depending on the endosomal uptake of PEI which causes a dramatic swelling and rupture of the endosome. While this release process, called 'proton sponge effect' seems crucial for the delivery of nucleic acid into the cytoplasm, the thereby generated intracellular stress can induce apoptosis via the intrinsic/mitochondrial pathway.

This redox-sensitive caused response process will have to be balanced by the cellular antioxidant and detoxification machinery (*Cyp1b1*, *Cryab*, *Hmox2*, *Gsr*, *Hspb1*, and *Ugt1a2*).

In summary, both benchmark particles revealed significant expression changes only within the first 6 h of treatment. CS induced pathways related to oxidative stress, inflammation and cytotoxicity, and NZO particles yielded a characteristic early stress protein response. The three PEI-based polymers showed certainly related expression pattern, but proinflammatory pathways were primarily induced by PEG modified PEI-based copolymers. In addition, the response upon PEI 25 kDa could be distinguished through apoptotic pathways triggered in the later phase, after 24 h of treatment (Fig.4). The observed alteration of expression levels of genes involved in apoptosis and cytokine signaling should be avoided on the one hand, but to some extent might also be beneficial for tumour targeting with improved anti-tumour effects on the other hand [47-50]. The higher inflammatory potential of the PEG modified PEI copolymers should however be considered as one limitation for their pulmonary application for various lung diseases where repeated and permanent dosing is required. To examine the in vivo relevance of the here described alarming proinflammatory PEI-PEG properties, detailed animal studies are currently executed in our lab which shall provide important information about degree and persistence of any relevant inflammatory responses.

Acknowledgment

Financial support of the Deutsche Forschungsgemeinschaft (DFG, Forschergruppe 627) is gratefully acknowledged. We would like to thank Birgit Frankenberger for her excellent technical assistance.

4.6 Supporting Information

S1: Gene table

Gene table of the RT² Profiler™ PCR Array Mouse Stress & Toxicity PathwayFinder provided by the manufacturer.

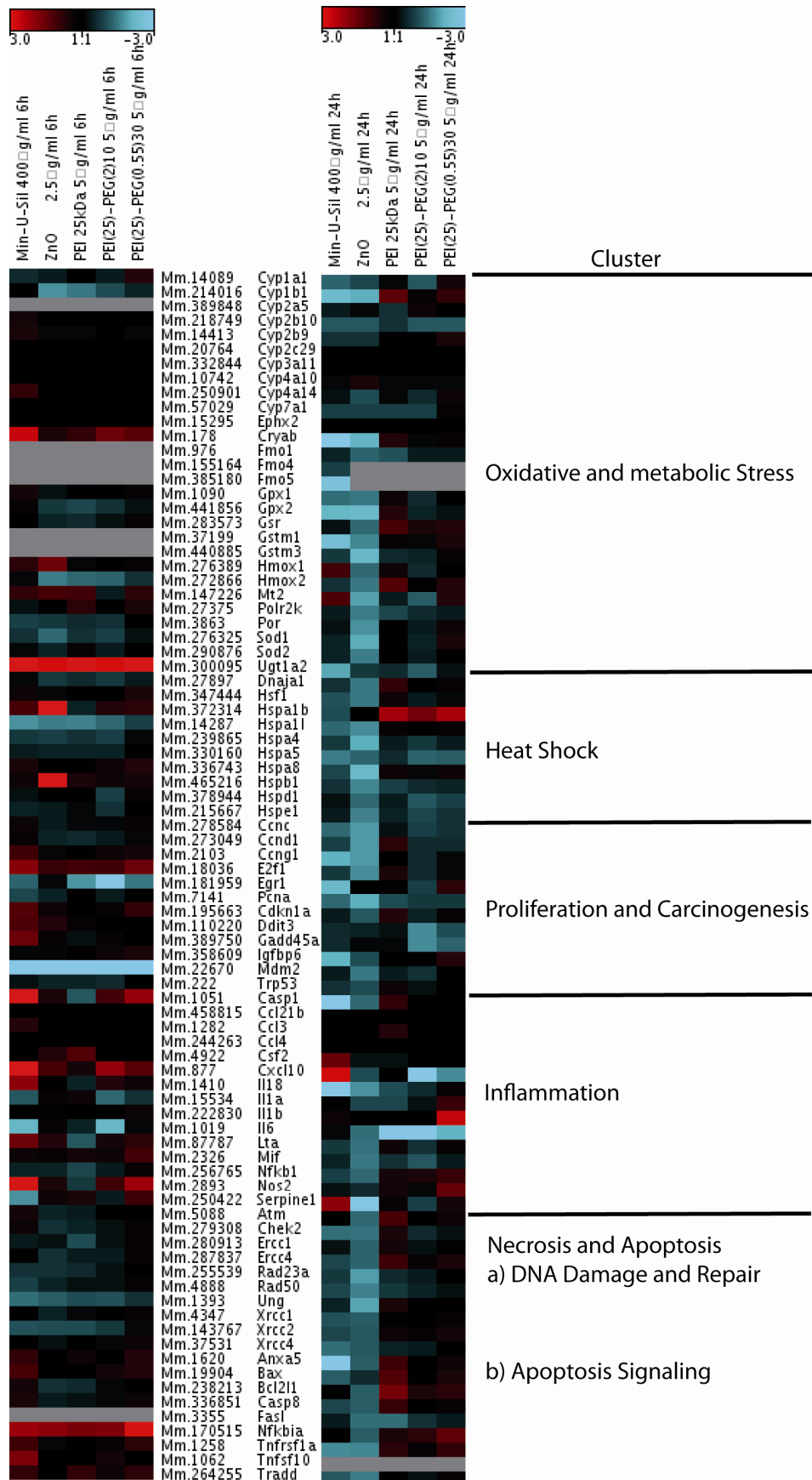
PCR Array Catalog #:	PAMM-003				
Position	Unigene	Refseq	Symbol	Description	Gencode
A01	Mm.1620	NM_009673	Anxa5	Annexin A5	Anx5/R74653
A02	Mm.5088	NM_007499	Atm	Ataxia telangiectasia mutated homolog (human)	AI256621/C030026E19Rik
A03	Mm.19904	NM_007527	Bax	Bcl2-associated X protein	BAX
A04	Mm.238213	NM_009743	Bcl2l1	Bcl2-like 1	Bcl(X)L/Bcl-XL
A05	Mm.1051	NM_009807	Casp1	Caspase 1	ICE/II1bc
A06	Mm.336851	NM_009812	Casp8	Caspase 8	Caspase-8/FLICE
A07	Mm.458815	NM_011124	Ccl21b	Chemokine (C-C motif) ligand 21b	6CKBAC2/6Ckine
A08	Mm.1282	NM_011337	Ccl3	Chemokine (C-C motif) ligand 3	AI323804/G0S19-1
A09	Mm.244263	NM_013652	Ccl4	Chemokine (C-C motif) ligand 4	Act-2/MIP-1B
A10	Mm.278584	NM_016746	Ccnc	Cyclin C	AI451004/AU020987
A11	Mm.273049	NM_007631	Ccnd1	Cyclin D1	AI327039/Cyl-1
A12	Mm.2103	NM_009831	Ccng1	Cyclin G1	AI314029
B01	Mm.195663	NM_007669	Cdkn1a	Cyclin-dependent kinase inhibitor 1A (P21)	CAP20/CDKI
B02	Mm.279308	NM_016681	Chek2	CHK2 checkpoint homolog (S. pombe)	CHK2/Cds1
B03	Mm.178	NM_009964	Cryab	Crystallin, alpha B	Crya-2/Crya2
B04	Mm.4922	NM_009969	Csf2	Colony stimulating factor 2 (granulocyte-macrophage)	Csfgm/Gm-CSf
B05	Mm.877	NM_021274	Cxcl10	Chemokine (C-X-C motif) ligand 10	C7/CRG-2
B06	Mm.14089	NM_009992	Cyp1a1	Cytochrome P450, family 1, subfamily a, polypeptide 1	AHH/AHRR
B07	Mm.214016	NM_009994	Cyp1b1	Cytochrome P450, family 1, subfamily b, polypeptide 1	CP1B/P4501b1
B08	Mm.389848	NM_007812	Cyp2a5	Cytochrome P450, family 2, subfamily a, polypeptide 5	Coh/Cyp15a2
B09	Mm.218749	NM_009998	Cyp2b10	Cytochrome P450, family 2, subfamily b, polypeptide 10	Cyp2b/Cyp2b20
B10	Mm.14413	NM_010000	Cyp2b9	Cytochrome P450, family 2, subfamily b, polypeptide 9	Cyp2b
B11	Mm.20764	NM_007815	Cyp2c29	Cytochrome P450, family 2, subfamily c, polypeptide 29	AHOH/AHOHase

B12	Mm.332844	NM_007818	Cyp3a11	Cytochrome P450, family 3, subfamily a, polypeptide 11	AI256190/Cyp3a
C01	Mm.10742	NM_010011	Cyp4a10	Cytochrome P450, family 4, subfamily a, polypeptide 10	AI647584/Cyp4a
C02	Mm.250901	NM_007822	Cyp4a14	Cytochrome P450, family 4, subfamily a, polypeptide 14	AI314743
C03	Mm.57029	NM_007824	Cyp7a1	Cytochrome P450, family 7, subfamily a, polypeptide 1	CYP7A1
C04	Mm.110220	NM_007837	Ddit3	DNA-damage inducible transcript 3	CHOP-10/CHOP10
C05	Mm.27897	NM_008298	Dnaja1	DnaJ (Hsp40) homolog, subfamily A, member 1	Hsj2/Nedd7
C06	Mm.18036	NM_007891	E2f1	E2F transcription factor 1	E2F-1/mKIAA4009
C07	Mm.181959	NM_007913	Egr1	Early growth response 1	A530045N19Rik/ETR103
C08	Mm.15295	NM_007940	Ephx2	Epoxide hydrolase 2, cytoplasmic	AW106936/Eph2
C09	Mm.280913	NM_007948	Ercc1	Excision repair cross-complementing rodent repair deficiency, complementation group 1	Ercc-1
C10	Mm.287837	NM_015769	Ercc4	Excision repair cross-complementing rodent repair deficiency, complementation group 4	AI606920/Xpf
C11	Mm.3355	NM_010177	FasL	Fas ligand (TNF superfamily, member 6)	APT1LG1/CD178
C12	Mm.976	NM_010231	Fmo1	Flavin containing monooxygenase 1	FMO1
D01	Mm.155164	NM_144878	Fmo4	Flavin containing monooxygenase 4	D1ErtD532e
D02	Mm.385180	NM_010232	Fmo5	Flavin containing monooxygenase 5	5033418D19Rik/AI195026
D03	Mm.389750	NM_007836	Gadd45a	Growth arrest and DNA-damage-inducible 45 alpha	AA545191/Ddit1
D04	Mm.1090	NM_008160	Gpx1	Glutathione peroxidase 1	AI195024/AL033363
D05	Mm.441856	NM_030677	Gpx2	Glutathione peroxidase 2	GPxGI/GSHPx-2
D06	Mm.283573	NM_010344	Gsr	Glutathione reductase	AI325518/D8ErtD238e
D07	Mm.37199	NM_010358	Gstm1	Glutathione S-transferase, mu 1	Gstb-1/Gstb1
D08	Mm.440885	NM_010359	Gstm3	Glutathione S-transferase, mu 3	AI042769/Fsc2
D09	Mm.276389	NM_010442	Hmox1	Heme oxygenase (decycling) 1	D8Wsu38e/HO-1
D10	Mm.272866	NM_010443	Hmox2	Heme oxygenase (decycling) 2	HO-2/HO2
D11	Mm.347444	NM_008296	Hsf1	Heat shock factor 1	AA960185
D12	Mm.372314	NM_010478	Hspa1b	Heat shock protein 1B	Hsp70/Hsp70-1
E01	Mm.14287	NM_013558	Hspa1l	Heat shock protein 1-like	Hsc70t/Msh5
E02	Mm.239865	NM_008300	Hspa4	Heat shock protein 4	70kDa/AI317151
E03	Mm.330160	NM_022310	Hspa5	Heat shock protein 5	78kDa/AL022860
E04	Mm.336743	NM_031165	Hspa8	Heat shock protein 8	2410008N15Rik/Hsc70
E05	Mm.465216	NM_013560	Hspb1	Heat shock protein 1	27kDa/Hsp25

E06	Mm.378944	NM_010477	Hspd1	Heat shock protein 1 (chaperonin)	60kDa/Hsp60
E07	Mm.215667	NM_008303	Hspe1	Heat shock protein 1 (chaperonin 10)	10kDa/mtcpn10
E08	Mm.358609	NM_008344	Igfbp6	Insulin-like growth factor binding protein 6	IGFBP-6
E09	Mm.1410	NM_008360	Il18	Interleukin 18	Igif/Il-18
E10	Mm.15534	NM_010554	Il1a	Interleukin 1 alpha	Il-1a
E11	Mm.222830	NM_008361	Il1b	Interleukin 1 beta	IL-1beta/Il-1b
E12	Mm.1019	NM_031168	Il6	Interleukin 6	Il-6
F01	Mm.87787	NM_010735	Lta	Lymphotoxin A	LT/LT-[a]
F02	Mm.22670	NM_010786	Mdm2	Transformed mouse 3T3 cell double minute 2	1700007J15Rik/AA415488
F03	Mm.2326	NM_010798	Mif	Macrophage migration inhibitory factor	GIF/Glif
F04	Mm.147226	NM_008630	Mt2	Metallothionein 2	AA409533/MT-II
F05	Mm.256765	NM_008689	Nfkb1	Nuclear factor of kappa light chain gene enhancer in B-cells 1, p105	NF-KB1/NF-kappaB
F06	Mm.170515	NM_010907	Nfkbia	Nuclear factor of kappa light chain gene enhancer in B-cells inhibitor, alpha	AI462015/Nfkbi
F07	Mm.2893	NM_010927	Nos2	Nitric oxide synthase 2, inducible, macrophage	NOS-II/Nos-2
F08	Mm.7141	NM_011045	Pcna	Proliferating cell nuclear antigen	PCNA
F09	Mm.27375	NM_023127	Polr2k	Polymerase (RNA) II (DNA directed) polypeptide K	MafY/Mt1a
F10	Mm.3863	NM_008898	Por	P450 (cytochrome) oxidoreductase	4933424M13Rik/CPR
F11	Mm.255539	NM_009010	Rad23a	RAD23a homolog (<i>S. cerevisiae</i>)	2310040P19Rik/AL024030
F12	Mm.4888	NM_009012	Rad50	RAD50 homolog (<i>S. cerevisiae</i>)	Mrell/Rad50l
G01	Mm.250422	NM_008871	Serpine1	Serine (or cysteine) peptidase inhibitor, clade E, member 1	PAI-1/PAI1
G02	Mm.276325	NM_011434	Sod1	Superoxide dismutase 1, soluble	B430204E11Rik/Cu
G03	Mm.290876	NM_013671	Sod2	Superoxide dismutase 2, mitochondrial	MnSOD/Sod-2
G04	Mm.1258	NM_011609	Tnfrsf1a	Tumor necrosis factor receptor superfamily, member 1a	CD120a/FPF
G05	Mm.1062	NM_009425	Tnfsf10	Tumor necrosis factor (ligand) superfamily, member 10	A330042I21Rik/AI448571
G06	Mm.264255	NM_001033161		Tradd TNFRSF1A-associated via death domain	9130005N23Rik/AA930854
G07	Mm.222	NM_011640	Trp53	Transformation related protein 53	bb1/bfy
G08	Mm.300095	NM_013701	Ugt1a2	UDP glucuronosyltransferase 1 family, polypeptide A2	UGTBr/p

G09	Mm.1393	NM_011677	Ung	Uracil DNA glycosylase	UNG1/UNG2
G10	Mm.4347	NM_009532	Xrcc1	X-ray repair complementing defective repair in Chinese hamster cells 1	Xrcc-1
G11	Mm.143767	NM_020570	Xrcc2	X-ray repair complementing defective repair in Chinese hamster cells 2	4921524O04Rik/8030409M04Rik
G12	Mm.37531	NM_028012	Xrcc4	X-ray repair complementing defective repair in Chinese hamster cells 4	2310057B22Rik/AW413319
H01	Mm.3317	NM_010368	Gusb	Glucuronidase, beta	AI747421/Gur
H02	Mm.299381	NM_013556	Hprt1	Hypoxanthine guanine phosphoribosyl transferase 1	C81579/HPGRT
H03	Mm.2180	NM_008302	Hsp90ab1	Heat shock protein 90kDa alpha (cytosolic), class B member 1	90kDa/AL022974
H04	Mm.343110	NM_008084	Gapdh	Glyceraldehyde-3-phosphate dehydrogenase	Gapd
H05	Mm.328431	NM_007393	Actb	Actin, beta, cytoplasmic	Actx/E430023M04Rik
H06	N/A	SA_00106	MGDC	Mouse Genomic DNA Contamination	MIGX1B
H07	N/A	SA_00104	RTC	Reverse Transcription Control	RTC
H08	N/A	SA_00104	RTC	Reverse Transcription Control	RTC
H09	N/A	SA_00104	RTC	Reverse Transcription Control	RTC
H10	N/A	SA_00103	PPC	Positive PCR Control PPC	
H11	N/A	SA_00103	PPC	Positive PCR Control PPC	
H12	N/A	SA_00103	PPC	Positive PCR Control PPC	

S2: Heat map



S2: *Heat map*

Fold induction of each gene after 6h treatment (left) and 24h treatment (right).is shown (based on our qRT-PCR stress and toxicity pathways focused gene array). Red (blue) color indicates up-(down-)regulation and gene symbols and Unigene IDs are shown. Genes are sorted according to the seven clusters of the RT² Profiler™ PCR Array Mouse Stress & Toxicity PathwayFinder provided by the manufacturer (except for Ugt1a2 and Casp1).

4.7 References

- 1 Howarth, J.L., Y.B. Lee, and J.B. Uney, *Using viral vectors as gene transfer tools (Cell Biology and Toxicology Special Issue: ETCS-UK 1 day meeting on genetic manipulation of cells)*. Cell Biol Toxicol, 2009.
- 2 Lufino, M.M., P.A. Edser, and R. Wade-Martins, *Advances in high-capacity extrachromosomal vector technology: episomal maintenance, vector delivery, and transgene expression*. Mol Ther, 2008. 16(9): p. 1525-38.
- 3 Akinc, A., M. Thomas, A.M. Klibanov, and R. Langer, *Exploring polyethylenimine-mediated DNA transfection and the proton sponge hypothesis*. J Gene Med, 2005. 7(5): p. 657-63.
- 4 Gao, K. and L. Huang, *Nonviral methods for siRNA delivery*. Mol Pharm, 2009. 6(3): p. 651-8.
- 5 Kleemann, E., L.A. Dailey, H.G. Abdelhady, T. Gessler, T. Schmehl, C.J. Roberts, M.C. Davies, W. Seeger, and T. Kissel, *Modified polyethylenimines as non-viral gene delivery systems for aerosol gene therapy: investigations of the complex structure and stability during air-jet and ultrasonic nebulization*. J Control Release, 2004. 100(3): p. 437-50.
- 6 Petersen, H., P.M. Fechner, A.L. Martin, K. Kunath, S. Stolnik, C.J. Roberts, D. Fischer, M.C. Davies, and T. Kissel, *Polyethylenimine-graft-poly(ethylene glycol) copolymers: influence of copolymer block structure on DNA complexation and biological activities as gene delivery system*. Bioconjug Chem, 2002. 13(4): p. 845-54.
- 7 Zintchenko, A., A. Philipp, A. Dehshahri, and E. Wagner, *Simple modifications of branched PEI lead to highly efficient siRNA carriers with low toxicity*. Bioconjug Chem, 2008. 19(7): p. 1448-55.
- 8 Rudolph, C., J. Lausier, S. Naundorf, R.H. Muller, and J. Rosenecker, *In vivo gene delivery to the lung using polyethylenimine and fractured polyamidoamine dendrimers*. J Gene Med, 2000. 2(4): p. 269-78.
- 9 Poma, A. and M.L. Di Giorgio, *Toxicogenomics to improve comprehension of the mechanisms underlying responses of in vitro and in vivo systems to nanomaterials: a review*. Curr Genomics, 2008. 9(8): p. 571-85.
- 10 Xia, T., M. Kovochich, M. Liang, L. Madler, B. Gilbert, H. Shi, J.I. Yeh, J.I. Zink, and A.E. Nel, *Comparison of the mechanism of toxicity of zinc oxide and cerium oxide nanoparticles based on dissolution and oxidative stress properties*. ACS Nano, 2008. 2(10): p. 2121-34.
- 11 Kunath, K., A. von Harpe, D. Fischer, H. Petersen, U. Bickel, K. Voigt, and T. Kissel, *Low-molecular-weight polyethylenimine as a non-viral vector for DNA delivery: comparison of physicochemical properties, transfection efficiency and in vivo distribution with high-molecular-weight polyethylenimine*. J Control Release, 2003. 89(1): p. 113-25.
- 12 Jackson, A.L., S.R. Bartz, J. Schelter, S.V. Kobayashi, J. Burchard, M. Mao, B. Li, G. Cavet, and P.S. Linsley, *Expression profiling reveals off-target gene regulation by RNAi*. Nat Biotechnol, 2003. 21(6): p. 635-7.
- 13 Fedorov, Y., E.M. Anderson, A. Birmingham, A. Reynolds, J. Karpilow, K. Robinson, D. Leake, W.S. Marshall, and A. Khvorova, *Off-target effects by siRNA can induce toxic phenotype*. Rna, 2006. 12(7): p. 1188-96.
- 14 Beyerle, A., O.M. Merkel, T. Stoeger, and T. Kissel, *PEGylation affects cytotoxicity and cell-compatibility of poly(ethylene imine) for lung application: structure-function-relationships* Toxicol Appl Pharmacol, 2009. in press.

- 15 Thakur, S.A., C.A. Beamer, C.T. Migliaccio, and A. Holian, *Critical role of MARCO in crystalline silica-induced pulmonary inflammation*. *Toxicol Sci*, 2009. 108(2): p. 462-71.
- 16 Oberdorster, G., A. Maynard, K. Donaldson, V. Castranova, J. Fitzpatrick, K. Ausman, J. Carter, B. Karn, W. Kreyling, D. Lai, S. Olin, N. Monteiro-Riviere, D. Warheit, and H. Yang, *Principles for characterizing the potential human health effects from exposure to nanomaterials: elements of a screening strategy*. Part *Fibre Toxicol*, 2005. 2: p. 8.
- 17 Gordon, T. and J.M. Fine, *Metal fume fever*. *Occup Med*, 1993. 8(3): p. 504-17.
- 18 Lindahl, M., P. Leanderson, and C. Tagesson, *Novel aspect on metal fume fever: zinc stimulates oxygen radical formation in human neutrophils*. *Hum Exp Toxicol*, 1998. 17(2): p. 105-10.
- 19 Aravindan, L., K.A. Bicknell, G. Brooks, V.V. Khutoryanskiy, and A.C. Williams, *Effect of acyl chain length on transfection efficiency and toxicity of polyethylenimine*. *Int J Pharm*, 2009. 378(1-2): p. 201-10.
- 20 Petersen, H., P.M. Fechner, D. Fischer, and T. Kissel, *Synthesis, Characterization, and Biocompatibility of Polyethylenimine-graft-poly(ethylene glycol) Block Copolymers*. *Macromolecules*, 2002. 35(18): p. 6867-6874.
- 21 Mosmann, T., *Rapid colorimetric assay for cellular growth and survival: application to proliferation and cytotoxicity assays*. *J Immunol Methods*, 1983. 65(1-2): p. 55-63.
- 22 Minko, T., P. Kopeckova, V. Pozharov, and J. Kopecek, *HPMA copolymer bound adriamycin overcomes MDR1 gene encoded resistance in a human ovarian carcinoma cell line*. *J Control Release*, 1998. 54(2): p. 223-33.
- 23 Choksakulnimitr, S., S. Masuda, T. Hideaki, Y. T., and H. Mitsuru, *In vitro cytotoxicity of macromolecules in different cell culture systems*. *J Control Release*, 1995. 34: p. 233-214.
- 24 Rainer, J., F. Sanchez-Cabo, G. Stocker, A. Sturn, and Z. Trajanoski, *CARMAweb: comprehensive R- and bioconductor-based web service for microarray data analysis*. *Nucleic Acids Res*, 2006. 34(Web Server issue): p. W498-503.
- 25 Prabhakar, U., E. Eirikis, M. Reddy, E. Silvestro, S. Spitz, C. Pendley, 2nd, H.M. Davis, and B.E. Miller, *Validation and comparative analysis of a multiplexed assay for the simultaneous quantitative measurement of Th1/Th2 cytokines in human serum and human peripheral blood mononuclear cell culture supernatants*. *J Immunol Methods*, 2004. 291(1-2): p. 27-38.
- 26 Merkel, O.M., A. Beyerle, D. Librizzi, A. Pfestroff, T.M. Behr, B. Sproat, P.J. Barth, and T. Kissel, *Nonviral siRNA delivery to the lung: investigation of PEG-PEI polyplexes and their in vivo performance*. *Mol Pharm*, 2009. 6(4): p. 1246-60.
- 27 Donaldson, K. and P.J. Borm, *The quartz hazard: a variable entity*. *Ann Occup Hyg*, 1998. 42(5): p. 287-94.
- 28 Sayes, C.M., K.L. Reed, and D.B. Warheit, *Assessing toxicity of fine and nanoparticles: comparing in vitro measurements to in vivo pulmonary toxicity profiles*. *Toxicol Sci*, 2007. 97(1): p. 163-80.
- 29 Nemmar, A.H.M.F., Hoet Peter H.M., Vermynen Josef, Nemery Benoit, *Size effect of intratracheally instilled particles on pulmonary inflammation and vascular thrombosis*. *Toxicol Appl Pharmacol*, 2003. 186: p. 38-45.
- 30 Ogris, M., S. Brunner, S. Schuller, R. Kircheis, and E. Wagner, *PEGylated DNA/transferrin-PEI complexes: reduced interaction with blood components, extended circulation in blood and potential for systemic gene delivery*. *Gene Ther*, 1999. 6(4): p. 595-605.
- 31 Walthera, U.I. and W. Fortha, *Influence of zinc on protein metabolism in various lung cell lines* *Tox in vitro*, 1999. 13(6): p. 905-914.

- 32 Hanada, T. and A. Yoshimura, *Regulation of cytokine signaling and inflammation*. Cytokine Growth Factor Rev, 2002. 13(4-5): p. 413-21.
- 33 Rogoff, H.A. and T.F. Kowalik, *Life, death and E2F: linking proliferation control and DNA damage signaling via E2F1*. Cell Cycle, 2004. 3(7): p. 845-6.
- 34 Rogoff, H.A., M.T. Pickering, F.M. Frame, M.E. Debatis, Y. Sanchez, S. Jones, and T.F. Kowalik, *Apoptosis associated with deregulated E2F activity is dependent on E2F1 and Atm/Nbs1/Chk2*. Mol Cell Biol, 2004. 24(7): p. 2968-77.
- 35 Yu, F., J. Megyesi, R.L. Safirstein, and P.M. Price, *Involvement of the CDK2-E2F1 pathway in cisplatin cytotoxicity in vitro and in vivo*. Am J Physiol Renal Physiol, 2007. 293(1): p. F52-9.
- 36 Ichinose, M., *Differences of inflammatory mechanisms in asthma and COPD*. Allergol Int, 2009. 58(3): p. 307-13.
- 37 Hollins, A.J., M. Benboubetra, Y. Omid, B.H. Zinselmeyer, A.G. Schatzlein, I.F. Uchegbu, and S. Akhtar, *Evaluation of generation 2 and 3 poly(propylenimine) dendrimers for the potential cellular delivery of antisense oligonucleotides targeting the epidermal growth factor receptor*. Pharm Res, 2004. 21(3): p. 458-66.
- 38 Regnstrom, K., E.G. Ragnarsson, M. Fryknas, M. Koping-Hoggard, and P. Artursson, *Gene expression profiles in mouse lung tissue after administration of two cationic polymers used for nonviral gene delivery*. Pharm Res, 2006. 23(3): p. 475-82.
- 39 Tagami, T., J.M. Barichello, H. Kikuchi, T. Ishida, and H. Kiwada, *The gene-silencing effect of siRNA in cationic lipoplexes is enhanced by incorporating pDNA in the complex*. Int J Pharm, 2007. 333(1-2): p. 62-9.
- 40 Omid, Y., A.J. Hollins, M. Benboubetra, R. Drayton, I.F. Benter, and S. Akhtar, *Toxicogenomics of non-viral vectors for gene therapy: a microarray study of lipofectin- and oligofectamine-induced gene expression changes in human epithelial cells*. J Drug Target, 2003. 11(6): p. 311-23.
- 41 Donaldson, K. and V. Stone, *Current hypotheses on the mechanisms of toxicity of ultrafine particles*. Ann Ist Super Sanita, 2003. 39(3): p. 405-10.
- 42 Stoeger, T., C. Reinhard, S. Takenaka, A. Schroepel, E. Karg, B. Ritter, J. Heyder, and H. Schulz, *Instillation of six different ultrafine carbon particles indicates a surface area threshold dose for acute lung inflammation in mice*. Environ Health Perspect, 2006. 114(3): p. 328-33.
- 43 Oberdorster, G., E. Oberdorster, and J. Oberdorster, *Nanotoxicology: an emerging discipline evolving from studies of ultrafine particles*. Environ Health Perspect, 2005. 113(7): p. 823-39.
- 44 Plank, C., K. Mechtler, F.C. Szoka, Jr., and E. Wagner, *Activation of the complement system by synthetic DNA complexes: a potential barrier for intravenous gene delivery*. Hum Gene Ther, 1996. 7(12): p. 1437-46.
- 45 Ovrevik, J., M. Lag, J.A. Holme, P.E. Schwarze, and M. Refsnes, *Cytokine and chemokine expression patterns in lung epithelial cells exposed to components characteristic of particulate air pollution*. Toxicology, 2009. 259(1-2): p. 46-53.
- 46 Warheit, D.B., T.R. Webb, and K.L. Reed, *Pulmonary toxicity screening studies in male rats with M5 respirable fibers and particulates*. Inhal Toxicol, 2007. 19(11): p. 951-63.
- 47 Dufes, C., W.N. Keith, A. Bilsland, I. Proutski, I.F. Uchegbu, and A.G. Schatzlein, *Synthetic anticancer gene medicine exploits intrinsic antitumor activity of cationic vector to cure established tumors*. Cancer Res, 2005. 65(18): p. 8079-84.
- 48 Moroson, H., *Polycation- treated tumor cells in vivo and in vitro*. Cancer Res, 1971. 31(3): p. 373-80.

- 49** Akhtar, S. and I. Benter, *Toxicogenomics of non-viral drug delivery systems for RNAi: potential impact on siRNA-mediated gene silencing activity and specificity*. *Adv Drug Deliv Rev*, 2007. 59(2-3): p. 164-82.
- 50** Seymour, L., *Synthetic Polymers with Intrinsic Anticancer Activity*. *Journal of Bioactive and Compatible Polymers*, 1991. 6: p. 178.

5 Investigations on mutant frequency induced by Poly(ethylene imine) in FE1-Muta™ Mouse lung epithelial cells

Andrea Beyerle, Alexandra Long, Paul White, Thomas Kissel, Tobias Stoeger

In preparation for *Toxicology letters*

Author's Contributions:

A.B. prepared the manuscript draft and wrote the manuscript, did the experimental work except for the lacZ analysis, analyzed and interpreted the data, A.L. did the lacZ analysis, P.W. provided the FE1 cells and the exposure protocol, and analyzed the data, T.K. reviewed and edited the manuscript, T.S. reviewed and edited the manuscript. All authors read and approved the final version of the manuscript.

5.1 Abstract

Genotoxicity data of polymeric nanomaterial are scant, but of great concern, especially when polymeric non-viral vector systems are used for cancer treatment.

In this study, we analyzed the mutant frequency (MF) caused by three different poly(ethylene imine) (PEI) -based polymers and nanosized zinc oxide particles (NZO) in a transgenic lung epithelial cell culture model following eight repeated 72 h incubations. The level of 8-OH-dG was additionally determined by using ELISA technique. NZO was included as lung toxicity benchmark. The concentrations used in this study served no cytotoxic effects but represented PEI-concentrations normally used for in-vitro transfection studies.

NZO and PEI25kDa showed no mutagenic potential, whereas the two polyethylene glycol (PEG) modified PEI copolymers caused slight increase in MF (PEI(25)-PEG(2)10: 1.4-fold, and PEI(25)-PEG(0.55)30: 1.2-fold increase in MF vs. ctrl.), but without oxidative damage of DNA. In addition, PEI(25)-PEG(2)10 appeared to have proliferative properties due to increased levels of cell counts after all exposure rounds (1.3-fold increase vs. ctrl.).

With regard to genotoxicity PEI-based nanocarriers and NZO particles showed no dramatically effects in MF in the FE1 in vitro model. Further clarification of the mutagenic potential is still needed for such polymeric non-viral nanocarriers and the FE1 MutaTMMouse in vitro model is appropriate to screen the MF, but further analysis for the underlying mechanisms should be followed.

Key words: PEI, mutant frequency, FE1, 8-OH-dG

5.2 Introduction

Poly(ethylene imine) (PEI) has widely been used as non-viral gene carrier due to its capability to form stable complexes by electrostatic interactions with nucleic acids. The major drawback of PEI is its high toxicity due to aggregation of huge clusters of PEI on the cell membrane and its interaction with blood component [1, 2]. To reduce the cytotoxicity of PEI several studies have introduced modified PEIs such as block or graft copolymers containing cationic and hydrophilic non-ionic components [3, 4]. Copolymers of PEI and hydrophilic poly(ethylene glycol) (PEG) with various molecular weights and graft densities were shown to possess improved cytotoxicity and potential for DNA and siRNA delivery [5-7].

To the best of our knowledge and despite the strong interaction of PEI with nucleic acids, no information is available about any mutagenicity or genotoxicity after treatment with PEI polymers. Non-viral vectors based on PEI usually contain an excess of free PEI that is not complexed with nucleic acids [8]. Therefore, it is of great interest to evaluate the mutant frequency induced by different free PEI polymers in *lacZ* transgenes of Muta™ Mouse lung epithelial cells (FE1). Previous studies comprehensively analyzed the safety and biocompatibility of different PEGylated PEI polymers in murine epithelial like type II cells (LA4) and alveolar macrophages (MH-S). We found that the degree of PEGylation correlated both with cytotoxicity and with oxidative stress, but not with proinflammatory effects. AB type copolymers with long PEG blocks caused high membrane damage and significantly decreased the metabolic activity of lung cells. Moreover AB type PEI copolymers with long PEG blocks significantly increased the release of lipid mediators such as 8-isoprostanes (8-IP) and prostaglandin E2 (PGE₂) in a dose-dependent manner. The cytokine profiles showed high levels of acute-phase cytokines such as TNF, IL-6, and G-CSF but without any structure-function relationship [9].

In this study, three different PEI-based polymers and nanosized zinc oxide (NZO) are investigated on their influence to induce mutations using an recently established lung cell in vitro model [10, 11] and the level of 8-hydroxy-2'-desoxyguanosine (8-OH-dG), one of the most

abundant oxidative products of cellular DNA, was determined using enzyme-linked immunosorbent assay (ELISA) technique. The concentrations which are used in this study ruled out any cytotoxic effects according to previous studies in different representative murine lung cell lines [9, 12]. Therefore, cytotoxicity was regarded as negligible in this set up. Regarding the repeated dosing scheme in this study, the overall concentration during the hole exposures (exposure round 1-8) are in one dose range for the PEI-based nanocarriers and NZO, which not normally cause any cytotoxic effects[9, 12]. However, it has been shown that modification on the PEI 25kDa backbone reduces cytotoxicity, but on costs of proinflammatory events and to some extent of oxidative stress parameters [12, 13]. Free radicals could also generated by inflammation, but it is unlikely that all such substances are carcinogens solely because they are able to cause inflammation. For ultrafine particles (UFP) it has been reported that they could enter mitochondria and induce mitochondrial damage because of their small size [14]. UFP may pass through cell membranes and combine with DNA. NZO induced also very high oxidative stress and inflammation [12, 15, 16] and could therefore also be able to direct interact with DNA to cause mutations and contribute to carcinogenesis. Due to its high positive charge density PEI is also able to interact directly with DNA. Therefore, the potential of genotoxicity of such PEI-based polymers for gene therapy or siRNA delivery as well as for NZO requires further clarification and the presented mutagenicity analysis should support the understanding of the underlying toxicity pathway of these non-viral vector systems for optimized development of promising pulmonary nanocarriers.

5.3 Materials and Methods

Particles and polymer solutions

Benzo[a]pyrene (B[a]P) was purchased from Alfa Aesar GmbH & Co KG, Karlsruhe, Germany and prepared as a stock solution of 1 mg in 10 ml DMSO (Merck, Darmstadt, Germany). Nanosized zinc oxide (NZO) was obtained from Alfa Aesar GmbH & Co KG, Karlsruhe, Germany and a stock solution of 1 mg in 1 ml double distilled water was prepared by vigorous vortexing and sonication for 5 min and three times. Branched poly(ethylene imine) (PEI) with a molecular weight of 25 kDa (Polymin, water-free, 99 %) was a gift of BASF, Ludwigshafen. The copolymers poly(ethylene imine)-graft-poly(ethylene glycol) (PEI-PEG) with a PEG content of approximately 50 % (w/w) were synthesized as previously described [4, 17] by grafting linear PEG of 0.55, 2 kDa onto branched PEI 25 kDa. These graft copolymers were designated using following nomenclature: PEI(25k)-g-PEG(x)_n. The number in brackets (25 k or x, where x= 0.55 k, 2 k) represents the molecular weight of the PEI or PEG block in Da, and the index n is the average number of PEG blocks per PEI molecule. This number was calculated on the basis of ¹H-NMR spectra as described previously [4]. Polymer dilutions were prepared in sterile, sodium chloride solution (150mM) to obtain a final concentration of 0.5 µg/ml PEI.

FE1 MML Cell line

The development and characterization of the FE1 MML epithelial cell line has been described previously by [10]. The cells were cultured in growth medium containing DMEM F12 (1:1) medium containing L-glutamine (Invitrogen, Gibco, Germany) supplemented with 2 % FBS (Biochrom AG, Germany), 100 U/ml Penicillin G (Biochrom AG, Germany), 100 mg/ml streptomycin (Biochrom AG, Germany), and 1 ng/ml human epidermal growth factor (Roche, Germany).

Phase contrast microscopy

FE1 MML epithelial cells were observed under an invert microscop (Axiovert 135, Zeiss, Jena, Germany) using phase-contrast II module to detect alteration in cell morphology over all eight exposure rounds and the washing step.

Cell incubations for analysis of mutant frequency (repeated dosing scheme)

The exposure setup was carried out as described previously by [11]. Briefly, 300,000 FE1 MML cells were seeded in 10ml growth medium in petri dishes (90 mm; Corning[®], Sigma-Aldrich, Germany) and incubated at 37 °C and 5 % CO₂ for 24 h before exposure. The negative control were incubated in pure exposure medium whereas the positive control represented 0.1 µg/ml B[a]P. The cells were incubated for 72 h, washed with PBS, trypsinized, and centrifuged at 1200 x g for 5 min at 4 °C. After resuspension in medium cells were counted and 300,000 cells were reseeded in a new dish. After 24 h, new exposure medium (only containing DMEM F12 (1:1) medium containing L-glutamine and supplemented with 1 ng/ml human epidermal growth factor (Roche, Germany)) with or without the test substance was added. After 6 h treatment exposure medium was removed and fresh growth medium was added to the cells. In a total of eight exposure rounds the cells were exposed to the particles or polymers, making the total exposure time (8 x 72 h) 576 h. The cumulative dose added was (8 x 0.5µg x 10) 40 µg for PEI polymers and (8 x 1µg x10) 80 µg for nanosized ZnO and (5 x 0.1µg x 10) 50 µg for B[a]P. B[a]P exposure was only repeated five times because after five times treatment the cells began to grow markedly slower than all other cells and only yielded 25 % confluence compared with about 80 % for all other samples. Therefore, they received pure growth medium for the remaining three exposure rounds. After the eight treatments the dishes were washed thoroughly with PBS to remove the excess of the particle. To further reduce the load of particles, and thereby easing mutation analysis, the cells were trypsinized and reseeded without test substance for 72 h.

Isolation of high molecular weight DNA for mutant analysis

After the ninth exposure/ washing round cells were digested overnight in lysis buffer containing 10 mM Tris pH 7.6, 10 mM EDTA, 10 mM NaCl, 1 mg/ml proteinase K and 1 % SDS. DNA was isolated from FE1 MML cells using chloroform/ phenol extraction and precipitation in ethanol as previously described [10]. Freshly isolated DNA was dissolved in TE buffer and stored at 4°C for further investigation of mutant frequency.

LacZ Mutation Analysis

Transgene mutant frequency was determined using P-gal positive selection assay described by [18]. Briefly, *galE*⁻ host bacterium was used to facilitate isolation and enumeration of mutant copies of the *lacZ* transgene [19]. λ gt10*lacZ* DNA copies were rescued from genomic Muta™ Mouse DNA using the Transpack™ lambda packaging system (Stratagene, La Jolla, CA). Packaged phage particles were mixed with the host bacterium (*Escherichia coli* Δ *lacZ*, *galE*⁻, *recA*⁻, pAA119 with *galT* and *galK* [19, 20]), plated on minimal agar with 0.3 % w/v P-gal, and incubated overnight at 37 ° C. Concurrent titers on nonselective minimal agar were employed to enumerate total plaque-forming units (pfu). Mutant frequency was expressed as the ratio of the mutant plaques to total pfu.

8-OH-dG enzyme-linked immunosorbent assay

8-OH-dG was determined using 8-OH-dG ELISA kit from Japan Institute of the Control of Aging, NIKKEN SEIL Co., Ltd. (Catalo-No. KOG-HS10E). DNA samples were directly used without further dilution and the 8-OH-dG detection was carried out following the manufacturer's instructions.

Statistics

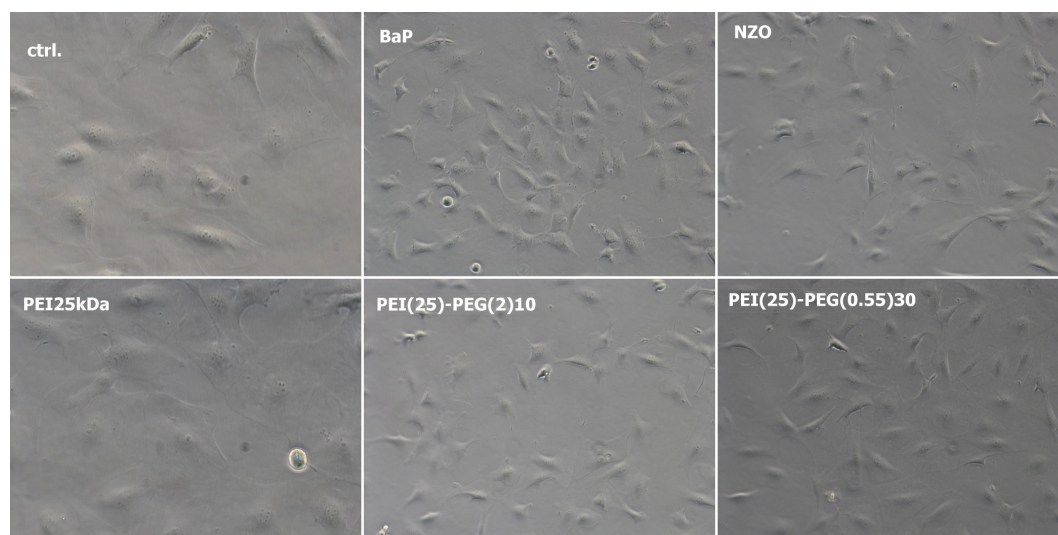
All mutant frequency data were tested for equal variance using F-test. All data sets were analyzed using Student's t-test in the SAS system v. 8.02 Windows (SAS Institute, Cary, NC).

5.4 Results and Discussion

To study mutagenicity a lot of transgenic rodent models are introduced. One of the convenient and effective in vivo mutation assay system is the MutaTMMouse system, which contains 80 copies of a stably integrated $\lambda gt10lacZ$ shuttle vector in the mouse genome [21]. The lung epithelial cell line used in this study was derived from the MutaTMMouse, and is a useful in vitro tool for assessing mutagenic activity [10]. Cell shape and confluence was observed under phase-contrast microscopy (Figure 1).

Figure 1: *Phase-contrast microscopy*

A



B

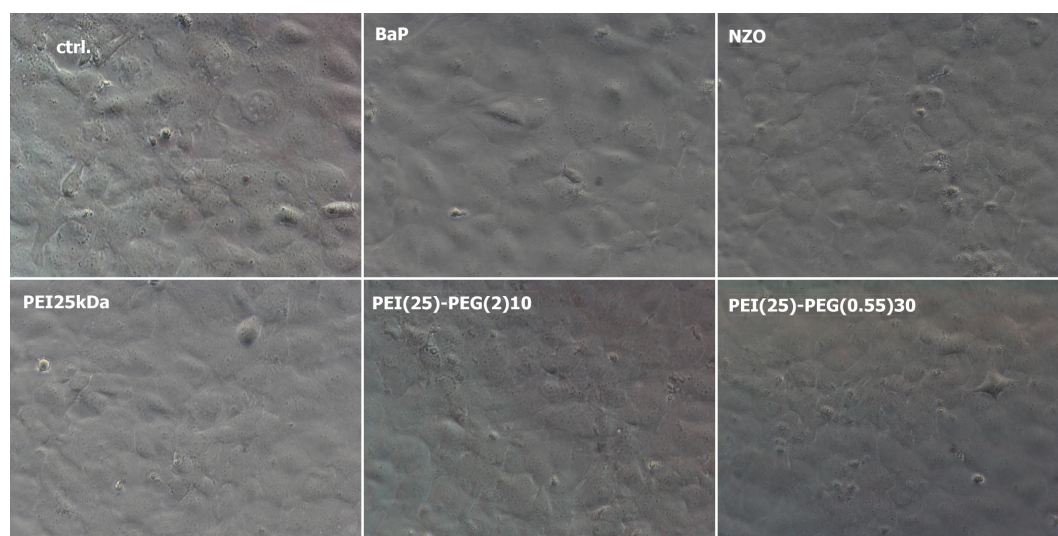


Figure 1: Phase-contrast microscopy

Phase-contrast images of MutaTMMouse flat epithelium isolate 1 (FE1) cells cultured on polystyrene dishes 6 h (A) and 72 h post exposure (B). Images are representative for all exposure rounds and all samples out of one group (n=10).

At low density, directly after reseeding and 6 h post exposure, the cells are large with distinct subcellular inclusions. Whereas at higher density (after 72 h exposure), the cells display less cytoplasm and form tight, uniform monolayer according to previously published data [10]. Depending on the exposure and the time (exposure round) cell counts were statistically impaired after B[a]P (0.1 µg/ml) (Figure 2) and phase-contrast images confirmed this quantification for the positive control. None of the particles and polymers tested altered the cell count rate. Interestingly, PEI(25)-PEG(2)10 seemed to increase the cell counts, which could be related to a slight proliferative effect, but without any statistical significance.

Figure 2: Cell counts

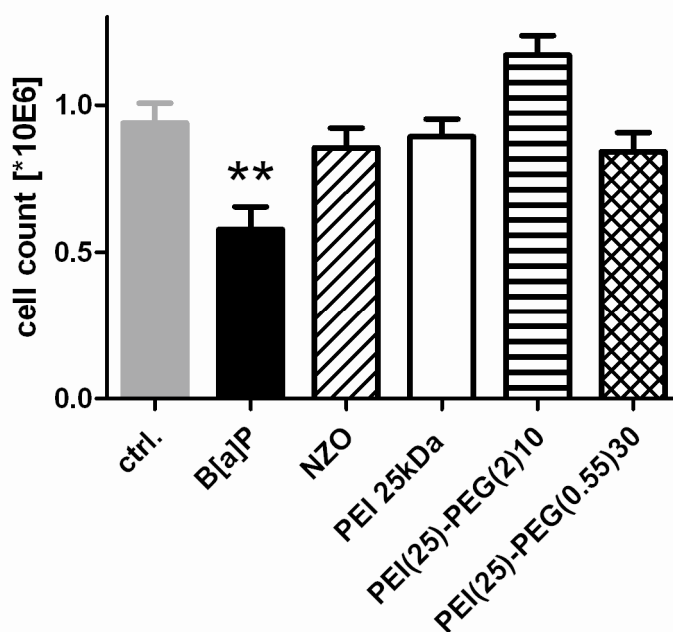


Figure 2: Cell counts

Cells counts were determined using CASY®Technology (innovatis AG, Reutlingen, Germany). 300.000 cells were seeded after each exposure round (for detailed information see material and methods) and cell counts were taken after 72h of exposure. Values represent mean±SD (n=10) of all exposure rounds (in total 8) plus washing phase (round 9). Statistical significance is marked as asterisk, **p<0.01 compared to negative control (ctrl.).

The effect of nanosized zinc oxide (NZO) and PEI-based polymers on the mutant frequency is shown in Table 1. It is obviously that the positive control dramatically elevated the mutant frequency (25.5 –fold increase vs. negative control), which is in good accordance to the results from Jacobsen et al.[11].

Table 1: The Effect of PEI-based nanocarriers on the Frequency of LacZ

Sample	No	Pfu _{screened}	total mutants _{counted}	MF*10 ⁵	MF *10 ⁵	
					mean	SD
negative control	1	247175	189	76.3	67.8	9.5
	2	285775	152	53.0		
	3	250571	179	71.2		
	4	223981	167	74.3		
	5	276995	178	64.1		
positive control	6	138746	2387	1720.4	1733.8	118.7
	7	187535	3066	1634.9		
	8	212302	3602	1696.4		
	9	161608	2713	1678.8		
	10	168483	3267	1938.8		

Table 1(continued): The Effect of PEI-based nanocarriers on the Frequency of LacZ

Sample	No	Pfu screened	total mutants counted	MF*10 ⁵	MF *10 ⁵	
					mean	SD
ZnO 1 ug/ml	11	252890	180	71.0	73.5	7.9
	12	226798	197	86.6		
	13	222490	149	66.7		
	14	277326	191	68.7		
	15	247755	184	74.3		
PEI(25) 0.5 ug/ml	16	217520	203	93.1	74.4	19.3
	17	219923	117	53.2		
	18	217686	189	86.6		
	19	200622	171	85.2		
	20	240962	130	54.0		
PEI(25)-PEG(2)10	21	215118	292	135.7	96.8	26.4
0.5 ug/ml	22	186209	159	85.4		
	23	147278	163	110.7		
	24	171879	120	69.8		
	25	172045	142	82.2		
PEI(25)-PEG(0.55)3026	26	208823	149	71.1	80.0	24.7
0.5 ug/ml	27	171962	87	50.6		
	28	168400	200	118.5		
	29	213047	163	76.5		

Table 1: The Effect of PEI-based nanocarriers on the Frequency of LacZ

The effect of polymers and particles on mutant frequency of lacZ mutants was determined. Bold values represent statistical significant values compare to negative control (***) $p < 0.001$. Pfu screened represents total number of plaque forming units screened for each sample and MF is mutant frequency.

Exposure of FE1 cells to the two PEGylated PEI-based polymers caused slightly elevated levels of mutant frequency in comparison to control, but without any statistical significance. PEI(25)-PEG(2)10 caused a 1.4-fold increase in mutant frequency, and PEI(25)-PEG(0.55)30 1.2-fold increase. NZO and PEI 25kDa exposure yielded mutant frequency comparable to the negative control. From that data, we conclude that PEI(25)-PEG(2)10 is slightly mutagenic and increase the proliferation rate in an eukaryotic lung epithelial cell line such as FE1. To get more insight in the potency of PEI-based polymers and NZO to induce DNA damage, we investigated the effect on oxidation of 8-OH-dG in the cellular DNA with ELISA technique. Again, the positive control showed high potential for DNA damage (Figure 3), but none of our polymers and NZO caused oxidative damage to DNA detected as 8-OH-dG. Accumulation of 8-OH-dG could lead to increased genomic instability that in turn could lead to a more malignant phenotypic behaviour of tumours [22]. The presence of 8-OG-dG in DNA leads to G:C and T:A transversion, mutagenesis, or cell death unless uncorrectly repaired before DNA replication, which is mainly repaired by base excision repair , in case of 8-OH-dG DNA damage.

Figure 3: 8-OH-dG ELISA

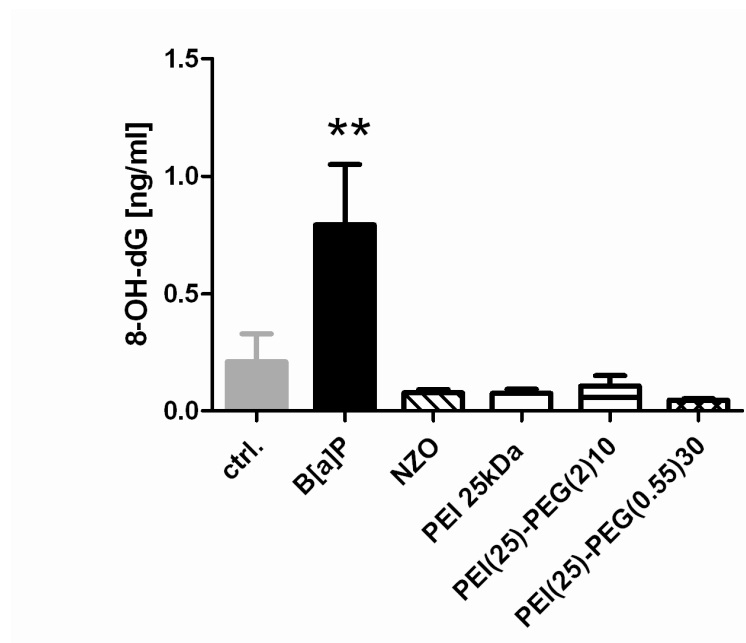


Figure 3:

DNA damage was analyzed using 8-OH-dG ELISA technique as described in materials and methods. Values represent mean \pm SD ($n=10$), and statistical significance represents $**p<0.01$ compare to negative control (ctrl.).

Thus, to clarify the potential of genotoxicity further investigations should be carried out to confirm the data presented in this study. To further elucidate the mechanism behind the slight increase in mutant frequency after treatment with PEI(25)-PEG(2)10, assays for determination of single strand breakage (comet assay), chromosome damage (micronuclei assay) or other mutation assays like the HPRT assay could be performed, but this was out of the scope of this study.

5.5 Conclusion

In conclusion, for the first time to our knowledge, the mutagenic property of PEI-based polymers and NZO was evaluated in a representative lung epithelial *in vitro* model. Since we recently described the higher proinflammatory potential and the induction of oxidative stress induced by these polymers and NZO [9, 13], we are now able to rule out mutagenicity for NZO and PEI25 kDa in an eukaryotic cell line. For the two PEGylated PEI-based nanocarriers the mutant frequency was slightly elevated, but without any sign of DNA damage, thus further analysis should be performed to understand the underlying mechanism. PEI(25)-PEG(2)10 seemed to be proliferative to a low extent, but with regard to carcinogenicity and the possible application of this nanocarrier for pDNA or siRNA delivery, e.g. for cancer treatment, this issue should be focused more in detail. Ongoing *in vivo* studies should further investigate the genotoxicity and mutagenesis of such polymeric non-viral vector systems.

5.6 References

- 1 Fischer, D., Y. Li, B. Ahlemeyer, J. Krieglstein, and T. Kissel, *In vitro cytotoxicity testing of polycations: influence of polymer structure on cell viability and hemolysis*. *Biomaterials*, 2003. 24(7): p. 1121-31.
- 2 Plank, C., K. Mechtler, F.C. Szoka, Jr., and E. Wagner, *Activation of the complement system by synthetic DNA complexes: a potential barrier for intravenous gene delivery*. *Hum Gene Ther*, 1996. 7(12): p. 1437-46.
- 3 Park, T.G., J.H. Jeong, and S.W. Kim, *Current status of polymeric gene delivery systems*. *Adv Drug Deliv Rev*, 2006. 58(4): p. 467-86.
- 4 Petersen, H., Fechner, P.M., Fischer, and Thomas Kissel, *Synthesis, Characterization, and Biocompatibility of Polyethylenimine-graft-poly(ethylene glycol) Block Copolymers*. *Macromolecules*, 2002. 35(18): p. 6867-6874.
- 5 Malek, A., F. Czubayko, and A. Aigner, *PEG grafting of polyethylenimine (PEI) exerts different effects on DNA transfection and siRNA-induced gene targeting efficacy*. *J Drug Target*, 2008. 16(2): p. 124-39.
- 6 Mao, S., X. Shuai, F. Unger, M. Wittmar, X. Xie, and T. Kissel, *Synthesis, characterization and cytotoxicity of poly(ethylene glycol)-graft-trimethyl chitosan block copolymers*. *Biomaterials*, 2005. 26(32): p. 6343-56.
- 7 Kunath, K., A. von Harpe, D. Fischer, H. Petersen, U. Bickel, K. Voigt, and T. Kissel, *Low-molecular-weight polyethylenimine as a non-viral vector for DNA delivery: comparison of physicochemical properties, transfection efficiency and in vivo distribution with high-molecular-weight polyethylenimine*. *J Control Release*, 2003. 89(1): p. 113-25.
- 8 Boeckle, S., K. von Gersdorff, S. van der Piepen, C. Culmsee, E. Wagner, and M. Ogris, *Purification of polyethylenimine polyplexes highlights the role of free polycations in gene transfer*. *J Gene Med*, 2004. 6(10): p. 1102-11.
- 9 Beyerle, A., O. Merkel, T. Stoeger, and T. Kissel, *PEGylation affects cytotoxicity and cell-compatibility of poly(ethylene imine) for lung application: structure-function relationships*. *Toxicol Appl Pharmacol*, 2010. 242(2): p. 146-54.
- 10 White, P.A., G.R. Douglas, J. Gingerich, C. Parfett, P. Shwed, V. Seligy, L. Soper, L. Berndt, J. Bayley, S. Wagner, K. Pound, and D. Blakey, *Development and characterization of a stable epithelial cell line from Muta Mouse lung*. *Environ Mol Mutagen*, 2003. 42(3): p. 166-84.
- 11 Jacobsen, N.R., A.T. Saber, P. White, P. Moller, G. Pojana, U. Vogel, S. Loft, J. Gingerich, L. Soper, G.R. Douglas, and H. Wallin, *Increased mutant frequency by carbon black, but not quartz, in the lacZ and cII transgenes of muta mouse lung epithelial cells*. *Environ Mol Mutagen*, 2007. 48(6): p. 451-61.
- 12 Beyerle, A., M. Irmeler, J. Beckers, T. Kissel, and T. Stoeger, *Toxicity pathway focused gene expression profiling of PEI-based polymers for pulmonary applications*. *Mol Pharm*, under review.
- 13 Beyerle, A., A. Braun, A. Banerjee, N. Ercal, O. Eickelberg, T. Kissel, and T. Stoeger, *Side-effects of PEI-based siRNA nanocarriers for pulmonary application in mice*. *Eur Res J*, under review.
- 14 Li, N., C. Sioutas, A. Cho, D. Schmitz, C. Misra, J. Sempf, M. Wang, T. Oberley, J. Froines, and A. Nel, *Ultrafine particulate pollutants induce oxidative stress and mitochondrial damage*. *Environ Health Perspect*, 2003. 111(4): p. 455-60.
- 15 Lindahl, M., P. Leanderson, and C. Tagesson, *Novel aspect on metal fume fever: zinc stimulates oxygen radical formation in human neutrophils*. *Hum Exp Toxicol*, 1998. 17(2): p. 105-10.

- 16 Xia, T., M. Kovochich, M. Liong, L. Madler, B. Gilbert, H. Shi, J.I. Yeh, J.I. Zink, and A.E. Nel, *Comparison of the mechanism of toxicity of zinc oxide and cerium oxide nanoparticles based on dissolution and oxidative stress properties*. ACS Nano, 2008. 2(10): p. 2121-34.
- 17 Petersen, H., P.M. Fechner, A.L. Martin, K. Kunath, S. Stolnik, C.J. Roberts, D. Fischer, M.C. Davies, and T. Kissel, *Polyethylenimine-graft-poly(ethylene glycol) copolymers: influence of copolymer block structure on DNA complexation and biological activities as gene delivery system*. Bioconj Chem, 2002. 13(4): p. 845-54.
- 18 Vijg, J. and G. Douglas, *Bacteriophage lambda and plasmid lacZ transgenic mice for studying mutations in vivo*. Technologies for the detection of DNA damage and mutations ed. G. Pfeifer. 1996, New York: Plenum Press. 391-410.
- 19 Gossen, J.A. and J. Vijg, *A selective system for lacZ- phage using a galactose-sensitive E. coli host*. Biotechniques, 1993. 14(3): p. 326, 330.
- 20 Mientjes, E., J. vanDelft, B. op'tHof, J.A. Gossen, J. Vij, P. Lohman, and R. Baan, *An improved selection method for lacZ-phages based on galactose sensitivity*. Transgenic Res, 1994. 39: p. 245-253.
- 21 Myhr, B.C., *Validation studies with Muta Mouse: a transgenic mouse model for detecting mutations in vivo*. Environ Mol Mutagen, 1991. 18(4): p. 308-15.
- 22 Shen, J., P. Deininger, J.D. Hunt, and H. Zhao, *8-Hydroxy-2'-deoxyguanosine (8-OH-dG) as a potential survival biomarker in patients with nonsmall-cell lung cancer*. Cancer, 2007. 109(3): p. 574-80.

6 Side-effects of Poly(ethylene imine)-based siRNA nanocarriers for pulmonary application in mice

Andrea Beyerle, Andrea Braun, Atrayee Banerjee, Nuran Ercal, Oliver Eickelberg, Thomas Kissel, Tobias Stoeger

Submitted to European Respiratory Journal (ERJ-00161-2010)

Author's Contributions:

A.B. prepared the manuscript draft and wrote the manuscript, carried out all experimental work except for the oxidative stress measurements, designed the experiments, analyzed and interpreted the data, A.Br. provided the material and protocol for the IgM detection, A.Ba. carried out the measurement of the oxidative stress parameters in lung tissues, N.E. provided the protocol for the HPLC detection of the oxidative stress parameters, reviewed and edited the manuscript, O.E., T.K. and T.S. reviewed and edited the manuscript, T.S. was involved in the experimental design and the approval of the animal study. All authors read and approved the final version of the manuscript.

6.1 Abstract

Polymeric non-viral vector systems for pulmonary application of siRNA are promising carriers, but have failed to enter clinical trials because of safety and efficiency problems. Therefore, improving their transfection efficiency as well as their toxicological profile are subject of intensive research efforts.

Different promising poly(ethylene imine) (PEI) -based nanocarriers with hydrophilic and hydrophobic modifications were toxicologically evaluated for pulmonary application in mice. Nanocarriers were intratracheal instilled to determine their toxicological profile with particular focus on the inflammatory response in the lungs.

Nanocarriers from both groups caused high, acute inflammation in the lungs with different resolution kinetics and cytotoxicity. Hydrophobic modifications caused severe inflammatory response and elevated epithelial barrier permeability, but accompanied by an acute antioxidant response. The later might, especially for Jeffamine™ modified PEI-based nanocarriers, support rapid resolution of the acute inflammation. Hydrophilic modification, with high PEG-grafting degrees, reduced the proinflammatory effects without depletion of macrophages and disruption of the epithelial/endothelial barrier in the lungs and showed only a minor oxidative stress response.

For pulmonary application, the balance between the transfection efficiency and the cytotoxic profile, especially the local pro-inflammatory effects, should be optimized by further development of nanocarriers with highly grafted PEG-PEI-based carriers or Jeffamine™ modified hydrophobic PEI modifications.

Keywords: PEI, siRNA, toxicity, lung inflammation, oxidative stress, epithelial permeability

6.2 Introduction

siRNA delivery to the lung represents a promising non-invasive approach to treating lung cancer or lung diseases like acute lung injury or disorders like influenza [1-3]. Local delivery of siRNAs relevant to lung diseases via the airways is advantageous for gene therapy since the target organ is directly accessible. The large respiratory surface area provides improved transfection efficiency, with reduced systemic side-effects. Successful siRNA delivery using non-viral vector systems to the target cells or tissue is mainly dependent on well balanced electrostatic interactions between a positively charged polymer or liposome and a negatively charged phosphate backbone of the nucleic acid [4-6]. A wide range of polymers with different architectures and functionalities has been engineered to further optimize and to increase targeted delivery, biocompatibility and prolonged efficiency [7]. Non-viral vector systems provide an attractive alternative to recombinant viral vectors due to reduced pathogenicity and immunostimulation [8, 9]. However, cationic transfection reagents used for siRNA delivery often exhibited severe cytotoxicity, which precludes their clinical applications. Pulmonary delivery of plasmid DNA (pDNA) using poly(ethylene imine) (PEI) - based nanocarriers was frequently described in the literature [10-12], but only scant information is available for PEI mediated delivery of siRNA to the lungs. For instance, pulmonary siRNA application was investigated to differentiate off-target effects (caused by the polymers or siRNA sequence) from specific knockdown effects, and to explore the feasibility of cell specific RNA-targeting [8, 13].

In this study, we tested the hypothesis that modifications of the PEI backbone reduce not only the cytotoxic effects of PEI, but also the inflammatory and oxidative stress response caused upon administration of siRNA polyplexes to the lung of mice. Two series of PEI-based nanocarriers with different modifications, complexed with siRNA, were investigated to elucidate the influence of polymer design on cytotoxic, and inflammatory and oxidative stress responses in the lungs. Low (8.3 kDa) and high (25 kDa) molecular weight PEI modified with

hydrophobic and hydrophilic poly(ethylene glycol) (PEG) modifications, respectively, were analyzed. PEI25 kDa was grafted with hydrophilic PEG at different grafting degrees and molecular weights, in contrast to PEI 8.3 kDa which was linked with hydrophobic PEGs, one with fatty acid residues and one with a so-called Jeffamine™ residue. As point of reference to benchmark the lung toxicity, we included two well defined particulate materials, namely crystalline silica (CS) and nanosized zinc oxide (NZO), both extensively documented in the literature [14, 15]. Our results emphasize the double edged nature of nanoparticle formulations in medicine: For pharmaceutical reasons nano-materials get introduced to reduce toxicity and side-effects of drugs, however at the same time the carrier systems themselves may impose risks to the patient, possibly similar as known for occupational or environmental particle exposures [16, 17].

6.3 Materials and Methods

Materials

Specifications of the materials used in this study are summarized in the supplementary materials, S1.

Polyplex formation and particle suspension

Sense and antisense strand of siRNA against GFP (siGFP) was annealed, according to the annealing protocol from Metabion (München, Germany). siRNA polyplexes were formed, as previously described [6], by mixing equal volumes (25 μ l each) of siRNA and polymer dilution in Aqua ad injectabilia (Braun, Melsung, Germany) to obtain the desired nitrogen to RNA phosphate ratio (N/P ratio) of 6, using 35 μ g siGFP. Toxicological benchmark particles were applied at doses estimated to cause acute lung inflammation related to a level of approximately 50 % BAL PMNs. For specific calculation, see online supplement, S2.

Animal experiments

Animal experiments were carried out according to the German law of protection of animal life and were approved by an external review committee for laboratory animal care.

Eight-to-twelve-weeks old, female BALB/cAnNcrI (Charles River Laboratories, Sulzfeld, Germany) mice were intratracheal instilled as described by Merkel et al.[6]. 24 h, 3 d, or 7 d post instillation, mice were sacrificed with an overdose of ketamine/xylazin (1%/0.1%) and blood was retro-orbitally collected for further investigation. The lungs of the mice were lavaged with phosphate-buffered saline (PBS) solution (37 ° C) as previously described [6]. Cytocentrifuged slides of spun-down lavaged cells were prepared for cell differentiation, after staining with Mayer-Grünwald stain.

Body weight loss

Mice were weighed at the day of instillation and again on the day of dissection. For 7 day treatment, mice were additionally weighed at day 3. Body weight loss was calculated as the

difference between the day of dissection and the day of instillation for each mice in every group (n=8).

Total protein and lactate dehydrogenase (LDH)

Bronchoalveolar lavage fluid (BALF) was centrifuged at 1200 g x 15 min. at 4 ° C. Total protein was determined using Bradford method and LDH concentration was determined by using Cytotoxicity Detection Kit (Roche Applied Diagnostics, Germany).

Cytokine and Immunoglobulin M (IgM) measurements

Ten cytokines/chemokines were detected simultaneously in the BALF using Luminex technology (Linco Research, St. Charles, MO). In this study, the secretions of following cytokines/chemokines were investigated: IL-1 α , IL-6, IL-10, TNF-alpha, G-CSF, CXCL1, CXCL2, CXCL5, CXCL10, INF- γ . The assay was performed as described previously [18].

MCP-1 (CCL2) was quantified in the BALF using mouse CCL-2/JE DuoSet ELISA (R&D Systems, Inc., Minneapolis, USA), according to the manufacturer's instructions.

Levels of total IgM were measured by ELISA using complementary capture and detection antibody pairs. IgM levels were calculated based on a standard curve using recombinant IgM as previously described by Braun et al. [19]. Detection limits are summarized in the supplementary material (S3).

Blood parameters

Whole blood was retro-orbitally collected in EDTA-coated tubes and continuously moved prior to measurement by the ADVIA 120 Hematology System (Siemens Healthcare Diagnostics, Deerfield, USA).

Determination of oxidative stress parameters

Glutathione (GSH), malondialdehyde (MDA) levels and catalase activity in the lung tissue were determined by HPLC, as previously described by Banerjee et al.[20].

Statistics

All values are presented as mean \pm standard deviation (SD) of eight animals per group (n=8) unless otherwise stated. Significant differences between two groups were evaluated by Student's t-test, or between more than two groups by one-way ANOVA, followed by Tukey's multiple comparison test. Statistical analysis was performed using the program, GraphPad Prism 5.0 (GraphPad Software, Inc., La Jolla, CA 92037 USA).

6.4 Results

Body weight loss

We followed the body weight of each mouse throughout the experimental period to monitor eventual severe acute toxicity. PEI(8.3)-(C16-C18-EO25)1.4 was the only polyplex causing a significant body weight loss of almost 15 % at day 3, after exposure (Figure 1).

Figure 1: Body weight loss

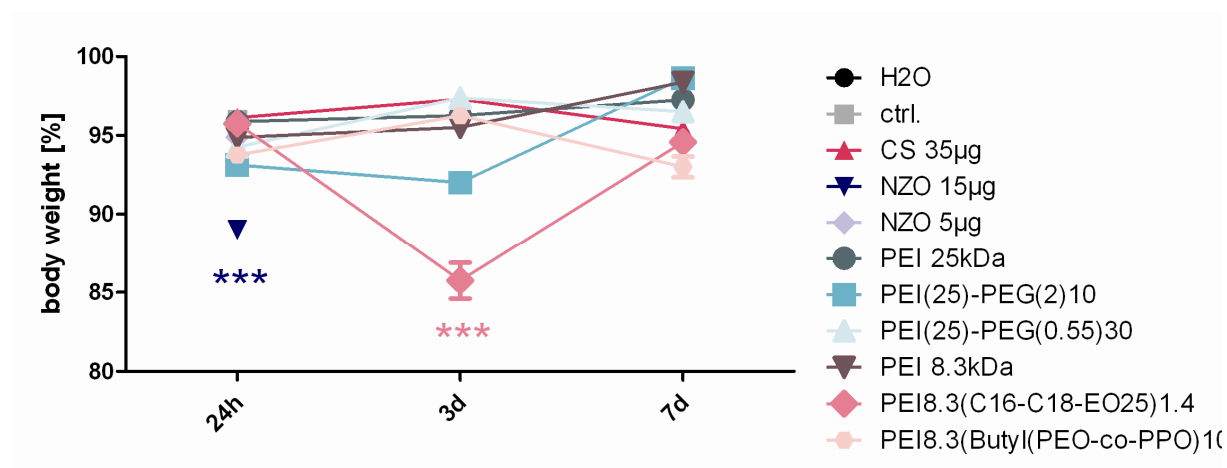


Figure 1: Body weight was determined on day of application and on day of dissection. Body weight loss [%] was calculated from the difference in body weight on day of application and day of dissection, and the percent was calculated as follow: $\text{Body weight loss [\%]} = (\text{BW}_{\text{application}} - \text{BW}_{\text{dissection}}) / \text{BW}_{\text{application}} * 100$. Values are given as mean \pm SD, $n=8$, asterisks indicate statistical significance with $***p < 0.001$ compare to control animals.

In contrast, NZO (15 µg) caused a weight loss of 10 %, already within the first 24 h after exposure, moreover the animals behaved very stressed, apathetic, and showed ruffled fur. As consequence, NZO (15 µg) experiments were terminated at this point for animal welfare reasons, and a low dose NZO (5 µg) was applied, where no body weight loss and no stress effects were detected.

Epithelial-endothelial permeability

Levels of total protein and immunoglobulin M (IgM) in the BALF were determined to evaluate the integrity of the alveolar blood-air-barrier. PEI(25)-PEG(2)10 caused a time-dependent increase in total protein (Fig.2A), after 24 h and 3 d, and increased IgM levels (Fig.2B) over all time points.

Figure 2A: Total protein

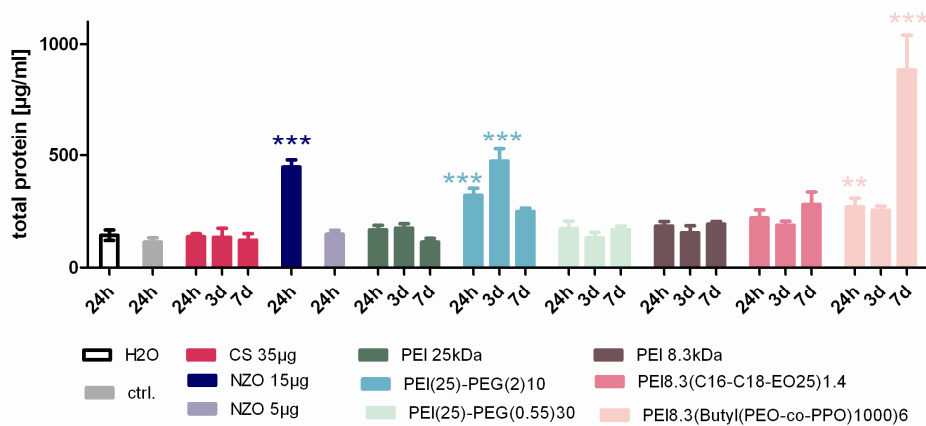


Figure 2A: Total protein was determined in broncho-alveolar lavage fluid (BALF) using Bradford-method. Values are given as mean±SD, n=8, asterisks represent significance compare to sham and control groups with *** $p < 0.001$, ** $p < 0.01$, * $p < 0.05$.

Figure 2B: Immunoglobulin M levels

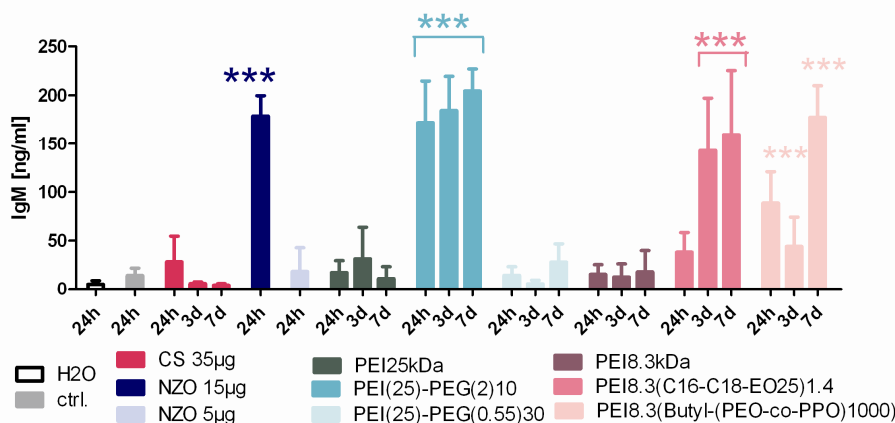


Figure 2B: Immunoglobulin M (IgM) levels were analyzed in broncho-alveolar lavage fluid (BALF) for each animal in each group. Values are given as mean±SD, n=8, and statistically significance as compare either to control or sham group, or both, as indicated by asterisks with *** $p < 0.001$, * $p < 0.01$, and * $p < 0.05$.

PEI 8.3(Butyl-(PEO-co-PPO)1000)6.2 yielded high levels of total protein and IgM with a maximum after 7 d treatment. IgM levels were increased after 3 d and 7 d treatment with PEI8.3(C16-C18-EO25)1.4, but no significant changes in total protein were detected at any time point. The effect levels observed upon nanoplex treatments indicated a breakdown in the integrity of the alveolar–capillary barrier to the same extent as observed for the high dose NZO (15 μ g) 24 h after treatment.

Cell membrane damage

Extracellular levels of the cytoplasmatic enzyme lactate dehydrogenase (LDH) were quantified in the BALF to determine disruptive effects on the cell membrane caused by the nanoplexes, indicating necrosis or late apoptosis. In our study, all nanoplexes caused elevated levels of LDH, but at different time points (Fig.3).

Figure 3: *LDH release*

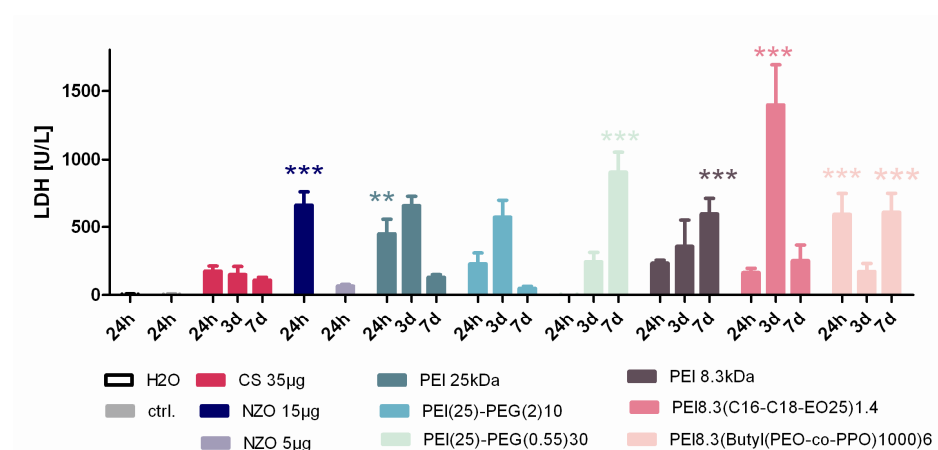


Figure 3: *Lactate dehydrogenase release was determined in broncho-alveolar lavage fluid (BALF). Values are given as mean \pm SD, n=8, and asterisks represent significance of comparison to the sham and control groups with ***p < 0.001, **p < 0.01, *p < 0.05.*

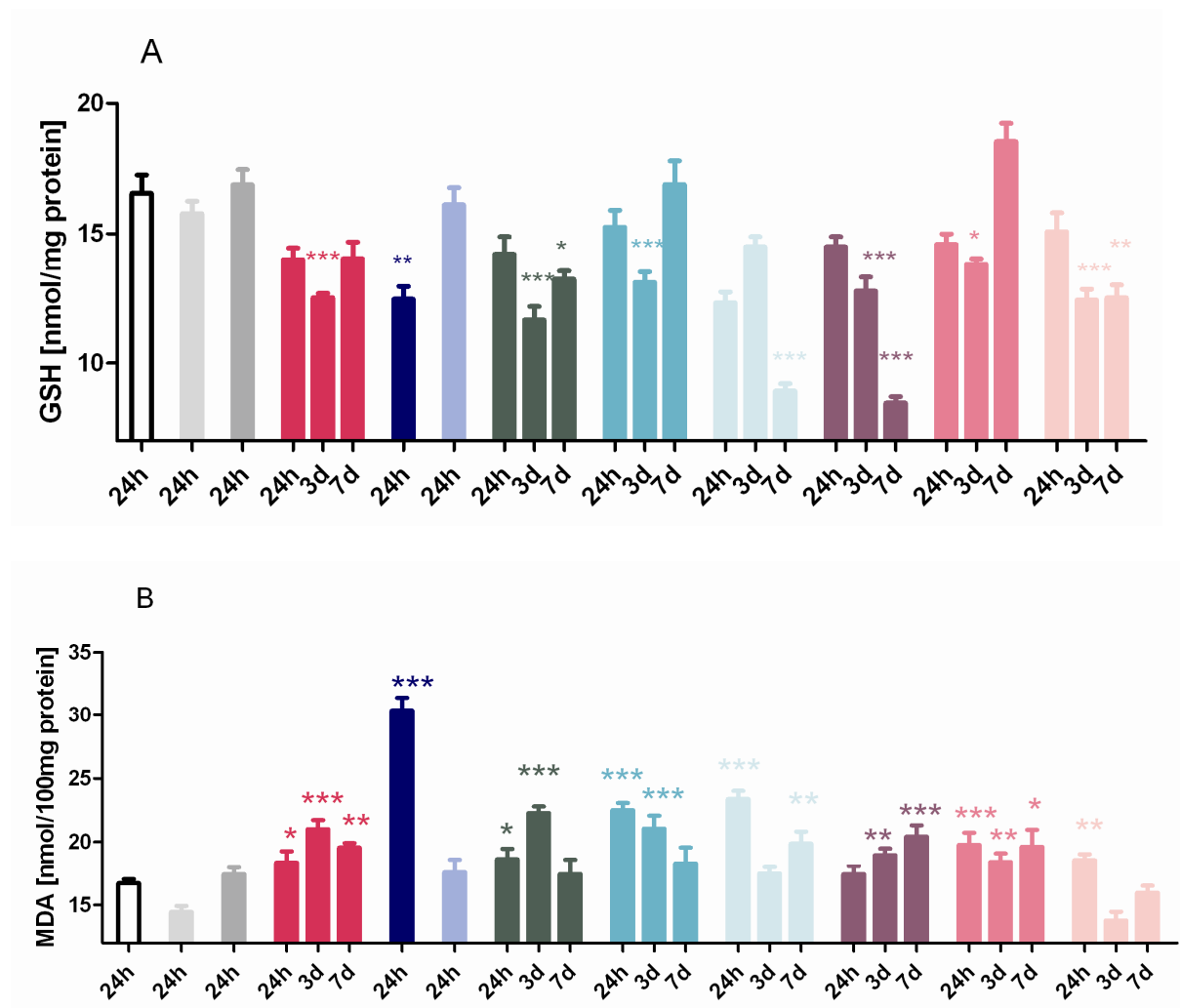
We could distinguish nanocomplexes which caused acute membrane damage (PEI25 kDa and PEI8.3(Butyl(PEO-co-PP)1000)6.2) and those which caused delayed disruptive effects, yet

after 3 d or 7 d treatment (PEI(25)-PEG(0.55)30, PEI8.3 kDa, PEI8.3(C16-C18-EO25)1.4 and PEI8.3(Butyl(PEO-co-PP)1000)6.2). Interestingly, PEI(25)-PEG(2)10 was the only nanocomplex which showed no significant membrane damage effects over all time points.

Oxidative stress response

Lung tissues of all animals were investigated for three oxidative stress parameters, depletion of the antioxidant glutathione (GSH), levels of the lipid-peroxidation by-product malondialdehyde (MDA), and the activity of the antioxidant enzyme catalase. We confirmed that the lavage procedure did not influence the oxidative status of the tissue (Fig 4A-C).

Figure 4: *Oxidative stress parameters*



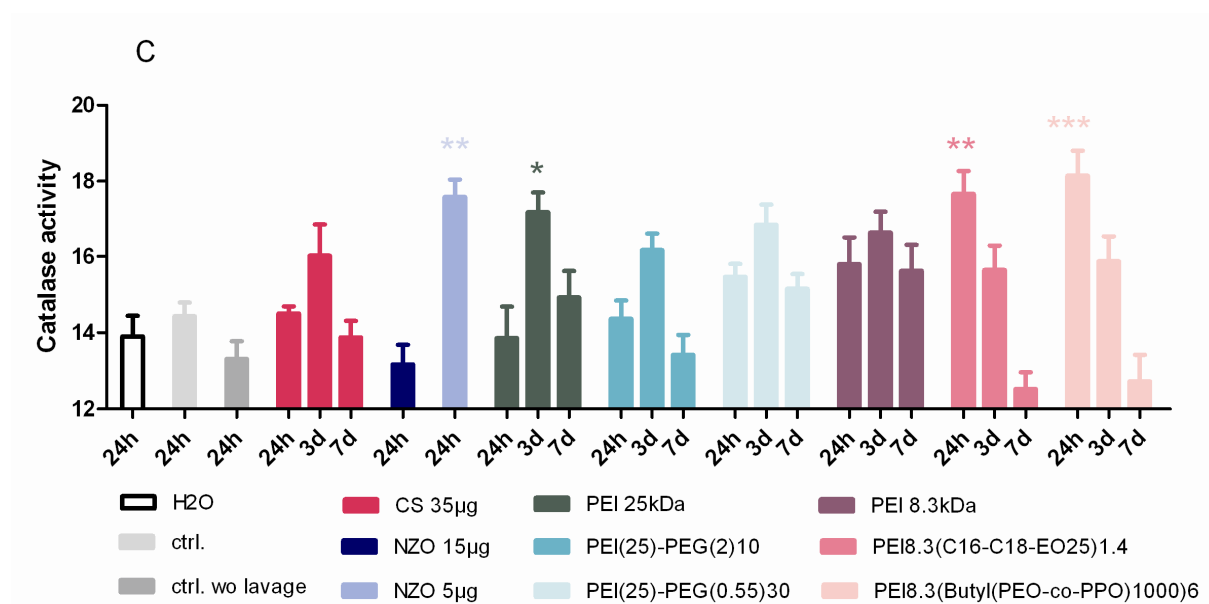


Figure 4: Glutathione (GSH, A) levels, malondialdehyde (MDA, B) levels and catalase activity (C) were determined in lung tissue from each animal in each group. Values represent mean \pm SD, $n=8$, and asterisks indicate statistical significance compare to control animals with *** $p<0.001$, ** $p<0.01$, * $p<0.05$.

After treatment with PEI(25)-PEG(0.55)30 and PEI8.3 kDa, GSH levels in the lungs were dramatically decreased, accompanied by elevated MDA levels indicating moderate lipid peroxidation (Fig. 4A and 4B). Interestingly, in contrast to all other polyplex treatments, we found good correlation between GSH and MDA levels and an acute increase in catalase activity after 24h for both modifications of low molecular weight PEI8.3 kDa. After treatment with PEI8.3(C16-C18-EO25)1.4, GSH levels were only slightly decreased after 3 d while MDA levels were significantly increased after 24 h and 3 d. PEI8.3(Butyl(PEO-co-PPO)1000)6.2 caused significantly decreased levels of GSH after 3 d and 7 d, but increased levels of MDA were found after 24 h. Thus, these two hydrophobic modifications appeared to prevent an acute oxidative stress response by increasing an adaptive antioxidant response indicated by the elevated activity of catalase in the lungs, after 24 h treatment (Fig 4C). The same antioxidative and protective effect was observed for low dose NZO (5 μ g) in contrast to high oxidative stress and lipid peroxidation after treatment with the cytotoxic high dose NZO

(15 µg). In general, the toxicological benchmarks caused high levels of lipid peroxidation and the levels caused by all nanoplexes were in the same range like that of CS, in contrast to more than 1.5-fold higher levels after NZO (15 µg).

Alteration of pulmonary leucocytes

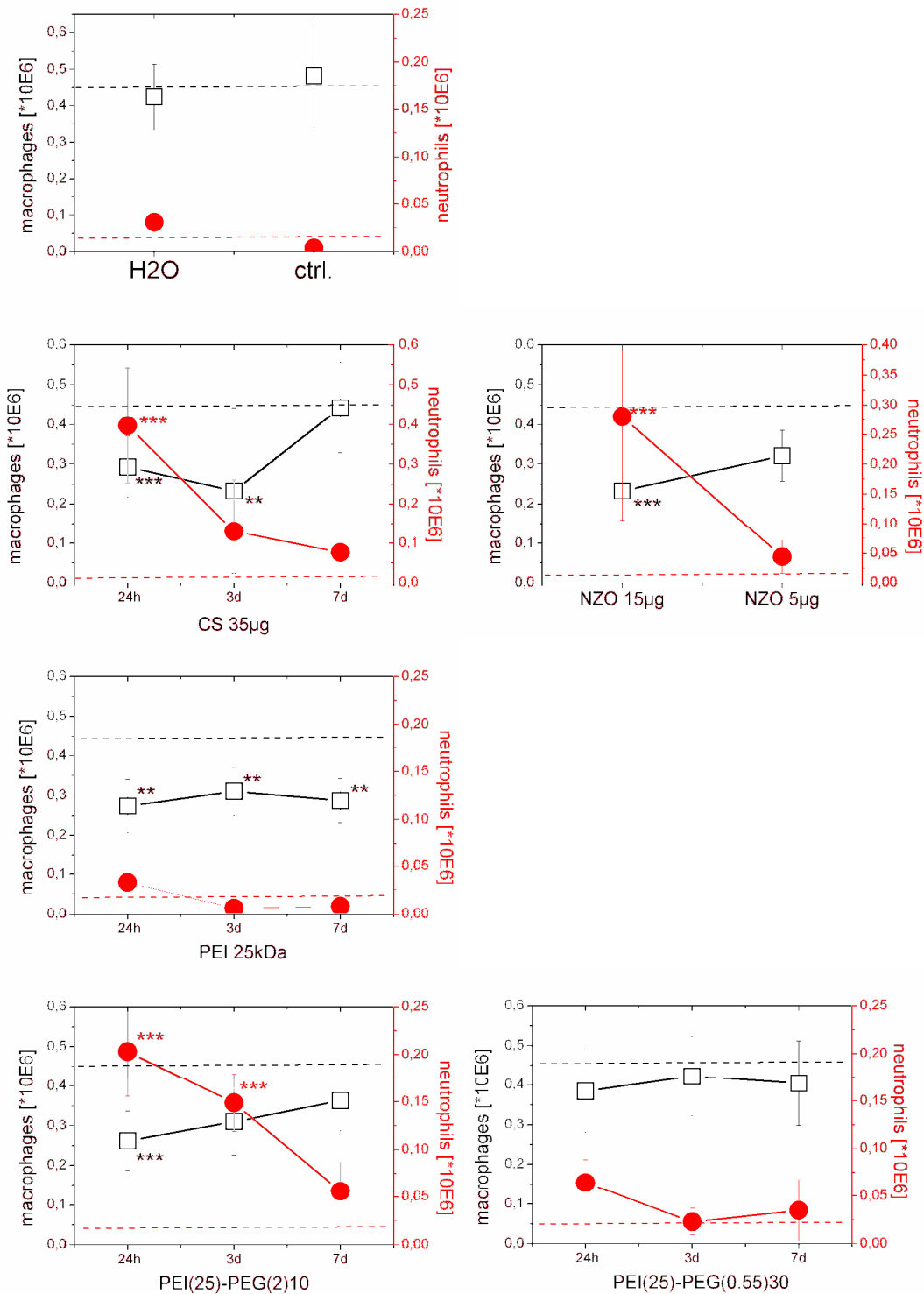
After 24 h treatment, all nanoplexes caused a strong PMN influx (>30 %), except for the standard PEI 25 kDa and the highly modified PEI(25)PEG(0.55)30. The two toxicological benchmark particles, CS and NZO, serving as positive control, and intended for causing a acute (after 24h) PMN influx around 40 % [14-16] Due to the dramatic toxic effect (loss in body weight and the alarming stressed behavior of the animals) we reduced the dose of NZO to 5 µg. This step eliminated the weight loss problem, but also reduced the inflammatory response (11.2 % PMN influx); therefore, we analyzed only the 24 h after treatment time point in case of NZO. The polyplexes PEI(25)-PEG(2)10 and PEI 8.3(Butyl(PEO-co-PPO)1000)6.2 even exceeded the level of acute inflammation caused by CS (more than 40 % PMN). For all groups, a time-depending resolution of inflammation was observed, resulting after 7 d in PMN levels corresponding to the sham group (7 % PMN), except for PEI(25)PEG(2)10 treated lungs (12 % PMN). Regarding the inflammatory burden in the lungs over the 7 days, nanoplexes could be ranked in the following order of decreasing inflammatory potential: PEI(25)-PEG(2)10 < PEI8.3-(C16-C18-EO25)1.4 < PEI8.3-(Butyl-(PEO-co-PPO)10000)6.2 < PEI8.3 kDa < PEI(25)-PEG(0.55)30 < PEI25 kDa.

Alveolar Macrophages

In comparison to the neutrophil response, no macrophage recruitment into the lungs was detected. In contrast, nanoplexes, in particular the PEI8.3 kDa derivates and PEI 25 kDa, even reduced the number of by BAL recovered alveolar macrophages to levels below 40 %. Interestingly, the depletion effect did recover till day 7 for CS but not for the nanoplexes (Fig.5).

Nanoplexes can be ranked, according to sustained depletion of alveolar macrophages in the following decreasing order: PEI8.3kDa > PEI8.3(C16-C18-EO25)1.4 > PEI25kDa > PEI8.3-(Butyl-(PEO-co-PPO)1000)6.2 > PEI(25)-PEG(2)10 > PEI(25)-PEG(0.55)30.

Figure 5: Correlation macrophages-neutrophils



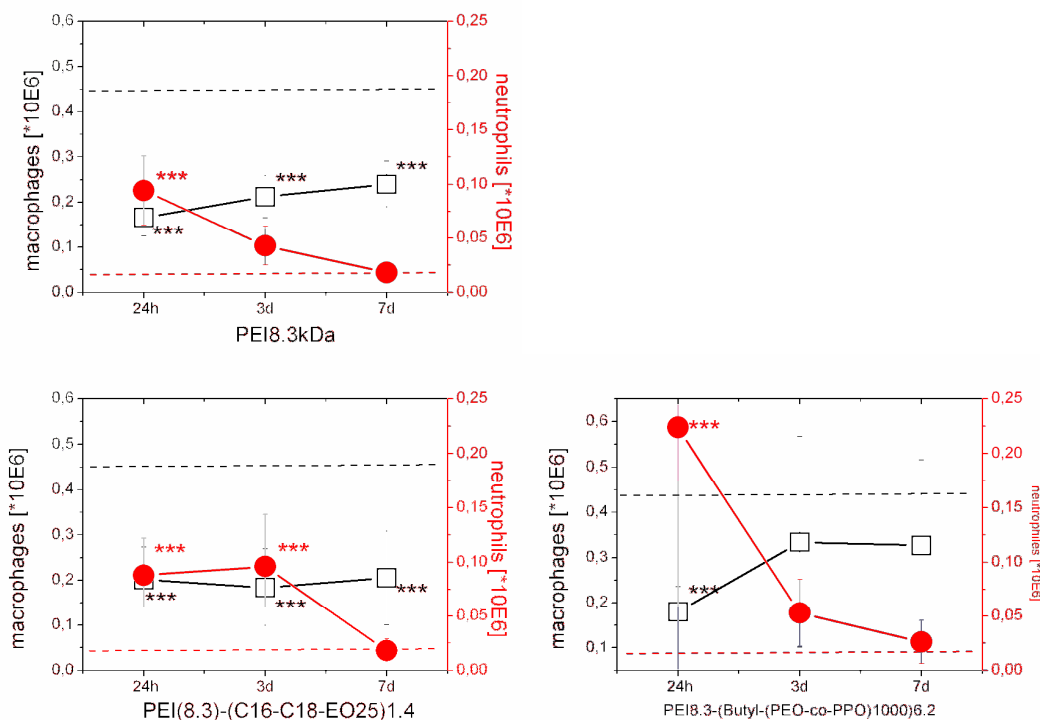


Figure 5: Correlation macrophages-neutrophils

Macrophage and neutrophil cell numbers [$\times 10^6$ cells] were calculated from broncho-alveolar lavage (BAL) where, for each animal in each group, 2 x 200 cells per cytopspin ($n=2/\text{animal}$) were counted. Macrophage numbers (y1-axis, left, black squares) were correlated with neutrophil numbers (y2-axis, right, red circles) to determine respective treatment and each time point. Dashed lines (macrophages in black and neutrophils in red) approximately represent the baseline levels in all figures for better comparison. Values are given as mean \pm SD, $n=8$, asterisks indicate statistical significance compare to control animals with *** $p < 0.001$, ** $p < 0.01$, * $p < 0.05$.

Cytokine release

The release of representative inflammatory cytokines into BALF was determined to further characterize the inflammatory and immunomodulatory effects of the nanoplexes. Overall, treatment with PEI(25)-PEG(2)10, PEI8.3(Butyl-(PEO-co-PPO)1000)6.2 and PEI8.3-(C16-C18-EO25)1.4 caused the highest pro-inflammatory cytokine response. 24 h after treatment PEI(25)-PEG(2)10 polyplexes yielded high levels of CXCL10, G-CSF, and IL-6 with decreasing cytokine levels till day 3 and 7, being in good correlation with BAL PMN numbers

(supplementary material, S4). In the same way, but to a different extent CXCL1 peaks at day 3 after treatment with PEI(25)-PEG(2)10 and PEI(25)-PEG(0.55)30. The low molecular weight PEI polyplexes showed a different cytokine pattern. PEI8.3(C16-C18-EO25)1.4 caused elevated levels of IL-6, CXCL1, CXCL10, and G-CSF with a maximum after 3 d treatment in accordance to the PMN numbers in the BAL. After polyplex treatment with PEI 8.3kDa only CXCL1 levels were increased, and this only acutely, PEI8.3(Butyl(PEO-co-PPO)1000)6.2 polyplexes however caused high levels of G-CSF after 24 h treatment and elevated levels of CXCL10 after 7d. After 3d treatment, PEI(25)-PEG(2)10 caused high levels of TNF- α , in contrast to CS that caused elevated levels of TNF- α after 24 h and 7 d (Fig. 6A).

Figure 6A: *TNF- α release*

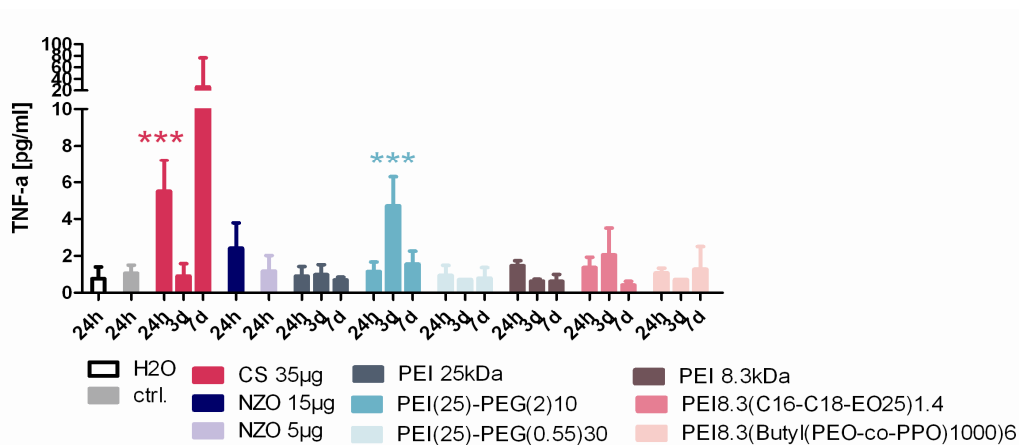


Figure 6B: *CXCL 5 release*

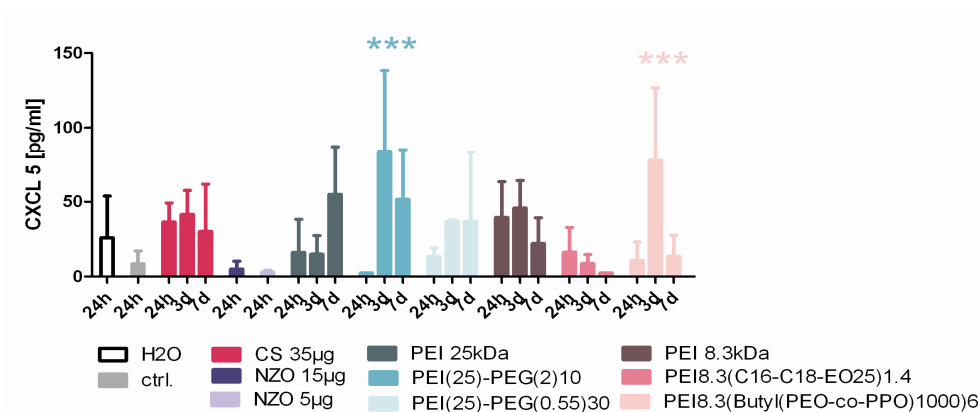


Figure 6C: MCP-1 release

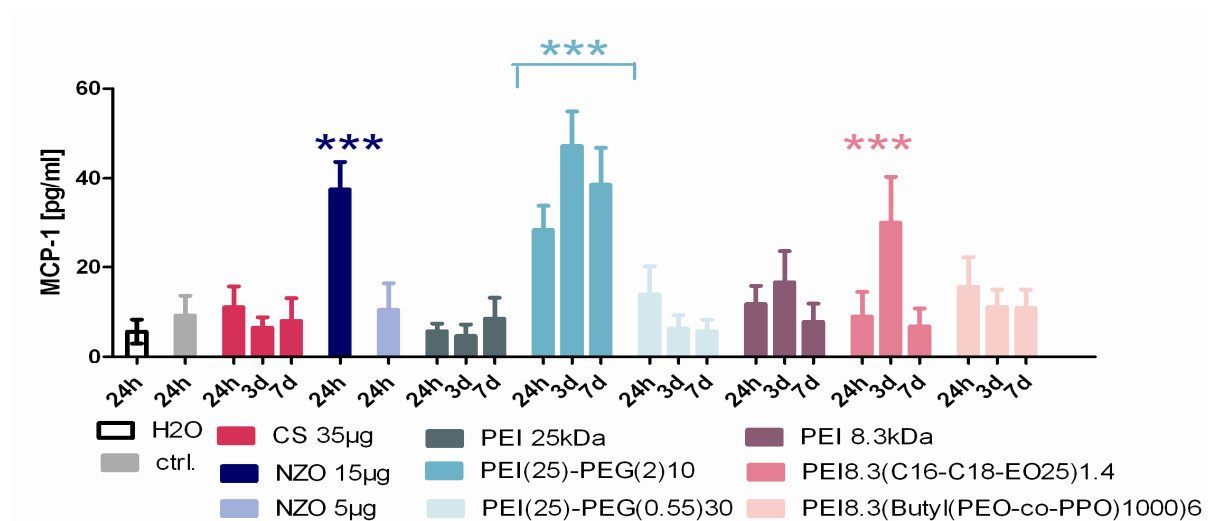


Figure 6: Tumor necrosis factor- α (TNF- α) (A), CXCL5 (B), and monocyte chemoattractant protein 1 (MCP-1/CCL-2) (C) release were determined in broncho-alveolar lavage fluid (BALF) for each animal in each group. Values are given as mean \pm SD, $n=4$ (TNF- α , CXCL5) and $n=8$ (MCP-1), and statistical significance compare to control animals are indicated by asterisks with *** $p<0.001$, * $p<0.01$, and * $p<0.05$.

High levels of CXCL5 could be observed in a reverse manner compared to the neutrophils influx into the lungs, especially for PEI25 kDa, PEI(25)-PEG(055)30, PEI8.3 kDa, and PEI8.3(Butyl-(PEO-co-PPO)1000)6.2 nanoplexes (Fig. 6B). PEI(25)-PEG(2)10 caused the highest release of MCP-1 for all time points and all treatments with a maximum after 3d treatment in accordance to levels of total protein and LDH in the BALF, as well as losses of body weight. Low molecular weight PEI8.3 kDa and its fatty acid modification also caused high levels of MCP-1 with peaks after 3 d treatment, that were comparable to the high body weight loss and elevated levels of LDH in BALF of the animals in that group. In comparison, MCP-1 levels were highly elevated in mice treated with the high dose of NZO (15 μ g) and reduced to control levels with the low dose of NZO (5 μ g) (Fig6C).

Systemic effects

A detailed hematological analysis was conducted in all mice to determine systemic effects related to the pulmonary nanoplex applications (supplementary material, S5). While white blood cell counts (WBC) remained unchanged over almost all nanoplex treatments and time points, as well as for the toxicological benchmarks, PEI25 kDa, PEI(25)-PEG(2)10, PEI8.3(C16-C18-EO25)1.4, and PEI8.3(Butyl(PEO-co-PPO)1000)6.2 polyplexes strongly decreased WBC counts after 24h treatment. Blood neutrophil numbers increased over time for PEI(25)-PEG(2)10 (after 24 h and 3 d), PEI8.3(C16-C18-EO25)1.4 (after 3 d), and PEI8.3(Butyl(PEO-co-PP)1000)6.2 (after 24 h) treatment. A comparable systemic response has not been observed for CS, but for NZO (15 µg) exposed mice after 24 h with 1.5-fold higher numbers of neutrophils in comparison to that of the nanoplexes. Red blood cell numbers (RBC) remained unaffected, except for the high dose NZO (15 µg), but platelet numbers (PLT) were increased after day 7 by PEI8.3(C16-C18-EO25)1.4 and PEI8.3(Butyl(PEO-co-PPO)1000)6.2 treatment to a similar extent as detected for NZO (15 µg).

6.5 Discussion

This study comprehensively describes the side-effects of six different PEI-based/siGFP polyplexes in the mouse lungs, after intratracheal administration. Two series of PEI-based nanocarriers were investigated because of their promising properties regarding pulmonary application and safety/cytotoxicity profiles previously assessed *in vitro* [18, 21]. One series represents high molecular weight PEI (PEI25 kDa), with hydrophilic PEG modifications, and the other consists of low molecular weight PEI (PEI8.3 kDa), with two different hydrophobic PEG modifications (namely C16-C18-fatty acid residues and so-called Jeffamine™ residues). PEG modification has been discussed to reduce cytotoxicity of the high positively charged branched PEI 25 kDa [18, 22, 23], possibly by the PEG groups shielding the positive PEI amine groups, and thus resulting in a reduced zeta potential of the polyplex, which in turn, might lead to decreased interactions with negatively charged structures such as the cell membrane. In contrast, the hydrophobic modifications of the PEI backbone (represented by PEI8.3(C16-C18-EO25)1.4 and PEI8.3(Butyl-(PEO-co-PPO)1000)6.2 respectively) is thought to enhance transfection efficiency due to stronger membrane interactions [24, 25] and, therefore, to facilitate cellular uptake of the nanocomplexes and to counteract protein adsorption, which should ultimately enhance siRNA delivery to the cytosol. However, aiming pulmonary applications, these aspects need to be carefully investigated in the lungs.

Toxicological analysis

Table 1 summarized the observed side-effects caused by PEI-based nanocarriers and provides a recommendation for the possible clinical relevance of the respective future application in human. PEI-based nanocarriers caused an acute inflammatory response in the lungs, mostly independent of the modification and the molecular weight of PEI.

Table 1: Summary of the side-effects caused by the nanoplexes and their clinical relevance

Polymer design (PEI-based nanocarriers)		Applied dosis		Side-effects											Clinical relevance	
backbone	modification	PEI	siGFP	Cytotoxicity			Inflammation			Disruption of alveolar- capillary barrier		Oxidative stress (lung tissue)			Clinical Categories: - : not suitable +/- : optimization + : promising carrier	
				BW	LDH	Depletion of macrophag es	PMN (%) in BALF			Cytokines in BALF	Total protein	IgM	GSH	MDA		catalase
							24h	3d	7d							
PEI 25kDa	non	30µg	35µg	-	+++	+++	11	2	3	CXCL1, CXCL5, CXCL10, G-CSF	-	-	+++	++	+	-
PEI 25kDa	PEG(2kDa)10			+/-	+	+	44	33	12	IL-6, CXCL1, CXCL10, G-CSF, MCP-1	+++	+++	+++	++	-	+/-
PEI 25kDa	PEG(0.55kDa)30			-	++	+/-	15	5	8	IL-6, CXCL1, CXCL5, G-CSF	-	-	+++	++	-	+
PEI8.3kDa	non			-	++	+++	35	17	7	IL-6, CXCL1, CXCL5, G-CSF, MCP-1	-	-	+++	++	-	-
PEI8.3kDa	(C16-C18-EO25)1.4			+++	+++	+++	31	35	7	IL-6, CXCL1, CXCL5, CXCL10, G-CSF, MCP-1	++	+++	++	++	++	+/-
PEI8.3kDa	Butyl(PEO-co-PPO) 1000)6.2			+/-	+++	++	41	14	6	IL-6, CXCL1, CXCL5, CXCL10, G-CSF, MCP-1	+++	+++	++	+	++	+/-
CS	non	35µg		-	+/-	+	39	20	7	TNF-a, CXCL1, G-CSF	-	-	+++	++	-	n.a.
NZO	non	15µg		+++	+++	++	50	n.d	n.d	IL-6, CXCL1, CXCL10, G-CSF, MCP-1	+++	+++	+++	+++	-	n.a.
NZO	non	5µg		-	-	+	11	n.d	n.d	IL-6, CXCL1, G-CSF	-	-	-	-	++	n.a.

Table 1: Summary of the side-effects caused by the nanoplexes and their clinical relevance. Side-effects of nanoplexes and benchmark particles are shown after intratracheal instillation in mice. Effects are summarized over all three time points (24 h, 3 d, 7 d) regarding significant changes compared to control animals. (+++) indicates statistical significant changes with $p < 0.001$, (++) $p < 0.01$, (+) $p < 0.05$, and (+/-) indicates changes which are not of statistical significance but different over time, (-) indicates no statistical changes over time in comparison to control animals. Clinical relevance is given in three categories with (+) compound represents promising properties for clinical trials, efficacy should be tested, (+/-) compound needs optimization regarding inflammatory potential, should be tested for efficacy, (-) compound offers strong toxicity and needs more optimization to reduce toxicity, and (--) shows compound which are not of clinical relevance.

Interestingly, PEI 25 kDa, the gold standard for transfection studies, offered the best pro-inflammatory profile, but caused dramatic depletion of macrophages in the lungs reducing the number of BAL macrophages substantially to less than 60 % of control values. This phenomenon could be related to high cytotoxicity caused by strong apoptotic polymer properties [26, 27] and eventually also related to alterations in surfactant metabolism [28]. In contrast to the cytotoxic standard PEI 25 kDa, the highly PEGylated PEI(25)-PEG(0.55)30 which also caused only minor inflammatory responses (15 % PMN influx vs. 1 % PMN ctrl.), showed no impairment of the BAL macrophage numbers, as compared to the sham or control group. However, then again reducing the grafting degree of PEG on PEI25kDa, increased the pro-inflammatory potential dramatically as also previously described *in vitro* [18].

PEI(25)-PEG(2)10 caused a pronounced PMN recruitment after 24 h that lasted until day 3 but was resolved by day 7. It also showed disruption of the alveolar-capillary barrier, resulting in high levels of total BAL protein and IgM till 7 d after treatment. Noteworthy PMN levels were as similar as seen for the highly toxic NZO (15 μ g). In addition, PEI(25)-PEG(2)10 caused over time a severe depletion of macrophage counts, an effect that in fact was not compensated by new recruitment of macrophages into the lungs, as would be expected because of the extremely high BAL levels of the monocyte chemotactic protein 1 (MCP-1) (Fig 6C). The three PEI 8.3 kDa containing polyplexes yielded a strong PMN influx after 24 h

together with a dramatic depletion of macrophage numbers over all time points. But since PEI8.3kDa polyplexes did not affect markers of epithelial – endothelial barrier integrity, a direct correlation between inflammation and barrier disruption seems unlikely. On the other hand the two hydrophobic modifications, PEI8.3(C16-C8-EO25)1.4 and PEI8.3(Butyl-(PEO-co-PPO)1000)6.2 disrupted the epithelial – endothelial barrier. In addition, to the inflammatory effects observed for almost all polyplexes, we detected high levels of LDH in BALF and reduced levels of GSH in the lungs that indicated high cytotoxicity of PEI-based polymers and an imbalance in the redox-system in the lungs, but to a different extent. The most prominent release of LDH from lung cells was found for PEI8.3(C16-C18-EO25)1.4 at day 3, at this time point also the highest cytokine levels for IL6, CXCL10 and G-CSF have been detected accompanied by increased blood neutrophil numbers and body weight loss. A sequence indicating together with the till day 3 persisting local, pulmonary inflammation and macrophage depletion also severe systemic toxicity of PEI8.3(C16-C18-EO25)1.4 to that extent as for the toxicity benchmark NZO (15 µg) .

Blood cell parameters were determined to obtain information about systemic effects that epidemiological studies have described, including sustained local lung inflammation that could cause adverse cardiovascular side effects [17]. High systemic inflammation was detected after treatment with the highly pro-inflammatory, and disruptive polymers like PEI(25)-PEG(2)10, PEI8.3(Butyl-(PEO-co-PPO)1000)6.2, and PEI8.3(C16-C18-EO25)1.4. In the same way, lymphocyte counts in the blood were decreased. Thus, these PEI-based nanocarriers should be applied with caution to the lungs, especially when considering repeated dosing. Lipid peroxidation occurred after all treatments, but was only moderate compared to NZO (15 µg). Interestingly, in the same way like low dose NZO (5 µg), we observed an acute antioxidant response indicated by high catalase activity after 24 h treatment with the two hydrophobic modification of PEI8.3 kDa.

Clinical relevance

To the best of our knowledge this is the first study that evaluated the inflammatory potential of different PEI-based nanocarriers for siRNA delivery in the mouse lungs. Clinical progress of non-viral vector alternatives is still of huge research interest but has been stopped by their inflammatory potential [29] and their lower or lost transfection efficacy [30]. Thus, the urgent need of optimal polymer design is still high and the requirement of overcoming the inflammatory and immunomodulatory potential beside reduced cytotoxicity, but high efficacy has to be more concentrated. Regarding repeated dosing, the inflammatory potency is critical due to massive damage of tissue surrounding the target site of action, but e.g. when treating lung cancer in a specific way that only tumor cells are targeted the inflammatory potency could enhance the elimination of the dead tumor cells. With regard to inflammatory lung diseases like chronic obstructive pulmonary disease or viral infections of the lungs, the inflammatory potential is most critical because of additive effects which are to be expected and might lead to aggravation or exacerbation of the clinical picture.

In summary, pulmonary application of all polyplexes caused considerable levels of acute lung inflammation accompanied by signs of oxidative stress, tissue damage, and systemic inflammation depending on the polymer structure. These results suggest that acute lung inflammation is one of the critical hurdles for pulmonary application of PEI based gene delivery systems. Optimized polymers with reduced cytotoxicity and inflammatory potential are required to proceed from bench to bedside.

Acknowledgements

Financial support of the Deutsche Forschungsgemeinschaft (DFG, Forschergruppe 627) is gratefully acknowledged. We would like to thank Birgit Frankenberger for her excellent technical assistance.

6.6 Supplementary Material

S1 Specifications of polymers and particles

Poly(ethylene imine) copolymers of PEI 25kDa with hydrophilic modifications

Branched poly(ethylene imine) (PEI) with a molecular weight of 25 kDa (Polymin™, water-free, 99 %), was a gift of BASF, Ludwigshafen. The poly(ethylene imine)-graft-poly(ethylene glycol) (PEI-PEG), with a PEG content of approximately 50 % (w/w), was synthesized as previously described [23, 31] by grafting linear PEG of 0.55 kDa and 2 kDa, respectively, onto branched PEI 25 kDa. These graft copolymers were designated using following nomenclature: PEI(25k)-g-PEG(x)n, where the numbers in brackets indicate the molecular weight of the PEI and the PEG block polymer in Daltons (25 k or x = 0.55 k, or 2 k), and the index n is the average number of PEG blocks per PEI molecule. This number was calculated based on the ¹H-NMR spectra, as described previously [31].

Poly(ethylene imine) copolymers of PEI 8.3kDa with hydrophobic modifications

PEI was synthesized by acid initiated polymerisation from aziridine using ethylenediamine as initiator. PEI 8.3 kDa was grafted by N-acylation with butyl-(poly(ethylenoxid-co-propylenoxid) (Butyl-(PEO-co-PPO)1000) or palmityl-/stearyl-polyethylenoxid (C16-C18-EO)25 mixture, as previously described by [21]. The nomenclature of these polymers is as follows: PEI8.3-(x)n, where x represent the respective hydrophobic polyethylenoxid derivate and n is the average number of x units per PEI molecule, calculated on the basic of ¹H-NMR spectra.

Lung benchmark particles

Crystalline silica, CS (Min-U-Sil 5), obtained from U.S. Silica Company, Berkeley Springs, WV, USA, had a median diameter of 1.7 μm and a BET surface area of 5.1 m²/g (declared on the datasheet from the manufacturer). Nanosized zinc oxide, NZO (CAS-No: 1314-13-2) was obtained from Alfa Aesar (A Johnson Matthey Company, Karlsruhe, Germany); the

manufacturer declares an average particle diameter of 70 nm and a BET surface area from 12.1 m²/g.

siRNA

siRNA against green fluorescence protein (siGFP) was obtained from Metabion (München, Germany) with the following sequence –

for sense strand: 5'-GGCUACGUCCAGGAGCGCACC-dTdT

and for antisense strand: 5'-GGUGCGCUCCUGGACGUAGCC-dTdT.

S2 Calculation of the applied dose for lung benchmark particles and PEI polymers

The applied doses for the toxicological benchmark particles was calculated from the respective particle surface area dose (BET), estimated to cause an acute pulmonary inflammatory response characterized by approximately 50 % BAL PMNs. The dose response calculation was performed according to Stoeger and Schmid 2009[32].

In brief: a 50% PMN influx is caused by a surface area dose of 0.001m² per gram lung weight (mouse lung weight: 0.18 g, and BET surface area for crystalline silica: 5.1 m²/g and for NZO: 12.1 m²/g.). According to this, we applied 35 µg CS = (0.001 m²/g x 0.18 g)/ 5.1 m²/g) and 15 µg NZO = (0.001 m²/g x 0.18 g)/12.1 m²/g) to cause around 50 % PMN influx in the lungs.

35 µg siGFP (2.39 nmol) was complexes with respective PEI polymer at N/P=6. Thus, we applied 28.43 µg of PEI to each animal which received PEI/siGFP polyplex.

S3 Detection limits for enzyme – linked immunosorbent assay

The lower limits of detection were 4.32 pg/ml for G-CSF, 3.77 pg/ml for IFN- γ , 5.39 pg/ml for IL-1a, 2.82 pg/ml for IL-6, 10.71 pg/ml for IL-10, 6.17 pg/ml for CXCL10, 0.69 pg/ml for CXCL1, 2.47 pg/ml for CXCL5, 16.56 pg/ml for Mip2, 0.6 pg/ml for TNF-a, 0.98 pg/ml for MCP-1, and 7.81 ng/ml for IgM.

S4: Cytokine release

	IL-1a		IL-6		IL-10		TNF-a		CXCL1		CXCL5		CXCL10		G-CSF		IFN- γ		
	mean	SD	mean	SD	mean	SD	mean	SD	mean	SD	mean	SD	mean	SD	mean	SD	mean	SD	
ctrl.	63.9	5.5	2.8	0.0	35.1	18.9	1.1	0.4	14.8	2.5	8.6	7.7	5.5	1.6	3.5	0.9	9.8	5.6	
Aq.inj.	50.6	10.0	2.8	0.0	38.7	16.9	0.8	0.6	27.3	14.4	25.9	24.1	8.9	4.7	6.6	1.1	9.2	6.8	
Min-U-Sil 35 μ g	57.4	11.7	1.8	1.0	26.7	19.8	5.5	1.5	175.9	32.7	36.4	11.1	11.9	8.8	47.5	8.3	8.1	6.7	
ZnO 15 μ g	56.8	9.4	1356.1	990.6	46.2	33.1	2.4	1.2	349.9	183.8	5.1	4.5	108.3	34.1	1933.4	374.2	12.0	1.0	
ZnO 5 μ g	29.0	10.3	4.7	3.3	10.6	6.4	1.2	0.7	25.3	9.6	3.1	1.0	6.2	0.0	9.0	7.1	3.8	0.0	
PEI 25kDa	43.0	3.8	2.8	0.0	14.6	6.6	0.9	0.4	23.7	4.8	16.1	19.2	8.7	1.7	6.0	2.9	8.3	7.8	
PEI(25)-PEG(2)10	22.3	6.2	228.1	54.0	10.7	7.9	1.2	0.45	137.7	42.9	2.5	0.0	1087.8	163.4	1888.8	242.8	3.8	0.0	
PEI(25)-PEG(0.55)30	54.1	15.7	7.6	3.8	23.8	14.7	0.9	0.5	71.1	11.3	13.5	5.0	7.0	1.4	8.7	2.3	6.6	4.9	
PEI8.3	50.4	16.6	8.8	8.7	18.6	5.3	1.5	0.2	220.5	139.7	39.6	20.7	6.7	5.0	48.6	22.3	5.0	2.2	
PEI8.3(C16-C18-EO25)1.4	37.0	13.7	36.3	38.5	12.8	9.5	1.4	0.5	116.0	29.4	16.3	14.3	118.0	135.1	215.0	258.3	3.4	0.6	
PEI8.3 (Butyl-(PEO-co-PPO)1000)6.2	44.7	15.3	69.5	36.2	12.8	8.1	1.1	0.2	113.8	47.8	10.8	10.6	90.5	101.9	1217.2	608.2	4.0	0.4	
3d																			
Min-U-Sil 35 μ g	43.8	12.4	2.8	0.0	14.9	9.4	0.9	0.6	92.7	10.4	41.6	13.8	6.2	0.0	10.6	2.8	3.8	0.0	
PEI 25kDa	74.2	12.2	2.3	1.7	49.0	21.4	1.0	0.5	32.2	4.7	14.9	10.8	20.2	12.2	2.8	0.2	15.4	4.7	
PEI(25)-PEG(2)10	12.3	5.7	203.8	87.2	5.3	4.0	4.7	1.4	685.8	125.8	84.1	47.0	561.1	183.7	487.6	97.0	5.9	2.9	
PEI(25)-PEG(0.55)30	63.9	46.2	3.9	0.0	70.5	55.5	0.7	0.0	106.6	52.5	36.9	0.8	21.7	8.4	3.6	1.2	14.6	9.0	
PEI8.3	82.5	44.8	4.2	2.5	32.7	16.7	0.6	0.1	134.4	9.8	45.8	15.9	76.7	23.9	25.5	17.7	8.5	5.2	
PEI8.3(C16-C18-EO25)1.4	14.7	6.1	761.9	758.8	6.8	6.8	2.1	1.3	433.0	243.5	8.6	5.2	1050.3	379.8	1629.5	726.0	5.0	1.0	
PEI8.3 (Butyl-(PEO-co-PPO)1000)6.2	17.0	4.8	6.0	4.7	10.7	2.6	0.7	0.0	231.8	98.6	77.9	42.4	74.8	42.0	39.8	19.7	5.1	0.9	
7d																			
Min-U-Sil 35 μ g	48.0	35.9	2.8	0.0	14.0	9.8	25.9	43.6	53.5	15.6	30.2	27.3	6.2	0.0	8.7	8.1	3.8	0.6	
PEI 25kDa	54.2	7.5	2.8	0.0	26.9	22.9	0.7	0.1	39.0	14.7	54.9	28.0	6.2	0.0	4.2	1.8	5.5	2.9	
PEI(25)-PEG(2)10	14.3	6.1	4.1	2.0	5.1	4.3	1.6	0.6	333.9	116.0	51.7	29.0	99.0	31.7	25.4	8.0	3.8	0.0	
PEI(25)-PEG(0.55)30	47.3	23.8	2.8	0.0	8.7	6.5	0.8	0.5	42.2	22.5	37.1	40.3	8.9	4.8	4.7	2.5	6.3	3.0	
PEI8.3	55.8	14.2	2.8	0.0	27.0	11.0	0.6	0.3	34.5	5.0	22.1	14.1	6.2	0.0	4.5	1.1	3.8	0.0	
PEI8.3(C16-C18-EO25)1.4	20.6	17.5	2.8	0.0	7.0	8.6	0.4	0.2	22.3	3.6	2.5	0.0	18.5	11.6	10.5	6.7	3.8	0.0	
PEI8.3 (Butyl-(PEO-co-PPO)1000)6.2	29.2	17.9	2.6	0.4	17.9	16.9	1.3	1.1	32.6	17.1	13.5	12.2	67.6	33.9	6.0	0.9	3.8	0.0	

S4: Cytokine release was determined in broncho-alveolar lavage fluid (BALF) by multiplex-based ELISA technique analyzing 10 characteristically pro- and antiinflammatory cytokines. Values are given in pg/ml for each cytokine as mean±SD, n=4. Values for Cxcl2 (Mip2) were below the detection limit of the kit used and not shown in the table. Bold values represent statistically significant values compare to control and sham groups, p-values are at least <0.05.

S5: Blood parameters

S5 A *White blood cell parameters*

	WBC		Neutrophils				Lymphocytes				Monocytes			
	(x10E03 cells/ μ L)		(%)		(x10E03 cells/ μ L)		(%)		(x10E03 cells/ μ L)		(%)		(x10E03 cells/ μ L)	
24h	mean	SD	mean	SD	mean	SD	mean	SD	mean	SD	mean	SD	mean	SD
ctrl.	6.5	1.5	12.9	2.7	0.8	0.2	82.9	2.8	5.4	1.3	1.7	0.6	0.1	0.1
Aq.inj.	7.1	1.3	13.6	3.2	1.0	0.2	82.1	3.7	5.8	1.1	1.5	0.7	0.1	0.1
CS 35 μ g	5.2	1.0	17.7	3.1	0.9	0.2	78.2	3.1	4.1	0.8	1.3	0.4	0.1	0.0
NZO 15 μ g	4.4	1.7	40.8	13.2	1.9	1.2	54.2	13.5	2.2	0.7	2.0	1.6	0.1	0.1
NZO 5 μ g	4.7	1.4	17.4	3.3	0.8	0.2	78.3	3.5	3.7	1.2	1.4	0.5	0.1	0.0
PEI 25kDa	4.5	1.1	14.4	2.8	0.7	0.2	81.6	2.3	3.7	0.9	1.1	0.3	0.1	0.0
PEI(25)-PEG(2)10	4.3	1.9	21.6	4.4	0.9	0.2	73.3	4.7	3.2	1.6	1.8	1.0	0.1	0.1
PEI(25)-PEG(0.55)30	5.1	1.7	16.4	2.2	0.8	0.3	79.6	2.3	4.1	1.4	1.3	0.3	0.1	0.0
PEI8.3kDa	4.9	1.8	15.6	5.4	0.7	0.3	79.9	5.8	3.9	1.6	1.3	0.5	0.1	0.0
PEI8.3-(C16-C18-EO25)1.4	4.5	1.0	14.1	4.6	0.6	0.2	81.4	4.7	3.6	0.8	1.4	0.4	0.1	0.0
PEI8.3(Butyl-(PEO-co-PPO)1000)6.2	3.4	1.1	24.7	8.0	0.8	0.2	70.9	8.3	2.4	0.9	1.5	0.3	0.1	0.0
3d														
CS 35 μ g	5.4	1.6	16.0	3.7	0.9	0.4	79.3	3.7	4.2	1.2	2.2	0.7	0.1	0.0
PEI 25kDa	5.5	1.3	15.2	6.6	0.8	0.4	80.7	6.8	4.4	1.1	1.6	0.4	0.1	0.0
PEI(25)-PEG(2)10	5.5	1.2	21.0	4.2	1.1	0.2	74.6	4.8	4.2	1.1	2.1	0.7	0.1	0.0
PEI(25)-PEG(0.55)30	6.2	1.5	16.4	2.6	1.0	0.2	79.2	2.7	4.9	1.3	2.0	0.4	0.1	0.0
PEI8.3kDa	5.1	1.1	13.9	2.6	0.7	0.2	82.1	3.1	4.2	0.9	1.6	0.3	0.1	0.0
PEI8.3-(C16-C18-EO25)1.4	6.0	2.0	26.8	6.9	1.5	0.5	67.2	7.8	3.8	1.6	2.0	0.5	0.1	0.1
PEI8.3(Butyl-(PEO-co-PPO)1000)6.2	6.0	1.6	18.1	3.6	1.1	0.5	77.8	3.9	4.6	1.1	1.7	0.5	0.1	0.0

	WBC		Neutrophils		Lymphocytes		Monocytes							
	(x10E03 cells/ μ L)	(%)	(x10E03 cells/ μ L)	(%)	(x10E03 cells/ μ L)	(%)	(x10E03 cells/ μ L)	(%)	(x10E03 cells/ μ L)	(%)	(x10E03 cells/ μ L)	(%)	(x10E03 cells/ μ L)	(%)
7d	mean	SD	mean	SD	mean	SD	mean	SD	mean	SD	mean	SD	mean	SD
CS 35 μ g	5.5	2.8	17.0	5.8	0.8	0.3	78.7	6.2	4.5	2.5	1.5	0.4	0.1	0.1
PEI 25kDa/	5.2	1.3	14.8	3.5	0.8	0.3	80.8	3.5	4.2	1.0	1.8	0.7	0.1	0.0
PEI(25)-PEG(2)10	4.9	1.6	16.7	3.2	0.8	0.3	79.4	3.0	3.9	1.2	1.7	0.8	0.1	0.1
PEI(25)-PEG(0.55)306.0	6.0	2.0	13.1	3.2	0.8	0.4	82.7	3.2	4.9	1.6	1.7	0.4	0.1	0.1
PEI8.3kDa	5.3	1.3	19.0	4.1	1.0	0.3	77.2	3.9	4.1	1.0	1.6	0.3	0.1	0.0
PEI8.3-(C16-C18-EO25)1.4	5.9	1.7	20.2	2.1	1.2	0.4	75.3	2.4	4.4	1.2	2.3	0.4	0.1	0.1
PEI8.3(Butyl-(PEO-co-PPO)1000)6.2	5.5	1.9	15.9	4.2	0.8	0.2	79.3	4.6	4.4	1.8	1.8	0.4	0.1	0.1

S5 A: *White blood cell parameters*

*White blood cell (WBC) parameters are given as mean \pm SD, n=8 in total numbers [10E3 cells/ μ l] and for the different cell populations in percent [%] and total cell number [*10E3 cells/ μ l]. Blood parameters were determined from hole blood after respective time point for each animal in each group using ADVIA 120 Hematology System (Siemens Healthcare Diagnostics, Deerfield, USA). Bold values represent statistical significance, $p<0.05$ compare to control group.*

S5 B: Red blood cell and platelet numbers

	<i>RBC (x10E06 cells/μL)</i>		<i>PLT (x10E03 cells/μL)</i>	
	mean	SD	mean	SD
24h				
ctrl.	9.9	0.4	965.3	102.7
Aq.inj.	10.2	0.3	1068.4	67.6
CS 35 μ g	10.2	0.3	1008.3	108.9
NZO 15 μ g	11.0	1.2	1210.3	164.2
NZO 5 μ g	10.1	0.3	979.0	90.2
PEI 25kDa	9.5	0.5	962.9	104.5
PEI(25)-PEG(2)10	10.1	0.8	995.3	97.9
PEI(25)-PEG(0.55)30	10.2	0.3	1061.8	69.1
PEI8.3kDa	9.3	1.1	951.0	168.7
PEI8.3(C16-C18-EO25)1.4	9.8	0.3	1049.4	120.1
PEI8.3(Butyl-(PEO-co-PPO)1000)6.2	10.1	0.4	1077.5	97.9
3d				
CS 35 μ g	10.0	0.3	969.3	66.1
PEI 25kDa	9.9	0.2	1071.5	117.3
PEI(25)-PEG(2)10	9.8	0.2	1063.4	65.1
PEI(25)-PEG(0.55)30	9.8	0.3	1015.5	100.9
PEI8.3kDa	10.0	0.3	1085.6	115.6
PEI8.3(C16-C18-EO25)1.4	10.3	0.7	912.1	228.4
PEI8.3(Butyl-(PEO-co-PPO)1000)6.2	9.7	0.2	1055.4	57.5
7d				
CS 35 μ g	10.1	0.3	1054.5	89.4
PEI 25kDa	9.8	0.3	1013.8	50.2
PEI(25)-PEG(2)10	9.9	0.3	985.8	164.0
PEI(25)-PEG(0.55)30	9.8	0.6	991.5	129.8
PEI8.3kDa	10.0	0.3	1058.5	83.6
PEI8.3(C16-C18-EO25)1.4	9.4	0.2	1233.2	141.8
PEI8.3(Butyl-(PEO-co-PPO)1000)6.2	10.0	0.2	1275.9	199.2

S5 B: Red blood cell parameters

Red blood cell (RBC) parameters are given as mean±SD, n=8. Red blood cell (RBC) and platelets (PLT) counts are given in 10E3 cells/μl. Blood parameters were determined from whole blood after respective time point for each animal in each group using ADVIA 120 Hematology System (Siemens Healthcare Diagnostics, Deerfield, USA). Bold values represent statistical significance, p<0.05 compare to control group.

6.7 References

- 1 Gary, D.J., N. Puri, and Y.Y. Won, *Polymer-based siRNA delivery: perspectives on the fundamental and phenomenological distinctions from polymer-based DNA delivery*. J Control Release, 2007. 121(1-2): p. 64-73.
- 2 Ge, Q., L. Filip, A. Bai, T. Nguyen, H.N. Eisen, and J. Chen, *Inhibition of influenza virus production in virus-infected mice by RNA interference*. Proc Natl Acad Sci U S A, 2004. 101(23): p. 8676-81.
- 3 Thomas, M., J.J. Lu, J. Chen, and A.M. Klibanov, *Non-viral siRNA delivery to the lung*. Adv Drug Deliv Rev, 2007. 59(2-3): p. 124-33.
- 4 Grayson, A.C., A.M. Doody, and D. Putnam, *Biophysical and structural characterization of polyethylenimine-mediated siRNA delivery in vitro*. Pharm Res, 2006. 23(8): p. 1868-76.
- 5 Grzelinski, M., B. Urban-Klein, T. Martens, K. Lamszus, U. Bakowsky, S. Hobel, F. Czubayko, and A. Aigner, *RNA interference-mediated gene silencing of pleiotrophin through polyethylenimine-complexed small interfering RNAs in vivo exerts antitumoral effects in glioblastoma xenografts*. Hum Gene Ther, 2006. 17(7): p. 751-66.
- 6 Merkel, O.M., A. Beyerle, D. Librizzi, A. Pfestroff, T.M. Behr, B. Sproat, P.J. Barth, and T. Kissel, *Nonviral siRNA delivery to the lung: investigation of PEG-PEI polyplexes and their in vivo performance*. Mol Pharm, 2009. 6(4): p. 1246-60.
- 7 Park, T.G., J.H. Jeong, and S.W. Kim, *Current status of polymeric gene delivery systems*. Adv Drug Deliv Rev, 2006. 58(4): p. 467-86.
- 8 Akhtar, S. and I.F. Benter, *Nonviral delivery of synthetic siRNAs in vivo*. J Clin Invest, 2007. 117(12): p. 3623-32.
- 9 Sakurai, H., K. Kawabata, F. Sakurai, S. Nakagawa, and H. Mizuguchi, *Innate immune response induced by gene delivery vectors*. Int J Pharm, 2008. 354(1-2): p. 9-15.
- 10 Kleemann, E., L.A. Dailey, H.G. Abdelhady, T. Gessler, T. Schmehl, C.J. Roberts, M.C. Davies, W. Seeger, and T. Kissel, *Modified polyethylenimines as non-viral gene delivery systems for aerosol gene therapy: investigations of the complex structure and stability during air-jet and ultrasonic nebulization*. J Control Release, 2004. 100(3): p. 437-50.
- 11 Rudolph, C., R.H. Muller, and J. Rosenecker, *Jet nebulization of PEI/DNA polyplexes: physical stability and in vitro gene delivery efficiency*. J Gene Med, 2002. 4(1): p. 66-74.
- 12 Rudolph, C., U. Schillinger, A. Ortiz, C. Plank, M.M. Golas, B. Sander, H. Stark, and J. Rosenecker, *Aerosolized nanogram quantities of plasmid DNA mediate highly efficient gene delivery to mouse airway epithelium*. Mol Ther, 2005. 12(3): p. 493-501.
- 13 Akhtar, S. and I. Benter, *Toxicogenomics of non-viral drug delivery systems for RNAi: potential impact on siRNA-mediated gene silencing activity and specificity*. Adv Drug Deliv Rev, 2007. 59(2-3): p. 164-82.
- 14 Sayes, C.M., K.L. Reed, and D.B. Warheit, *Assessing toxicity of fine and nanoparticles: comparing in vitro measurements to in vivo pulmonary toxicity profiles*. Toxicol Sci, 2007. 97(1): p. 163-80.
- 15 Xia, T., M. Kovichich, M. Liong, L. Madler, B. Gilbert, H. Shi, J.I. Yeh, J.I. Zink, and A.E. Nel, *Comparison of the mechanism of toxicity of zinc oxide and cerium oxide nanoparticles based on dissolution and oxidative stress properties*. ACS Nano, 2008. 2(10): p. 2121-34.
- 16 Monteiller, C., L. Tran, W. MacNee, S. Faux, A. Jones, B. Miller, and K. Donaldson, *The pro-inflammatory effects of low-toxicity low-solubility particles, nanoparticles*

- and fine particles, on epithelial cells in vitro: the role of surface area.* Occup Environ Med, 2007. 64(9): p. 609-15.
- 17 Nemmar, A., M.F. Hoylaerts, P.H. Hoet, D. Dinsdale, T. Smith, H. Xu, J. Vermylen, and B. Nemery, *Ultrafine particles affect experimental thrombosis in an in vivo hamster model.* Am J Respir Crit Care Med, 2002. 166(7): p. 998-1004.
 - 18 Beyerle, A., O.M. Merkel, T. Stoeger, and T. Kissel, *PEGylation affects cytotoxicity and cell-compatibility of poly(ethylene imine) for lung application: structure-function-relationships* Toxicol Appl Pharmacol, 2009. in press.
 - 19 Braun, A., M. Bewersdorff, J. Lintelmann, G. Matuschek, T. Jakob, M. Gottlicher, W. Schober, J.T. Buters, H. Behrendt, and M. Mempel, *Differential impact of diesel particle composition on pro-allergic dendritic cell function.* Toxicol Sci, 2009.
 - 20 Banerjee, A., M.B. Trueblood, X. Zhang, K.R. Manda, P. Lobo, P.D. Whitefield, D.E. Hagen, and N. Ercal, *N-acetylcysteineamide (NACA) prevents inflammation and oxidative stress in animals exposed to diesel engine exhaust.* Toxicol Lett, 2009. 187(3): p. 187-93.
 - 21 Koch, F., *Synthese und Charakterisierung niedermolekularer Polyethylenimine und Polyethylenimin-Derivate für die Gentransfektion.* Master Thesis, 2009.
 - 22 Mao, S., X. Shuai, F. Unger, M. Wittmar, X. Xie, and T. Kissel, *Synthesis, characterization and cytotoxicity of poly(ethylene glycol)-graft-trimethyl chitosan block copolymers.* Biomaterials, 2005. 26(32): p. 6343-56.
 - 23 Petersen, H., P.M. Fechner, A.L. Martin, K. Kunath, S. Stolnik, C.J. Roberts, D. Fischer, M.C. Davies, and T. Kissel, *Polyethylenimine-graft-poly(ethylene glycol) copolymers: influence of copolymer block structure on DNA complexation and biological activities as gene delivery system.* Bioconjug Chem, 2002. 13(4): p. 845-54.
 - 24 Masotti, A., F. Moretti, F. Mancini, G. Russo, N. Di Lauro, P. Checchia, C. Marianecchi, M. Carafa, E. Santucci, and G. Ortaggi, *Physicochemical and biological study of selected hydrophobic polyethylenimine-based polycationic liposomes and their complexes with DNA.* Bioorg Med Chem, 2007. 15(3): p. 1504-15.
 - 25 Neamark, A., O. Suwanton, C.R. K, C.Y. Hsu, P. Supaphol, and H. Uludag, *Aliphatic Lipid Substitution on 2 kDa Polyethylenimine Improves Plasmid Delivery and Transgene Expression.* Mol Pharm, 2009.
 - 26 van Rooijen, N., A. Sanders, and T.K. van den Berg, *Apoptosis of macrophages induced by liposome-mediated intracellular delivery of clodronate and propamide.* J Immunol Methods, 1996. 193(1): p. 93-9.
 - 27 Beyerle, A., M. Irmeler, J. Beckers, T. Kissel, and T. Stoeger, *Toxicity pathway focused gene expression profiling of PEI-based polymers for pulmonary applications.* Mol Pharm, under review.
 - 28 Forbes, A., M. Pickell, M. Foroughian, L.J. Yao, J. Lewis, and R. Veldhuizen, *Alveolar macrophage depletion is associated with increased surfactant pool sizes in adult rats.* J Appl Physiol, 2007. 103(2): p. 637-45.
 - 29 Tan, Y. and L. Huang, *Overcoming the inflammatory toxicity of cationic gene vectors.* J Drug Target, 2002. 10(2): p. 153-60.
 - 30 de Fougerolles, A., H.P. Vornlocher, J. Maraganore, and J. Lieberman, *Interfering with disease: a progress report on siRNA-based therapeutics.* Nat Rev Drug Discov, 2007. 6(6): p. 443-53.
 - 31 Petersen, H., P.M. Fechner, D. Fischer, and T. Kissel, *Synthesis, Characterization, and Biocompatibility of Polyethylenimine-graft-poly(ethylene glycol) Block Copolymers.* Macromolecules, 2002. 35(18): p. 6867-6874.
 - 32 Stoeger, T. and O. Schmid, *Dose response relations* second ed. Particle–Lung Interactions, ed. P. Gehr, et al. Vol. 241. 2009, New York.

7 Fatty acid modification of low molecular weight

Poly(ethylene imine)-mediated siRNA delivery to lung leucocytes after intratracheal instillation in mice

Andrea Beyerle, Andrea Braun, Felix Koch, Tobias Stoeger, Thomas Kissel

In preparation for Journal of Controlled Release

Author's Contributions:

A.B. prepared the manuscript draft and wrote the manuscript, carried out the experimental work, designed the animal study, analyzed and interpreted the data, A.Br. provided the FACS antibodies and supported the flow cytometry settings and analysis, F.K. synthesized the low molecular weight PEI polymers, W.v.W. discussed the FACS data, A.O.Y. supported the animal experiments, T.K. provided the PEI polymers, reviewed and edited the manuscript, T.S. reviewed and edited the manuscript. All authors read and approved the final version of the manuscript.

7.1 Abstract

Pulmonary siRNA delivery offers a new way to treat various lung diseases. Poly(ethylene imines) (PEIs) are promising cationic nanocarriers and various modifications are still under investigations to improve their cytotoxicity and efficacy for siRNA delivery.

In this study, we analyzed two series of PEI – based nanocomplexes, after *in-vitro* pre-selection, for pulmonary siRNA delivery. Ubiquitously enhanced green fluorescent protein (EGFP) expressing transgenic mice were intratracheally instilled with 35 µg siRNA complexed with the different PEI nanocarriers. Knock down of EGFP expression was analyzed by flow cytometry and fluorescence microscopy 5 days post instillation.

Three of the six polyplexes caused significant knock down of EGFP expression, but only the fatty acid modified low molecular weight PEI 8.3 kDa (C16-C18-EO25)_{1.4} specifically reduced EGFP expression in CD45⁺ leucocytes and CD11b⁻/CD11⁺ lung macrophages.

The hydrophobic/hydrophilic balance of the non-viral vector system appears to be one approach for safer and improved siRNA therapeutics for successful pulmonary siRNA delivery.

Key words: siRNA delivery, EGFP, intratracheal instillation, PEI

7.2 Background

RNA interference (RNAi) based therapeutics represent a fundamentally new way to treat human disease by addressing targets, that could not yet targeted with tools of the existing medicines [1, 2]. The nobel-prize winning discovery of RNAi in the worm *Caenorhabditis elegans* in 1998 [3], and the subsequent demonstration that RNAi operates in mammalian cells revolutionized the current understanding of endogenous mechanisms of gene regulation and provided powerful new tools for biological research and drug discovery.

The lung is becoming an attractive target organ to systemic and local treatment of various lung disorders using small interfering RNAs (siRNA), because of the enormously increasing number of pulmonary diseases with high mortality and morbidity. In addition, pulmonary targeting could be achieved by invasive (intravenous injection) as well as non-invasive (intranasal, intratracheal and inhalative) application. Delivery of siRNAs to the lungs has been described via different routes, using different delivery strategies [4-8]. The clinical success of siRNA-mediated treatment is still crucial due to safety and efficacy reasons.

In this study, we tested a wide range of different non-viral polycationic nanocarriers, with promising *in vitro* properties for siRNA delivery to the lungs [9-11], for their *in vivo* performance in mouse lungs. A lot of non-viral approaches have been made to successfully deliver siRNA. Poly(ethylene imine) (PEI) represents the most extensively studied cationic polymer for non-viral gene delivery, especially when focusing the lungs [6, 12-18]. Many factors such as the molecular weight, degree of grafting, ionic strength of the solution, zeta potential, particle size, cationic charge density, molecular structure, sequence and conformational flexibility influence the transfection efficiency and cytotoxicity of such non-viral vector systems. PEI polymers with different molecular weights and branching degrees as well as several modifications on the PEI backbone are still under intense investigations for successful *in vivo* use [4, 7, 19-21]. We analyzed the efficacy of two series of PEI-(polyethylene glycol) (PEG) copolymers, one series comprises of the high molecular weight

PEI 25 kDa with two different hydrophilic PEG modifications and another series of the low molecular weight PEI 8.3 kDa with two different hydrophobic PEG modifications. We hypothesized that the modification of the PEI backbone improves siRNA delivery in the lungs. The hydrophilic PEG modifications have been shown *in vitro* to reduce cytotoxicity [11, 22, 23], protein adsorption [24, 25] and it is intended to prolong the half life of the polyplexes *in vivo* due to minimizing recognition of the innate immune system and especially reducing macrophage clearance [26]. The hydrophobic PEG modifications built more amphiphilic polymer structures that appear to enhance transfection efficacy due to better interaction with the cell membrane and therefore improved endocytotic uptake [27-30]. Therefore, we intratracheally instilled siRNA against enhanced green fluorescent protein (siEGFP) complexed with six different PEI-PEG copolymers into EGFP transgenic mice and evaluated the knock down efficiency via flow cytometry and fluorescent microscopy.

7.3 Methods

Materials

Synthesis of the polymers and polyplex formation are described in the supplementary material, S1.

Particle size distribution

The hydrodynamic diameters of the polyplexes were analyzed by dynamic light scattering (DLS) measurements using HPPS Malvern Instruments (Malvern Instruments, Herrenberg, Germany).

In vitro cytotoxicity

Experiments were carried out using murine alveolar epithelial – like type II cells (LA4; ATCC No. CCL-196TM) and murine alveolar macrophages, (MH-S; ATCC No. CRL-2019).

Cell viability was determined using the Cell Proliferation Reagent WST-1 (Roche Diagnostics, Germany) according to [31]. Briefly, LA4 and MH-S cells were seeded at a density of 0.25×10^6 cells/well in 24-well-plate in cell culture medium containing FBS and grown overnight in an incubator at 37 ° C and 5 % CO₂. Medium was replaced before cells were treated. Cells were incubated with three different polymer concentrations (0.5 µg/ml, 5 µg/ml, 50 µg/ml corresponding to PEI concentration). After 24 h treatment, the relative viability [%] related to control samples (untreated cells) was calculated by following equation: Cell viability = $(OD_{\text{sample}}/OD_{\text{control}}) * 100$.

Lactate dehydrogenase (LDH) was determined using Cytotoxicity Detection Kit (Roche Diagnostics, Germany) according to the manufacturer's protocol. Briefly, cells were cultured and seeded like that in the WST-1 assay. To avoid interference with assay reagents, the cell culture medium was replaced with serum-reduced (2 % FBS) cell culture medium without antibiotics before addition of polymers. LDH kinetic was observed after 0.5 h, 1 h, 2 h, 4 h, 6 h, and 24 h exposure time. The LDH concentration in the cell culture supernatant was determined spectrophotometrically at a wavelength of 492 nm using an ELISA reader

(Labsystems iEMS Reader MF). Cells treated with 2 % (w/v) Triton X-100 served as a control according to the manufacturer's protocol and revealed maximum LDH release (100 %) corresponding to $OD_{\text{high control}}$. The relative LDH release is defined by the ratio of LDH released over total LDH (high control) and was calculated as follows: Cytotoxicity [%] = $(OD_{\text{sample}} - OD_{\text{low control}})/(OD_{\text{high control}} - OD_{\text{low control}}) * 100$, where $OD_{\text{low control}}$ was the absorption from the supernatant of the untreated cells. Less than 10 % LDH release was regarded as non-toxic effect level in our experiments according to [32].

In vitro cytokine release

Ten inflammatory cytokines/chemokines were simultaneously detected in the cell culture supernatant using a multiplexing Luminex assay (Linco Research, St. Charles, MO). In this study, the secretion of IL-1 α , IL-6, TNF- α , G-CSF, CXCL1, CXCL5, CXCL10, IFN- γ , IL-10, and CCL3 was measured. The assay was performed as described previously [33] and mean fluorescence intensity (MFI) was detected by the Multiplex plate reader (Luminex System, Bio-Rad Laboratories, Germany) for each sample (50 μ l) with a minimum of 100 beads per region being analyzed. The raw data (MFI) were captured using the Multiplex plate reader software (Bioplex Manager, Version 2.0). For data analysis, a 5-parameter logistic curve fit was applied to each standard curve and sample.

Animal experiments

Animal experiments were carried out according to the German law of protection of animal life and were approved by an external review committee for laboratory animal care.

Eight-to-twelve-weeks old, female C57BL/6J-Tg(Bos/GFP)CaBaBii011Dcm (Helmholtz Zentrum München, Germany) mice were intraperitoneal (i.p.) injected with a mixture of Medetomidin (500 μ g/kg body weight), Midazolam (5 mg/kg body weight), and Fentanyl (50 μ g/kg body weight) and fixed in a supine position on a 60 ° incline board by holding their upper incisor teeth. The tongue was gently extended using coated tweezers. Mice were intubated through mouth and trachea using the flexible tube of a 24-gauge catheter (BD

Insyte, Becton Dickinson GmbH, Heidelberg, Germany). Polyplexes (50 μ l) were instilled followed by 100 μ l air. Directly after instillation mice were subcutaneously injected with the antagonist mixture of Atipamezol (2.5 mg/kg body weight), Flumazenil (500 μ g/kg body weight), and Naloxon (1200 μ g/kg body weight) to recover from anaesthesia within 5-10 min. Mice were treated with siRNA polyplexes for five days.

Lung homogenate for flow cytometer analysis

Mice were sacrificed with an overdose of a mixture of ketamine and xylacin (1 %/0.1 %) and exsanguinated via vena cava caudalis. Lungs were perfused with 20 ml of sterile HBSS until free of blood by visual inspection. The right lungs were fixed, carefully removed and transferred into petri dishes containing 0.7 mg/ml collagenase A (Roche, Germany) and 1 mg/ml DNase I (Roche, Germany) in RPMI-1640 medium (Biochrom AG, Germany). Lungs were minced and cut into small pieces, incubated at 37 ° C for 45 min in a humidified atmosphere containing 5 % CO₂. Cell aggregates were dispersed by repeated passage through a syringe, and filtered through a 200 μ m falcon and a 40 μ m cell strainer (BD Biosciences), to obtain single cell suspension. Subsequently, cells were rinsed with HBSS and PBS containing 2 mM EDTA and 0.5 % FCS.

Flow cytometer analysis

For flow cytometer analysis cells were resuspended in PBS containing 2 mM EDTA and 0.5 % FCS and Fc receptor-mediated and non-specific antibody binding was blocked by addition of excess non-specific immunoglobulin (Fc-block, CD16/CD32 purified, clone 2.4G2, BD Pharmingen). The following monoclonal antibodies were used at appropriate dilutions for cell specific staining: CD11c-PE (HL3, BD Pharmingen), CD11b-APC (M1/70, BD Pharmingen), GR-1-PE (RB6-8C5, Biolegend), CD19-PE (1D3, BD Pharmingen), CD45-biotinylated (30-F11, BD Pharmingen), CD-4-PE (RM4-5, BD Pharmingen), CD-8a-PE (Ly-2, 53, -67, BD Pharmingen), CD-19-PE (1D3, BD Pharmingen), MHC II – biotinylated (2G9, BD Pharmingen). Staining was performed at 4 ° C in the dark for 30 min. After staining, cells

were washed twice in PBS containing 2 mM EDTA and 0.5 % FCS. Biotinylated primary antibodies were further incubated for 5 min with APC-conjugated streptavidin (BD Pharmingen), followed by one additional wash with PBS containing 2 mM EDTA and 0.5 % FCS. A FACSCalibur flow cytometer (BD Biosciences) was used for flow cytometric characterization of cell populations. The BD Cell quest Pro software package was used for data analysis (BD Biosciences).

Lung histology

Left lungs were inflated with 4 % paraformaldehyde (PFA), pH 7.4 via the trachea after dissection and fixed in 4 % PFA, pH 7.4 solution before they were paraffin-embedded using standard procedure. Paraffin sections (3 μ m) were deparaffinized and stained with 4',6-diamidino-2-phenylindole (DAPI) (Molecular Probes, Invitrogen, Germany) for fluorescent detection. A total of 6 individual images from different regions of the lung per animal were analyzed and representative images are shown.

Fluorescent microscopy

A Olympus BX51 fluorescent microscope was used to determine the EGFP expression in lung tissue slides. For excitation of EGFP fluorescence, an excitation filter with a wavelength of 470/40 nm was used and fluorescence emission was detected using a 525/50 nm long-pass filter. DAPI was detected using a 350/50 nm excitation filter and fluorescence was detected by a 460/50 nm long-pass filter. All of the fluorescent images were acquired with the same settings with respect to exposure time using CellF Imaging Software for Fluorescence microscopy (Olympus Deutschland GmbH, Hamburg, Germany).

Statistics

All values are presented as mean \pm standard error (SEM) of four to six animals per group (n=4-6) unless otherwise stated. Significant differences between two groups were evaluated by Student's t-test, or between more than two groups by one-way ANOVA, followed by Tukey's

or Dunnett's multiple comparison test. Statistical analysis was performed using the program, GraphPad Prism 5.0 (GraphPad Software, Inc., La Jolla, CA 92037 USA).

7.4 Results

Particle size distribution

Particle size distribution was determined because nanocomplex size limits the desired uptake and transfection efficiency in the target cells. Nanocomplexes showed average diameters in the range of 100nm to highly aggregated nanocomplexes with an average diameter of 600 nm (Fig 1). Interestingly, the highly positively-charged polymer, PEI25 kDa, yielded the smallest nanocomplexes with an average diameter of 91.5 ± 84 nm. In contrast, the low molecular weight PEI8.3 kDa formed the largest and most polydisperse nanocomplexes with an average diameter of 596.3 ± 104.5 nm, indicating a strong agglomeration in water. The two hydrophobic modifications of PEI8.3 kDa formed nanocomplexes in an acceptable size range of 120-200 nm. The excessive PEGylated modification of PEI25kDa, PEI(25)-PEG(0.55)30, caused high agglomeration, with average diameters around 400nm, whereas the more moderately PEGylated PEI(25)-PEG(2)10 was characterized by a more preferable size spectrum of 110.6 ± 92.8 nm.

Figure 1: *Particle size distribution*

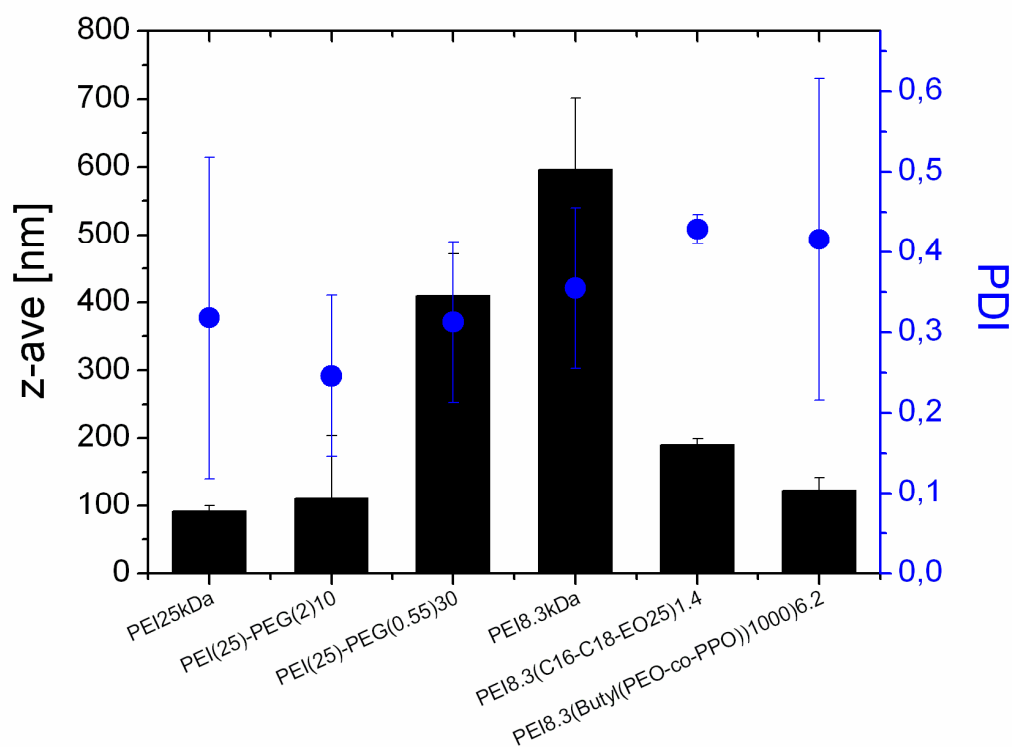
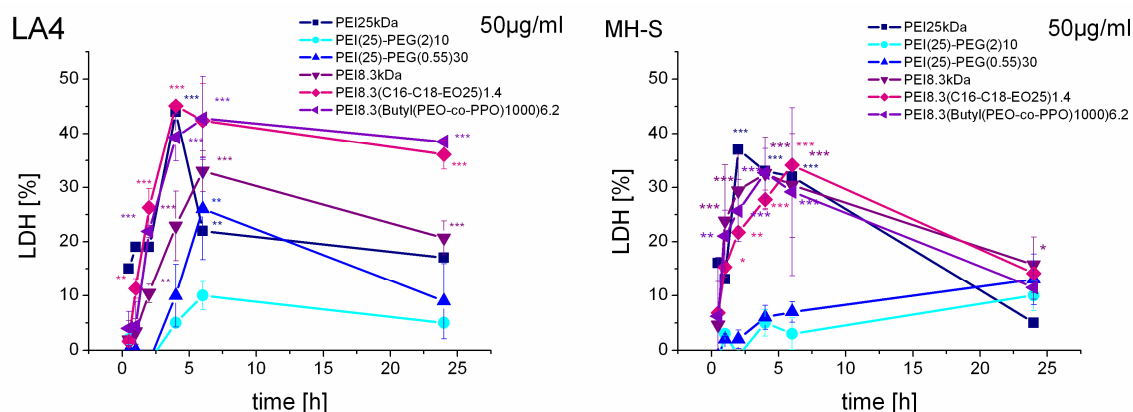


Figure 1: Particle size distribution

Hydrodynamic diameter (z-ave, black bars) and polydispersity index (PDI, blue circles) were determined using dynamic light scattering (DLS) measurements. Values are given as mean \pm SD for each treatment group, measurements were repeated three times. All polyplex solutions were prepared in Aqua ad injectabilia (Braun AG, Melsung, Germany) as described in supplement material, S1.

In vitro cytotoxicity

Cell viability was tested for free polymers after 24 h treatment of two alveolar cell lines representing the pneumocytes type II (LA4) and macrophages (MH-S). This *in vitro* testing represents a worst case scenario because it is well described in the literature that after release of siRNA and also during complex formation a huge amount of free polymer remains in the cytoplasm [34], and the free PEI polymer seemed to be necessary for optimal siRNA delivery [35] and in addition, the toxic part of the polyplexes used *in vivo* is the polycationic carrier. Cell viability was reduced in a dose-dependent manner for all polymers (supplementary material, S2) and the hydrophilic PEG modified PEI-PEG copolymers strongly reduced the cytotoxicity *in vitro* as previously described [10, 11, 23]. However, the hydrophobic modification of the PEI 8.3 kDa showed comparable cytotoxicity as seen for PEI 8.3 kDa, but still lower than PEI 25 kDa, and strong membrane interaction indicated by a huge amount of lactate dehydrogenase (LDH) in the supernatant in a time-dependent manner in both cell lines tested (Fig.2). The stronger membrane disruption could be explained by the more hydrophobic properties of these polymers that enhance the interaction with the negatively charge phospholipids in the cell membrane.

Figure 2: LDH kinetic**Figure 2:** LDH kinetic

LDH release was determined using Cytotoxicity detection kit (Roche) after 0.5 h, 1 h, 2 h, 4 h, 6 h, and 24 h polymer treatment in LA4 cells (left) and MH-s cells (right). For each time point three independent experiments were carried out and the values were expressed as mean \pm SD. Less than 10% LDH release were regarded as non-toxic effect level in our experiments [32]. Significant difference to control was presented as asterisk with * p <0.05, ** p <0.01; *** p <0.0001. It has to mentioned that data for PEI25 kDa, PEI(25)-PEG(2)10, and PEI(25)-PEG(0.55)30 already published by Beyerle et al. [10].

Cytokine release *in vitro*

Beside the cytotoxic effect, the proinflammatory effect of such nanocarriers is crucial, especially when nanocarriers were directly applied to the lungs. Thus, the supernatants of the cell viability testing in the two alveolar cell lines (LA4 and MH-S) were further analyzed to determine the release of ten characteristically inflammatory cytokines. As recently described [10] the reduced cytotoxicity of the hydrophilic PEI-PEG copolymers is on cost of a moderate proinflammatory potential of these polymers, more prominent for PEI(25)-PEG(2)10 than PEI(25)-PEG(0.55)30. The low molecular weight PEI 8.3 kDa and its hydrophobic modifications showed only slightly increased levels of CXCL1, CXCL10, and IL-6 in LA4 and MH-S, but without any statistical significance (Table 1).

Table 1: Cytokine release

A		Cytokine release							
LA4 fold change	CXCL1		CXCL10		G-CSF		IL-6		
	mean	SD	mean	SD	mean	SD	mean	SD	
PEI25kDa									
0.5µg/ml	0.41	0.03	0.62	0.26	0.31	0.00	8.68	2.83	
5µg/ml	0.39	0.05	1.11	0.15	0.24	0.09	6.24	1.67	
50µg/ml	0.11	0.03	2.88	0.08	0.28	0.04	1.29	0.21	
PEI(25)-PEG(2)10									
0.5µg/ml	1.10	0.48	0.79	0.44	0.41	0.44	1.49	0.50	
5µg/ml	4.36	0.41	2.38	2.80	12.29	10.92	9.72	8.38	
50µg/ml	4.32	0.37	2.34	2.80	8.94	0.39	7.25	3.62	
PEI(25)-PEG(0.55)30									
0.5µg/ml	0.51	0.00	2.23	2.19	0.31	0.00	15.29	4.19	
5µg/ml	0.52	0.24	38.01	42.11	0.31	0.00	6.60	5.29	
50µg/ml	0.60	0.37	9.59	8.53	0.31	0.00	4.76	2.46	
PEI8.3kDa									
0.5µg/ml	0.55	0.25	b.d.l.		b.d.l.		b.d.l.		
5µg/ml	0.65	0.20	b.d.l.		b.d.l.		b.d.l.		
50µg/ml	1.94	1.00	b.d.l.		b.d.l.		b.d.l.		
PEI8.3(C16-C18-EO25)1.4									
0.5µg/ml	0.50	0.53	b.d.l.		b.d.l.		b.d.l.		
5µg/ml	0.61		b.d.l.		b.d.l.		b.d.l.		
50µg/ml	1.52		b.d.l.		b.d.l.		b.d.l.		
PEI8.3(Butyl-(PEO-co-PPO)1000)6.2									
0.5µg/ml	0.83	0.40	b.d.l.		b.d.l.		b.d.l.		
5µg/ml	2.35	0.55	b.d.l.		b.d.l.		b.d.l.		
50µg/ml	0.34	0.21	b.d.l.		b.d.l.		b.d.l.		
B									
MH-S fold change	CXCL1		CXCL10		G-CSF		IL-6		
	mean	SD	mean	SD	mean	SD	mean	SD	
PEI25kDa									
0.5µg/ml	0.54	0.06	b.d.l.		4.71	2.78	1.23	0.07	
5µg/ml	0.76	0.11	b.d.l.		5.10	5.52	1.83	0.57	
50µg/ml	0.64	0.23	b.d.l.		10.23	12.34	2.13	1.27	
PEI(25)-PEG(2)10									
0.5µg/ml	1.76	1.24	1.03	0.03	5.47	2.98	0.50	0.01	
5µg/ml	2.91	1.07	1.03	0.01	36.12	31.83	17.25	17.34	
50µg/ml	2.01		1.03		1.79		1.00		
PEI(25)-PEG(0.55)30									
0.5µg/ml	0.48	0.01	b.d.l.		4.34	4.79	1.27	0.80	
5µg/ml	0.61	0.13	b.d.l.		4.73	0.93	1.57	0.40	
50µg/ml	0.77	0.26	b.d.l.		1.24	0.21	1.20	0.57	
PEI8.3kDa									
0.5µg/ml	0.86	0.10	0.79	0.50	2.41	3.40	1.54	0.94	
5µg/ml	1.11	0.49	1.29	1.12	1.40	1.63	1.60	0.60	
50µg/ml	0.91	0.45	1.12	0.65	1.61	1.12	2.17	0.41	
PEI8.3(C16-C18-EO25)1.4									
0.5µg/ml	0.51	0.45	1.78	0.74	b.d.l.		b.d.l.		
5µg/ml	1.52		1.51		b.d.l.		b.d.l.		
50µg/ml	0.14		0.33		b.d.l.		b.d.l.		
PEI8.3(Butyl-(PEO-co-PPO)1000)6.2									
0.5µg/ml	0.85	0.58	1.44	0.94	b.d.l.		1.50	0.51	
5µg/ml	1.47	0.27	1.44	0.52	b.d.l.		2.01	0.25	
50µg/ml	0.76	0.75	2.71	3.21	b.d.l.		b.d.l.		

Table 1: Cytokine release

Cytokine release was determined in LA4 (A) and MH-S(B) cells after 24h polymer exposure. Values are given as mean \pm SD (n=3) of the fold change compare to control (untreated cells), b.d.l. is below detection limit. Bold values are statistically significant, * p <0.05.

Thus, from that *in vitro* data we conclude that these polymers could be applied *in vivo* for evaluating their performance in RNAi.

Quantification of EGFP down regulation by FACS Analysis

After intratracheal instillation of 35 μ g siRNA complexed six different polyplexes we detected a significant knock down of enhanced green fluorescent protein (EGFP) expression in the lungs compare to untreated animals (ctrl.) for three polyplexes (PEI(25)-PEG(2)10: 75 \pm 4 %; PEI8.3kDa: 66 \pm 9 % ; PEI8.3(C16-C18-EO25)1.4: 69 \pm 9 % (Fig. 3 and supplementary material, S3). However comparing siEGFP results to the treatment with the unspecific siRNA against luciferase (siGL3), failed to detect any anti-EGFP specific significant knock down effect (p <0.05), even though the EGFP expression appeared still higher in the animals treated with the unspecific siGL3 as compared to siEGFP. In comparison to control animals and the other three specific polyplexes, the EGFP expression was slightly reduced with the unspecific siGL3 (PEI(25)-PEG(2)10: 50 \pm 11 %; PEI8.3 kDa: 58 \pm 9 %; PEI8.3(C16-C18-EO25)1.4: 30 \pm 16 %) From that data, the most unspecific off-target effect was seen for the treatment with the low molecular weight PEI 8.3 kDa polymer used to complex and delivery siRNA. Keeping that in mind, the most effective polyplexes could be arranged in following order with decreasing specific knock down efficacy: PEI8.3(C16-C18-EO25)1.4 > PEI(25)-PEG(2)10 > PEI8.3 kDa. Fluorescence microscopy confirmed the obvious knock down effect in lung EGFP expression with these three polyplexes mentioned above, which seem to be more prominent in the alveolar region of the lungs (Fig. 4).

Figure 3: FACS analysis

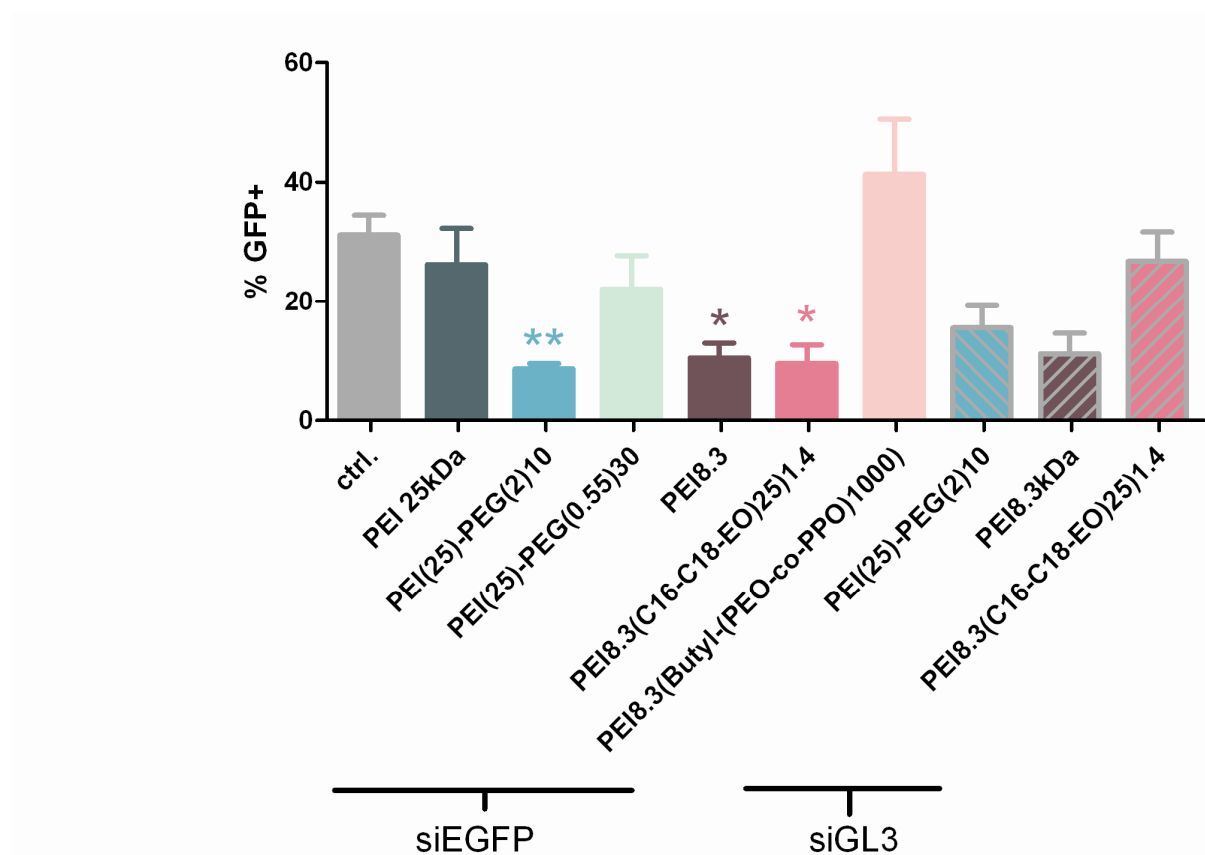


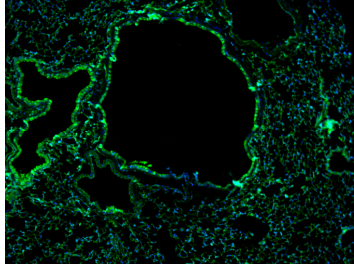
Figure 3: FACS analysis

Flow cytometer data from GFP transgenic mouse lungs 5 day postinstillation with six different polyplexes with specific siGFP or as indicated in the figure with unspecific siGL3. 10,000 cells were counted and dead cells were excluded by propidium iodide (PI) staining. Values shows the percent of the vital GFP+ cell population and represents mean \pm SEM (n=4-6). Asterisks represents statistical significance with * p <0.05, ** p <0.01 compare to control animals (gray bars).

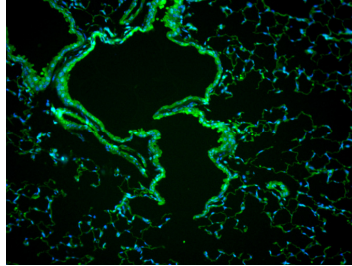
Figure 4: Fluorescence microscopy

A 4.1

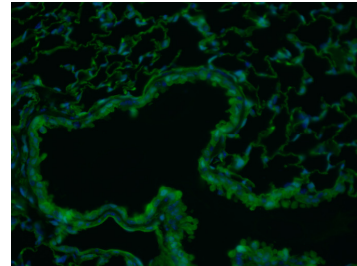
PEI25kDa



PEI(25)-PEG(2)10

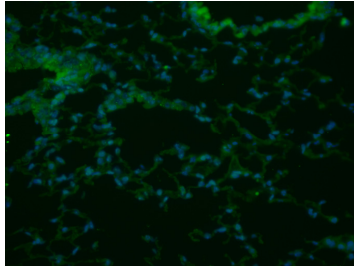


PEI(25)-PEG(0.55)30

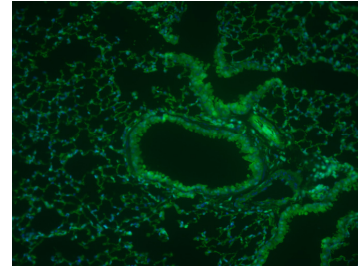
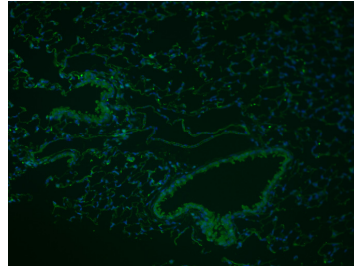


B 4.1

PEI8.3kDa

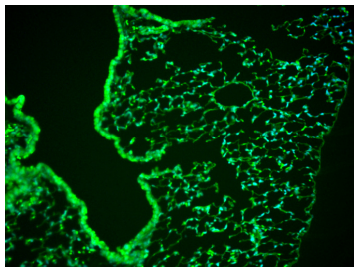


PEI8.3(C16-C18-EO25)1.4 PEI8.3(PEO-co-PPO)1000)6.2

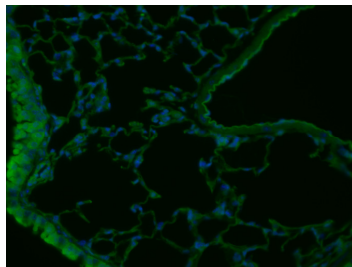


C 4.1

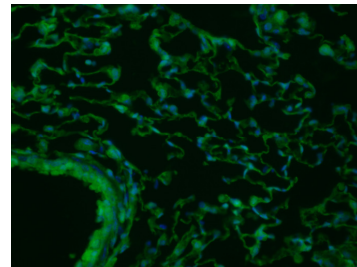
PEI(25)-PEG(2)10/siGL3



PEI8.3kDa/siGL3

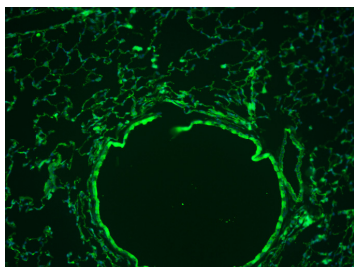


PEI8.3(C16-C18-EO25)1.4/siGL3

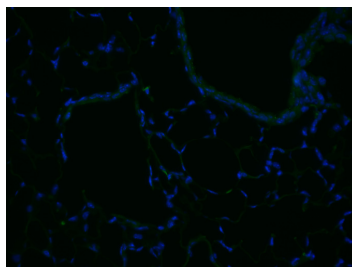


D 4.1

CABA ctrl.

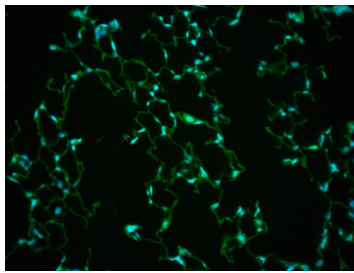


C57/BL6 ctrl.

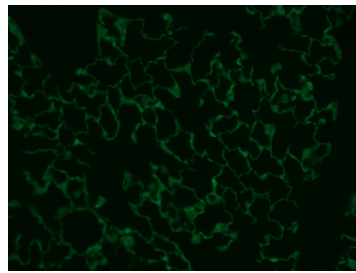


A 4.2

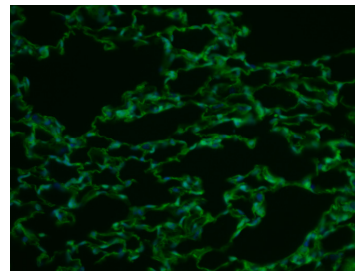
PEI25kDa



PEI(25)-PEG(2)10

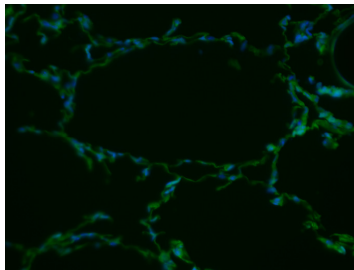


PEI(25)-PEG(0.55)30

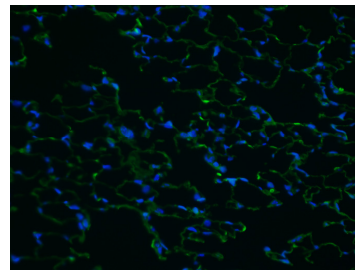


B 4.2

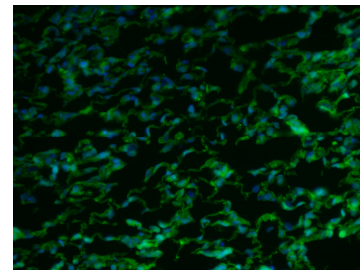
PEI8.3kDa



PEI8.3(C16-C18-EO25)1.4

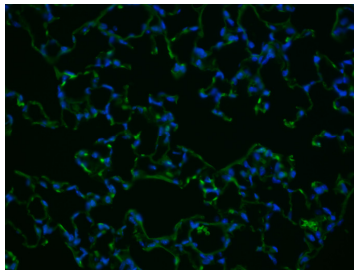


PEI8.3(PEO-co-PPO)1000)6.2

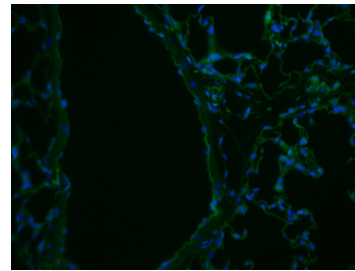


C 4.2

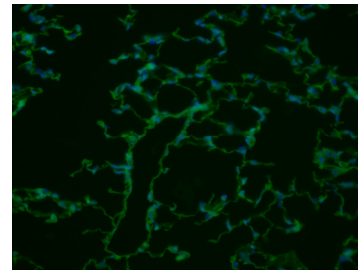
PEI(25)-PEG(2)10/siGL3



PEI8.3kDa/siGL3

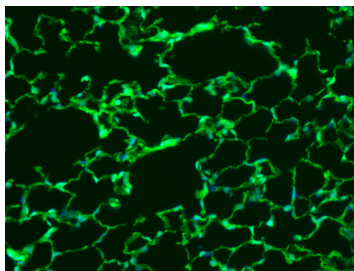


PEI8.3(C16-C18-EO25)1.4/siGL3



D 4.2

CABA ctrl.



C57/BL6 ctrl.

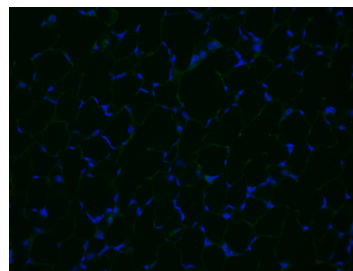


Figure 4.1-4.2: Fluorescence microscopy

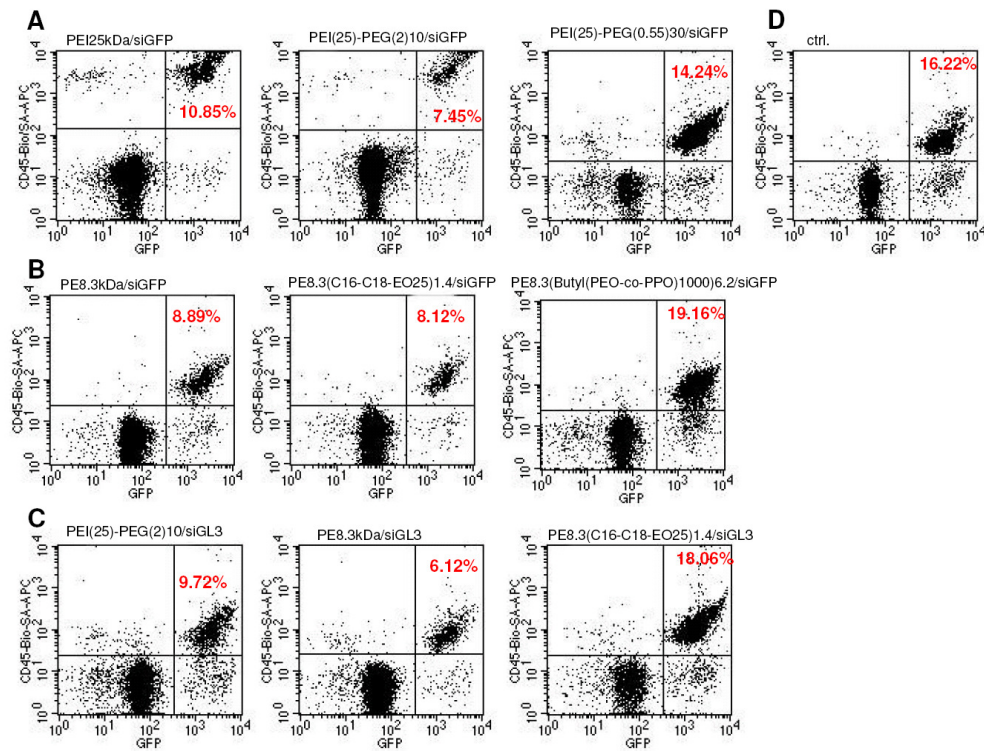
5 days post instillation the left lungs were paraffin-embedded and processed for fluorescent microscopy. Nuclei are shown in blue (DAPI), and EGFP signal is shown in green. Exposure time was kept constant to compare the EGFP signal in the different treatment groups. Images are representative images out of 6 individual images from the respective region of the lungs per animal, magnification 40 x. Figure 4.1 is showing the upper airways and Figure 4.2 the alveolar region. A represents PEI25kDa, PEI(25)-PEG(2)10, PEI(25)-PEG(0.55)30 from left to right, B showed PEI8.3kDa, PEI8.3(C16-C18-EO25)1.4 from left to right, in C is given the unspecific complexes with siGL3 of PEI(25)-PEG(2)10, PEI8.3kDa, PEI8.3(C16-C18-EO25)1.4 from left to right, D showed the controls, enhanced green fluorescent protein expressing CBA mice and C57/BL6 control mice.

Cell specific targeting

To get an impression about a selective (cell-type) targeting of specific leukocyte subtypes by the PEI-based nanocarriers, we investigated the lung homogenate by flow cytometry using different leukocyte specific cell surface markers to differentiate leukocytes (CD45+), from B-lymphocytes (CD45+/CD19+), T-lymphocytes (CD4+ positive: CD45+/CD4+ and CD8+ positive: CD45+/CD8+), granulocytes (Gr1+), neutrophilic granulocytes (Gr1+/CD11b+), lung macrophages (CD11b-/CD11c+), and dendritic cells (CD11b+/CD11c+ or HCII+/CD11c+). Particular high reduction of the EGFP expression was found for CD45+/GFP+ cells after treatment with PEI(25)-PEG(2)10/siGFP, PEI8.3(C16-C18-EO25)1.4/siGFP, and PEI8.3kDa/siGL3 (Fig 5.). Again PEI8.3 kDa showed very high off-target effect and the knock down efficacy was not specific, because the knock down effect with the unspecific siGL3 was stronger than with the specific siGFP when using PEI 8.3 kDa polymer for siRNA complexation.

Figure 5: Cell specific targeting

A leukocytes (GFP+/CD45+)



B lung macrophages (GFP+/CD11b-/CD11c+)

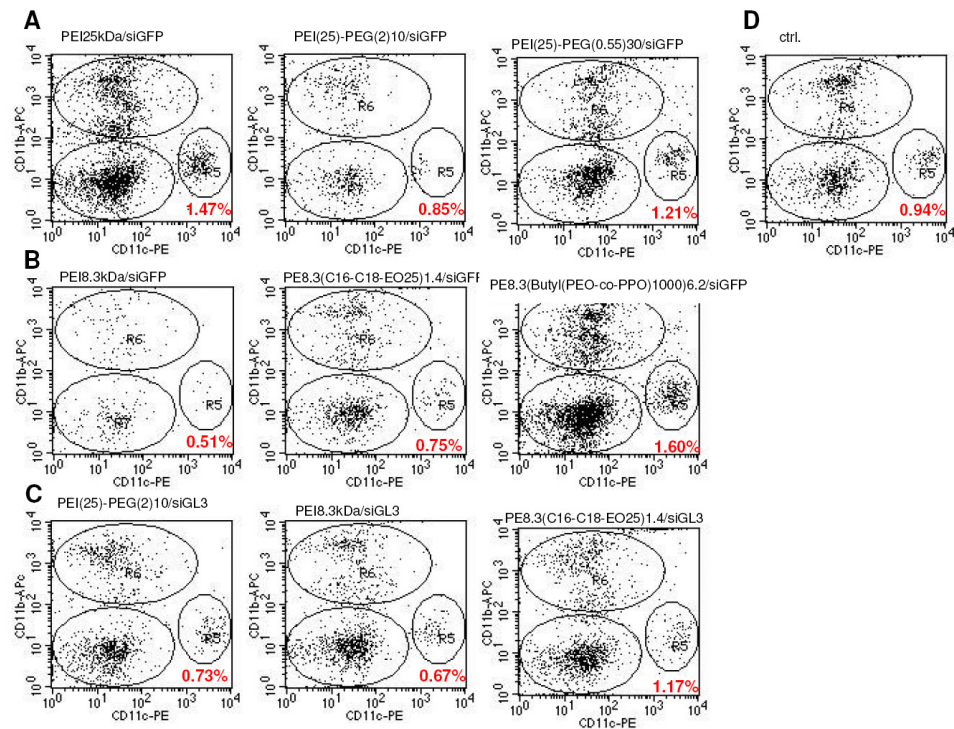


Figure 5: Cell specific targeting

Single-cell suspension obtained from collagenase/DNAse digested lungs from enhanced green fluorescent protein (EGFP) transgenic CABA mice, stained with CD45 (A) and CD11b (B) and CD11c (B). Treatment groups are mentioned above each dot plot and percent of total GFP+/CD45+ (A) or GFP+/CD11c+, CD11b- (B) cells is indicated in red as mean of n=4-6.

Because of the small amount of lung macrophage numbers [36] in the homogenate the reduction of EGFP expression was not statistically significant, but a trend was seen in macrophage specific targeting for specific (siEGFP) and unspecific (siGL3) treatment with polyplexes containing PEI(25)-PEG(2)10 and PEI 8.3 kDa polymer and for specific (siEGFP) treatment with PEI8.3(C16-C18-EO25)1.4 polymer (Figure 6B). Interestingly, it appeared that the fatty acid modified low molecular weight PEI-PEG copolymer was intended for slight knock down EGFP expression in lung macrophages (CD11b-/CD11c+:21 %, MHCII-/CD11c+: 29 %), and to a much stronger extent in leucocytes (39 %). PEI 8.3kDa/siGFP showed also slight knock down in lung macrophages (CD11b-/CD11c+:17 %, MHCII-/CD11c+: 33 %), but this data should be regarded with caution because of the high off-target effects observed after treatment with this polymer when regarding cell specific targeting, e.g. CD45+ leucocytes.

7.5 Discussion

Treatment of lung diseases by tools of combined cell specific targeting and RNAi technique represents a new way for novel treatment strategies and would be a great challenge for nanomedicine. So far, pulmonary application of siRNA *in vivo* is still rare and entry to clinical trials often failed due to safety or efficacy reasons. Therefore, new and improved approaches for promising nanocarriers for pulmonary siRNA delivery are still needed and under intense investigations. In this study, we analyzed the efficacy of six different PEI-based non-viral vector systems on siRNA delivery directly to the lungs focusing leucocytes as target cells because it would be a great challenge to target this cell type for lung disease like chronic obstructive pulmonary disorder (COPD) or asthma bronchiale. Two series of PEI modifications (high molecular weight vs. low molecular weight and hydrophilic vs. hydrophobic PEGs) were investigated because of their promising *in vitro* properties [10, 11, 23]. High molecular weight PEI 25 kDa has been successfully delivered siRNA as well as pDNA to the lungs [4, 8, 35], but the cytotoxicity is very high and limits the dosing regime. Therefore, low molecular weight PEI and several modifications on the PEI backbone were developed and analyzed [22, 37]. Low molecular weight PEI was shown to transfect various cell lines *in vitro* with pDNA [38, 39]. Hydrophilic PEG-PEI copolymers were used to reduce cytotoxicity, protein binding, and increase solubility *in vitro* [11, 19, 23, 40, 41] and have been shown to successfully deliver siRNA to mouse lungs [7]. Fatty acid modification on a natural occurring, cationic charged molecule like spermine was shown to successfully deliver pDNA in to the dermis and intramuscular in mice [42]. They found an increase in toxicity with increasing length of hydrocarbon chains, which could be explained by the detergents-like properties which are more prominent with longer hydrocarbon chains on the polycation spermine and could cause higher membrane disruption than more hydrophobic molecules. The higher membrane damage effect of the more hydrophobic modified PEI-PEGs in our study revealed similar results like that in the above mentioned study and the decrease in cell

viability was much stronger for the low molecular weight PEI8.3 kDa polymers than for PEI25 kDa polymers and more prominent in the alveolar epithelial cell line. Alshamsan et al. [27] has investigated the *in vitro* transfection efficacy of oleic acid and stearic acid modified PEIs for siRNA delivery in B16 melanoma cells and found a pronounced higher transfection efficacy for the hydrophobically modified PEI-based polymers over a wide range of other commercially available transfection reagents for siRNA delivery.

In our study, we tried to introduce a panel of promising variations on the PEI backbone to study the efficacy of the *in vitro* tested carriers for siRNA directly to the lung. Although, recently published studies [4, 35] described successful delivery of siRNA against different proteins of the influenza virus A to the lungs by using PEI 25 kDa, we were not able to show specific knock down in EGFP expression in our mouse model using PEI25 kDa. Nevertheless, one of the hydrophilic PEG modification PEI(25)-PEG(2)10, and the low molecular weight PEI8.3 kDa, and the fatty acid modification PEI8.3(C16-C18-EO25)1.4 yielded strong reduction of EGFP expression in the lungs. To test if these knock down effects were sequence-specific for EGFP we applied the three most effective polyplexes complexed with an unspecific siRNA against luciferase (GL3). Surprisingly, we found for all unspecific polyplexes also slight reduction of EGFP expression, whereas the low molecular weight PEI8.3kDa (58±9 %) and PEI(25)-PEG(2)10 (50±11 %) caused the highest unspecific knock down effect and PEI8.3(C16-C18-EO25)1.4 (30±16 %) showed only a moderate unspecific knock down compare to control animals. PEI25kDa, PEI(25)-PEG(0.55)30 and PEI8.3(Butyl-PEO-co-PPO)1000)6.2 polyplexes induced no significant changes in EGFP expression in comparison to control animals, therefore we did not look for unspecific knock down effects using siGL3. Regarding the cell specific targeting in the lung, we could distinguished a broad range of leucocytes-related cell types and found out that with the most efficient carrier PEI8.3(C16-C18-EO25)1.4 targeted in most cases leucocytes (CD45+) and to a small extent lung macrophages (CD11b-/Cd11c+), but knock down efficiencies were not higher than the

overall knock down in EGFP expression. Therefore, it seemed to be likely that leucocytes-related cell types in the lung are targeted to a small amount but the main target cell types are out of our staining strategy and represent rather endothelium or epithelium [4, 5, 36]. The fatty acid modification on the PEI 8.3 kDa backbone offers some advanced properties for transfection. The hydrophobic residue caused i) weaker interaction between the polymer and siRNA, which could facilitate siRNA delivery, and ii) stronger membrane interaction for improved uptake. Successful targeting lung macrophages was also described by a study of Griesenbach et al. [5], where they found FITC-labeled siRNA complexed with the cationic lipid Genzyme lipid (GL69) most likely in alveolar macrophages in comparison to antisense oligonucleotides (asODN), which were found to target alveolar epithelial cells.

Because of the high proinflammatory potential of the analyzed polymers and polyplexes *in vitro* as well as *in vivo* as recently described [9, 10] and the high unspecific knock down effects observed in this study, further evaluation of the stimulation of the innate immune system after polyplex application is still needed to improve polymer design with limited off-target effects.

For the first time, we could describe the leucocytes specific cell type targeted following intratracheal instillation of PEI-based nanocarriers by siRNA delivery. In that way, the hydrophobic moiety, namely the fatty acid residue (C16-C18-EO25) on PEI8.3 kDa, appear to be most promising for specific knock down in lung cells and offers new strategies to develop more effective nanocarriers. The next generation of cationic polymers for siRNA should balance the hydrophilic and hydrophobic properties for improved polyplex uptake, reduced cytotoxicity and immunostimulation and efficient delivery of siRNA.

7.6 Supplementary data

S1 Synthesis of the polymers and siRNA information

Poly(ethylene imine) copolymers of PEI 25 kDa with hydrophilic modifications

Branched poly(ethylene imine) (PEI) with a molecular weight of 25 kDa (Polymin™, water-free, 99 %) was a gift of BASF, Ludwigshafen. The polyethylene imine-graft-poly(ethylene glycol) (PEI-PEG) with a PEG content of approximately 50 % (w/w) was synthesized as previously described [22, 23] by grafting linear PEG of 0.55 kDa and 2 kDa, respectively, onto branched PEI 25 kDa. These graft copolymers were designated using following nomenclature: PEI(25k)-g-PEG(x)n. The number in brackets (25 k or x, where x=0.55 k, 2 k) represents the molecular weight of PEI or PEG block in Daltons, and the index n is the average number of PEG blocks per PEI molecule. The number was calculated on the basis of ¹H-NMR spectra as described previously [22].

Poly(ethylene imine) copolymers of PEI 8.3 kDa with hydrophobic modifications

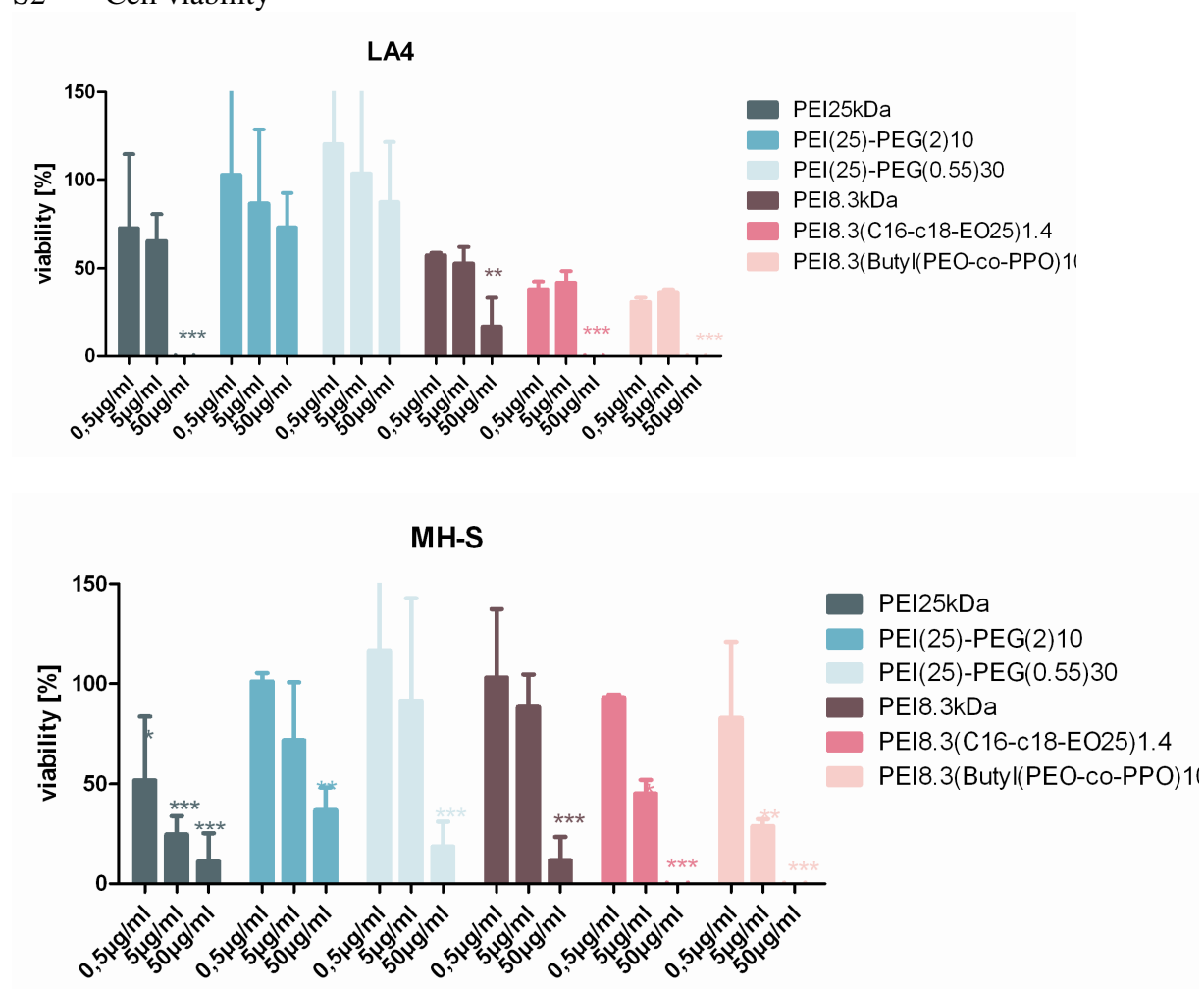
PEI was synthesized by acid initiated polymerisation from aziridine using ethylenediamine as initiator. PEI 8.3 kDa was grafted by N-acylation with butyl-(poly(ethylenoxid-co-propylenoxid) (Butyl-(PEO-co-PPO)1000) or palmityl-/stearyl-polyethylenoxid (C16-C18-EO)25 mixture as previously described by [37]. The nomenclature of these polymers are following: PEI8.3-(x)n, where x represent the respective hydrophobic polyethylenoxid derivate and n is the average number of x units per PEI molecule, which is calculated on the basis of ¹H-NMR spectra.

siRNA against green fluorescence protein (GFP) was obtained from Metabion (München, Germany) with following sequence for sense strand: 5'-GGCUACGUCCAGGAGCGCACC-dTdT and for antisense strand: 5'-GGUGCGCUCCUGGACGUAGCC-dTdT. siRNA against luciferase GL3 (siGL3) was purchased from MWG (Ebersberg, München) with following sequence for the sense: 5'-CTTACGCTGAGTACTTCGATT -3' and the antisense strand: 5'-AATCGAAGTACTCAGCGTAAG-3'.

Polyplex formation

Sense and antisense strand for siRNA against GFP was annealed using annealing buffer containing 30 mM HEPES-KOH pH 7.4, 100 mM KCl, 2 mM MgCl₂, 50 mM NH₄Ac according to the annealing protocol from Metabion. siRNA polyplexes were formed as previously described [7]. siGL3 was purchased already as annealed double-strand and was directly used. Polyplexes were formed by mixing equal volumes (25 μ l each) of siRNA and polymer dilution in Aqua ad injectabilia to obtain the desired nitrogen to RNA phosphate ratio (N/P ratio) of 6 using 35 μ g siRNA. Polymers were diluted in Aqua ad injectabilia (Braun AG, Melsung, Germany) and vigorously vortexed directly before use.

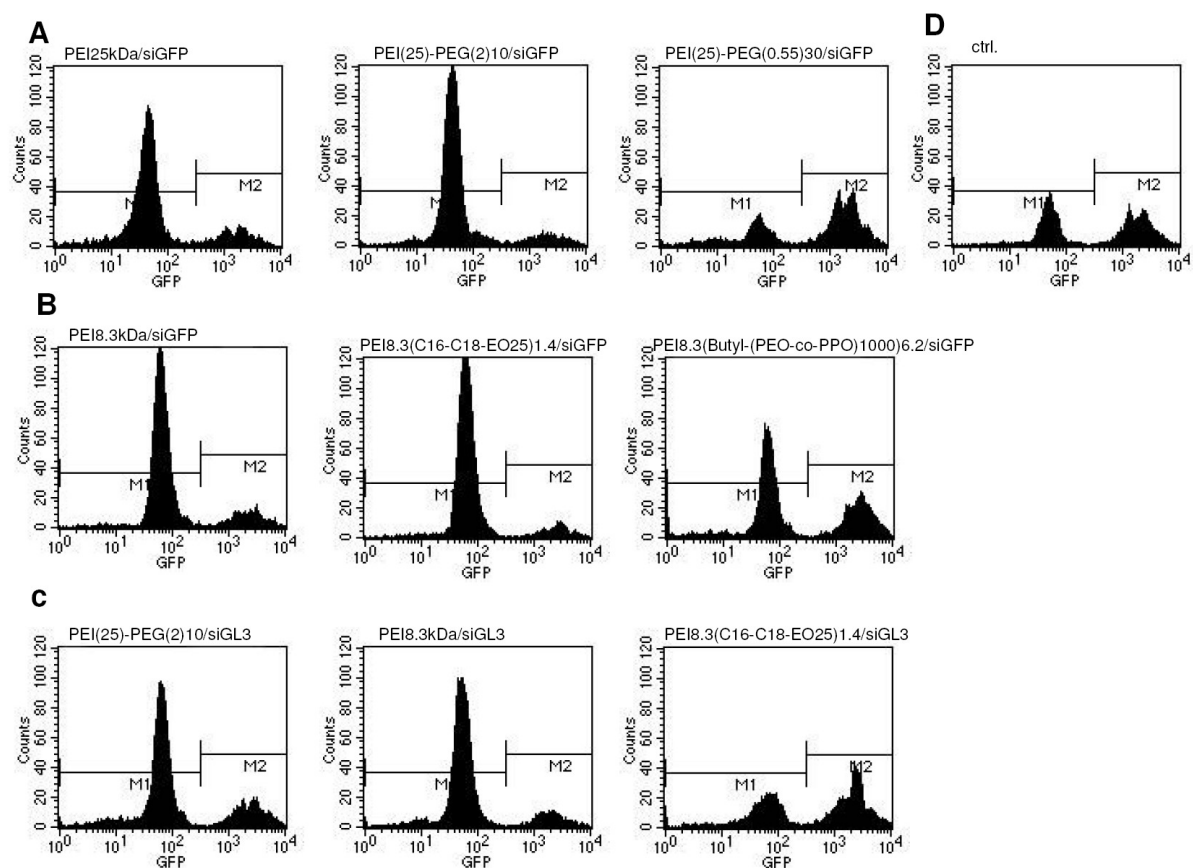
S2 Cell viability



S2 Cell viability

Cell viability was determined by using WST-1 reagent (Roche Diagnostics, Germany) after 24 h polymer treatment. Values represents mean \pm SD of three independent experiments and statistical significance is indicated by asterisks with * p <0.05, ** p <0.01, *** p <0.001.

S3 GFP expression



S3: Histograms of EGFP expression in all treatment groups. y-axis shows the cell counts and x-axis the EGFP signal. M1 is the cell population containing low EGFP expressing cells and M2 represents the cell population which expressing high EGFP (cells of interest). Histograms were depicted as representative from $n=4-6$ animals of each group.

7.7 References

- 1 de Fougerolles, A., H.P. Vornlocher, J. Maraganore, and J. Lieberman, *Interfering with disease: a progress report on siRNA-based therapeutics*. Nat Rev Drug Discov, 2007. 6(6): p. 443-53.
- 2 Novina, C.D. and P.A. Sharp, *The RNAi revolution*. Nature, 2004. 430(6996): p. 161-4.
- 3 Fire, A., S. Xu, M.K. Montgomery, S.A. Kostas, S.E. Driver, and C.C. Mello, *Potent and specific genetic interference by double-stranded RNA in Caenorhabditis elegans*. Nature, 1998. 391(6669): p. 806-11.
- 4 Ge, Q., L. Filip, A. Bai, T. Nguyen, H.N. Eisen, and J. Chen, *Inhibition of influenza virus production in virus-infected mice by RNA interference*. Proc Natl Acad Sci U S A, 2004. 101(23): p. 8676-81.
- 5 Griesenbach, U., C. Kitson, S. Escudero Garcia, R. Farley, C. Singh, L. Somerton, H. Painter, R.L. Smith, D.R. Gill, S.C. Hyde, Y.H. Chow, J. Hu, M. Gray, M. Edbrooke, V. Ogilvie, G. MacGregor, R.K. Scheule, S.H. Cheng, N.J. Caplen, and E.W. Alton, *Inefficient cationic lipid-mediated siRNA and antisense oligonucleotide transfer to airway epithelial cells in vivo*. Respir Res, 2006. 7: p. 26.
- 6 Kim, W.J. and S.W. Kim, *Efficient siRNA delivery with non-viral polymeric vehicles*. Pharm Res, 2009. 26(3): p. 657-66.
- 7 Merkel, O.M., A. Beyerle, D. Librizzi, A. Pfestroff, T.M. Behr, B. Sproat, P.J. Barth, and T. Kissel, *Nonviral siRNA delivery to the lung: investigation of PEG-PEI polyplexes and their in vivo performance*. Mol Pharm, 2009. 6(4): p. 1246-60.
- 8 Thomas, M. and A.M. Klibanov, *Enhancing polyethylenimine's delivery of plasmid DNA into mammalian cells*. Proc Natl Acad Sci U S A, 2002. 99(23): p. 14640-5.
- 9 Beyerle, A., A. Braun, A. Banerjee, N. Ercal, O. Eickelberg, T. Kissel, and T. Stoeger, *Side-effects of PEI-based siRNA nanocarriers for pulmonary application in mice*. Eur Res J, under review.
- 10 Beyerle, A., O.M. Merkel, T. Stoeger, and T. Kissel, *PEGylation affects cytotoxicity and cell-compatibility of poly(ethylene imine) for lung application: structure-function-relationships* Toxicol Appl Pharmacol, 2009. in press.
- 11 Mao, S., X. Shuai, F. Unger, M. Wittmar, X. Xie, and T. Kissel, *Synthesis, characterization and cytotoxicity of poly(ethylene glycol)-graft-trimethyl chitosan block copolymers*. Biomaterials, 2005. 26(32): p. 6343-56.
- 12 Boussif, O., F. Lezoualc'h, M.A. Zanta, M.D. Mergny, D. Scherman, B. Demeneix, and J.P. Behr, *A versatile vector for gene and oligonucleotide transfer into cells in culture and in vivo: polyethylenimine*. Proc Natl Acad Sci U S A, 1995. 92(16): p. 7297-301.
- 13 Demeneix, B. and J.P. Behr, *Polyethylenimine (PEI)*. Adv Genet, 2005. 53: p. 217-30.
- 14 Densmore, C.L., F.M. Orson, B. Xu, B.M. Kinsey, J.C. Waldrep, P. Hua, B. Bhogal, and V. Knight, *Aerosol delivery of robust polyethyleneimine-DNA complexes for gene therapy and genetic immunization*. Mol Ther, 2000. 1(2): p. 180-8.
- 15 Di Gioia, S. and M. Conese, *Polyethylenimine-mediated gene delivery to the lung and therapeutic applications*. Drug Design, Development and Therapy, 2008. 2: p. 163-188.
- 16 Goula, D., C. Benoist, S. Mantero, G. Merlo, G. Levi, and B.A. Demeneix, *Polyethylenimine-based intravenous delivery of transgenes to mouse lung*. Gene Ther, 1998. 5(9): p. 1291-5.
- 17 Grayson, A.C., A.M. Doody, and D. Putnam, *Biophysical and structural characterization of polyethylenimine-mediated siRNA delivery in vitro*. Pharm Res, 2006. 23(8): p. 1868-76.

- 18 Rudolph, C., J. Lausier, S. Naundorf, R.H. Muller, and J. Rosenecker, *In vivo gene delivery to the lung using polyethylenimine and fractured polyamidoamine dendrimers*. *J Gene Med*, 2000. 2(4): p. 269-78.
- 19 Glodde, M., S.R. Sirsi, and G.J. Lutz, *Physicochemical properties of low and high molecular weight poly(ethylene glycol)-grafted poly(ethylene imine) copolymers and their complexes with oligonucleotides*. *Biomacromolecules*, 2006. 7(1): p. 347-56.
- 20 Philipp, A., X. Zhao, T. P. W. E, and Z. A, *Hydrophobically modified oligoethylenimines as highly efficient transfection agents for siRNA delivery*. *Bioconjug Chem*, 2009. 20(11): p. 2055-61.
- 21 Zintchenko, A., A. Philipp, A. Dehshahri, and E. Wagner, *Simple modifications of branched PEI lead to highly efficient siRNA carriers with low toxicity*. *Bioconjug Chem*, 2008. 19(7): p. 1448-55.
- 22 Petersen, H., P.M. Fechner, D. Fischer, and T. Kissel, *Synthesis, Characterization, and Biocompatibility of Polyethylenimine-graft-poly(ethylene glycol) Block Copolymers*. *Macromolecules*, 2002. 35(18): p. 6867-6874.
- 23 Petersen, H., P.M. Fechner, A.L. Martin, K. Kunath, S. Stolnik, C.J. Roberts, D. Fischer, M.C. Davies, and T. Kissel, *Polyethylenimine-graft-poly(ethylene glycol) copolymers: influence of copolymer block structure on DNA complexation and biological activities as gene delivery system*. *Bioconjug Chem*, 2002. 13(4): p. 845-54.
- 24 Moore, N.M., T.R. Barbour, and S.E. Sakiyama-Elbert, *Synthesis and characterization of four-arm poly(ethylene glycol)-based gene delivery vehicles coupled to integrin and DNA-binding peptides*. *Mol Pharm*, 2008. 5(1): p. 140-50.
- 25 Pathak, A., P. Kumar, K. Chuttani, S. Jain, A.K. Mishra, S.P. Vyas, and K.C. Gupta, *Gene expression, biodistribution, and pharmacoscintigraphic evaluation of chondroitin sulfate-PEI nanoconstructs mediated tumor gene therapy*. *ACS Nano*, 2009. 3(6): p. 1493-505.
- 26 Gref, R., M. Luck, P. Quellec, M. Marchand, E. Dellacherie, S. Harnisch, T. Blunk, and R.H. Muller, *'Stealth' corona-core nanoparticles surface modified by polyethylene glycol (PEG): influences of the corona (PEG chain length and surface density) and of the core composition on phagocytic uptake and plasma protein adsorption*. *Colloids Surf B Biointerfaces*, 2000. 18(3-4): p. 301-313.
- 27 Alshamsan, A., A. Haddadi, V. Incani, J. Samuel, A. Lavasanifar, and H. Uludag, *Formulation and delivery of siRNA by oleic acid and stearic acid modified polyethylenimine*. *Mol Pharm*, 2009. 6(1): p. 121-33.
- 28 Aravindan, L., K.A. Bicknell, G. Brooks, V.V. Khutoryanskiy, and A.C. Williams, *Effect of acyl chain length on transfection efficiency and toxicity of polyethylenimine*. *Int J Pharm*, 2009. 378(1-2): p. 201-10.
- 29 Forrest, M.L., G.E. Meister, J.T. Koerber, and D.W. Pack, *Partial acetylation of polyethylenimine enhances in vitro gene delivery*. *Pharm Res*, 2004. 21(2): p. 365-71.
- 30 Gabrielson, N.P. and D.W. Pack, *Acetylation of polyethylenimine enhances gene delivery via weakened polymer/DNA interactions*. *Biomacromolecules*, 2006. 7(8): p. 2427-35.
- 31 Mosmann, T., *Rapid colorimetric assay for cellular growth and survival: application to proliferation and cytotoxicity assays*. *J Immunol Methods*, 1983. 65(1-2): p. 55-63.
- 32 Choksakulnimitr, S., S. Masuda, T. Hideaki, Y. T., and H. Mitsuru, *In vitro cytotoxicity of macromolecules in different cell culture systems*. *J Control Release*, 1995. 34: p. 233-214.
- 33 Prabhakar, U., E. Eirikis, M. Reddy, E. Silvestro, S. Spitz, C. Pendley, 2nd, H.M. Davis, and B.E. Miller, *Validation and comparative analysis of a multiplexed assay for the simultaneous quantitative measurement of Th1/Th2 cytokines in human serum*

- and human peripheral blood mononuclear cell culture supernatants.* J Immunol Methods, 2004. 291(1-2): p. 27-38.
- 34 Boeckle, S., K. von Gersdorff, S. van der Piepen, C. Culmsee, E. Wagner, and M. Ogris, *Purification of polyethylenimine polyplexes highlights the role of free polycations in gene transfer.* J Gene Med, 2004. 6(10): p. 1102-11.
- 35 Zou, S.M., P. Erbacher, J.S. Remy, and J.P. Behr, *Systemic linear polyethylenimine (L-PEI)-mediated gene delivery in the mouse.* J Gene Med, 2000. 2(2): p. 128-34.
- 36 Stone, K., R.R. Mercer, P. Gehr, B. Stockstill, and J.D. Crapo, *Allometric relationships of cell numbers and size in the mammalian lung.* Am J Resp Cell Mol Biol, 1992. 6: p. 235-243.
- 37 Koch, F., *Synthese und Charakterisierung niedermolekularer Polyethylenimine und Polyethylenimin-Derivate für die Gentransfektion.* Master thesis, 2009.
- 38 Fischer, D., T. Bieber, Y. Li, H.P. Elsasser, and T. Kissel, *A novel non-viral vector for DNA delivery based on low molecular weight, branched polyethylenimine: effect of molecular weight on transfection efficiency and cytotoxicity.* Pharm Res, 1999. 16(8): p. 1273-9.
- 39 Kunath, K., A. von Harpe, D. Fischer, H. Petersen, U. Bickel, K. Voigt, and T. Kissel, *Low-molecular-weight polyethylenimine as a non-viral vector for DNA delivery: comparison of physicochemical properties, transfection efficiency and in vivo distribution with high-molecular-weight polyethylenimine.* J Control Release, 2003. 89(1): p. 113-25.
- 40 Kichler, A., M. Chillon, C. Leborgne, O. Danos, and B. Frisch, *Intranasal gene delivery with a polyethylenimine-PEG conjugate.* J Control Release, 2002. 81(3): p. 379-88.
- 41 Ogris, M., S. Brunner, S. Schuller, R. Kircheis, and E. Wagner, *PEGylated DNA/transferrin-PEI complexes: reduced interaction with blood components, extended circulation in blood and potential for systemic gene delivery.* Gene Ther, 1999. 6(4): p. 595-605.
- 42 Viola, J.R., H. Leijonmarck, O.E. Simonson, Oprea, II, R. Frithiof, P. Purhonen, P.M. Moreno, K.E. Lundin, R. Stromberg, and C.I. Smith, *Fatty acid-spermine conjugates as DNA carriers for nonviral in vivo gene delivery.* Gene Ther, 2009. 16(12): p. 1429-40.

8 Summary and Perspectives

8.1 Summary

In this thesis, toxicity of PEI-based non-viral vector systems for siRNA application into the lungs was comprehensively described and analyzed in vitro as well as in vivo.

Chapter 1 introduced in basic information about the lung anatomy and physiology and general considerations for pulmonary application as well as gave an overview of the two major groups of non-viral vector systems for pulmonary application and highlighted their impact in nanomedicine and nanotoxicology. The search for more predictive toxicity tools for (polymeric) non-viral vector systems is still of great concern in the community and was pointed out in this chapter.

Chapter 2 described the toxicological and immunomodulatory effects of two different PEI-based nanocarriers for siRNA delivery in different murine lung cells. Two different PEI nanocarriers (branched vs. linear, and low vs. high molecular weight PEI) were evaluated regarding standard toxicity endpoints, but also immunomodulatory effects caused by the pure polymers and their respective polyplexes with siRNA. The results pointed out, that epithelial cells were much more sensitive in response to such polymers and the polyplexes appeared to be less toxic than the pure polymers. In addition, the immunomodulatory effects of such polymeric non-viral vector systems should be further investigated for their underlying mechanism.

Chapter 3 hypothesized that poly(ethylene glycol) (PEG) reduces the cytotoxicity of high molecular weight, branched PEI25 kDa and investigated the cell-compatibility and cytotoxicity of a panel of different PEI-PEG polymers in vitro. This in vitro study highlighted the inflammatory potential of such PEI-PEG polymers which seemed to be higher when cytotoxicity was extremely reduced.

Hypothesizing that inflammatory and oxidative stress response play an important role when using PEI-based nanocarriers, especially for pulmonary application, in *Chapter 4* a toxicity and stress pathway focused gene expression profiling was described for selected PEI-PEG

polymers. This gene array clearly stressed the inflammatory potential of the modified PEI-PEG polymers with reduced apoptotic signalling pathways, but increasing inflammatory and oxidative stress response, in contrast to PEI25 kDa.

Due to the higher proinflammatory potential and elevated oxidative stress parameters, the question of genotoxicity was addressed in *Chapter 5*. The mutant frequency of selected PEI-based nanocarriers was investigated by using a transgenic lung epithelial cell culture in vitro model, but was regarded to be less and PEI-based nanocarriers were not mutagenic in such an in vitro model.

After toxicity analysis in vitro two main questions raised (i) what kind of effects would be induced by the polymers or their polyplexes in vivo when directly administered to the lungs and (ii) could we find any in vitro/ in vivo correlation for biomarkers indicating toxicity, inflammation and/or oxidative stress?

Chapter 6 focused on the in vivo toxicity, inflammatory, and oxidative stress response of selected PEI-based nanocarriers for siRNA in mice after intratracheal instillation and tried to answer the two upcoming questions from the in vitro studies. Almost all modified PEI-based nanocarriers showed very high acute inflammation, but with different resolving kinetics. Hydrophobic modification of low molecular weight PEI and highly hydrophilic PEGylated PEI-based nanocarriers seemed to be well tolerable in contrast to moderate hydrophilic PEGylated and fatty-acid modified PEI-based polymers which showed very high and sustained inflammation in the lungs.

In contrast to safety issues (which represent the main part of this thesis) in *chapter 7* the in vivo efficacy and the cell-type specific targeting was reported of PEI-based nanocarriers, same carriers selected as in *Chapter 6*, for pulmonary siRNA delivery. Surprisingly, the highly inflammatory PEI-based nanocarriers yielded high knock down effects, but only the fatty acid modified PEI-based nanocarrier, seemed to avoid off-target effects. Leucocytes

were targeted to some extent, but seemed not to be the main targeted cell type in the lung after PEI-based nanocarriers application for siRNA delivery.

Thus, for clinical trials the polymers should be carefully optimized and evaluated for cytotoxicity, high acute inflammatory and oxidative stress response and their in vivo performance of siRNA delivery. Development of polymers with reduced cytotoxicity and negligible off-target effects, but high in vivo efficacy represents one of the biggest challenges for the next decades before entry to clinics. In addition, optimized in vitro models for predictive toxicity are still needed.

8.2 Perspectives

Predictive in vitro tools for cytotoxicity is one issue to be overcome when using so called nanocarriers for human application. A lot of information of the behaviour and properties of nanocarriers in the lungs could be obtained from the intense investigations of ultrafine particles (UFP) in the field of environmental health. In all our studies two anorganic particles were included, namely crystalline silica (CS) and nanosized zinc oxide (NZO), which are well known for their cytotoxicity and inflammatory effects in the lungs. These particles were for the first time introduced as lung toxic benchmarks. Further investigations and establishments of in vitro models should include such as particles to obtain an idea of the relevance of the in vitro results with regard to risk assessment and safety. Considering the rapid growth of nanotechnology and the variety of nanomaterials potentially used in the future, identifying, quantifying and managing potential health risks is essential, especially in the respiratory tract that may serve as the portal of entry for inhaled nanoparticles and nanofibers. Epidemiological studies have shown that a sudden surge in the level of UFP can be linked to increased cardio-respiratory morbidity and mortality including asthma, chronic obstructive pulmonary disease (COPD) and arteriosclerosis. Thus, the potential risk of therapeutic

nanoparticles should be carefully evaluated, and robust and reliable predictive in vitro tools should be introduced.

In this thesis, the *Chapter 2-5* dealt with a wide range of in vitro analysis in different lung mono cell culture systems and described various toxicity endpoint measurements. To integrate the lung cell interplay, between the over 40 different cell types in the lung, and to be more realistic, the main focus in future should be addressed on the development of robust and reliable in vitro models. More than one cell type in culture should be included and the co-culture models should be easy to handle, but more predictive in regard to the interaction between the different cell types. In parallel, more than one mono cell line representing different origin (human vs. murine) and/or cell type (e.g. epithelial, endothelial cells, fibroblasts, macrophages) should be analyzed for cytotoxicity. Nevertheless, in this thesis the mono cell culture systems (using different cell types) highlighted the immunomodulatory and proinflammatory potential from such PEI-based non-viral vector systems (*Chapter 2-5*), which could be confirmed in the vivo toxicity study in *Chapter 6*. To uncover the underlying mechanism of inflammation and oxidative stress as well as cytotoxicity caused by polymeric non-viral vector systems for siRNA delivery into the lungs represents one challenge for the near future to develop safe and efficient carrier systems. Further studies should be analyze more in detail the underlying toxicity pathways regarding gene expression pattern and following the "hits" by measuring protein expression of relevant proteins involved in the respective pathway, e.g. cytochrom c release for the intrinsic apoptotic pathway detected by Bcl or Bax. For more evidence of the apoptotic behaviour of PEI assays should be included which analyze more in detail the two distinct apoptotic pathways, e.g. regarding caspase activity. With regard to the higher inflammatory potential of the PEI-modifications further models are still needed to evaluate the mechanism behind, e.g. complement activation.

Little is known about the cell-type-specific targeting of non-viral vector systems for siRNA delivery into the lungs. Combination of cell specific targeting and RNAi technique represents

a new way for treatment of various diseases and would be a great challenge for nanomedicine. *Chapter 7* described for the first time, in addition to the in vivo performance of six different PEI-based nanocomplexes with siRNA, the cell-type specific targeting of such polymeric non-viral vector systems. Since leucocytes were targeted to some extent, but do not represent the major cell-type which was addressed by polymeric siRNA delivery systems, further evaluation of other cell types, which are more represented in the lung, like epithelium or endothelium, but also interstitial cell types like fibroblasts or smooth muscle cells, is still needed. More sophisticated techniques, e.g. immunofluorescence and MACS technology for flow cytometry or the combination with non-invasive imaging techniques (e.g. PET, MRT, CT) may help to distinguish more in detail the main targeted lung regions (upper vs. lower airways).

In summary, the in vitro/ in vivo correlation of the obtained data is still needed to provide more information for an optimized development of predictive toxicity in vitro models and better guidance of sophisticated in vivo studies.

8.3 Zusammenfassung

Die vorliegende Arbeit beschreibt sehr ausführlich die Toxizität von Polyethylenimine (PEI)-basierten nicht-viralen Vektorsystemen für die pulmonare Verabreichung von siRNA und zeigt die toxikologische Analyse dieser Carrier in vitro als auch in vivo.

Kapitel 1 führt in die Lungenanatomie sowie –physiologie ein und gibt allgemeine Hinweise, die bei einer pulmonaren Applikation von Bedeutung sind. Außerdem wird ein Überblick gegeben über die zwei bedeutendsten Gruppen von nicht-viralen Vektorsystemen für eine pulmonare Verabreichung und die Bedeutung dieser Klassen im Zusammenhang mit der sogenannten „Nanomedizin“ und „Nanotoxikologie“ dargestellt. Die Entwicklung und der Nutzen von geeigneten in vitro Toxizitätsuntersuchungs- und -beurteilungsmöglichkeiten für polymer-basierte nicht-virale Vektorsysteme zur besseren Vorhersage ihrer Toxizität in vivo stellt eine große Herausforderung an alle Wissenschaftler im Bereich der „Nanomedizin“ dar und ist in *Kapitel 1* besonders hervorgehoben worden.

Kapitel 2 beschreibt die toxikologischen und immunmodulatorischen Effekte von zwei PEI-basierten Nanocarriern für siRNA Freisetzung in verschiedenen Mauszelllinien. Die zwei PEI-basierten Nanocarrier (verschweigt gegenüber linear und PEI mit geringem und hohem Molekulargewicht, sowie reine Polymere gegenüber den Komplexe mit siRNA) wurden hinsichtlich ihrer Toxizität und immunmodulierender Effekte mit klassischen toxikologischen Endpunktmessungen untersucht. Die Ergebnisse zeigen eine deutlich höhere Empfindlichkeit der alveolaren Epithelzellen nach Behandlung mit PEI, wobei die Polyplexe eine geringere Toxizität aufweisen als die reinen Polymere. Außerdem zeigen die Polymere und Polyplexe ein gewisses immunmodulatorisches Potential, das weiter hinsichtlich des zugrundeliegenden Mechanismus untersucht werden sollte.

Kapitel 3 postuliert, dass die Kopplung von Polyethylenglycol (PEG) an PEI die Zytotoxizität von hochmolekular, verzweigtem PEI 25kDa reduzieren kann und untersucht die Zell-Kompatibilität und Zytotoxizität von mehreren unterschiedlich PEGylierten PEI-PEG

Kopolymeren in vitro. Diese in vitro Studie zeigt klar, dass mit zunehmender PEGylierung die Zytotoxizität zwar abnimmt, dafür aber das entzündungsfördernde Potential der PEG-PEI Kopolymere zunimmt.

Ausgehend davon, dass eine möglicherweise auftretende Entzündungsantwort und ein oxidativer Stresseffekt eine entscheidende Rolle bei der Verabreichung und Anwendung solcher PEI-basierten Nanocarrier, vor allem für die pulmonare Anwendung, spielt, beschreibt *Kapitel 4* ein Toxizitäts- und Stress-basiertes Genexpressionsprofiling für ausgewählte PEI-PEG Polymere. Dieser Genarray hebt wiederum deutlich das entzündungsfördernde Potential der PEI-PEG Copolymere gegenüber dem reinen PEI 25kDa hervor, wobei mit zunehmender PEGylierung apoptotische Signalwege vermindert auftreten und Entzündungsprozesse sowie oxidative Stresseffekte verstärkt werden.

Wegen des erhöhten entzündungsfördernden Potentials und der verstärkten oxidativen Stressantwort, wurde die Frage einer möglichen Genotoxizität der PEI-basierten Polymere in *Kapitel 5* untersucht. Die Mutationsfrequenz von ausgewählten PEI-basierten Polymeren wurde in einem transgenen Lungenepithelzell - Zellkultur-Model getestet. Es konnte gezeigt werden, dass das mutagene Potential von diesen PEI-basierten Nanocarriern in diesem Model als sehr gering bis vernachlässigbar klein eingestuft werden konnte.

Nachdem die Toxizität in vitro ausführlich getestet wurde, stellten sich folgende zwei Fragen:

- a) Was für Effekte werden hervorgerufen nach direkter pulmonarer Verabreichung der Polymere oder ihrer Polyplexe in der Lunge?
- b) Gibt es eine mögliche in vitro/ in vivo Korrelation für einen oder mehrere Biomarker, die Hinweise auf Toxizität, Entzündung und oxidativen Stress geben?

Kapitel 6 beschäftigt sich in erster Linie mit der Beurteilung der Toxizität, Entzündung und der oxidativen Stressantwort in vivo nach intratrachealer Verabreichung von ausgewählten PEI-basierten Nanocarriern für siRNA in Mäusen und versucht die oben genannten zwei Fragen zu beantworten.

Fast alle modifizierten PEI-basierten Nanocarrier zeigen eine sehr starke, akute Entzündungsreaktion in der Lunge, jedoch mit unterschiedlichen Kinetiken hinsichtlich der Entzündungsauflösung. Hydrophobe Modifikationen an gering molekularem PEI 8.3 kDa als auch hydrophile, stark PEGylierte PEI 25 kDa Kopolymere scheinen gut vertragen zu werden, im Gegensatz zu eher weniger PEGylierten PEI 25 kDa Kopolmeren und Fettsäure-modifizierten PEI 8.3 kDa Kopolymeren, die eine sehr starke und anhaltende Entzündungsreaktion in der Lunge hervorrufen.

Zusätzlich zu den Toxizitätsstudien, die den Hauptteil der vorliegenden Arbeit ausmachen, wird in *Kapitel 7* die Wirksamkeit und ein Zelltyp spezifisches Targeting von PEI-basierten Nanocarriern (die gleichen, die auch in der Toxizitätstudie in *Kapitel 6* untersucht wurden), nach intratrachealer Verabreichung in transgenen EGFP-Mäusen analysiert. Interessanterweise zeigt sich, dass die, in *Kapitel 6* beschriebenen stark entzündungsfördernden PEI-basierten Polymere die höchste Knockdown Effizienz zeigen, allerdings mit einem hohen Anteil an "off-Target" Effekten. Nur das Fettsäure modifizierte PEI -Polymer scheint weniger bis keine "off-Target" Effekte zu erzeugen. Es konnte weiterhin gezeigt werden, dass Leukozytenpopulation zu einem gewissen Anteil Zielzellen nach Verabreichung der PEI-basierten siRNA-Komplexe in der Lunge darstellen, allerdings scheinen zusätzlich noch Epithel- oder auch Endothelzellen in der Lunge erreicht zu werden. Welche Zellpopulationen außer Leukozyten noch von siRNA/PEI Komplexen nach intratrachealer Verabreichung erreicht werden, soll in weiterführenden Studien mit diesen Polyplexen untersucht werden.

Für klinische Studien im Menschen sollten die Polymere weiterhin sorgfältig optimiert und untersucht werden, um eine sichere und effiziente Anwendung zu gewährleisten. Die Entwicklung von PEI-basierten Polymeren mit einer verminderten bis vernachlässigbaren Zytotoxizität, vernachlässigbaren "off-Target" Effekten, aber einer ausreichenden

Wirksamkeit, stellt eine der wichtigsten Herausforderung im Bereich der Nanomedizin und siRNA Therapie für die nächsten Jahre dar.

8.4 Ausblick

Die Entwicklung geeigneter, vorhersagender und verlässlicher *in vitro* Testmöglichkeiten für Zytotoxizitätsbeurteilung von sogenannten Nanocarriern für die Anwendung beim Menschen stellt eine große Herausforderung für die Wissenschaft im Bereich der "Nanomedizin" dar. Viele Informationen über das Verhalten und die Eigenschaften von Nanocarriern in der Lunge sind bereits aus den sehr intensiven Untersuchungen mit ultrafeinen Partikeln im Bereich der Umweltmedizin und -gesundheit bekannt. Aus diesem Grund, wurden zwei anorganische Partikel, nämlich kristallines Silica (CS) und "nanogrosses" Zinkoxid (NZO), in allen Studien untersucht, da ihre Toxizität sowie die Entzündungsauslösung in der Lunge hinreichend bekannt sind. Zum ersten Mal wurden diese Partikel als sogenannte Referenzpartikel für Lungentoxizität eingeführt. Weiterführende Untersuchungen sowie bei der Entwicklung geeigneter *in vitro* Modelle sollten solche Partikel mit untersuchen, um eine bessere Risikoabschätzung und Beurteilung des Risiko für eine erhöhte Sicherheit der zu untersuchenden Partikel zu erhalten.

Berücksichtigt man die enorme und schnelle Verbreitung von Nanotechnologien und die Vielfalt verschiedenster Materialien im Nanobereich, die bereits genutzt und eingesetzt werden, aber auch die, die sich noch in der Entwicklung befinden, so stellt die richtige Beurteilung, Identifizierung, Quantifizierung und das Management des potentiellen Gesundheitsrisikos, vor allem in Bezug auf den Respirationstrakt, eine essentielle Herausforderung für die Wissenschaft dar. Viele epidemiologische Studien konnten bereits beweisen, dass ein Zusammenhang zwischen der erhöhten Exposition von ultrafeinen Partikeln und kardiovaskulären sowie respiratorischen Erkrankungen und damit auch von Morbidität und Mortalität besteht. Deshalb ist es von entscheidender Bedeutung, das potentielle Risiko von therapeutisch eingesetzten Nanopartikeln genau zu untersuchen und

robuste sowie verlässliche, vorhersagbare in vitro Modelle zu entwickeln, um eine sichere Anwendung am Menschen zu gewährleisten.

In der vorliegenden Arbeit, werden eine Vielzahl von in vitro Analysen in verschiedenen Lungenzellmodellen in *Kapitel 2-5* beschrieben und die Toxizität von PEI-basierten nicht-viralen Vektorsystemen mit verschiedenen Toxizitätsempfindungsmessungen untersucht.

Um die große Anzahl an verschiedenen Zellen in der Lunge (mehr als 40) zu berücksichtigen und die Interaktionen zwischen den verschiedenen Zelltypen realistischer untersuchen zu können, wäre die Entwicklung von einfachen, robusten und verlässlichen in vitro Zellkulturmodellen mit mehr als einem Zelltyp wünschenswert. Parallel zu solchen Modellen wäre auch die Untersuchung in Monokulturen, aber von verschiedenen Zelltypen (z.B. Epithel-, Endothelzellen, Fibroblasten, Makrophagen) oder auch von unterschiedlichen Spezies (Mensch gg. Maus) sinnvoll. Trotzdem lässt sich sagen, dass in der Mono-Zellkultur, wie sie in der vorliegenden Arbeit verwendet wurde, auch erste brauchbare Ergebnisse finden lassen können. Zumindest konnte das in *Kapitel 2-5* gefundene entzündungsfördernde und immunomodulatorische Potential der PEI-basierten nicht-viralen Vektorsysteme in vivo (*Kapitel 6*) bestätigt werden. Nun sollte in weiterführenden Studien der zugrundeliegende Mechanismus der Entzündung und des oxidativen Stress sowie der Zytotoxizität genauer untersucht werden, um bessere und sichere polymer-basierte Nanocarrier zu entwickeln. Weiterführende Studien sollten den zugrundeliegenden Mechanismus aufklären, indem ausgehend von Genexpressionmustern verschiedene relevante Proteine untersucht werden, die in einem bestimmten Pathway eine Schlüsselrolle spielen, z.B. Freisetzung von Cytochrom C beim intrinsischen Zelltod. Um eine erhöhte Evidenz für das apoptotische Verhalten von PEI zu erhalten, sollten weitere Untersuchungen hinsichtlich einer Caspaseaktivierung für eine bessere Unterscheidung von intrinsischen und extrinsischen apoptotischen Pathway durchgeführt werden. Im Hinblick auf das erhöhte entzündungsfördernde Potential der PEI-Modifikationen

sind weitere Modelle notwendig, die den zugrundeliegenden Mechanismus aufklären können, z.B. Untersuchungen zur Komplementaktivierung.

Bisher wenig untersucht ist das Zelltyp spezifische Targeting von nicht-viralen Vektorsystemen für siRNA Freisetzung in der Lunge. Die Kombination von Zelltyp spezifischen Targeting und RNAi Technik stellt einen neuartigen Weg zur Behandlung verschiedener Erkrankungen dar und wäre eine Revolution für die „Nanomedizin“.

Kapitel 7 beschreibt, zusätzlich zur Wirksamkeit in vivo, das Zelltyp spezifische Targeting (Leukozyten) von sechs verschiedenen PEI-basierten Nanocarriern für siRNA Freisetzung. Es konnte gezeigt werden, dass Leukozyten zwar zu einem gewissen Teil erreicht werden, dass sie aber nicht den Hauptanteil an Zellen ausmachen, in denen eine spezifische Runterregulation von "enhanced green-fluorescent protein" (EGFP) beobachtet werden konnte. Weiterführende Studien sollten andere Zelltypen wie Epithel- oder Endothelzellen, die einen Großteil der Lungenzellen ausmachen, miteinbeziehen und von weiterführenden Techniken wie Immunfluoreszenz und MACS Technology für die Durchflusszytometrie sowie die Einbindung von nicht-invasiven bildgebenden Verfahren (PET, MRT, CT) Gebrauch machen, um eine genaue Unterscheidung der verschiedenen Lungenbereiche (Bronchial vs. Alveolar) und Zelltypen zu erreichen.

Zusammenfassend läßt sich sagen, dass eine in vitro/ in vivo Korrelation der vorliegenden Daten noch durchzuführen ist, um noch mehr Informationen liefern zu können für eine optimierte Entwicklung von vorhersagenden Toxizitäts- in vitro Modellen und für eine bessere Anleitung aussagekräftiger in vivo Versuche.

9 Appendices

9.1 Abbreviations

AMD	Age related macular degeneration
ATP	Adenosine triphosphate
CF	Cystic fibrosis
COPD	Chronic obstructive pulmonary disease
d_{ae}	Aerodynamic diameter
DC	Dendritic cell
DE	Deposition
DME	Diabetic Macular Edema
dsRNA	Double stranded RNA
FRC	Functional residual capacity
EGF	Epidermal growth factor
GTP	Guanosine trisphosphate
KSP	Kinesin spindle protein
MAPK	Mitogen-activated protein kinase
MF	Mutant frequency
mRNA	Messenger RNA
miRNA	micro RNA
NfKB	Nuclear factor kappa beta
NOD	Nucleotide-binding oligomerization domain
8-OH-dG	8-hydroxy-2'-deoxyguanosine
PAI I	Plasminogen activator inhibitor
PEG	Poly(ethylene) glycol
PEI	Poly(ethylene imine)
PM	Particular matter
RNAi	RNA interference

RSV	Respiratory-Syncytial-Virus
RV	Residual volume
shRNA	Short hairpin RNA
siRNA	Small interfering RNA
t	Time
TGF-beta	Transforming growth factor beta
TLR	Toll-like receptor
V	Volume
VC	Vital capacity
Vd	Dead space volume
VEGF	Vascular epidermal growth factor
Vt	Tidal volume
UFP	Ultrafine particles

9.2 List of publications

Andrea Beyerle, Alexandra Long, Paul White, Thomas Kissel, Tobias Stoeger

Investigations on mutant frequency induced by Poly(ethylene imine) in FE1-MutaMouse lung epithelial cells

In preparation for Toxicology Letters

Andrea Beyerle, Andrea Braun, Felix Koch, Tobias Stoeger, Thomas Kissel

Fatty acid modification of low molecular weight Poly(ethylene imine) (PEI) mediate siRNA delivery in leucocytes and lung macrophages after intratracheal instillation in mice

In preparation for J Control Rel

Andrea Beyerle, Andrea Braun, Atrayee Banerjee, Nuran Ercal, Oliver Eickelberg, Thomas Kissel, Tobias Stoeger

Side-effects and their clinical relevance of Poly(ethylene imine)-based siRNA nanocarriers for pulmonary application in mice

Submitted to European Respiratory Journal (ERJ-00161-2010)

Olivia M. Merkel, Damiano Librizzi, Andrea Beyerle, Thomas Merdan, and Thomas Kissel: **In vitro and in vivo siRNA delivery with an integrin-targeting small molecule bioconjugate** in preparation for Gene Therapy

Olivia M. Merkel*, Andrea Beyerle*, Benedikt M. Beckmann, Roland K. Hartmann, Tobias Stoeger, and Thomas Kissel

Off-target effects in non-viral siRNA delivery – A study on the effect of polymer genomics under in vitro cell culture conditions

Submitted to Molecular Therapy

Andrea Beyerle, Martin Irmeler, Johannes Beckers, Thomas Kissel, Tobias Stoeger

Toxicity pathway focused gene expression profiling of PEI-based polymers for pulmonary applications

Submitted to Molecular Pharmaceutics (mp-2009-00278x)

Furong Tian, Adriele Prina-Mello, Giovanni Estrada, Andrea Beyerle, Winfried Möller, Holger Schulz, Wolfgang Kreyling, Tobias Stoeger

Macrophage Cellular Adaptation, Localization and Imaging of Different Size Poly-styrene Particles

Nano Biomedicine and Engineering, Vol 1, No 1 (2009)

Andrea Beyerle, Olivia Merkel, Tobias Stoeger, Thomas Kissel.

PEGylation affects cytotoxicity and cell-compatibility of Poly(ethylene imine) for lung application: structure-function-relationships.

Toxicol Appl Pharmacol. 2010 Jan 15;242(2):146-54.

Olivia M. Merkel, Andrea Beyerle, Damiano Librizzi, Andreas Pfestroff, Thomas M. Behr, Brian Sproat, Peter J. Barth, Thomas Kissel:

Nonviral siRNA Delivery to the Lung: Investigation of PEG-PEI Polyplexes and Their In Vivo Performance

Mol Pharm. 2009 Aug 3;6(4):1246-1260.

Furong Tian, Daniel Razansky, Giovanni Gomez Estrada, Manuela Semmler-Behnke, Andrea Beyerle, Wolfgang Kreyling, Vasilis Ntziachristos, and Tobias Stoeger
Surface modification and size dependence in particle translocation during early embryonic development

Inhalation Toxicology, 2009 Jul;21(S1):92-96

Andrea Beyerle, Sabrina Höbel, Frank Czubayko, Holger Schulz, Thomas Kissel, Achim Aigner, and Tobias Stoeger.

In vitro cytotoxic and immunomodulatory profiling of low molecular weight polyethylene-imines for pulmonary application.

Tox in vitro, 23 (2009) 500–508

Andrea Beyerle, Holger Schulz, Thomas Kissel and Tobias Stoeger.

Screening strategy to avoid toxicological hazards of inhaled nanoparticles for drug delivery: the use of α -quartz and nano zinc oxide particles as benchmark.

Journal of Physics: Conference Series: 151 (2009) 012034

Furong Tian, Adriele Prina-Mello, Giovanni Gomez-Estrada, Andrea Beyerle, Wolfgang Kreyling, Tobias Stöger

A novel assay for the quantification of internalised nanoparticles in macrophages.

Journal of physics: 151: 2009

Furong Tian, Adriele Prina-Mello, Giovanni Gomez-Estrada, Andrea Beyerle, Winfried Möller, Holger Schulz, Wolfgang Kreyling, Tobias Stöger

Development of a fast and reliable method to quantify the amount of internalized nano-structured materials in macrophages

Nanotoxicology. 2008, 2 231-242

9.3 Poster presentations

Olivia M. Merkel, Andrea Beyerle, Damiano Librizzi, Thomas Kissel

Nuclear imaging of intratracheal siRNA delivery with PEG-PEI copolymers

4th European Molecular Imaging Meeting, Barcelona, Spain, May 2009

Olivia M. Merkel, Andrea Beyerle, Damiano Librizzi, Thomas Kissel

Nuclear imaging of intratracheal siRNA delivery with PEG-PEI copolymers

17th International Congress of the International Society for Aerosols in Medicine, Monterey, CA, USA, May 2009

Andrea Beyerle, Thomas Kissel, Holger Schulz, Tobias Stoeger

Structure-function-relationships of modified Nanocarriers for pulmonary application: PEGylation affects biocompatibility of poly(ethylene imine)

2nd European Conference for Clinical Nanomedicine, Basel, CH, April 2009

Andrea Beyerle, Olivia M. Merkel, Thomas Kissel, Holger Schulz, Tobias Stoeger

Safety profiling of non-viral vector systems for pulmonary gene and siRNA delivery

14th International Symposium on Recent Advances on Drug Delivery Systems, Salt Lake City, US, Februar 2009

Andrea Beyerle, Holger Schulz, Thomas Kissel, Tobias Stoeger
Screening strategy to avoid toxicological hazards of inhaled nanoparticles for drug delivery: the use of a-quartz and nano zinc oxide particles as benchmark
Inhaled Particles X Conference, Sheffield, UK, September 2008

Andrea Beyerle, Sabrina Höbel, Frank Czubayko, Holger Schulz, Thomas Kissel, Achim Aigner, Tobias Stoeger
Comprehensive cytotoxicity and proinflammatory in-vitro testing of two low molecular weight poly(ethylene imine) particles exposed to pulmonary target cells
INIS Hannover, Hannover, Juni 2008)

Andrea Beyerle, Olivia M. Merkel, Holger Schulz, Thomas Kissel, Tobias Stoeger
Cytotoxic and proinflammatory evaluation of various PEI particles on lung target cells
PBP World Meeting Barcelona, Barcelona, April 2008

Andrea Beyerle, Anke-Gabriele Lenz, Holger Schulz, Sabrina Höbel, Beate Urban-Klein, Achim Aigner, Thomas Kissel, Tobias Stoeger
Screening Strategy for Toxicological Hazards of Inhaled Nanoparticles for Drug Delivery
Interact Munich, München, Dezember, 2007

Andrea Beyerle, Anke-Gabriele Lenz, Holger Schulz, Sabrina Höbel, Beate Urban-Klein, Achim Aigner, Tobias Stoeger
Cytotoxic and proinflammatory investigations of two siRNA stabilizing polyethyleneimines (PEI) in murine lung cells
EuroNanoForum, Düsseldorf, Juni, 2007

Andrea Beyerle, Anke-Gabriele Lenz, Holger Schulz, Sabrina Höbel, Beate Urban-Klein, Achim Aigner, Tobias Stoeger
Analysis of cytotoxic and proinflammatory effects of two siRNA stabilizing polyethyleneimines (PEI) in murine lung cells
48.DGPT –Tagung, Mainz, März, 2007

9.4 Lectures

Olivia M. Merkel, Andrea Beyerle, Damiano Librizzi, Thomas Kissel
Nuclear imaging of intratracheal siRNA delivery with PEG-PEI copolymers
Oral Presentation, Meditrans Second Annual Meeting, Weizmann Institute of Science, Rehovot, Israel, March, 2009

Andrea Beyerle, Holger Schulz, Thomas Kissel, Tobias Stoeger
Nanohale - Cytotoxic and proinflammatory evaluation of various PEI particles on lung target cells
Oral Presentation, 49. DGPB Tagung, Lübeck, April 2008

9.5 Curriculum vitae

Persönliche Daten:

Name: Beyerle, Christiane Andrea Barbara
 Beruf: Apothekerin
 Geburtsdatum: 10.09.1979
 Geburtsort: Neuss
 Nationalität: Deutsch

Schulbildung:

1985 - 1989 Martin-Luther-Grundschule in Neuss
 1989 - 1995 Marienberg Gymnasium in Neuss – mittlere Reife
 1995 - 1998 Quirinus Gymnasium in Neuss – Allgemeine Hochschulreife

Berufsausbildung:

1998 - 2001 Ausbildung zur pharmazeutisch technischen Assistentin an der
 PTA – Lehranstalt in Duisburg

Hochschulausbildung:

2001 - 2005 Studium der Pharmazie an der Philipps- Universität in Marburg
 05/2005 - 10/2005 Praktikum bei Sanofi - Aventis, Pharmaceutical Sciences,
 Early Formulation/Preformulation; Labor Dr. Kamm
 11/2005 - 04/2006 Praktikum in der Metropolitan Pharmacy, Apotheke am internationalen
 Flughafen Frankfurt, Inhaber: Frank Füßl

Promotion:

07/2006-02/2010 Wissenschaftliche Mitarbeiterin am Helmholtz Zentrum München,
 Comprehensive Pneumology Center, Institut für Lungenbiologie, in
 Kooperation mit der Philipps-Universität Marburg unter der Leitung von
 Prof. Kissel (Institut für Pharmazeutische Technologie und Biopharmazie)
 Anfertigung der vorliegenden Dissertation

Post Doc:

03/2010 - recent Research Associate at Newcastle University in the Northern Institute for
 Cancer Research

Berufserfahrung:

als PTA während der Semesterferien:

2001 - 2002	Bären-Apotheke, Zollstr. 7, 41460 Neuss
2002 - 2003	Malteser-Apotheke, Venloerstr.103, 41462 Neuss
2003 - 2004	St.Cosmas Apotheke, Kaarster Str.50, 41462 Neuss
2005	Struwelpeter-Apotheke, An der Hauptwache 10, 60313 Frankfurt

als Apothekerin während der Promotion:

10/2006 – 01/2010	St.Peter Apotheke, Leopoldstr. 171a, 80804 München
-------------------	----------------------------------------------------

Weiterbildung zum Fachtoxikologen DGPT/Fachtoxikologin DGPT:

10/2007	Versuchstierkunde I (Theorie) & Biostatistik, Erfurt
02/2008	Molekulare Zellbiologie, München
06/2008	Versuchstierkunde II (Praxis), Jena
09/2008	Fremdstoffmetabolismus und Toxikokinetik, Dortmund
11/2008	Chemische Kanzerogenese & Mutagenese, München
02/2009	Fremdstoffallergie/Immuntoxikologie, Berlin
06/2009	Organtoxikologie und -pathologie II, Erfurt
02/2010	Safety Pharmacology, Basel
02/2010	Organtoxikologie und -pathologie I, Erfurt

9.6 Danksagung

Mein besonderer Dank gilt Herrn Prof. Dr. Thomas Kissel für die Betreuung meiner Doktorarbeit und sein in mich gesetztes Vertrauen. Sein großer Erfahrungsschatz und die stete Diskussionsbereitschaft haben maßgeblich zum Gelingen dieser Arbeit beigetragen. Er war ein verständnisvoller und motivierender Doktorvater für mich. Ich möchte mich besonders für seine großartige und ständige Unterstützung aus der Ferne bedanken und die Freiheiten, die er mir gegeben hat, mit deren Hilfe ich mich selbst weiter entwickeln und sehr viele Erfahrungen im weiten Gebiet der Wissenschaft sammeln konnte.

Im gleichen Maß möchte ich Dr. Tobias Stöger danken für die hervorragende Zusammenarbeit und Betreuung meiner Arbeiten in München. Für seinen unerschöpflichen Vorrat an Ideen und Energie in vielen Diskussionsrunden sowie seine stete Bereitschaft meine Ideen umzusetzen und seine Großzügigkeit und die Freiheit, die er mir im Laboralltag und beim Besuch aller nationalen und internationalen Kongresse gegeben hat.

Bei Prof. Dr. Werner Seeger sowie Prof. Dr. Eickelberg und auch Dr. Thomas Schmehl und Dr. Tobias Gessler möchte ich mich für die unkomplizierte und durchgängige Finanzierung meiner Doktorarbeit bedanken.

Im Helmholtz Zentrum München möchte ich mich ganz herzlich bei Prof. Dr. Holger Schulz und Dr. Wolfgang Kreyling bedanken, dass Sie mir mit dem Nanohale-Antrag ermöglicht haben, außerhalb von Marburg unter Anleitung und Betreuung von Prof. Dr. Thomas Kissel und Dr. Tobias Stöger meine Doktorarbeit in München im Institut für Lungenbiologie am Comprehensive Pneumology Center zu schreiben.

Bei Prof. Dr. Paul White und Alexandra Long vom Health Canada Institut in Ottawa bedanke ich mich recht herzlich für die hervorragende Zusammenarbeit und Diskussionsbereitschaft und die sorgfältige Bearbeitung meiner DNA-Proben. In diesem Zusammenhang soll auch Dr. Nicklas R. Jakobson ein besonderer Dank ausgesprochen werden für die gute und sehr interaktive Anleitung der Projektplanung und –durchführung.

Frau Prof. Dr. Nuran Ercal und Dr. Atrayee Banerjee von der Missouri University in Rolla danke ich für die tolle und lehrreiche Zusammenarbeit im Hinblick auf die oxidativen Stress Parameter in meinen Mauslungen.

Allen Mitgliedern der DFG-Forschergruppe „Nanohale“ möchte ich für die vielen Diskussionen und die Zusammenarbeit während meiner Doktorarbeit danken.

Desweiteren möchte ich mich ganz herzlich für die Unterstützung in der Zellkultur vor allem in der Anfangsphase meiner Doktorarbeit am Helmholtz Zentrum München bei Frau Dr. Anke-Gabriele Lenz und Michael Krumpel bedanken, die mir die Heranführung an die Zellkultur wesentlich erleichtert haben. Daniela Dittberner danke ich für die sehr produktiven und lernintensiven Stunden nebeneinander an der Bench mit allen mehr oder weniger lustigen Zwischenfällen von Tablettverlusten und geheimnissvollen Kontaminationen und die intensiven Exkurse in die Mikrobiologie.

Herzlich bedanken möchte ich mich außerdem bei Frau Dr. Maria Diedrich-Möhring aus der Arbeitsgruppe Immunbiologie in der Augenklinik der Universität München, die mich in die Luminex Technik eingeführt hat und mir mit ihrem großen Erfahrungsschatz die selbständige Durchführung aller meiner Zellkulturüberstandsmessungen auf pro- und antiinflammatorische Effekte wesentlich erleichtert hat.

Herrn Andreas Stampfl und Frau Melanie Mayer aus dem Institut für Toxikologie möchte ich ganz herzlich danken für die jederzeit unkomplizierte Hilfsbereitschaft und freundliche Art, auf alle meine Anfragen, am HPPS Malvern Instrument messen zu dürfen und die rechtzeitige Einschaltung des Gerätes.

Frau Dr. Andrea Braun aus der Klinischen Kooperationsgruppe „Umweltdermatologie und Allergie“, ZAUM (TU München) danke ich für alle gemeinsam besuchten Toxkurse der DGPT, die stets gut organisierten Unterkünfte und die gemeinsamen Lernstunden am Ende jedes Kurses. Außerdem danke ich Frau Dr. Andrea Braun für die Möglichkeit der sehr intensiven Nutzung des FACS-Gerätes aus ihrer Arbeitsgruppe in der letzten Phase meiner Doktorarbeit und allen

gemeinsamen Messungen, wertvollen Diskussionen und die stete Unterstützung in der Umsetzung meiner Ideen.

Jens Lipka danke ich für die vielen, morgendlichen Diskussionen auf dem Fahrrad beim gemeinsamen Weg zur Arbeit, für alle Hilfestellungen handwerklicher Art von Fahrradreifenwechsel bis Festplattensanierung meines Laptops.

Herrn Dr. Thomas Hofer danke ich für die exzellente Einführung in die Durchflusszytometrie und die schnelle und jederzeit unkomplizierte Beantwortung all meiner Fragen.

Einen ganz besonderen Dank möchte ich Tobias Lehardt aus der Arbeitsgruppe von Herrn Prof. Dr. Thomas Kissel aussprechen, für alle Übernachtungen während meiner Aufenthalte in Marburg zu wissenschaftlichen und auch privaten Zwecken und alle gemeinsamen Abendessen mit sehr intensiven Diskussionen und die vielen motivierende Worte. Die Reise nach Marburg war nicht zuletzt wegen seiner unkomplizierten und spontanen Gastfreundschaft immer wieder eine große Freude.

Aus dem Arbeitskreis von Prof. Dr. Thomas Kissel geht ein weiterer besonderer Dank an Frau Dr. Olivia Merkel, mit der ich die intensivsten und sehr lehr- und erfolgreichen in vivo Laborstunden in der Nuklearmedizin in der Uniklinik Marburg und im BMFZ verbracht habe. Ich danke ihr auch, für Ihre immer offenen Ohren und emails zu allen möglichen Tages – und Nachtzeiten, die sich meine Sorgen und Probleme bei meinen Arbeiten in München angehört haben und die mich immer wieder motiviert hat, weiterzumachen und das Ziel nicht aus den Augen zu verlieren.

Herrn Dr. Ali Önder Yildirim danke ich für die zwar sehr kurze, aber stets sehr lehrreiche und intensive Zusammenarbeit und Unterstützung sowie Motivation während meines letzten Projekt am Helmholtz Zentrum München im Institut für Lungenbiologie.

Für die beste labortechnische Unterstützung über einen langen Zeitraum meiner Doktorarbeit danke ich ganz herzlich Frau Birgit Frankenberger, die mir mit all ihrem Wissen und ihrer Erfahrung stets zur Seite stand. Auch außerhalb des Institut hat sie mich in die Schönheit der

Alpen geführt, mir meine tägliche Kondition durch viele, schöne, gemeinsame Läufe zum Nymphenburger Schloß, an der Isar oder auch durch den Englischen Garten um ein wesentliches verbessert und mich all meine täglichen Sorgen schnell vergessen lassen.

Weiterhin bedanke ich mich bei allen Mitgliedern des Instituts für Lungenbiologie insbesondere allen, die mich im Gebäude 34 begleitet haben. Dr. Konrad Maier, Dr. Ingrid Beck-Speier, Dr. Anke-Gabriele Lenz, Dr. Furong Tian, Dr. Dariusch Etehadieh, Dr. Shang Yu, Dr. Alex Götz, Renfu Yin, Birgit Frankenberger, Barbara Oswald, Gabriele Schumann, David Kutschke und Dr. Matthias Wjst, ihnen danke ich für alle gemeinsamen Unternehmungen in und um München, alle lustige Bürostunden und gemeinsam besuchten Kongresse.

Zum Schluß meiner Danksagung möchte ich meinen liebevollen Eltern für ihre stete Unterstützung in allen Lebenslagen und ihr Verständnis für all meine Entscheidungen von ganzem Herzen danken. Ohne sie wäre ich nicht der Mensch geworden, der ich bin.